

MArch Thesis

Building Performance Simulation

A Multicriteria analysis of Indoor
Environmental Quality of the H-IEQ
laboratory

MArch Thesis

Building Performance Simulation

**A Multicriteria analysis of Indoor
Environmental Quality of the H-IEQ**

laboratory



**DAD - Department of Architecture and Design
a.a 2019/2020
Master's Degree in Architecture**

**Supervisor:
Fabio Favoino**

**Advisor:
Luigi Giovannini**

**Candidate:
Stefano Cassano**

Acknowledgements

I would like to express my gratitude to my Supervisor Fabio Favoino and my advisor Luigi Giovannini for giving me the chance of accomplishing such a work. Without their knowledge, experience, availability and sense of duty, this dissertation would never have been possible.

I would also like to thank my family and friends for their indirect yet empowering support.

Sapore felice 25 giugno 1985

E' nell'aria,
tiepida sera d' estate,
fra le stelle e la falce rossiccia,
il raro gusto di vivere,
felice per esserci,
pace e silenzio,
assieme finalmente.

To my father...

Table of Contents

Abstract	15
Intro	17
Theory	24
- Thermal Comfort	26
- Visual Comfort	31
- Indoor Air quality	35
Objective and aims	37
Research Methods	38
- building performance simulation	38
- Workflow and test cases	38
Software	40
H-IEQ Lab - STATE OF THE ART	42
A. Climate Analysis	47
Simulations	57
B. Baseline	60
- b1. adaptive thermal comfort analysis	62

- b2. PMV comfort model	69
- b3. Influence of solar radiation on occupants	73
- b4. CBDM & Daylight Analysis	87
- b5. Ev + glare	91
- b6. Image based analysis Evalglare	105
- b7. Thermal + Visual Comfort	114
C. New Glass Specs	121
- c1. Thermal Comfort Analysis	122
- c2. CBDM & Daylight Analysis	126
- c3. Ev + glare	130
- c4. Thermal + Visual Comfort	144
D. Dynamic Shading	147
- d1. Thermal Comfort Analysis	148
- d2. CBDM & Daylight Analysis	151
- d3. Ev + glare	155
- d4. Thermal + Visual Comfort	168
E. Fixed Shading	171
- e1. Solar study & Shading masks	173
- e2. Thermal Comfort Analysis	176
- e3. CBDM & Daylight Analysis	178
- e4. Ev + glare	182
- e5. Thermal + Visual Comfort	196

F. Findings & Comments 199

References 215

Abstract

This Master Thesis work consists in performing a multicriteria analysis of the indoor environmental quality of an experimental facility for IEQ testing.

The facility, which stands for “Health Indoor Environmental Quality Lab”, wants to be in line with already built experimental prototypes used in the analysis for researched-based indoor quality studies. Whether the laboratory will host real life tests, its construction systems and flexibility make it interesting for the application of computer simulation software.

Building Performance simulation has supported a parametric study comparable to on-field testings. By iteratively using and changing different input parameters, software simulation can lay out specific findings among multiple scenarios. In this work, different input lead to different

outputs according to some environmental quality aspects, such as thermal comfort, daylight and glare. These very aspects are also placed together to find common design strategies with the aim of solving discomfort issues across multiple domains. After a brief climate analysis based on Turin Typical Meteorological Year data (TMY), simulations are displayed according to different configurations: a) a baseline configuration in free-running mode; b) a baseline configuration conditioned by means of HVAC system; c) the baseline configuration b) with improved glass specification; d) the baseline configuration b) with an external dynamic shading; e) the baseline configuration b) with an external optimised fixed shading. Simulations follows similar steps, from main thermal analysis, displaying annual plotting of over-heated, comfort and

under-heated %, to some of the principal daylight indexes, such as Daylight Autonomy, Spatial Daylight Autonomy and Useful Daylight illuminance. This work also provides a simplified evaluation of spatial glare. Eventually, baseline results indicate high quantity of overheating during spring and summer time. Moreover, exceeding illuminance and DGP are measured. Modification of glass properties for sun control and application of shadings lead to reduction in overheating, especially in case of fixed shading application, parallel to increase of under-heated % hours, with Thermal Comfort still being in the similar range. Yet, a sensible degree of delta in summer Overheated hours is found. Daylight results depict more effective changes towards acceptable conditions. Energy consumptions vary according to the four different scenarios.

Baseline case presents higher values in cooling vs. heating. This trend inverts in the other three cases (new glass, dynamic shading and fixed shading). Electrical Lighting consumptions in baseline case are the lowest among all scenarios, whereas Dynamic shading is the one with higher values in terms of indoor comfort levels. Overall, configuration with improved glass specification, results in the lowest global energy use.

Intro

By reading the 2014 Climate Change report, it's clear that the overheating process of our planet is ongoing. In the last decades, sea levels along with quantity of CO₂, N₂O, and acidity measured in the oceans, read all higher numbers (see charts page 19).

“Human influence on the climate system is clear, and recent anthropogenic emissions of greenhouse gases are the highest in history” [1]. If we give a look at the graphs, Global Mean Surface Temperature (GMST) and Global Average Sea Levels (GASL), values indicate highly rising measurements in the last decades and skewing graphs. Above pre-industrial levels, human activities have caused an increment in temperature of about 1 °C and it is growing with a rate of 0.2 °C per decade. If the trend will not be modified in the

next few years, there is a very high probability to increase the overall temperature further than 1.5 °C.

In 2015, all United Nations Member States adopt an agenda for “Sustainable development” to reach prosperity, equality and respect for the ecosystems and climate all over the world.

Moreover, 17 UN goals, called “SDGs”, are set, some symbolizing the reduction in inequality, others related to sustainable cities and communities...

In particular, Goal n.13 quotes “Take urgent action to combat climate change and its impacts”.

For this reason, one of the trendiest words in the architecture field in the last decade are “sustainable”, “resilient” ...

The concept of sustainability in its modern sense emerged in the early 1970s in response to growing understanding that modern development practices were leading to environmental and social crisis. The term is first used in 1972 by Donella Meadows in “The Limits to Growth”, but the concept traces its origin far deeper in the history of human evolution. Since with the philosopher Aristotle, such terms as “second nature” existed, as to state anything that was touched, modified and then altered by human action. The technical and social breakthroughs of the industrial revolution are usually badly depicted by Poets such as William Wordsworth, Shelley, Keats and in 1836 Contrasts by Augustus Pugin. But it is mainly in the 1900s that the sustainability definition enters

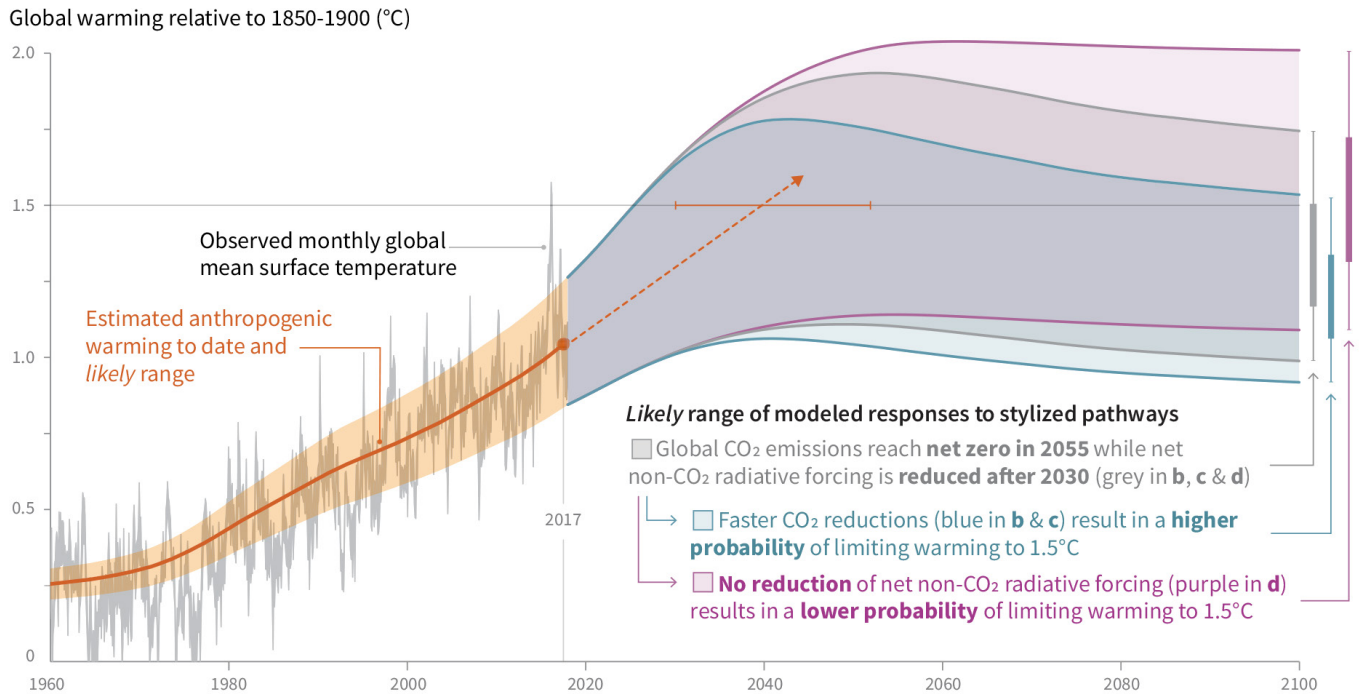


Figure 1. Global Warming in delta°C on decades plot basis

vocabularies and starts conquering people feelings, from the 1938 Lewis Mumford's Culture of Cities and 1972 United Nations Conference on the human Environment, that consists in a description of the greenhouse effect problem. Also, in 1972, a UN conference on Environment and Development is held in Stockholm. In the same year, in Limits to Growth,

Meadows and some other MIT researchers, predict a crash of the human system, by mid 21th century, based on some factors like resource consumption, pollution and global population.

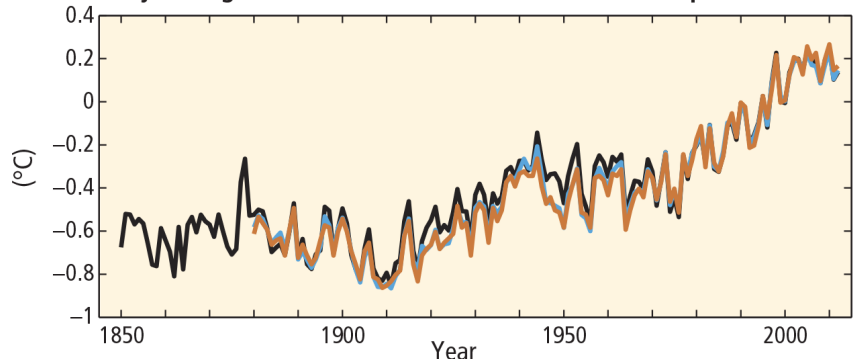
Climate change is about equal to 400000 Hiroshima nuclear bombs exploding each of 365 days per year. That is a huge amount of energy! But what is the

real responsible factor for this big amount of energy production? It is the building industry, which is like the infrastructure and factories industries combined. By looking at the Global Status Report (2017), "Buildings construction, including the manufacturing of materials for building such as steel and cement, accounted for an additional 26 EJ in estimated

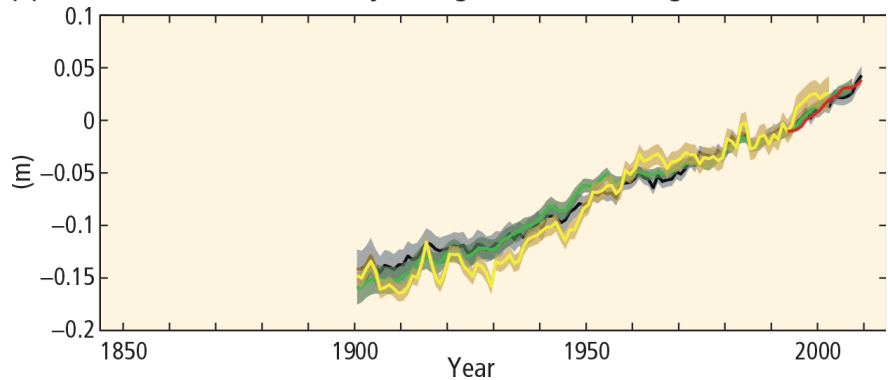
global final energy use”. In 2016, 30% of total energy use is consumed, a value corresponding to 125 EJ. Moreover, “Accounting for upstream power generation, buildings represented 28% of global energy-related CO₂ emissions, with direct emissions in buildings from fossil fuel combustion accounting for around one-third of the total. Buildings construction represented another 11% of energy sector CO₂ emissions”[2].

One of the principals aims to consider for a sustainable development approach in Building design is to reduce at maximum the production of fossil fuels and maximize the use of natural resources, like water collective systems and exploitation/reduction of Solar radiation. Passive Houses and net-zero energy buildings are a good way to empower this discourse, especially when using mechanical ventilation systems, thus limiting or even avoiding

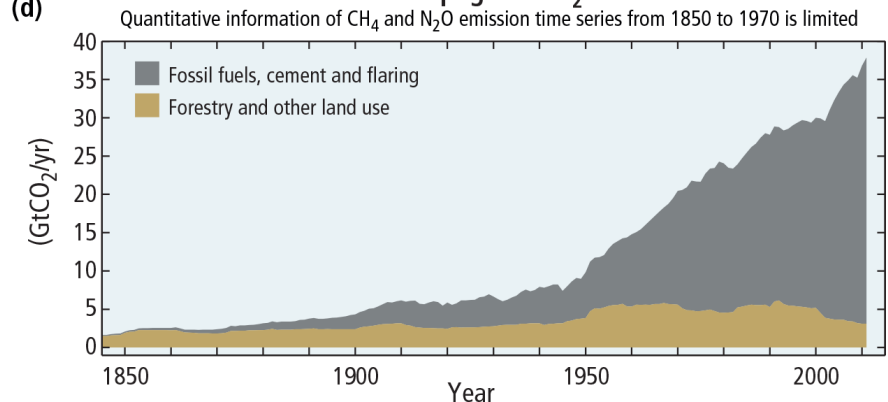
(a) Globally averaged combined land and ocean surface temperature anomaly



(b) Globally averaged sea level change



(d) Global anthropogenic CO₂ emissions



the use of air conditioning for heating and cooling.

In many countries there is a great amount of old buildings, in some case without necessary insulation applied. Thus, the energy consumption per year reaches high values, in addition to producing excessive heating and CO₂ for the environment, claiming need for retrofit campaigns. A perspective design should consider building green roofs, so to gain the multiple benefits of [...] improved air quality, increased biodiversity, storm water management, increased longevity of the building's waterproof membrane, assistance with urban food production, and contribution of a more liveable city [3]. Green roofs are also important in mitigating the heat-island effect, which is a well-known phenomenon in cities.

Architect and planners should design a building based on bioclimatic principles, so to

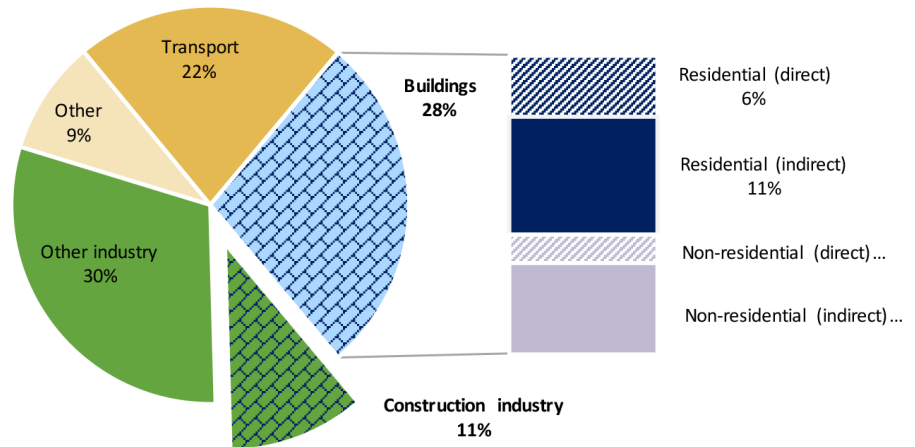


Figure 5. Global Status Report - Energy % consume per sector

minimise the costs on technical equipment and the technologies systems in projects. Not only has this to be applied on the smaller scales, but also on the greater one.

From the 90s and 2000s new companies are born to care about minimizing energy consumptions and recognizing better energy systems in buildings. “By one count, there are nearly 600 relevant green product certifications worldwide. These systems assist in the difficult task of determining how green a given building is “[4].

So, from “BREEAM” to “LEED” to “Living Building Challenge”, some architectural firms are already dealing with high performance energy buildings. In addition, Standards and normative keeps evolving and giving suggestions on how to achieve more sustainable design and maximize comfort.

Present and future design in Architecture must pursue a holistic approach more than ever, from a pure aesthetic reasoning to a more technical, scientific, and social one. Communication

between architects, engineers and communities must be easier and more direct and as close as ever.

Building simulation can be applied in the early phase of the design, in order to follow bioclimatic approaches and exploit the environment for passive energy implications, or simply find best strategies to reduce discomfort situations (e.g. overheating in summer). Yet, some climates (e.g. Mediterranean climate) can deploy some challenges given the presence of hot conditions in summer and cold ones in winter. In this cases, adaptation of the building to the outdoor climate is essential and, in parallel to state-of-the-art construction, installation of mechanical systems such as HVAC cannot always be avoided. Energy modelling can be applied to correctly size and preview the efficiency of HVAC, after indoor microclimates data has been

calculated and interpreted according to key factors.

Heating and cooling loads are mostly responsible for energy consumes in buildings and production of excessive CO₂. As the increase of urbanized areas and people living in cities is a well known phenomenon, urban density will remain pivotal in future and high rise buildings such as skyscrapers are being more preferable to build, for they cover less soil. It is especially with this types of buildings that architecture is constantly experimenting high glazed and transparent surfaces and reducing structural skeletons. Nonetheless, whether applying the greatest amount of transparent surfaces may be the dream of many designers, some factors such as solar radiation can have a huge impact on thermal and visual comfort.

Before last two decades, building

industry hardly considers solar radiation influence on indoor climate. Even now, it is an hard topic on modern research.

Nielsen and Blazejczyk (1994), McNeill and Parsons (1999), S. Hodder and Parsons (2007) [4] evidence that, when the subject is exposed to solar radiation, it determines thermal discomfort. In particular S. Hodder and Parsons find out that an increase of one scale unit in thermal sensation is linked to about 200 W/m² and that there is no significant relationship between thermal sensation response and the specific solar spectrum involved. Arens et al. (2015) [5] research paper proposes a model, named SolarCal, which takes into account the solar radiation falling on occupants. Here, Short-wave radiation is distinguished from long-wave radiation as it is evidenced how fundamental it is in thermal discomfort evaluation. Thanks to these implications, ASHRAE

Standard 55 implements the “SolarCal model”.

What solar radiation affects is primarily the Mean radiant temperature “tr” and the Operative temperature “top”.

Operative temperature, a mean between air temperature and mean radiant temperature, is the effective “felt” temperature by the occupants and what comfort models calculations are based on. Instead, air temperature perceived by thermostat, is what HVAC system activation is based on. Yet, air temperature does not account for solar radiation discomfort on occupants.

That is where a discrepancy in comfort evaluation and HVAC sizing occurs.

Building simulation outputs include different aspects of indoor climate, from proper thermal aspects to daylight. Only recently have designers been studying the influence of these aspects altogether. Since then, thermal aspects were conducted

in spite of daylight ones or vice-versa, outlying an incomplete vision of design. A combined visualization of such metrics and domains is necessary more than ever when seeking for a total design approach.

Theory

Main normative referenced in this work is based on US Standard ANSI ASHRAE 55 [6]. ASHRAE (American Society of Heating, Refrigerating and Air conditioning Engineers), founded in 1984, is a global society focusing on human well-being in the built environment.

An European version of the normative is CEN, in particular CEN 15251:2007, about “Indoor environmental input parameters for design and assessment of energy

Certification level	Points BD&C	Points BD&C (Core and Shell)	Points BD&C (Schools)	Points BD&C (Healthcare)
Certified	8	8	8	5
Silver	10	12	10	6
Gold	12	16	12	7
Platinum	16	20	15	9

Figure 8. LEED 4 certification categories with relative score

performance of buildings addressing indoor air quality, thermal environment, lighting and acoustics” [7], which is followed in Italy with UNI 7730.

For visual comfort, there is some reference to CEN/TC 169 “Daylight in buildings” [8].

Moreover, The International WELL Building Institute (IWBI) is another rating system, launched in October 2014, that combines aspects of Thermal, Visual and Air comfort to many others.

Nowadays, “The Well v2” is

type	WELL	LEED V4	BREEAM 3.0
indoor air quality	ASHRAE Standard 62.1 - 2013	ASHRAE Standard 62.1 - 2010 CEN Standards EN 15251 - 2007	BS EN 16798-3:2017 CIBSE AM10
thermal comfort	ASHRAE Standard 55	ASHRAE Standard 55 CEN Standard EN 15251 - 2007	CIBSE AM11 ANNEX A ISO 7730:2005 CIBSE TM52: The limits of thermal comfort: avoiding overheating in European Buildings CIBSE TM59
visual comfort	sDA300,50% for at least 55% of space ASE1000,250 <=10% of space	sDA300,50% for at least 55% of space (2pts) sDA300,50% for at least 75% of space (3pts) ASE1000,250 <=10% of space UDI300-3000 for 75% of time (2pts) UDI300-3000 for 95% of time (3pts)	(min req) 2% DF for 80% of space At least 300 lx for 2000 hrs per year for 80% of space (entire space) At least 90 lx for 2000 hrs per year for 80% of space (worst lit point) (exemplary) 4% DF (single storey) for 80% of space At least 300 lx for 3000 hrs per year for 80% of space (entire space) At least 120 lx for 300 hrs per year for 80 % of space (worst lit point)

Figure 9. Some of comfort parameters and prerequisites according to WELL, LEED and BREEAM standards

a newer version of “The Well Building Standard” and “The Well Community Standard”. This work references to “The Well Building Standard v1”, May 2016 [9].

One of the principal rating systems is “LEED”, Leadership in Energy and Environmental Design.

This is based on 4 types of recognised certification (from “Certified” to “Platinum”) according to the total sum of point per category and construction type (see figure 8).

Main categories for evaluation are:

- location and transportation
- sustainable sites
- water efficiency
- energy and atmosphere
- materials and resources
- indoor environmental quality

“BREEAM” is another leading sustainability assessment method for infrastructure and buildings.

Certification scale varies from “Pass” to “Outstanding”, through the achievement of benchmarks expressed in percentages.

Main categories for evaluations are:

- Management
- Energy
- Water
- Pollution
- Health and Wellbeing
- Transport

- Materials
- Land use and Ecology
- Innovation

Some of the “Indoor environmental quality” parameters refer to ANSI ASHRAE and CEN, as it is for thermal comfort.

Figure 9 lists some of the performance parameters according to indoor air

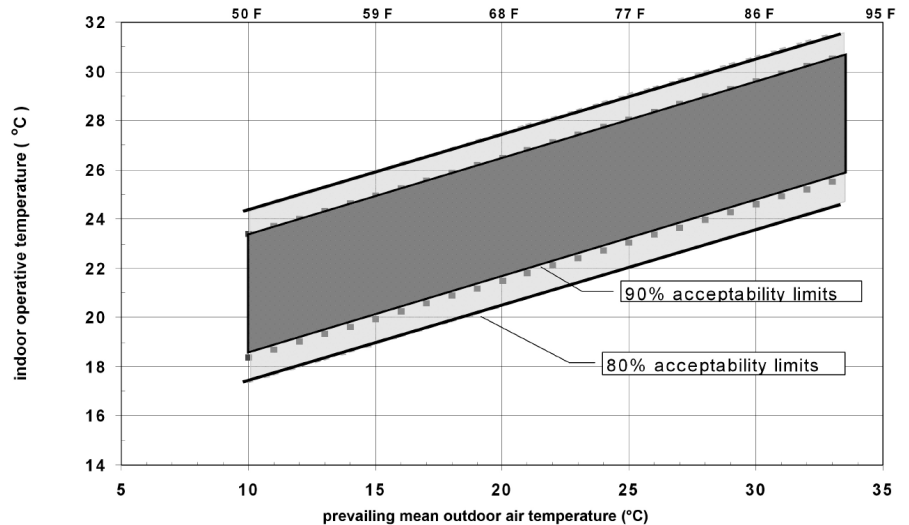


Figure 10. Indoor Operative temperature and Comfort Range - ASHRAE 55

quality, thermal and visual comfort among WELL, LEED and BREEAM.

Thermal Comfort

“Thermal comfort is the condition of mind that expresses satisfaction with the thermal environment and is assessed by subjective evaluation” [6].

Nowadays, there are two main known models to determine whether a space is comfortable or not. In particular, “it is first necessary to recognize that there has been an ongoing debate in the comfort science community over the last few decades that parallels the issues raised by a conditioned thermally neutral vs. a free-running thermally diverse environment” [10].

The adaptive model and the Fanger PMV comfort model are the actors of this debate.

The Adaptive Model

The adaptive model is based on statistical data coming from thousands of surveys and locates a comfort range based on a comparison between dry bulb outdoor temperature values and indoor operative temperature.

In particular, according to ASHRAE, the method defines “acceptable thermal environments only for occupant-controlled naturally conditioned spaces”.

Some criteria are required, such as that there is no mechanical system activated and the prevailing mean outdoor temperatures is greater than 10° C and lower than 33.5° C.

Moreover, occupants should have a metabolic rate between 1.0 and 1.3 met. The criteria followed to assess comfort can be based on 80% acceptability limits, but also 90% and 95% (which is the top value) are used.

The computation of the prevailing mean outdoor air

temperature “ $tp_{ma} (out)$ ”, should be based on no fewer than 7 days and no more than 30 sequential days. ANSI/ASHRAE 55 also gives these following equations, that refer to the lower and upper limit of the indoor operative temperature based on 80% acceptability criteria:

a. Lower limit:

$$0.31 * tp_{ma} (out) + 14.3^{\circ}$$

b. Upper limit:

$$0.31 * tp_{ma} (out) + 21.3^{\circ}$$

Prevailing mean outdoor temperature can also be more accurately calculated, applying a weighted running mean of some specific intervals of the year. For example, according to CEN, last 7 days temperature of each month is used to calculate a mean, weighted through a “climatic response” coefficient named “ α ”. If air speed is higher than 0.3 m/s, the standard suggests incrementing these boundary conditions of a ΔT equal to

1.2° C, 1.8° C, 2.2 ° C, according to an air speed of 0.6, 0.9 and 1.2 m/s, respectively.

PMV comfort Model

In 1970 Danish Fanger studies the correlation between climatic conditions in buildings and human subjective sensations. When it gets cold or hot, blood circulation changes according to vasomotor thermoregulation, so that it can adapt to exterior shifts such as those determined by temperature.

If it gets too cold or too hot, vasomotor thermoregulation is not enough and the mechanism of behavioural thermoregulation starts on, activating the body muscles by effect of bumps and shaking, or making the body into sweating, when it is hot outside. In this case, the thin layer of sweat, cools us down, when it evaporates and leaves our skin. Human body is a machine, more or less like a mechanical machine

Table 5.2.2.2A Clothing Insulation I_{cl} Values for Typical Ensembles

Clothing Description	Garments Included ^a	I_{cl} , clo
Trousers	(1) Trousers, short-sleeve shirt	0.57
	(2) Trousers, long-sleeve shirt	0.61
	(3) #2 plus suit jacket	0.96
	(4) #2 plus suit jacket, vest, t-shirt	1.14
	(5) #2 plus long-sleeve sweater, t-shirt	1.01
	(6) #5 plus suit jacket, long underwear bottoms	1.30
Skirts/dresses	(7) Knee-length skirt, short-sleeve shirt (sandals)	0.54
	(8) Knee-length skirt, long-sleeve shirt, full slip	0.67
	(9) Knee-length skirt, long-sleeve shirt, half slip, long-sleeve sweater	1.10
	(10) Knee-length skirt, long-sleeve shirt, half slip, suit jacket	1.04
	(11) Ankle-length skirt, long-sleeve shirt, suit jacket	1.10
Shorts	(12) Walking shorts, short-sleeve shirt	0.36
Overalls/coveralls	(13) Long-sleeve coveralls, t-shirt	0.72
	(14) Overalls, long-sleeve shirt, t-shirt	0.89
	(15) Insulated coveralls, long-sleeve thermal underwear tops and bottoms	1.37
Athletic	(16) Sweat pants, long-sleeve sweatshirt	0.74
Sleepwear	(17) Long-sleeve pajama tops, long pajama trousers, short 3/4 length robe (slippers, no socks)	0.96

Figure 11. Some “I_{cl}” values according to typical clothing ensembles

working by the principles of Thermodynamics, which means we can consider the equation:

$$\Delta U = Q - L \quad (1)$$

The variation of the energy of a system equals the work done by the system plus the heat absorbed.

Following the same principle, the internal energy of a human body equals the metabolic power “M” minus the heat interchanged with the environment “Q” and mechanical power “W”.

To write this down:

$$\Delta U = M - Q - W \quad (2)$$

In particular, we can write (2) like this:

$$M - W - C - R - Ck - Ed - Esw - Cve - Eve = dU/dt \quad (3)$$

Where “M” or “metabolic power” is based on the amount of oxygen consumed per Kg per minute. The amount of consume of an average seated person is 3.5 ml/kg/m.

Metabolic rate is also expressed in Met, which stands for “Metabolic Equivalent of Task”. As the name suggests, “M” depends on the activity the body is involved in. A physical activity makes our body consume more oxygen and, thus, energy. 1 Met is a power expressed in W/m². The value of a 1 Met, corresponding to a seated inactive person, is 58.2 W/m².

In equation (3), “Q” is translated into various components, such as:

- “C”, which is the sensible thermal power interchanged with the ambient through convection.

- “R” is the sensible thermal power interchanged through radiation.

- “Ck” is the sensible thermal power interchanged through conduction.

- “Ed” is the latent thermal power interchanged through transpiration by our skin.

- “Esw” is the latent thermal power through sweat evaporation.

- “Cve” is the sensible amount of energy through respiration.

- “Eve” is the latent amount of energy through respiration.

“W”, which is the energy that each human body interchanges with the ambient, has a very low efficiency, usually between 0 and 0.2, which means that “W” can be ignored in the general calculations.

Here explained terms of (3):

$$C = hc \cdot fcl \cdot (Tcl - Ta) \quad (4)$$

Where “hc” is the thermal convection coefficient, “fcl” is the area clothing coefficient, “Ta” is air temperature and “Tcl” is temperature of clothing.

In particular:

a. $fcl = 1 + 1.2 \cdot Icl$ if $Icl < 0.5$

clo

b. $fcl = 1.05 + 0.1 \cdot Icl$ if $Icl \geq 0.5$

clo

“Icl” is one of the input factors to take into account in the

calculations of micro-climate data. It indicates the thermal resistance that each body can have,

according to the types or numbers of clothing layers occupant is wearing. Standards give some of its typical values that can be used in analysis and simulations (see figure 11).

The power related to radiation exchanges can be calculated as:

$$R = 3,96 \cdot 10^{-8} \cdot Fcl \cdot [(Tcl + 273)^4 - (MRT + 273)^4] \quad (5)$$

Where “MRT” stands for Mean Radiant Temperature.

“Mrt” is the temperature that is

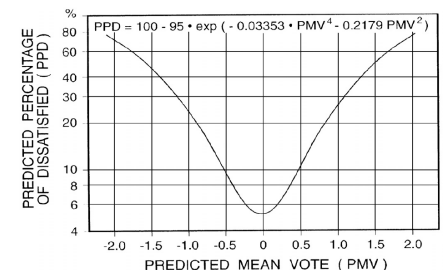


Figure 12. PMV/PPD chart

exchanged between the person in the ambient and all the surfaces around. In particular, it can be expressed as it follows:

$$MRT = \sum(F_{p,i} \cdot T_{s,i}) \quad (6)$$

Where “Fp” is the viewpoint factor based on the distance between each surface and the exact position of the body and “Ts” refers to the surface temperature of the ambient.

The sum of the product of each surface temperature by the factor point, gives mean radiant temperature, which is dependent of the body’s position in space.

This value is essential to calculate the kind of temperature that is actually felt by the occupants, that is the “Operative Temperature”. “top” can be expressed as an average between MRT and air temperature.

“Ck”, interchanged through conduction, depends on the surfaces and objects in direct contact with the body, such as the floor or a chair, if it is the case of a standing

person or a seated one. Usually, thermal exchange through convection is not considered.

$$Ed = 3.05 \cdot 10^4 \cdot (256 \cdot T_{sk} - 3373 - \phi_{pvs} \cdot T_a) \quad (7)$$

Where “Tsk” is the skin temperature and “φpvs,Ta” is the partial pressure of vapour air.

$$E_{sw} = 0.42 \cdot (M - 58.15) \quad (9)$$

Where “M” is metabolic power

$$C_{ve} = 0.0014 \cdot M \cdot (34 - T_a) \quad (10)$$

$$E_{ve} = 1.72 \cdot 10^{-5} \cdot M \cdot (5867 - \phi_{pvs} \cdot T_a) \quad (11)$$

Where “Ta” is air temperature.

Comfort condition occurs when the thermal balance of the body is equal to 0, which means that the variation of the inner energy of the body equals the members on the left of the equation (3).

Fanger model of comfort is expressed by two main values: PMV and PPD.

“Predicted Mean Vote” or “PMV” is a 7 scale - number from -3 to +3, whose values corresponds to the degree of comfort in a space.

In particular, negative numbers represent slightly cool, cool and cold sensation, with -3 being the coldest evaluation; positive numbers are associated to slightly warm, warm and hot instead. “0” stands for neutral position or ideal comfort.

According to the class of the building simulations may refer to, different classes of comfort are linked to specific in-between ranges of the PMV comfort scale (e.g. $-0.5 < PMV < +0.5$).

According to figure 12 , PMV is associated to PPD, which stands for “Percentage of People Dissatisfied”. PPD indicates discomfort % in the ambient. Usually, targeted PPD values are like 10% of people. The “highest” value is 5%. It is not possible to go lower because it is

impossible to have all people satisfied with the climate condition of the zone(s), given that comfort is in some part subjective dependant.

To sum up, by looking at Fanger research studies, thermal comfort depends on 6 main components:

- Metabolic rate
- Clothing level
- Air temperature
- Radiant temperature
- Air speed
- Humidity

The first two components can vary according to the human body, whereas the remaining four depends only on the ambient.

Finally, there are other things to consider, such as the Radiant Temperature Asymmetry, Vertical Air temperature difference and the surface temperature of the floor. These three aspects may cause discomfort and affect the overall

comfort criteria. Vertical radiant temperature asymmetry is the difference in temperature on a plane considering its opposite direction, whereas horizontal radiant asymmetry is in all direction. It is measured on average waist height at 0.6 m for a seated person and 1.1 m for a standing person.

Moreover, the difference between surface temperatures sometimes lead to convective drafts or loops, consequent to hotter indoor air that, mixing with cooler air near surfaces such as windows, becomes colder, determining additional circular movement of air inside a zone [11]. Whether this phenomenon could be acceptable or even useful in hot period of the year, through a more activated ventilation, it may result inconvenient during the winter season.

Vertical air temperature difference is measured between head level and ankle level and it shall not exceed 3° C for seated

occupants and 4° C for a standing person.

Finally, the difference in floor temperature should belong to the range from 19° C to 29° C.

Visual Comfort

Visible Light is the range of the electromagnetic field between 380 and 780 nm. According to these frequencies, the eye can perceive colours in relation to the moment of the day. Whether it is daytime or night time, our eye is more sensible to specific frequencies, according to photopic, mesopic and scotopic vision and the ability to distinguish colours diminishes when it gets darker.

Some principal photometry quantities related to light are:

- Luminous flux, which is the amount of energy distributed in all directions, is expressed in lumen (lm).
- Luminous intensity is the amount of light flux per solid unit angle, based on a specific direction. It is expressed in lm/sr or cd (candela).
- Luminance is the luminous intensity getting to or coming

from an area of space, thus being expressed as cd/m². This is what glare is based on.

- Illuminance is the amount of luminous flux per unit area, expressed in lx (lm/m²). This is the main SI photometry quantity used to assess minimum horizontal and vertical illumination values.

Just like thermal comfort, Visual comfort depends on various factors. Generally comfort is associated to the degree of natural light that can reach the indoor space. Indeed, Daylight factor, one of the assessment metrics in building simulations, is the ratio of indoor illuminance values “E_i” to “E₀”, which is the outdoor illuminance value relative to an unobstructed area. “E_i” is based on the sum of SC (solar direct sky component), ERC (reflected light from outside that reaches indoor) and IRC (reflected light that bounces

inside the ambient). Daylight factor, based on an overcast sky simulation, is one of the first methods to assess the degree of natural light in a space. Being it a ratio, it is expressed in %.

Daylighting simulations involve some of the following metrics:

- Daylight Autonomy (DA), that is the percentage of occupied time when the space or a point of space (e.g. sensor or target point) reaches the minimum target illuminance value by solely natural lighting. It is a way to express how much time during the occupied year the space of a building is autonomous from electrical lighting, in order to reach specified target illuminance values. In our case target is set on 500 lx (even though for some office spaces a value of 300 lx can be accepted).

- A similar metric, sDA_{300,50%},

indicates the percentage of occupied area (minimum of 55%), which, at least for 50% of occupied time, reaches the minimum target illuminance of 300 lx through solely natural lighting.

- Useful Daylight Illuminance (UDI), indicates the percentage of occupied time when a point is under, in-between or over a specific illuminance range. In this case study, lower and higher bounds are set to 100 and 3000 lx, which is named after UDI_{achieved}. A value in the range suggest an average good lighting, whereas a number lower than 100 lx indicates insufficient lighting. Values above 3000 lx points those cases when a high degree of glare can occur.

- Annual Solar Exposure (ASE), is a daylight metric that indicates how much area of the building receives 1000 lx or more, for at least 250h of occupied time. Alongside UDI>3000 lx, it is a metric that suggests potential glare. According to “The Well

Building Standard” (May 2016 edition), section 62 on Daylight Modelling, ASE1000,250 is achieved for no more than 10% of regularly occupied space. No more than 10% of the area can receive more than 1000 lx for 250 h per year or more.

Visual comfort is strictly related to possible high luminance values in the occupants’ field of view, caused by low Sun positions visible through the windows, but also artificial lighting installed in the ambient. Luminance values should be controlled as its variations all over the workspaces (e.g. in case of an office building) may determine discomfort. To assess this problem, metrics such as DGP or daylight glare probability are used.

Glare is a complex phenomenon in building design because it is strictly dependant on the position of the viewer, which is sometimes not easily assessable

in an early design stage. Moreover, glare calculations require high computational time, often limiting the results to only one or few points in the room [12].

DGP is introduced by Wienold and Christoffersen and its complex equation is:

$$DGP = c_1 \cdot E_v + c_2 \cdot \log \left(\sum \frac{L_{si}^2 \cdot \omega_{si}}{E_v^a \cdot P_i^2} \right) + c_3 \quad (12)$$

Where the first part deals with the vertical illuminance measured at eye level, due to direct solar radiation contribute, and the second term refers to the contrast between the background luminance and specific luminance of glare sources.

“c1”, “c2” and “c3” are constants (respectively equal to “5,87*10⁻⁵”, “9,18*10⁻²” and “0,16”.

“α”=0,16. E_v is the vertical illumination in lx, “ω” is the light source solid angle and “p” is the position index.

There are four main classes indicating DGP ranges, they are:

- $DGP < 0.35$, imperceptible glare
- $0.35 \leq DGP < 0.4$, perceptible glare
- $0.4 \leq DGP < 0.45$, perceptible glare
- $DGP \geq 0.45$, intolerable glare

According to Wienold and Christoffsen, as one can see from the formula above, there is a correlation between Vertical illuminance values and the glare potential. For this reason, given the high calculation times regarding the simulations, a simplified model to compute DGPs has been proposed.

A paper by Wienold [13] introduces the simplified method. In particular, whether the complete equation (12) accounts for glare derived by both overall vertical illuminance and contrasts between the former with lumi-

nance values present in the subject field of view, the simplified method or DGPs, is solely related to E_v . Moreover, the same author suggests its application when no direct sun or light reflection is present in the scene, which shall account for a determining value in the second term of the equation above. Indeed, whether the direct light is present or not, correlation between E_v s and DGP values changes dramatically, from $r^2=0.983$ to $r^2=0.506$

Simplified DGPs equation can be written as follows:

$$DGPs = (6.22 \cdot 10^{-5} \cdot E_v) + 0.184 \quad (13)$$

According to (13), the following ranges are set to determine visual comfort percentages for each point:

- Imperceptible to perceptible => $E_v = 2669 \text{ lx}$
- Perceptible to disturbing => $E_v = 3473 \text{ lx}$
- Disturbing to intolerable =>

$$E_v = 4277 \text{ lx}$$

According to CEN, there are three main levels for recommendation for glare protection, from minimum to high. In particular:

- minimum protection for $DGP_{e<5\%} = 0.45$
- medium protection for $DGP_{e<5\%} = 0.4$
- high protection for $DGP_{e<5\%} = 0.35$

where $DGP_{e<5\%}$ is the DGP value that does not exceed more than 5% occupational time. $DGP_{e < 5\%}$ is thus calculated as follows:

$$f_{DGP_{e,exceed}} = \frac{\text{glare exc. time}}{\text{occ. time}} = \frac{t_{\text{glare}}}{t_{\text{ref}}} \quad (14)$$

Visual comfort is related to other elements such as an adequate electric lighting system with appropriate colour temperature. Lamp temperatures

are expressed in K and usual values are 2000,3000 and 5000 K. The higher the temperature the colder the light, thus simulating the real temperature of the sun, which during daytime can be 6500 K. Colour temperature is important with the task held in the ambient. E.g. surgery rooms should present white colour lamps with really high lux levels (500 to 1000) in order to perform the task safely and correctly. Warmer color are usually associated with calm and relax. For example, when the sun sets, its color temperature changes from daylight cool white sun with 6000 K to warmer sun with 3200 K or lower. Finally, CRI, which stands for “Color Rendering Index” is a scale metric from 0 to 100 which indicates the fidelity of colours reachable through the light emitted by the lamp, compared to an ideal one. Minimum values should be 80, with 100 achieving best quality.

Another considerable factor in visual comfort is the view out from a window system. Basically, it refers to the quality the view has through a fenestration system. Daylight openings with a view out provide connection with surroundings. The view out should comprise of layers of sky, city or landscape, and ground. A natural view is preferred over a view towards man-made environment, and a wide and distant view is appreciated more than a narrow and near view [8]. A view is perceived good if there is a sufficient horizontal opening, a certain distance to the outside and a good number of “layers” included, such as ground, landscape etc... There are three categories of view – out, minimum, medium to high.

Indoor Air Quality

CEN final draft prEN 15251 gives some indications about air quality in the ambient. When an occupant breathes, to put it simply, he breathes in some of the oxygen present in the ambient and breathe out some CO₂ as a product. Levels of concentration of CO₂ cannot be high. Necessary ventilation and minimum amount of oxygen is required.

Air quality within an ambient can be expressed either in terms of CO₂ PPM levels or ACH, which stands for Air Change per Hour.

ACH is equal to the sum of the ventilation per person and ventilation per area contributes, then divided by the volume of the zone. Given that the amount of ventilation is expressed in m/s, it is necessary to convert this value in terms of hours, by multiplying it by 3600. To put it in formula:

$$\text{ACH} = (\text{Q}_s * 3600) / \text{V} \quad (15)$$

Where “Q_s” is the total amount of ventilation rate by person and area and “V” is the volume of the zone.

Ventilation rate per person is expressed as:

- Q_p = ventilation rate per person times the max number of people in the zone

- Q_b (the ventilation rate for emissions from building) = ventilation rate per area * max area of the zone

These two rates must be summed to obtain the total ventilation rate for the ambient (l/s or m/s). CEN lists IV category based on the ventilation rate per person and per area or the maximum total ventilation rate.

For an average low polluting office building, relative to II category, CEN suggests 7 l/s/p and 0.7 l/s/m² for ventilation rate per person and ventilation rate for building emissions respectively.

Indoor air quality also depends

on the presence of some potentially harmful substances such as formaldehyde, a gas produced in resins and wall paints. Another harmful substance is “VOC”, volatile organic compounds which can evaporate easily at air temperature. These substances are responsible for irritations and can cause health problems to liver and the nervous system. VOC can be present in paints and other products such as detergents, pesticides and cosmetics.

Objective and aims

This dissertation consists in the performance assessment of an under-construction research-based laboratory in Turin, according to thermal and daylight parameters across four main different scenarios. In particular, this work aims at tunnelling down an overall comfort/discomfort evaluation by developing a multicriteria approach in which thermal, daylight and glare aspects are analysed altogether. On the one hand, this is done to better understand the design envelope behaviour in each case study. On the other, this can narrow down the issues and define possible, efficient future strategies to achieve comfort, in line with the best trade-off among sometimes contrasting parameters.

Research methods

Building Performance Simulation

This Thesis focuses on Building Performance Simulation (BPS) on an experimental facility for Indoor Environmental Quality testing.

BPS is a computer-based model capable of quantifying and qualifying aspects of building performance useful to design.

In this work Overall Thermal and Daylight indexes are measured. In addition, three performance parameters are used as comfort reference, based on:

- a. Thermal Comfort
- b. UDI_{achieved}
- c. DGP

a) is achieved with 90% of space according to II category building comfort parameter.

b) is achieved with at least 80% of space for 80% of occupied time.

c) is achieved with 95% of points

where glare does not overtake 5% of occupancy time.

Workflow & test Cases

Before running main simulations, first step in this work concerns a brief climate analysis, based on radiation and shadow study on main laboratory façades.

In addition, clear sky days are chosen in line with sky coverage data retrieved from Typical Meteorological Year data (TMY). Next part covers simulation results according to four main different case studies.

Case scenario are:

- B. baseline scenario:
 - b1. free-running
 - b2. conditioned
- C. new glass scenario
- D. dynamic shading
- E. fixed shading

These are all based on two main domains, thermal and visual comfort. Thermal Comfort displays annual plotting of

over-heating, comfort and under-heated % of time plus thermal maps, which give a spatial representation of data, according to each of the analysed points.

Visual comfort displays Climate-Based Daylight Modelling (CBDM) results, such as Daylight Autonomy, Spatial Daylight Autonomy and Useful Daylight Illuminance. Moreover, annual plots and spatial representation of glare is also represented.

At the end of each simulation, thermal and visual comfort aspects are combined and supported by info-graphics (figure 6 shows a scheme of the Thesis Workflow).

Eventually, comparisons of four case studies results and main findings are shown.

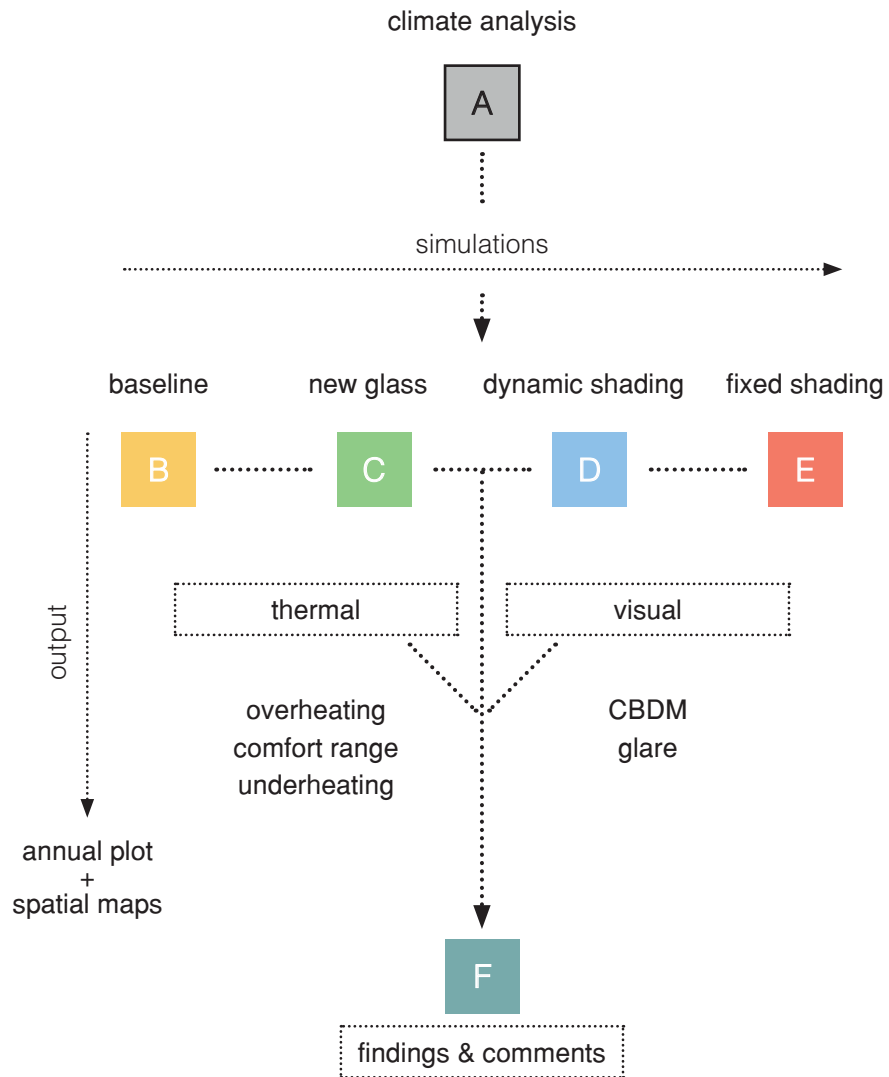


Figure 6. Main Thesis Workflow

Software

For Energy modelling analysis Honeybee Ladybug plug-ins for Rhino Grasshopper have been used.

Ladybug first version is released on 2013, being a collection of 28 components for weather data visualization, solar radiation studies, and sunlight hours analysis. A year later, honeybee is released, connecting grasshopper to some validated energy and daylighting simulation engines such as Radiance, Daysim, EnergyPlus and Openstudio. Mostapha S. Roudsari and Chris Mackey are the main founders, now co-working with thousands of experts, researchers, and professionals.

Honeybee and Ladybug components scripts involves some state of the art application in thermal and visual comfort studies. For instance, Honeybee Microclimate Maps component makes it possible to calculate

main temperature info including “Solar Cal” method (Arens, Hoyt & Zhou) and the effect of direct solar radiation falling on occupants.

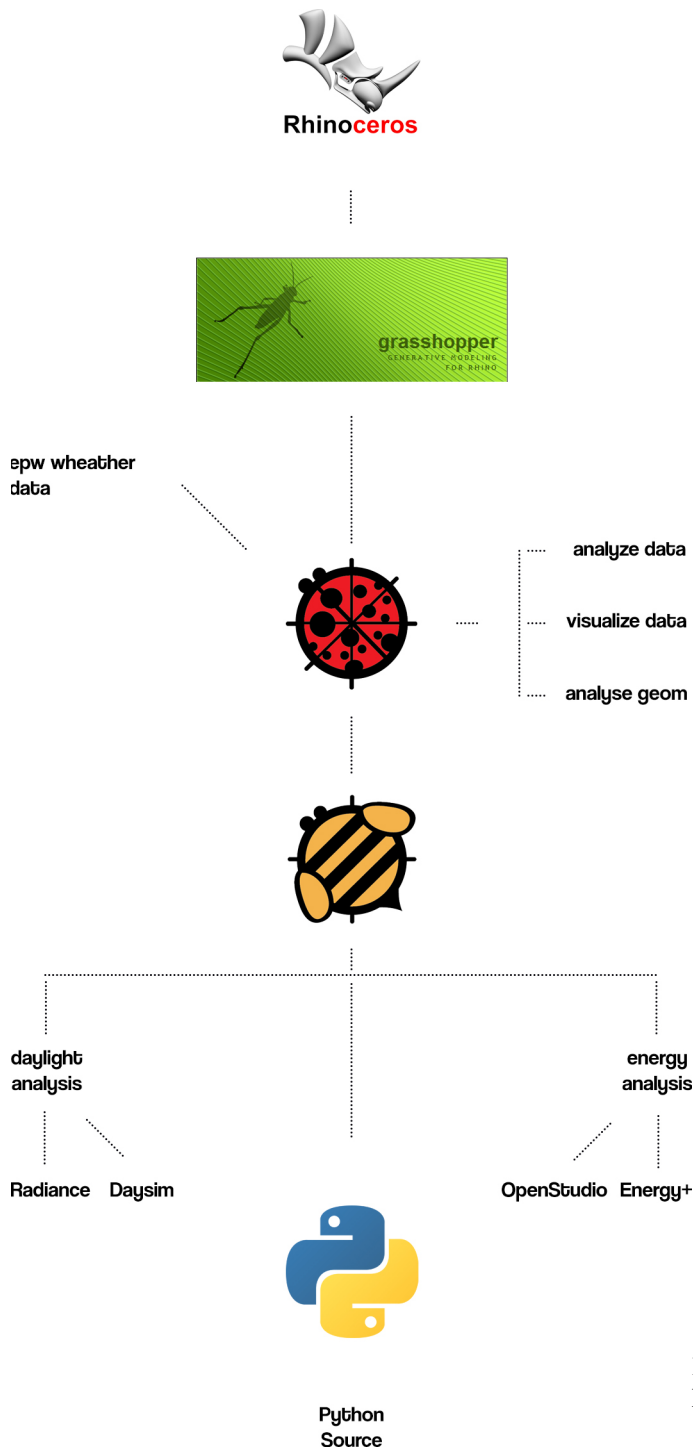


Figure 7. Workflow relative to Honeybee/Ladybug Grasshopper plug-ins

The HIEQ LAB

State of the Art

The facility is in line with previous labs such as FlexLab (USA), MoWitt (USA), MATElab (Cambridgen ENG), SENSElab (Delft, NED) [14], with more or less the following traits:

- Flexibility and structural modularity, with the ability to change elements of the façade systems (e.g. windows and shading systems) efficiently and in the cheapest way possible.
- Mechanical installations such as HVAC (Heating Ventilation Air Cooling) systems to control and better test different indoor climatic conditions in relation to microclimate factors.
- Sensor placement to compare digital analysis to on-field ones and have a better report.

In particular, HIEQ LAB is characterised by an average U

value of 1 W/m²K with specific indications for:

- Floor 0.3 W/m²K
- Opaque elements 0.25 W/m²K
- Transparent elements (Windows) 1.4 W/m²K
- Doors 1 W/m²K
- Upper horizontal partition (ceiling) 0.3 W/m²K

Air resistance should be fixed on 0.3 Vol/h and 0.5 Vol/h for interior walls. HVAC application can also be flexible as it is being designed both as air and water-based system, with radiant panels/beams or air emission plenum above workstations respectively. In particular, a first configuration follows the use of radiant floor panels, one for each zone, and plenum above workstations. Electrical and Lighting system can be more flexible: there is no specific choice on the type and way of installation, as one is free to make adjustments and modifications. For the time being,

simple lighting ducts can be fixed under the false ceiling. Lab plan covers a 7 x 13 m area and is 4.5 m high. A possible, curved shading element can be fixed on top of the roof, bringing the overall dimensions to 8.3 x 13.6 m. Lab is on a foundation 0.4 m high above the ground, serving as location for additional ducts and cables to pass through the structure.

There are three main rooms or “zones”, a room for main technical installations, a second “control” room and the last one, which is mainly used for testing.

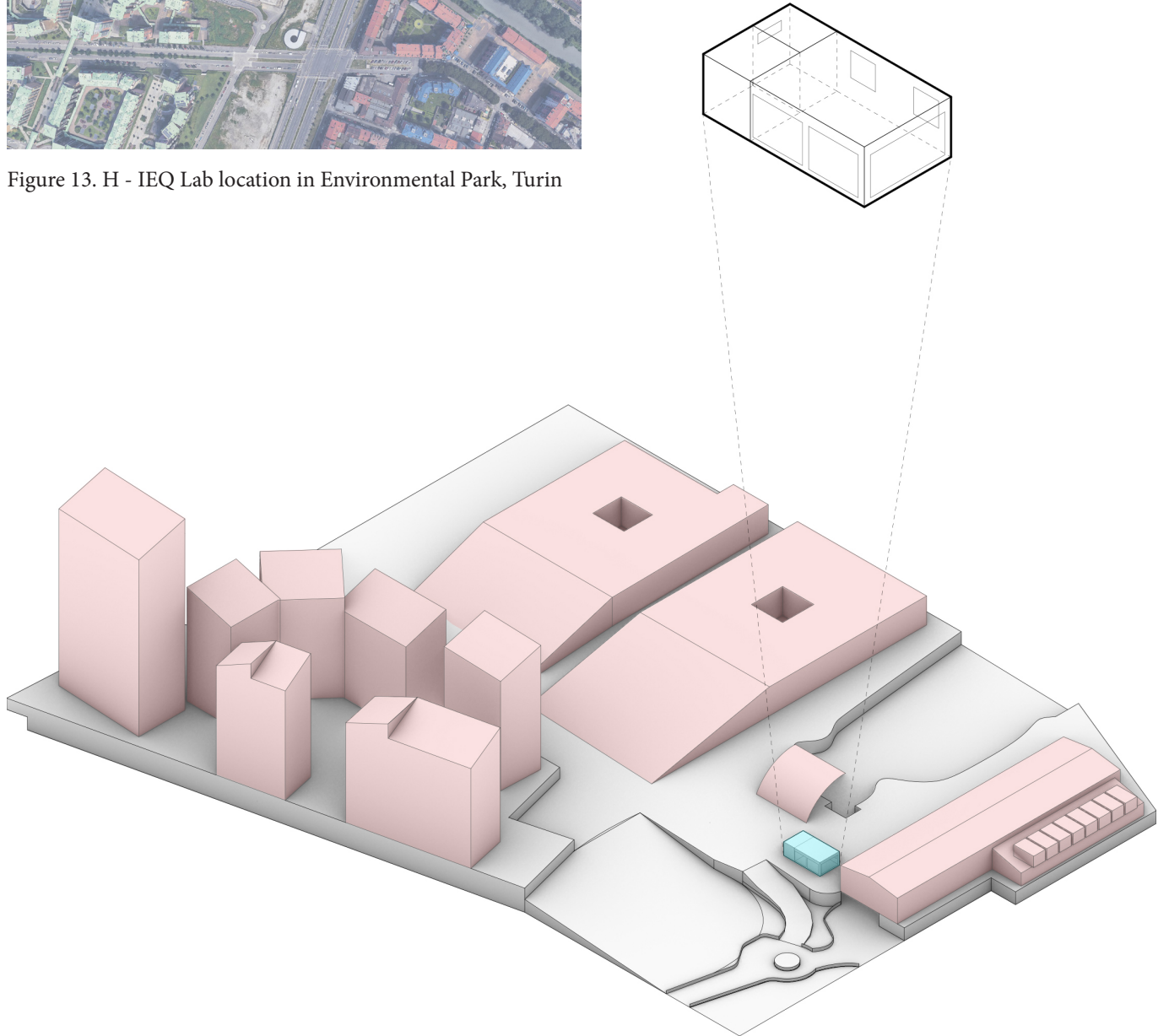
The facility is being built in Via Livorno n.60, in the Environmental Park area in Turin. Specific Coordinates are 45.0870, 7.6740.

Structure is made by a 0.3 m cement foundation layer and GLULAM (glued laminated timber) portals shaped by a 16 x 30 cm rectangular frame. Upright fir wood framing, 3 x 16 cm each, make vertical walls whereas

24 cm thick Crosslam panels are used for the roof.



Figure 13. H - IEQ Lab location in Environmental Park, Turin



- ceiling:
 - plasterboard
 - radiant panel with XPS
 - double warping for countertop
 - Crosslam panel
 - vapor barrier
 - wood fiber
 - OSB panels
 - waterproof layer
 - gravel

- exterior wall:
 - plaster
 - gypsumfiber panel
 - OSB panel
 - fir wood structural element
 - woodfiber
 - woodfiber DWD protect panel
 - OSB boards
 - compressed cork board
 - metal sheet

- interior wall:
 - plaster
 - gypsumfiber board
 - fir wood structural elements
 - gypsumfiber board
 - plaster

- floor:
 - floating floor
 - vapor barrier
 - OSB board
 - woodfiber
 - concrete bed
 - polystyrene XFOAM
 - lean concrete

- south window:
 - ipasol 7037 doubleglass
 - $U_g = 1.4 \text{ W/m}^2\text{K}$
 - $T_v = 0.7$
 - $g = 0.37$
- east window:
 - ipasol 7037 doubleskin facade
 - $U_g = 1 \text{ W/m}^2\text{K}$
 - $T_v = 0.7$
 - $g = 0.35$
- north window:
 - ipasol 7037 doubleglass
 - $U_g = 1.4 \text{ W/m}^2\text{K}$
 - $T_v = 0.7$
 - $g = 0.37$



Figure 14. Exploded Axonometry and building construction info

A - climate analysis

Outdoor Dry Bulb Temperature, Humidity and Radiation

Ladybug collects EnergyPlus weather data for simulations. These data are associated to a TMY (typical meteorological year), in particular to weather station data from Turin Caselle Airport.

Results show annual plot of dry-bulb temperature and outdoor relative humidity values. Climate alternate cold winter to hot summer, with temperatures around 0°C to 30°C and more in the hottest summer days. This is highlighted in figure a1 on the right, indicating monthly values of heating and cooling degree days.

Humidity is overall high in the morning and late evening, night-time. Scale varies from 30 to 100% humidity, where green values represent good to acceptable humidity, as we can see happening in the afternoon from January to August. These period of time could be

useful for some natural ventilation, also according to outdoor temperatures and indoor comfort.

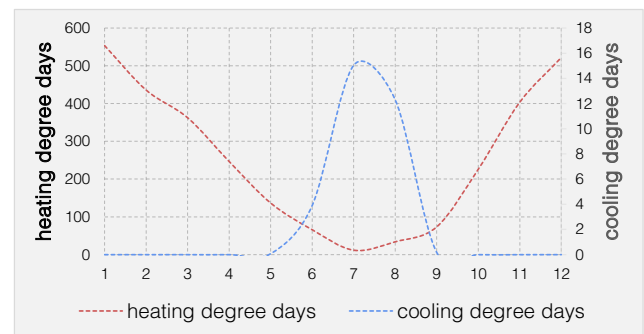


Figure a1 - Heating and Cooling Degree Days- monthly values

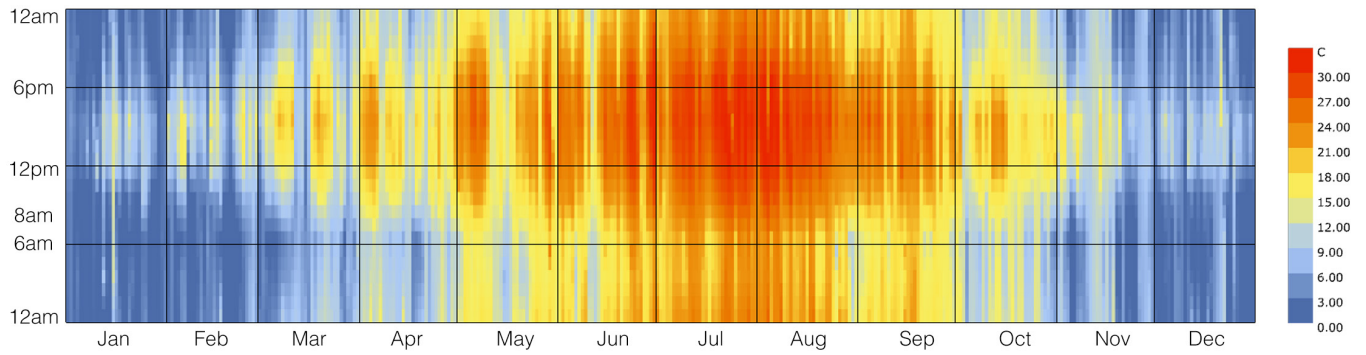


Figure a2 Outdoor dry bulb temperature

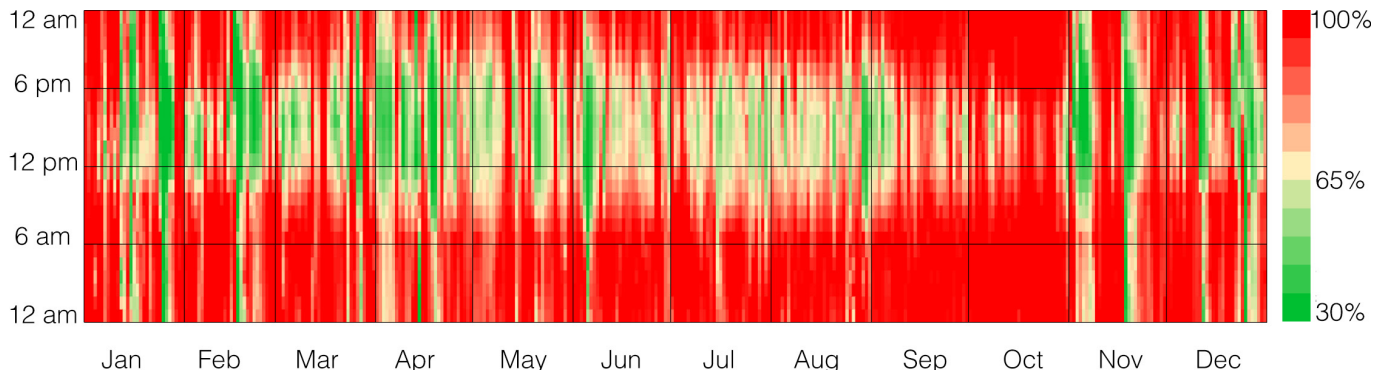


Figure a3 Outdoor Relative Humidity %

Before running main simulations, a radiation study is necessary to evaluate the amount of radiation falling on the main surfaces of the zones.

Then, both for delta MRT on horizontal grid and vertical illuminances on east and south grids at the height of 120 cm (seated person), three months are chosen for these analyses, such as December, June and September.

In order to highlight the worst-case scenarios, “clear sky” days in the second half of the each month are picked, according to the highest Global, Direct radiation levels and the least sky coverage, the latter based on a scale from 0 to 10, with 0 corresponding to the minimum and 10 the maximum sky coverage.

For the matter, an annual plot of climate-based Sky coverage results can be seen in figure a9 (see page 52).

To sum up, instead of simply choosing those days when equinoxes and solstices occurs, clear sky days are preferred

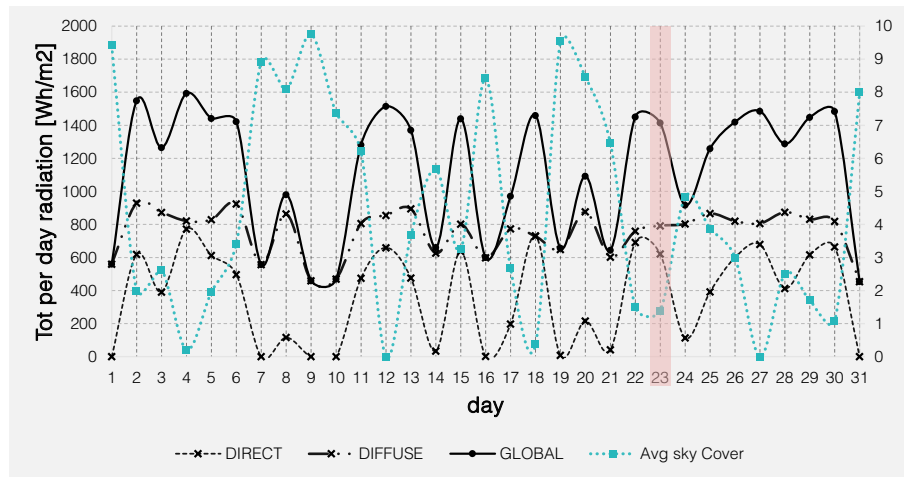


Figure a4. Radiation study and chosen “clear sky” day in June

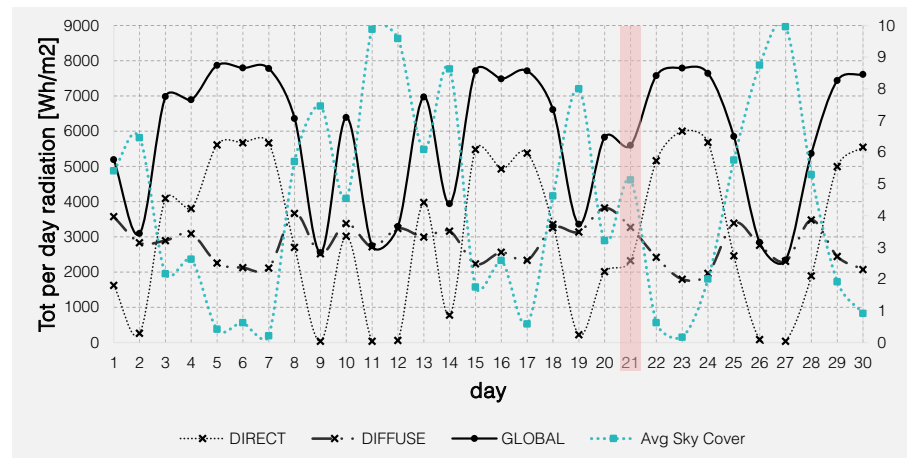


Figure a5. Radiation study and chosen “clear sky” day in September

instead, to highlight the worst situation possible according to direct radiation from the Sun, hence possible higher values in delta MRT and EVs.

In particular, as it is visible from figures a4, a5 and a6, , June 23rd, Sept 21st and December 18th are chosen. These charts refer to daily plot of global, direct, diffuse total solar radiation (sum of each hour of the day) for each day of the month. The reader can see the relationship between these values and the sky coverage plotted on a scale from 0 to 10.

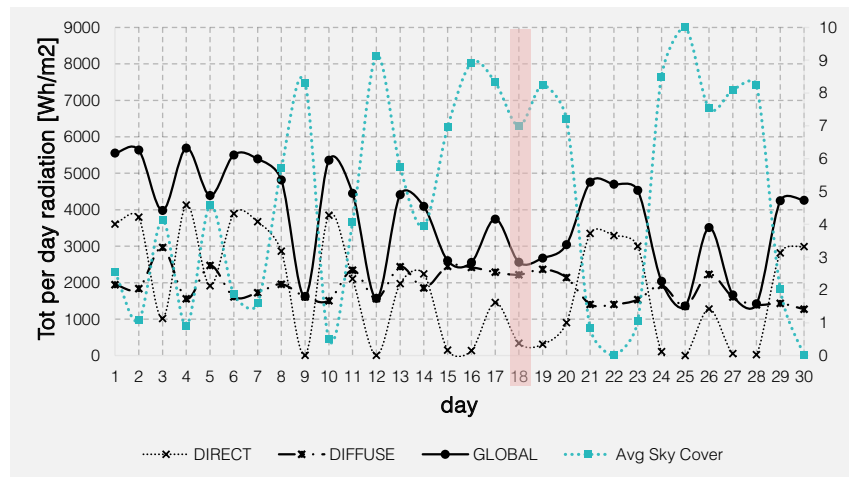


Figure a6. Radiation study and chosen “clear sky” day in December

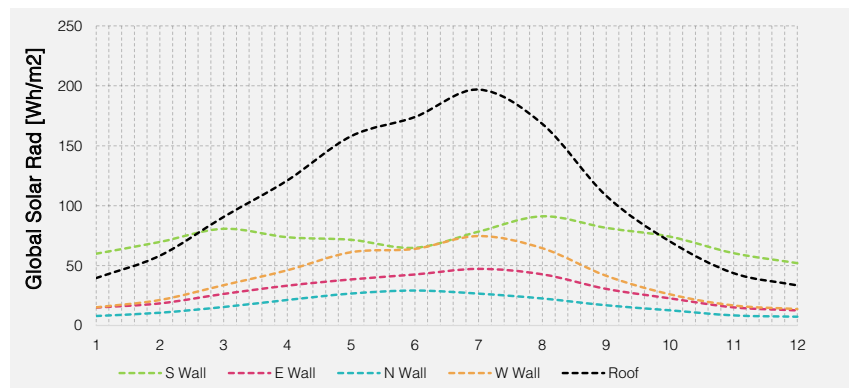


Figure a7. Monthly average of Global solar Radiation falling on main Lab facades

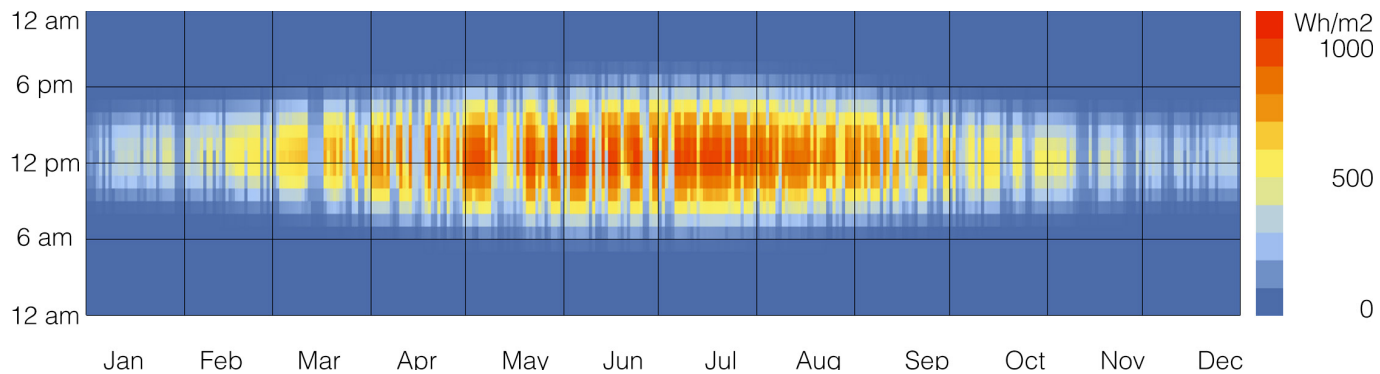


Figure a8 Annual plot of Global Solar Radiation

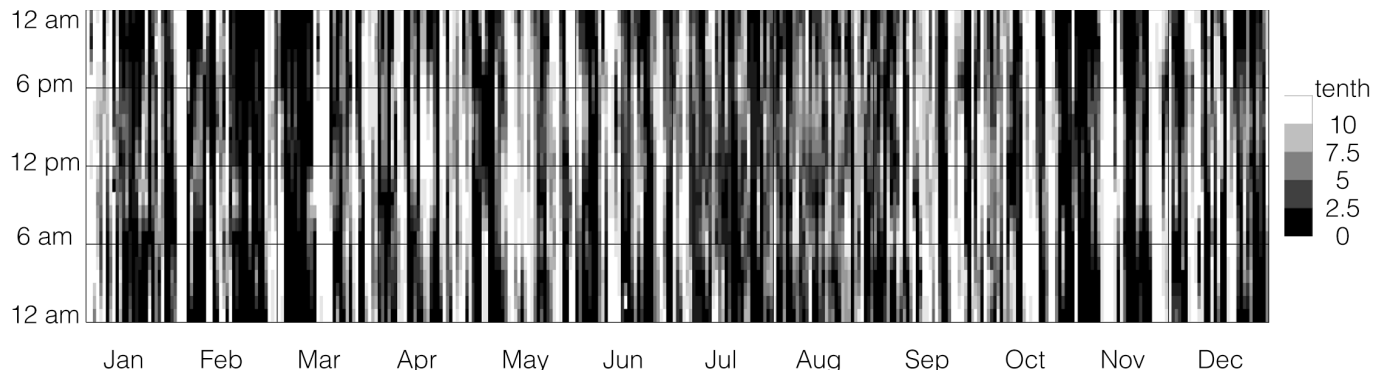


Figure a9 Annual plot of Sky Coverage

As we can see from Annual Sky cover, March to June presents higher quantity of cloudy skies alongside with September, November and first days of January, whereas June, August, February and March reveal higher quantity of “clear sky” days. This is reflected on the Annual Global Radiation plot, where parts of the month with high sky cover presents minor values of Radiation (see figure a.8).

Images on the right show shadow study with a black and white scale indicating number of hours in shadow.

In the following page, in the same days, charts related to Radiation values falling on East and South facade are displayed.

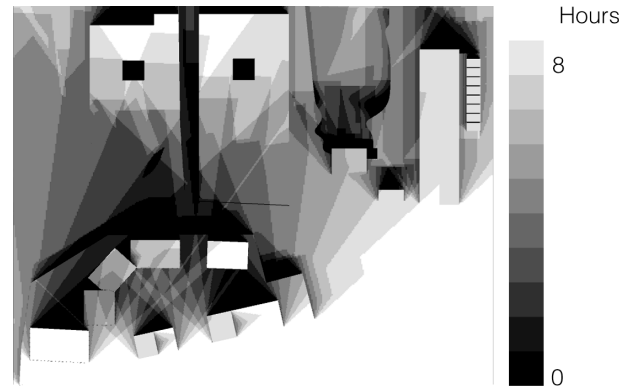


Figure a10 Shadow study - December 18th

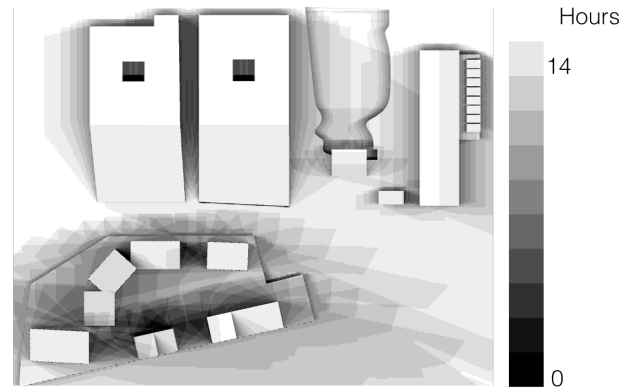


Figure a11 Shadow study - June 23rd

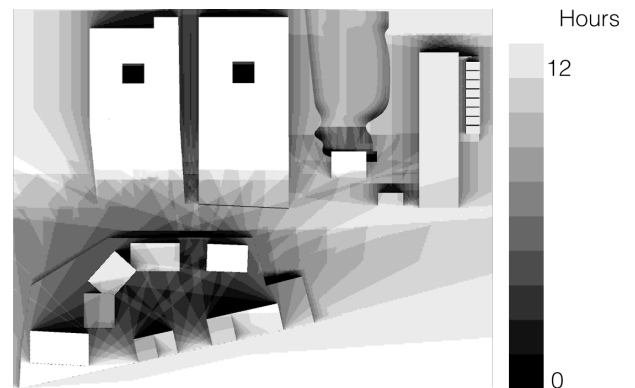


Figure a12 Shadow study - September 21st

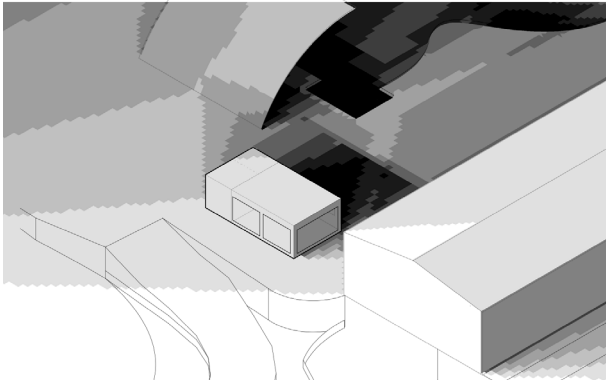


Figure a13 Shadow test on south and east facade on December 18th

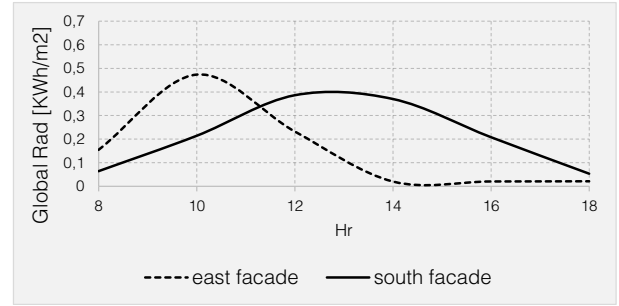


Figure a16 Global solar radiation on south and east facade on December 18th

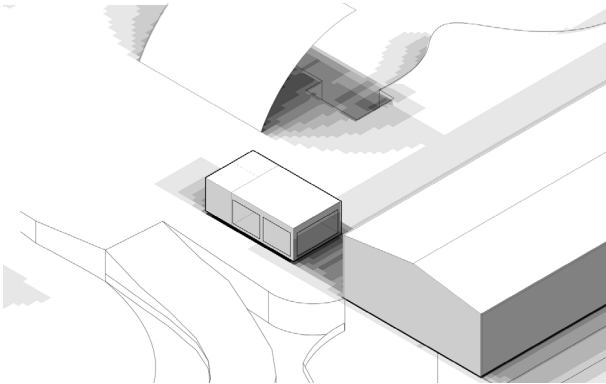


Figure a14 Shadow test on south and east facade on June 23rd

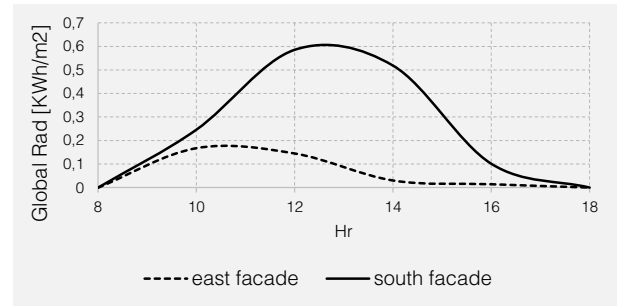


Figure a17 Global solar radiation on south and east facade on June 23rd

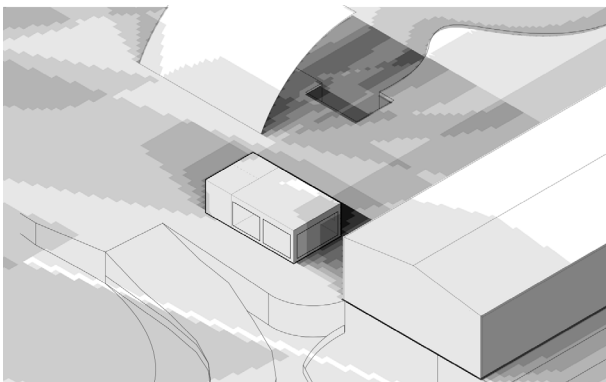


Figure a15 Shadow test on south and east facade on September 21st

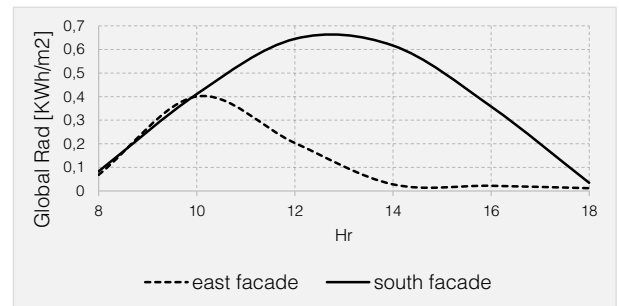


Figure a18 Global solar radiation on south and east facade on September 21st

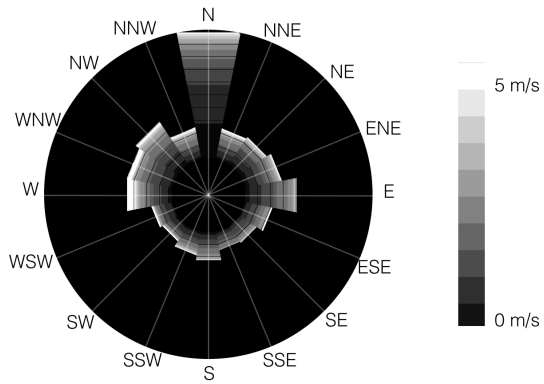


Figure a19 Wind Rose

Figure a19 represents wind Rose diagram with wind speed from 0 to 5 m/s. Notice that wind often blows from north, where cooler air could be exploited for natural ventilation strategies.

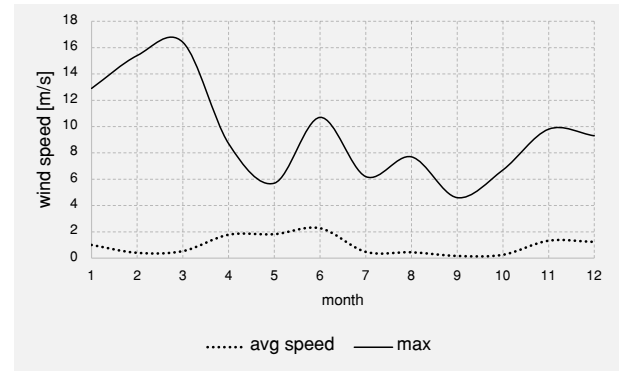


Figure a20 Average Wind speed with max monthly values

Simulations

The following simulations are based on data measured on 221 grid points at different heights above the floor according to the specific analysis. In particular:

- 1 grid for the thermal analysis at 0.8 m above floor level
- 2 grids for the daylight analysis, at 0.8 m and 1.2 m above the floor respectively. 1.2 m grid is both south and east oriented
- specific points (e.g. point 54 and 32) for annual glare simulations and overall thermal + daylight ambient evaluations

Moreover, analysis are characterized by sometimes common sometimes different inputs such as loads and schedules. Loads refer to quantity of infiltration air, temperature setpoints and general condition under which ideal air and temperature control system work. A type of schedule,

occupancy, which is related to the time the ambient is occupied by people, is expressed in ratio, from 0 to 1, with 1 meaning full occupancy. The facility is considered occupied from 8 in the morning till 18 in the evening from Monday to Friday. On Saturday, occupancy is limited to 8am to 12pm.

Schedules for lighting cannot be the same as for occupancy. A Daysim analysis based on an annual daylight simulation is used to generate annual profiles as an input for the schedule. For this matter, all 221 points work as sensors to detect whether the area of the ambient would get too dark and, if such the case, turn the lights on to reach a target illuminance value of 500 lux. Control strategy assigned is “automate switch-off with occupancy” with a power density of 7 W/m². Stand by power of 3 W and a switch off delay time of 2 minutes is assumed.

As for loads, temperature setpoints on thermostat are 20°C for heating and 26° C for cooling. Heating setback is 13°C and Cooling setback is 40°C. Air conditioning will turn on whenever these temperature are overreached during and beyond occupancy time.

In case of conditioned scenario, ventilation rate per person is set to 0,007 m³/s while ventilation per area is set to 0,0007 m³/s.

According to these loads and a peak number of people in the room equal to 8, ACH (air change per hour) can be calculated as around 2,1 (which means roughly 1 opening each half an hour).

Infiltration air per façade is constant in each simulation, with a value of 0.00015 m³/sm².

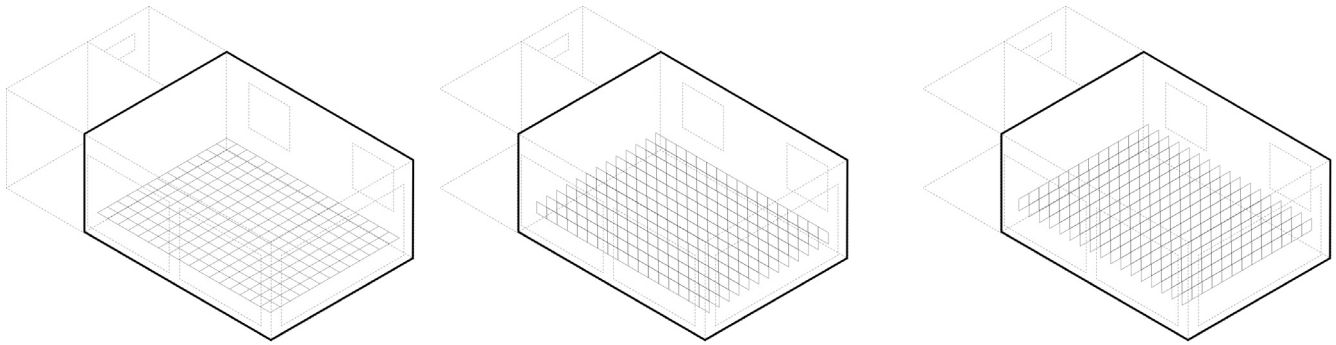


Figure a21. Grid sensor points used for simulations. From left to right: horizontal, south oriented and east oriented grid

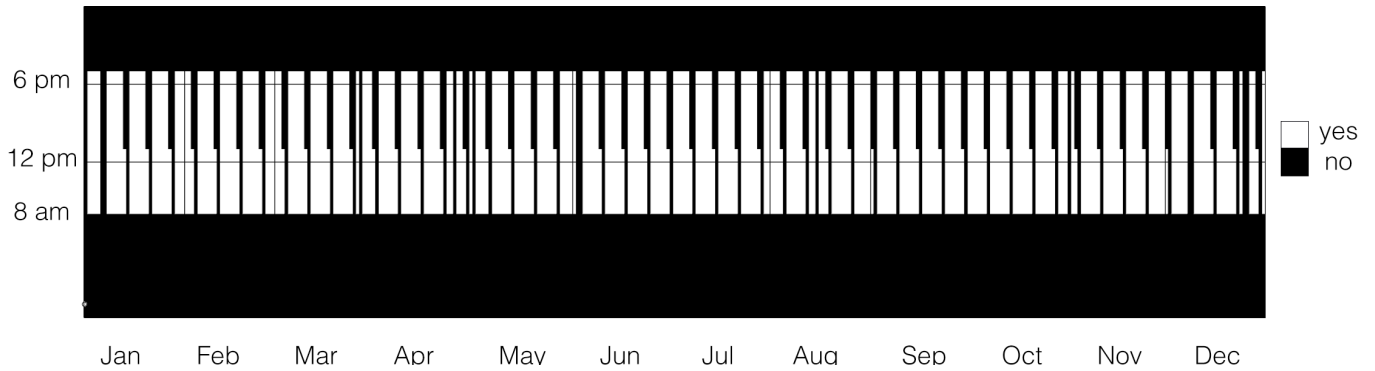


Figure a22. Occupancy profile. White area indicates occupied space

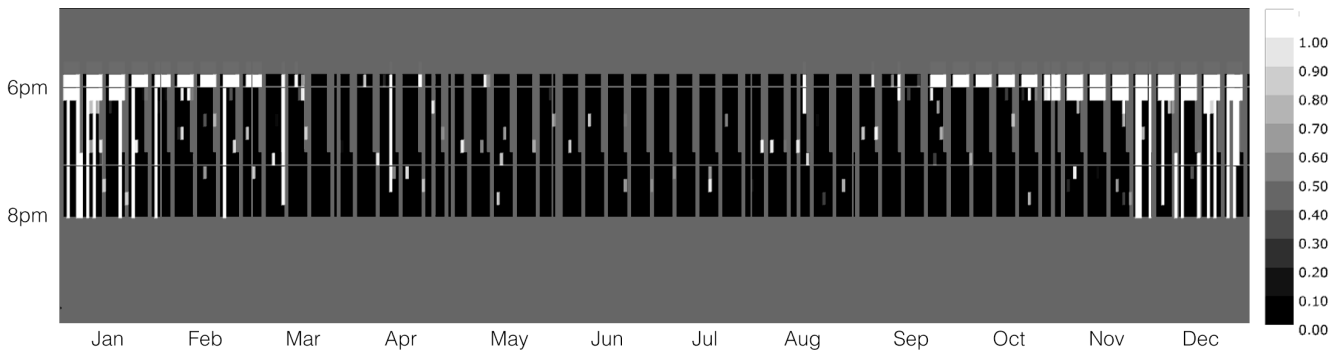


Figure a23. Example of Daysim annual lighting Profile (lighting schedule). 1 indicates lights working at highest regime (fully on).

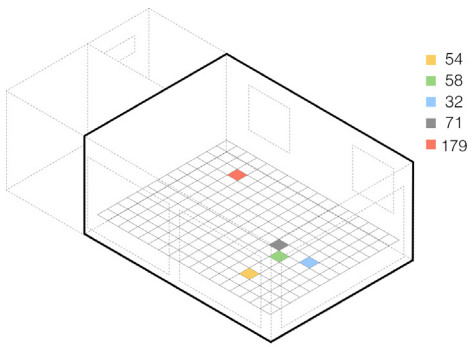


Figure a22. Grid sensor points chosen for glare and luminous autonomy insides

B - Baseline

Adaptive Model

First simulation is run with no HVAC system on. This means there are no thermostat setpoints and setbacks and no mechanical ventilation system with humidity control. Just constant infiltration air through the façade with a value equal to $0.00015 \text{ m}^3/\text{sm}^2$ is taken into account.

Within this first simulation, one analysis will consider no ventilation, while a second one, will apply ventilation based on operable windows. In particular, no schedule is applied, in order to see the maximum flexibility natural ventilation can reach. This means that window can be opened even outside the occupancy time, when people are actually inside the facility.

The following parameters are used to account for natural ven-

tilation by windows:

- a. Minimum and maximum indoor for natural ventilation equal to 21°C and 25°C respectively
- b. Minimum and maximum outdoor for natural ventilation equal to 18°C and 30°C respectively
- c. Fraction of glazing area operable equal to 30%
- d. Fraction of glazing height operable of 0.5 m

Wind driven cross ventilation is considered given the presence of opposite windows in the laboratory (north and south windows).

Images on next page show annual plot of indoor operative temperatures measured in zone 3, derived from analysis without HVAC and thermostat control in the zones. As the very term “adaptive” would suggest, the model used for this simulation wants to see the relationship between the designed envelope of the laboratory and how it responds “naturally” to the outdoor climate. It is basically a way to better understand the efficacy of the building mass and construction.

By looking at occupied time, figure b1.1 show cold condition in January, February, November and December, in particular in the morning and late evening. From mid February to October high over-heating occurs, even when not considering sun radiation influence.

Second image shows the same results for an almost identical analysis, except for natural

ventilation as input. Annual plot in figure b1.3 shows the energy loss or “heat loss” related to window ventilation. As we can see, red area from figure b1.1 is shortened at least by half, disappearing in June, part of July, September and October, solving some excessive overheating, yet with August still being too hot. Likely, during this month windows are closed for excessive outdoor temperatures and lack of cooler air. The reader can see a deep relationship between figure b1.2 and b1.3, with heat loss corresponding to red area resizing.

Moreover, other two results are shown here. Figure b1.4 plots indoor relative humidity, whose values result good to acceptable in the morning and some afternoons such as in April and June. Figure b1.5 results are related to ventilation autonomy which is based on minimum Air Change per Hour, comparable to the

actual indoor climate pollution and concentration of CO₂. As mentioned before, minimum Air Change per Hours is derived from the sum of Total ventilation per Area and Total ventilation per Person, a value expressed in m³/s and converted in ACH. Supposing a maximum number of people of 8, calculations suggests a minimum ACH for the zone equal to 2.1 which stands for at least 1 air change or window opening for each half an hour, in case of maximum occupancy.

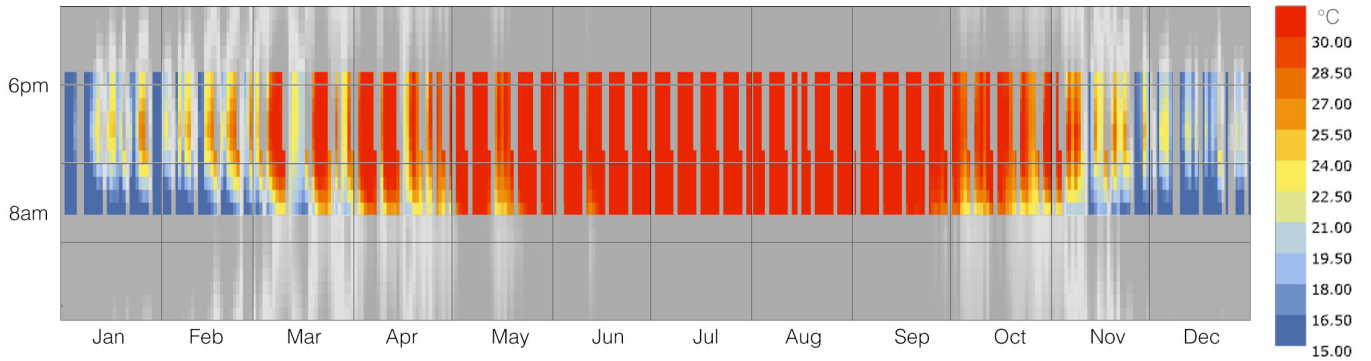


Figure b1.1 Indoor standard Operative Temperature - free running scenario

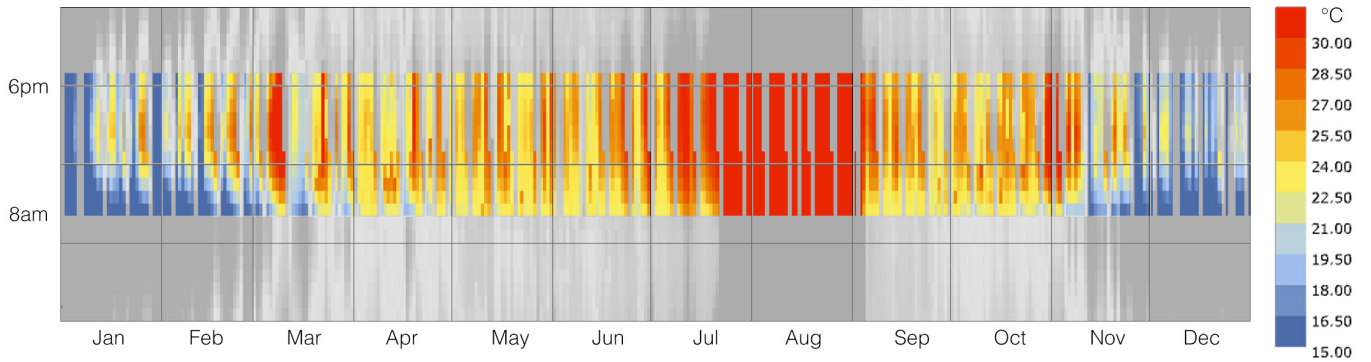


Figure b1.2 Indoor standard Operative Temperature - free running scenario

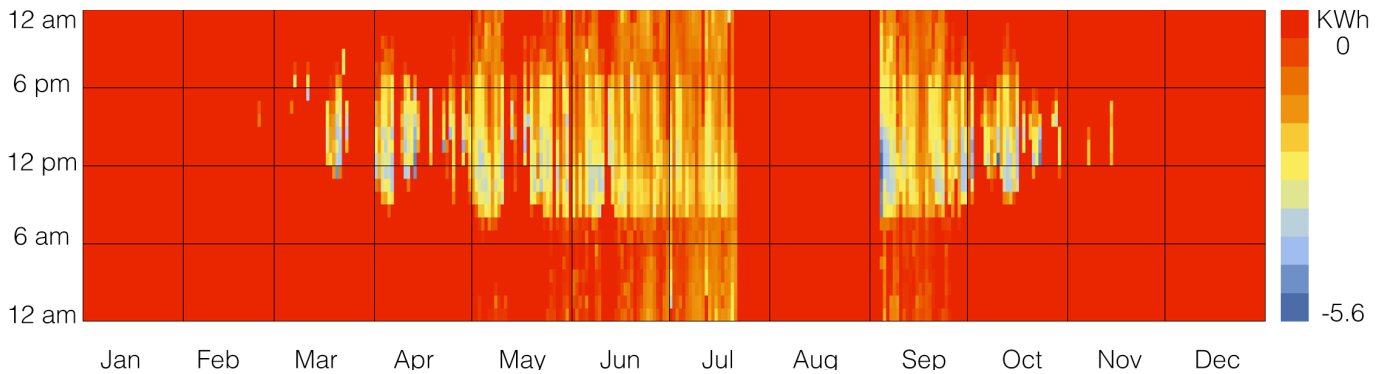


Figure b1.3 Natural ventilation Energy loss - annual plot

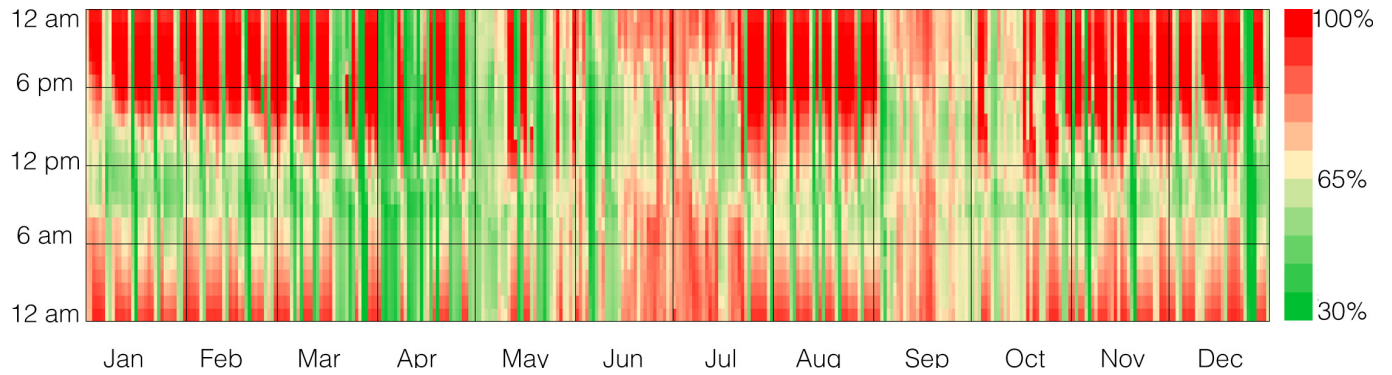


Figure b1.4 Indoor Relative Humidity - zone 3 - free running

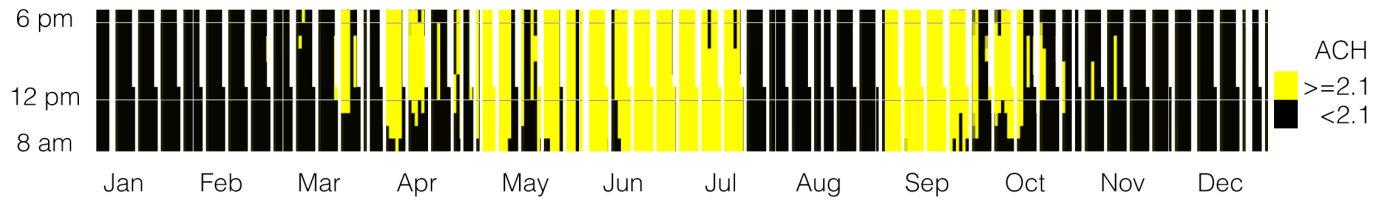
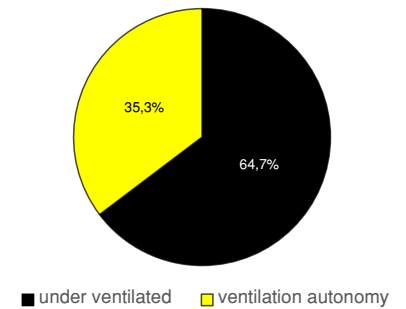


Figure b1.5 Ventilation Autonomy - zone 3 - free running



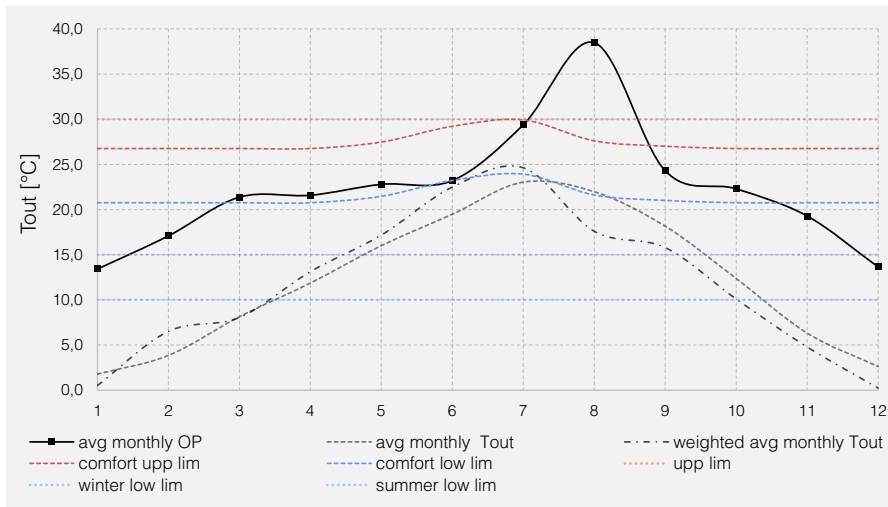


Figure b1.6. Standard and weighted monthly average outdoor temperature according to minimum and maximum ranges plus average monthly Operative Temperature

Following simulation uses Adaptive method for thermal comfort evaluation. According to ASHRAE 55 US standard, operative temperature upper and lower limits is determined based on equations “a” and “b” (see page 26). It is possible to use a simple average of monthly outdoor temperature, but it is preferable to use a prevailing outdoor mean temperature in conjunction with dynamic simulation software. In particular, “ T_{pma}_{out} ” is defined

as:

$$T_{pma}_{out} = (1-\alpha)te(n-1) + \alpha trm(n-1) \quad (16)$$

Where “ α ” is a constant between 0 and 1 coefficient, indicating temperature variation according to climate (e.g. humid tropical vs. mid-latitude climate). For Turin climate a coefficient of 0.6 will be used. “ $te(n-1)$ ” is the daily mean air temperature before the day in question and “ $trm(n-1)$ ” indicates the running mean

temperature before the day in question.

The following part of this simulation adopts CEN 15251 (2007) comfort parameters instead. In particular, exponentially weighted running mean is done for the last 7 days of each month applying the following equation [15]:

$$Trm = (T_{od-1} + 0.8 \cdot T_{od-2} + 0.6 \cdot T_{od-3} + 0.5 \cdot T_{od-4} + 0.4 \cdot T_{od-4} + 0.3 \cdot T_{od-5} + 0.2 \cdot T_{od-7}) / 3.8 \quad (17)$$

Once determined “ Trm ”, Comfort ranges of indoor Operative temperature are set according to CEN 15251:2007 upper and lower limits.

Turin climate presents harsh winter temperature that goes beyond the upper limit and lower limit of both US Standard and CEN 15251. As it is visible in figure b1.6, for the time when “ trm ” is below the indicated limit, the lowest boundary is taken into account (e.g. 15°C for heating

periods)

Image b1.7 and pie chart below represents mean temperature ranges. Simulation is run without considering the influence of solar radiation. As we can see, the only moment of the year being too hot is part of July and August, whereas the rest is mainly under heated (blue area).

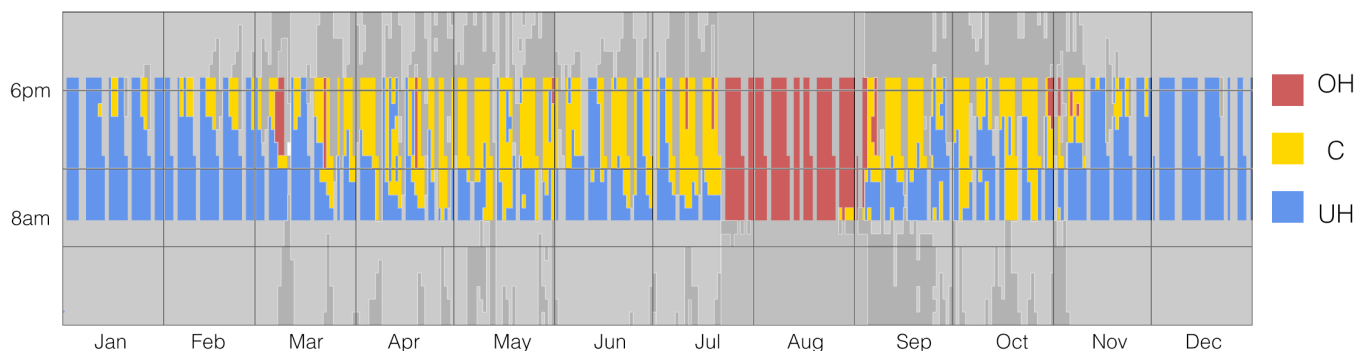
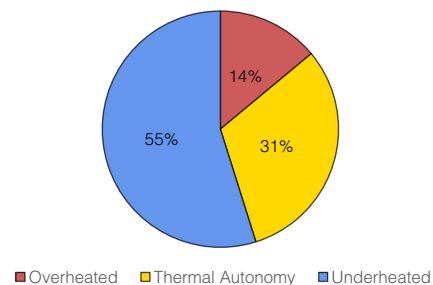


Figure b1.7 Mean Overheated, Comfort and Underheated annual plot ranges - free running simulation



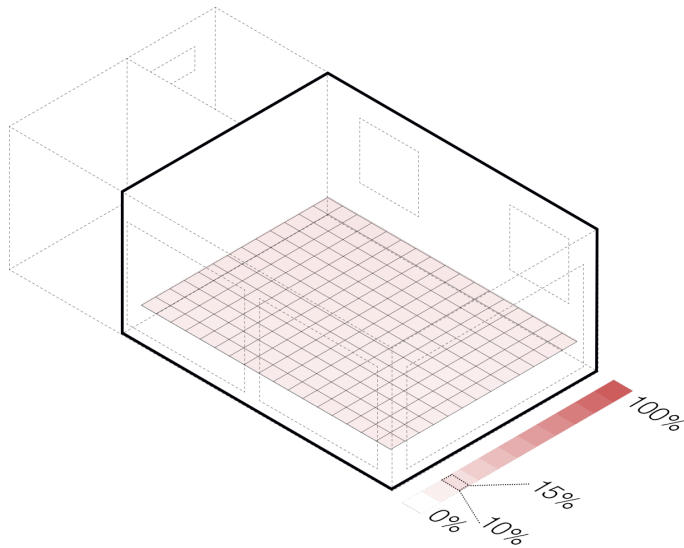


Figure b1.8 Overheated map

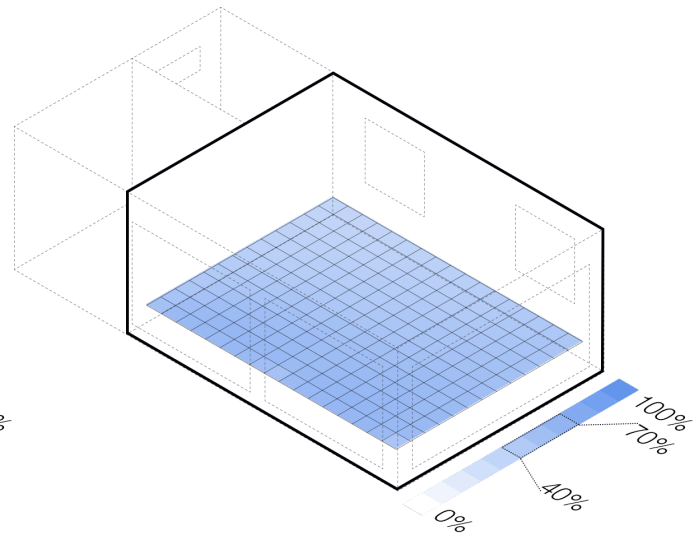
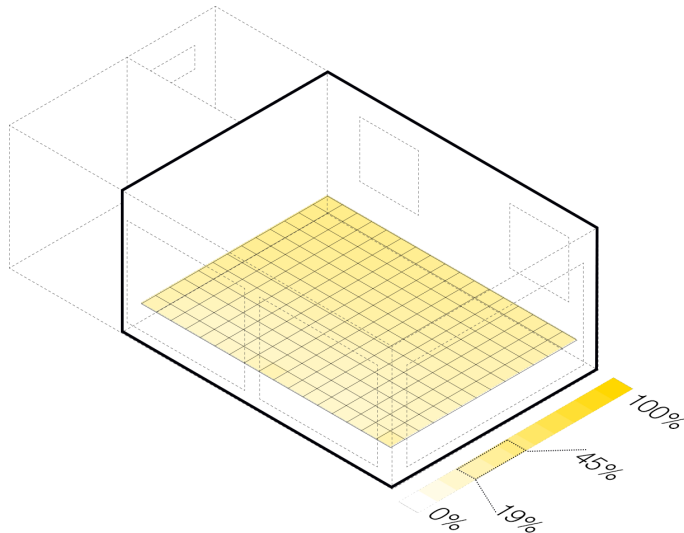


Figure b1.9 Under heated map



These page shows spatial map representation of overheated (red), under heated (blue) and comfort (thermal autonomy % in yellow).

Notice the area close to south and east window in the thermal autonomy maps, which is the least comfortable.

B2. PMV Comfort Model

Second simulation concerns the application of PMV comfort model on the baseline facility, considering the space like a proper office “conference room” with heating and cooling. With these assumptions, it is necessary to make some modifications and supplements to the loads used in previous analysis, while keeping schedules the same. In particular, minimum and maximum humidity values are specified, respectively as 30% and 50%. Moreover, in addition to the

same infiltration rate through the façade equal to 0.0015 m³/s, a ventilation per person of 0.007 m³/s and ventilation per area equal to 0.0007 m³/s are set. Lighting density and setpoints/setbacks are the same used for previous analysis.

In line with simulation b1, b2 results shows higher operative temperature values in summer, in particular from May to September, whereas in simulation b1, thanks to the effect of natural ventilation,

mainly August results in high operative temperature values solely. Winter and Autumn time presents values around 19°C. Relative humidity presents good values most of the occupancy time, given the presence of dehumidification system in the HVAC, as we can also see from the ventilation autonomy in pie chart on next page with a value of 83% of occupied time, against 35% of previous simulation.

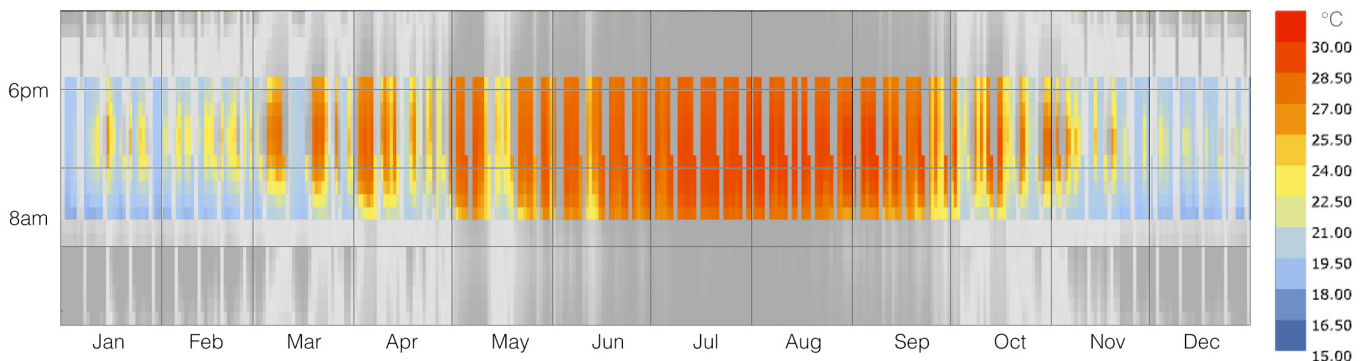


Figure b2.1 Indoor standard Operative Temperature - conditioned

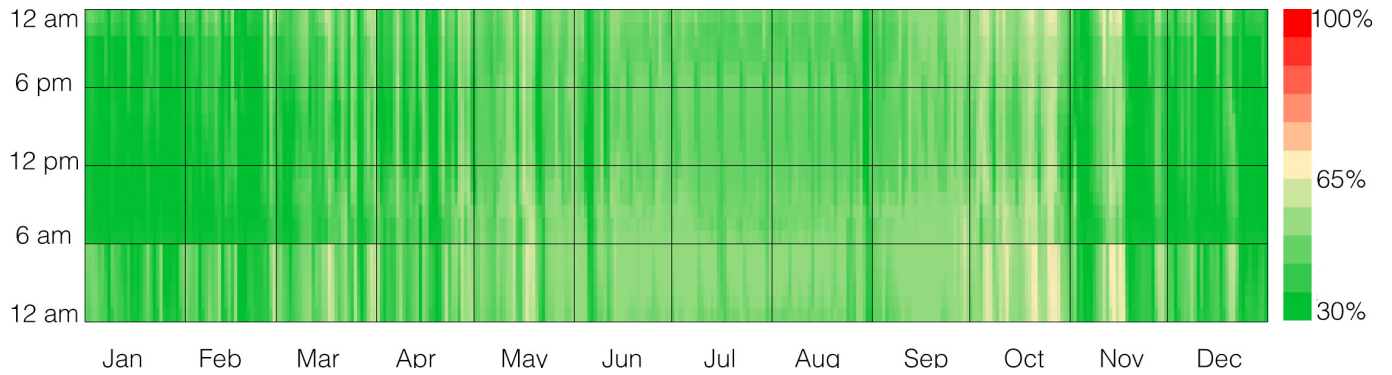


Figure b2.2 Indoor Relative Humidity - conditioned

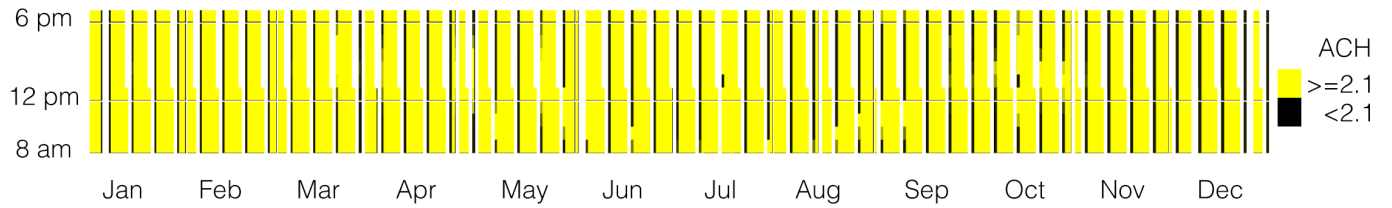
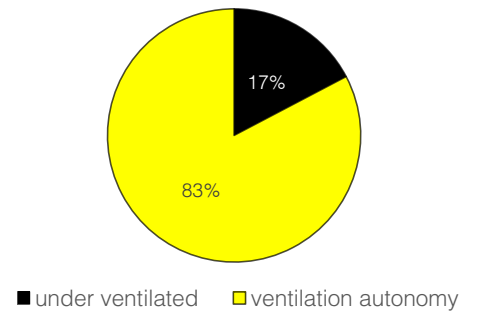


Figure b2.3 Ventilation Autonomy



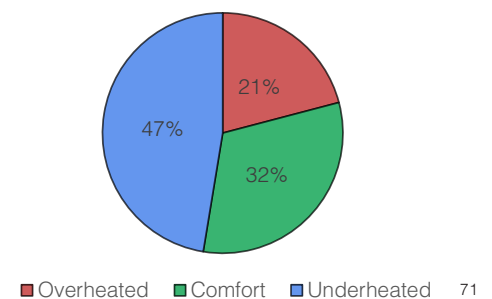
PMV comfort model uses Operative temperature ranges to set comfort zone for the occupants as well. The main difference with the adaptive model is that new inputs are considered, such as the metabolic rate and the clothing level of the occupants. According to CEN EN 15251, as we have also discussed in previous pages, comfort range is set with a Predicted Mean Vote in between -0.5 and +0.5,

corresponding to II building comfort class. In particular, for an office destination or “conference room” type and according to a sedentary metabolic rate equal or about to 1.2 met, upper and lower temperatures are 26°C (minimum for heating in winter season and 1 as clothing level) and 20° C (maximum for cooling in summer season with 0.5 clo). Thus, as one of the inputs for the

analysis, clothing level maximum and minimum values are considered as 1 for the coldest day and 0.5 clo for the hottest one. Hourly clothing levels in-between this range are calculated through Ladybug clothing function component. In addition, forced air system with diffusers is considered. Hence, no air stratification is computed, and air is considered well mixed.



Figure b2.4 Mean Overheated, Comfort and Under-heated annual plot ranges - free running simulation



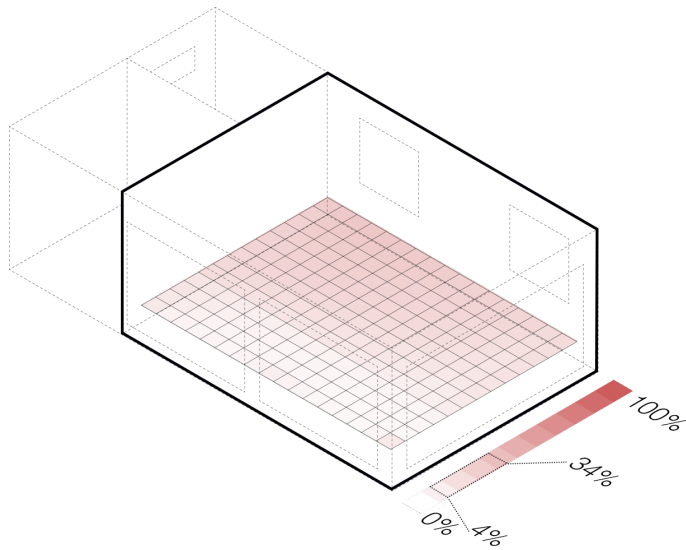


Figure b2.5 Overheated map

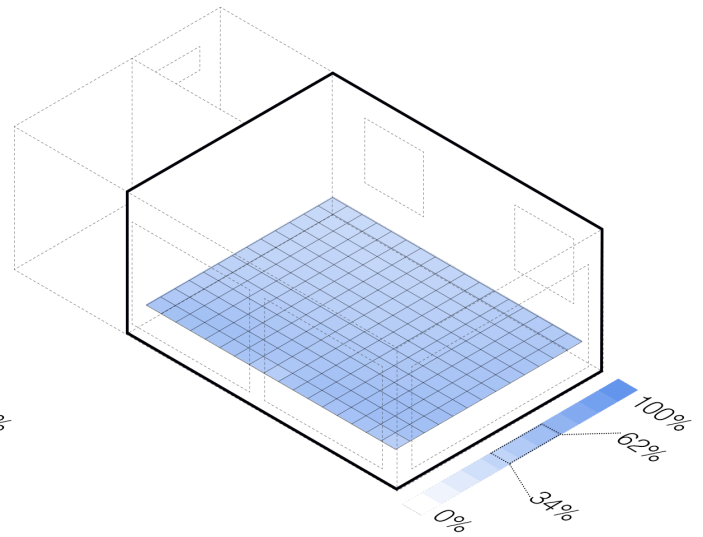
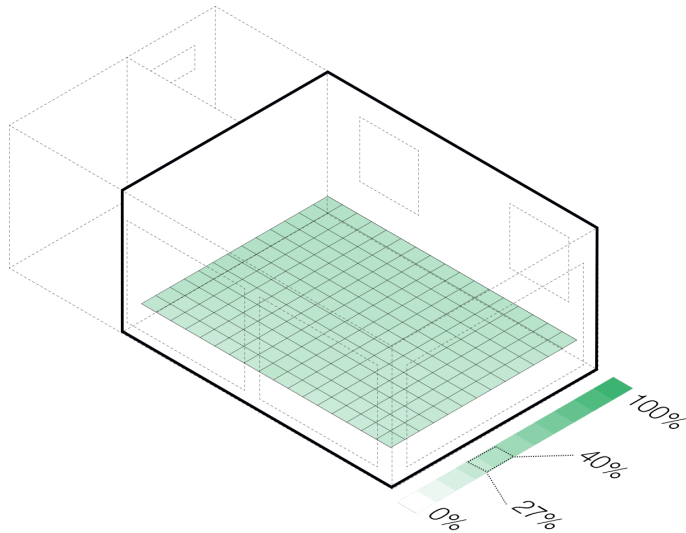


Figure b2.6 Under heated map



72 Figure b2.7 Thermal Autonomy map

Figure b2.4 and b2.6 reveal high quantity of Under-heating % of occupied time, from January to April (in the morning) and from October to December.

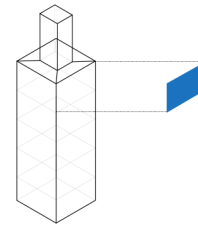
B3. Influence of Solar Radiation on occupants

As mentioned in previous pages, Total Mean Radiant Temperature is made up of two components, longwave radiation, which involves the longer wavelength of solar spectrum, and shortwave radiation, which is a stronger radiation related to UV and visible light range of solar spectrum. The latter is responsible of high temperature asymmetry, thus determining thermal discomfort. This work thesis follows main normative procedure from appendix C from ASHRAE 55 standard for calculating comfort impact of solar gains on occupants. A similar procedure to known published paper (e.g. Zani et Al. [16-17-18]) is followed to produce main results. Each point is translated into a seated simplified manikin, whose eye height correspond to 1.2 m. Zani et Al. focuses on the application of delta MRT and

indoor solar radiation studies on different types of manikin, from more detailed mesh to a simplified one. Whether a noticeable decrease in simulation computational time is observed, no such a difference is noticed in terms of correlation and results quality. Nonetheless, the paper evidences scarce correlations when running simulation with simplified manikin and shading systems at the same time. In such cases, more detailed manikins' application is suggested.

The main steps adopted in the computation of delta MRT are:

a. An annual daylight simulation with results expressed in terms of radiation as output for the analysis is run. Points are 221, which means that the analysis will produce results for 221 placed manikins. Each simplified manikin is made up of 30 meshes. At the end of the



Simplified Manikin and one (blue) of its mesh faces

simulation a total of 58.078.800 values is produced. This huge number stands for radiation values registered on each of the manikins meshes in an entire year.

b. Data is post processed to obtain annual data for each point, so that the overall radiation of each manikin is synthesized in 221 grid points. To do so, each of the 30 meshes results is multiplied by its area, thus obtaining a value expressed in “W”. After summing all of the

30 multiplications, the result is divided by average person area (1,88 m²), thus resulting in a value in W/m².

While Zani et Al. collect data for direct and diffuse solar radiation, annual simulation used in our case already comprehends direct and diffuse amount of radiation. For this reason, the final value in W/m² already represents the total Esol component, which, according to the relationship between long-wave and short-wave coefficients, leads to ERF (effective radiant field) as final output.

c. Applying the following equation, delta MRT is finally determined:

$$\text{delta MRT} = \frac{\text{ERF}}{f_{\text{eff}} * h_r} \quad (18)$$

where “ f_{eff} ” is the coefficient of body exposure of a seated or standing person and “ h_r ” is the radiant coefficient.

Following images show deltaMRT values on clear sky chosen days, from 10 am to 4pm.

Following images show spatial distribution of Delta MRT based on 15°C range. Annual plots (see figures b3.13-16 next pages) present values based on 4° Delta MRT range, in line with the work of Zani et Al. [16] and an example of Annual Solar Radiation computation

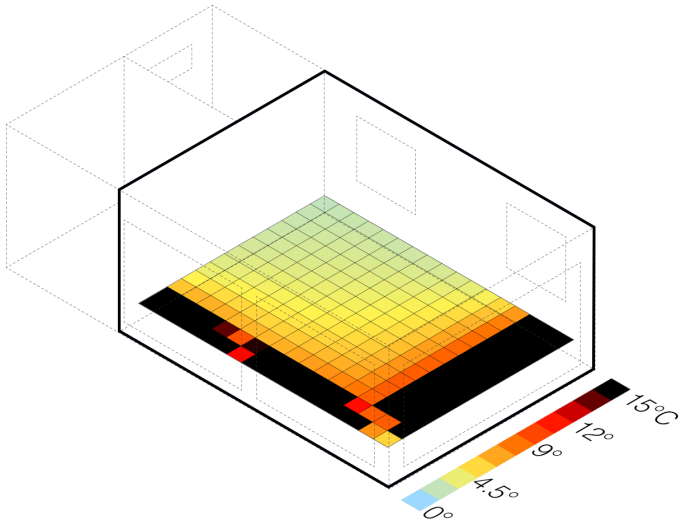


Figure b3.1 10 am

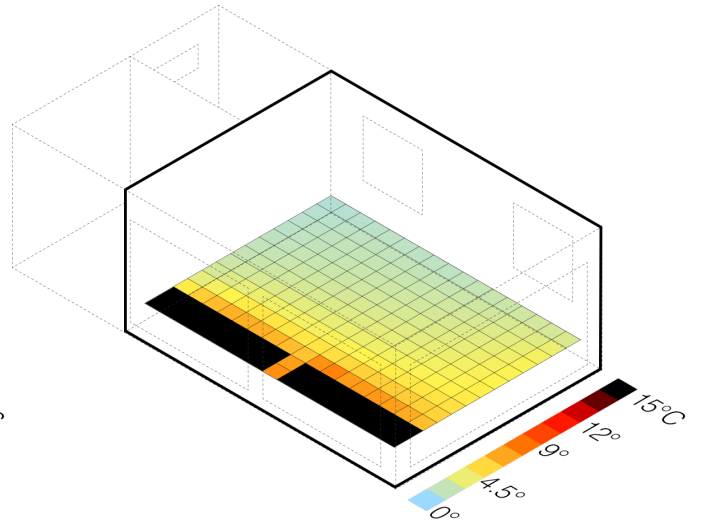


Figure b3.2 12 pm

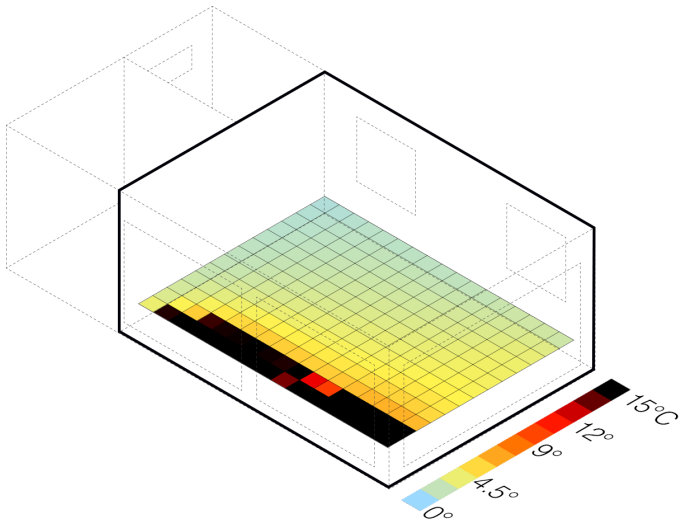


Figure b3.3 14 pm

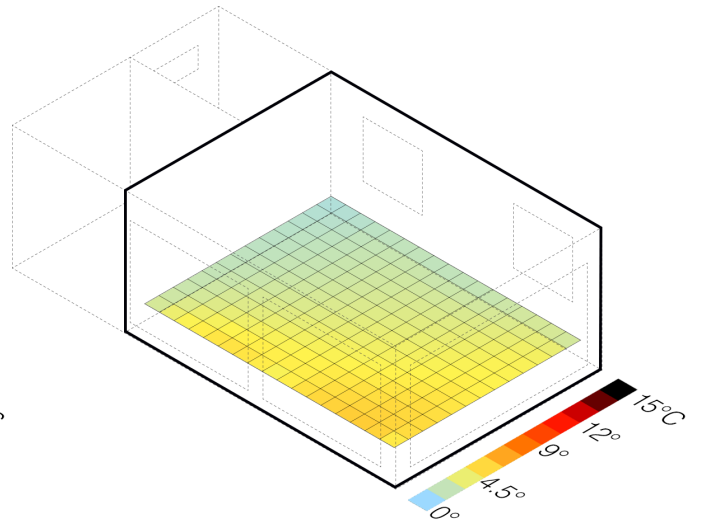


Figure b3.4 16 pm

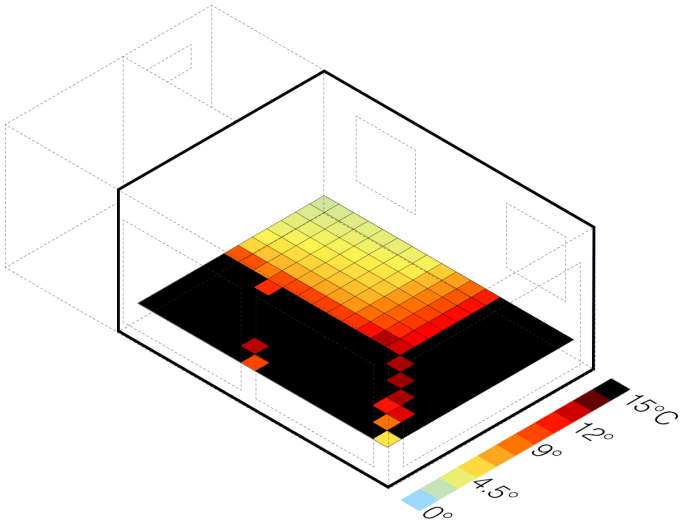


Figure b3.5 10 am

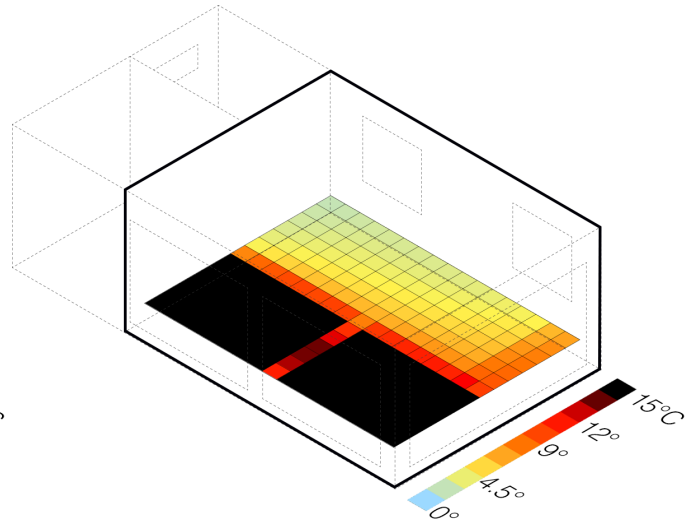


Figure b3.6 12 pm

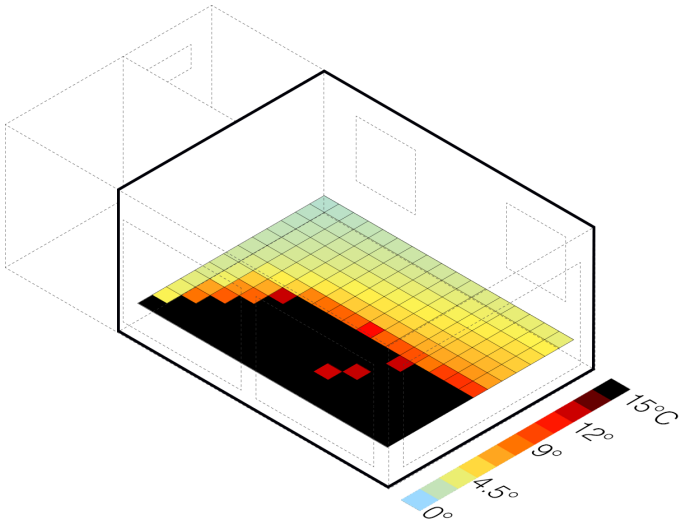


Figure b3.7 14 pm

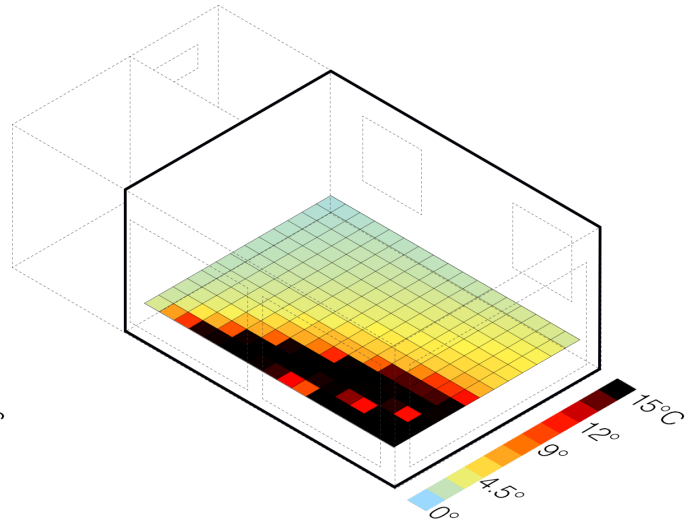


Figure b3.8 16 pm

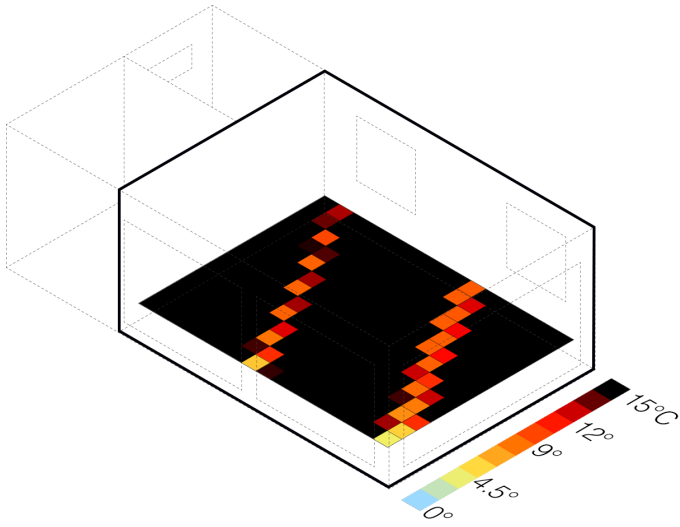


Figure b3.9 10 am

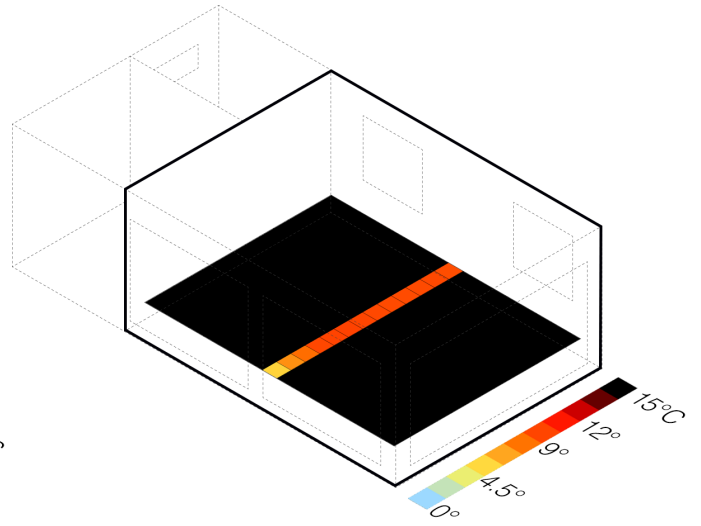


Figure b3.10 12 pm

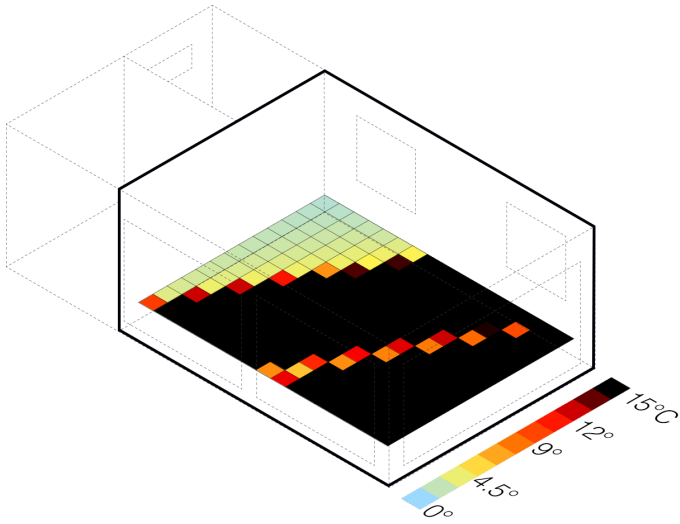


Figure b3.11 14 pm

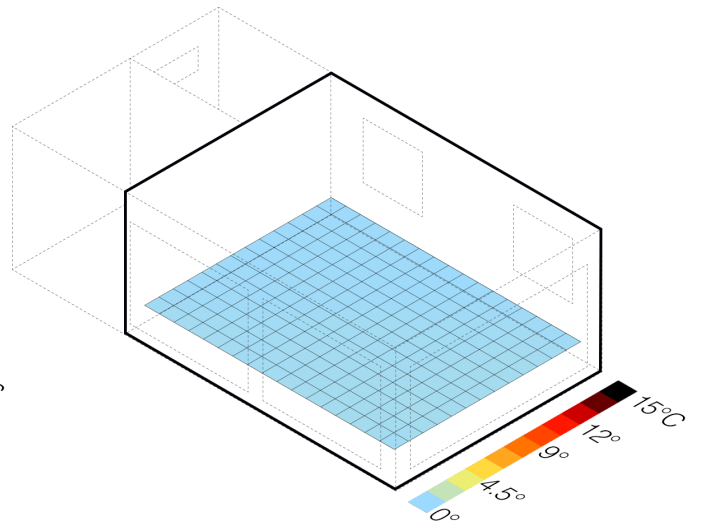


Figure b3.12 16 pm

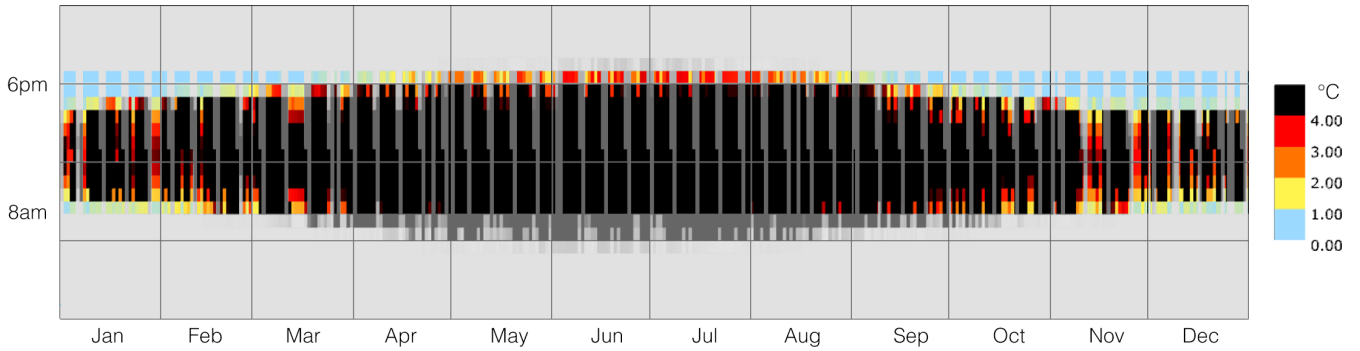


Figure b3.13 Annual radiation discomfort measured on point 54

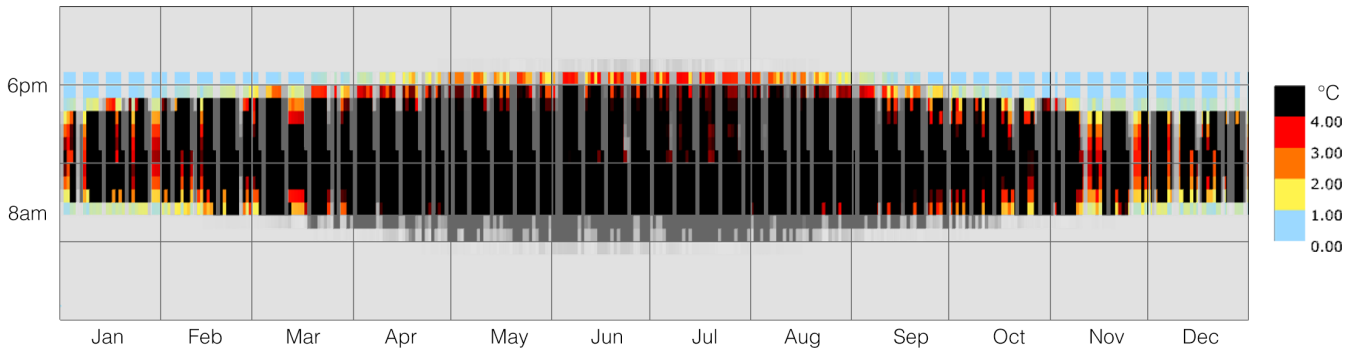
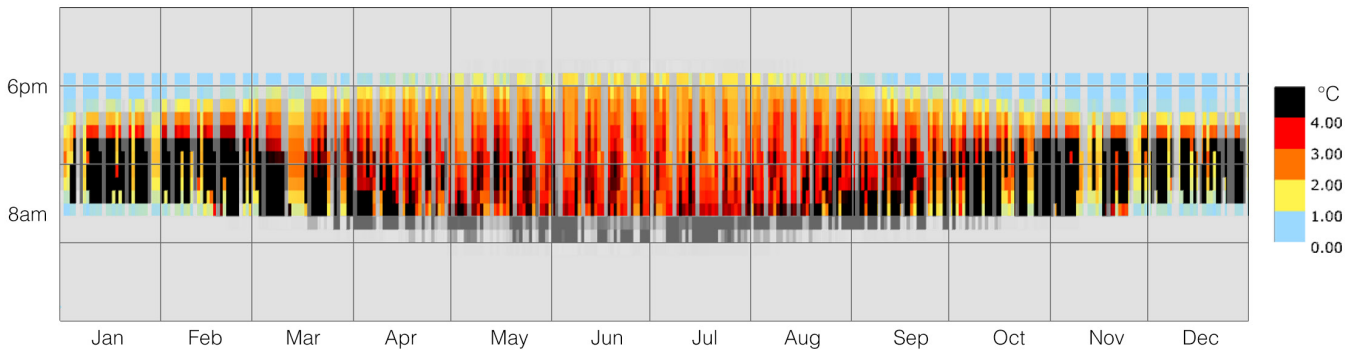


Figure b3.14 Annual radiation discomfort measured on point 32



78 Figure b3.15 Annual radiation discomfort measured on point 179

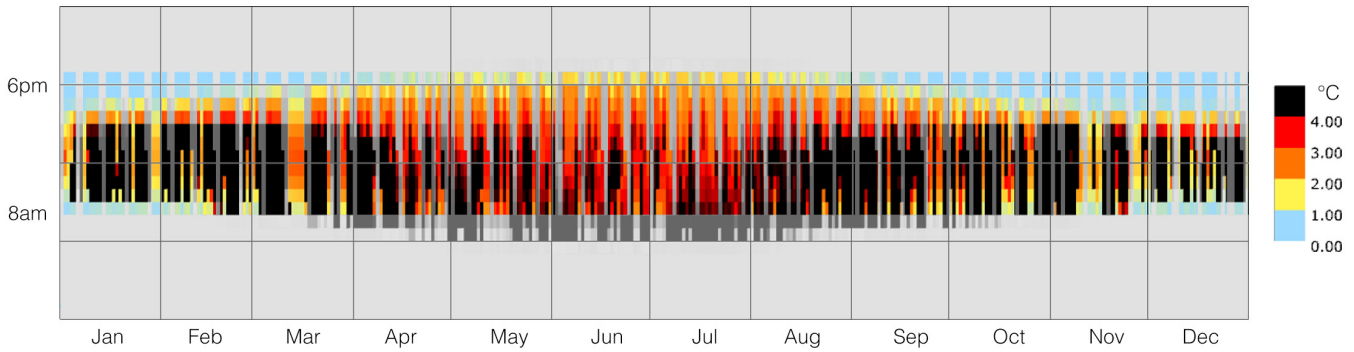


Figure b3.16 Annual radiation discomfort measured on point 188

Once delta MRT data is collected from every hour of the year for each grid point, we can observe its variation yearly. In particular, we can treat delta MRT and radiation data as a metric and we can express values according to occupancy (see images b3.13 to b3.16).

By calculating the occupied time when delta MRT exceeds 4°C [17], we calculate the percentage of time of discomfort by radiation, that is to say, annual radiation discomfort (ARD). Once percentages are calculated for each point of the

grid, we can draw a heat map. Unacceptable values are those, within 3 meters from façade, that exceeds 10 % of occupancy time.

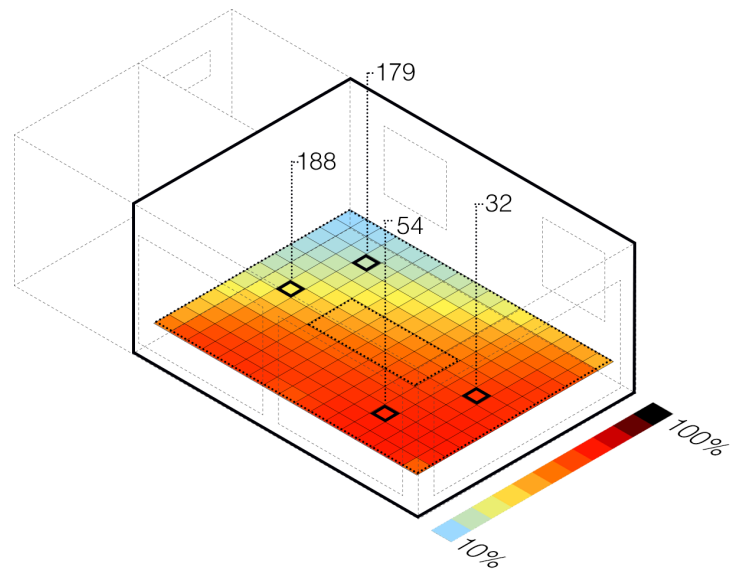


Figure b3.17 Annual Radiation Discomfort Map (%) based on 4° delta MRT

Following images show results of thermal comfort analysis, both Adaptive and PMV, considering the influence of Solar Radiation falling on Occupants.

As we can see from both the Operative temperature annual plots in figures b3.20 and b3.27 (pag. 81 -84), there is an increase in red and yellow areas, determining an increase of Overheated hours and decrease of both Under-heated and Thermal comfort %. This is reflected in respective pie charts, which are supported by heat maps visualizations (pag. 83-86).

Interestingly, adaptive comfort and PMV results vary differently. Whether they share a similar decrease in Under-heated % (adaptive: 55 to 14.7; PMV: 47 to 13.4), different is for comfort response to the changing situation (adaptive: 31 to 49.8; PMV: 32 to 33.7). This is associated to leap difference in the % of Overheated hours

(adaptive: 35,5; PMV: 53), with delta MRT being certainly more acceptable and exploitable in a case where there is no heating on. Thus, when HVAC system is on, month from May to September results too hot.

Adaptive Model p.2

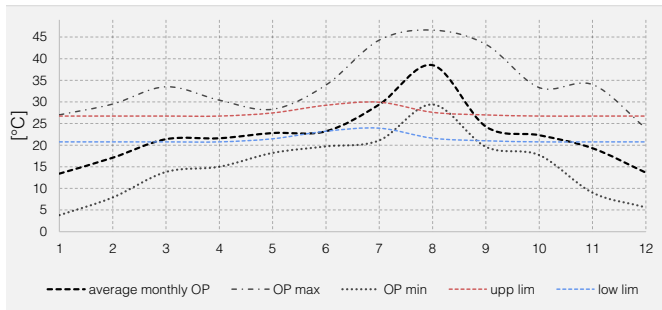


Figure b3.18
Average Op temperature and comfort zone
- no solar radiation

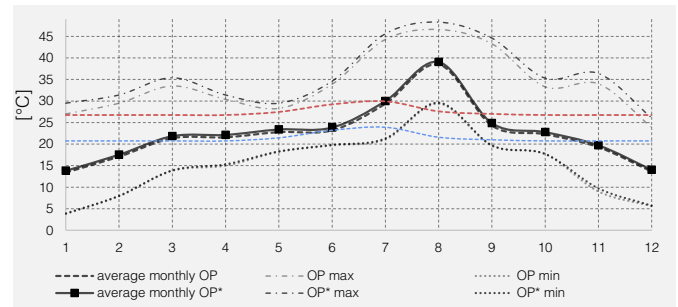


Figure b3.19 Average Op temperature and comfort zone - with solar radiation. (Standard Top and Adjusted Top in dashed and continuous black line respectively)

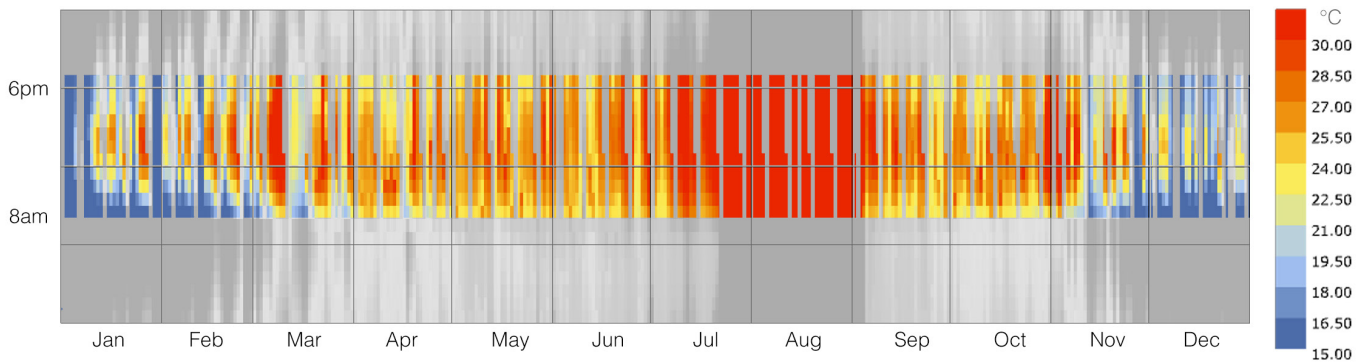


Figure b3.20 Indoor adjusted Operative Temperature - free running scenario

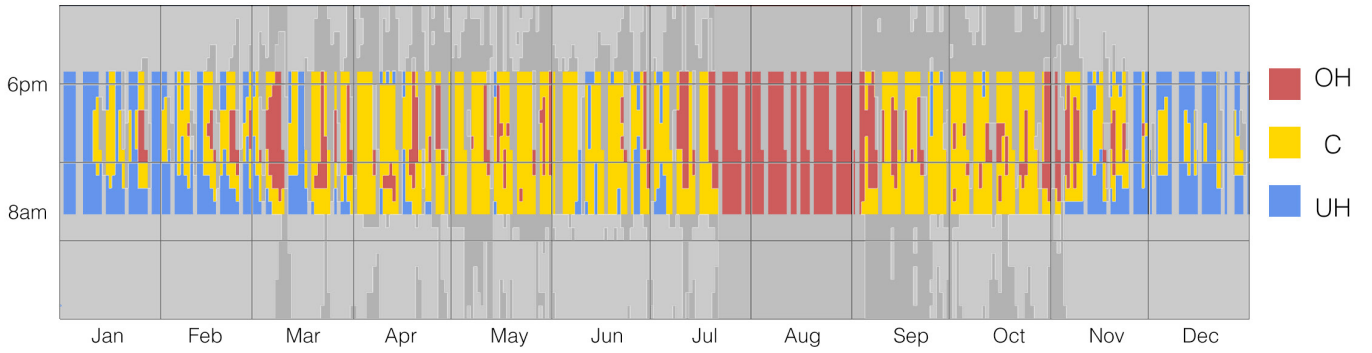
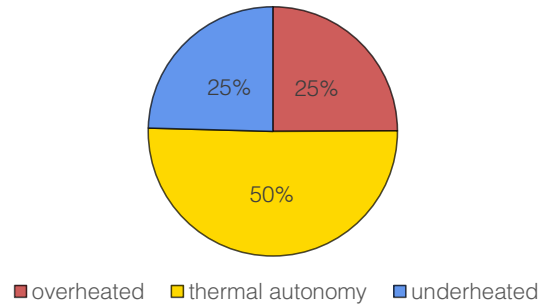
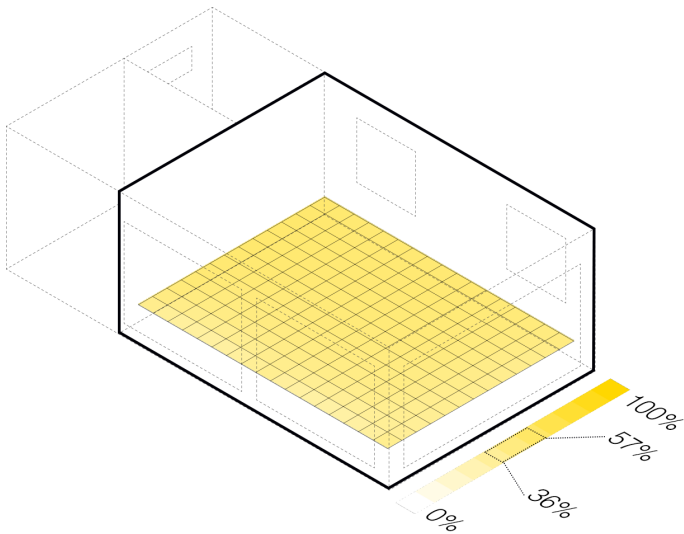
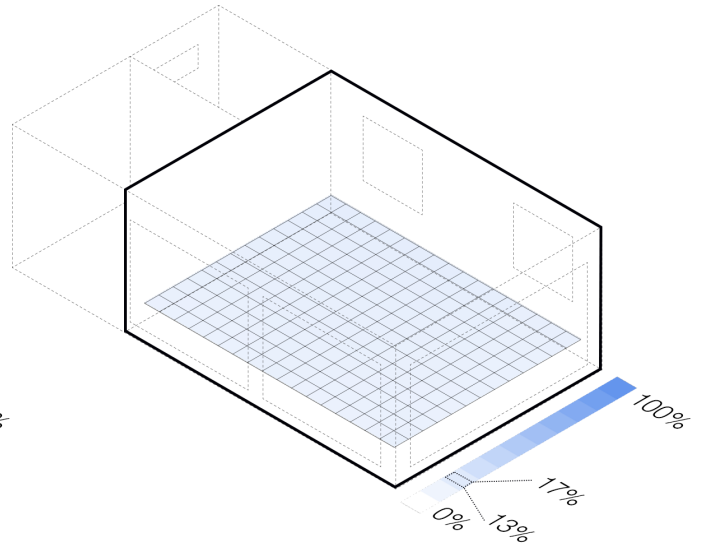
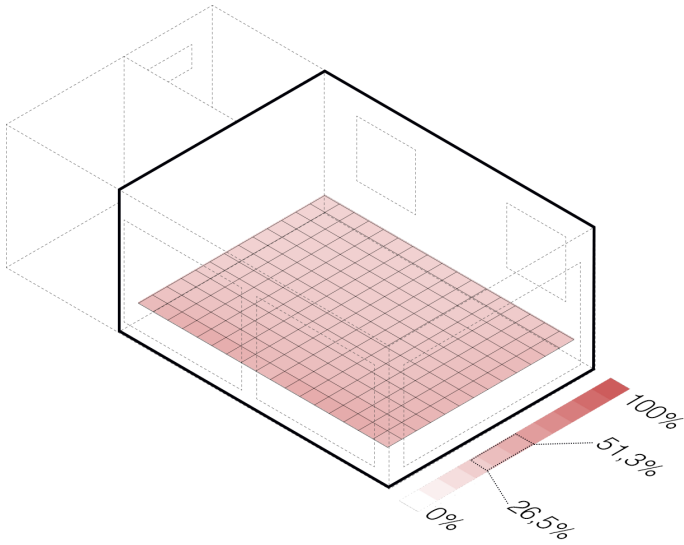


Figure b3.21 Mean Overheated, Comfort and Underheated annual plot ranges - free running simulation





PMV Model p.2

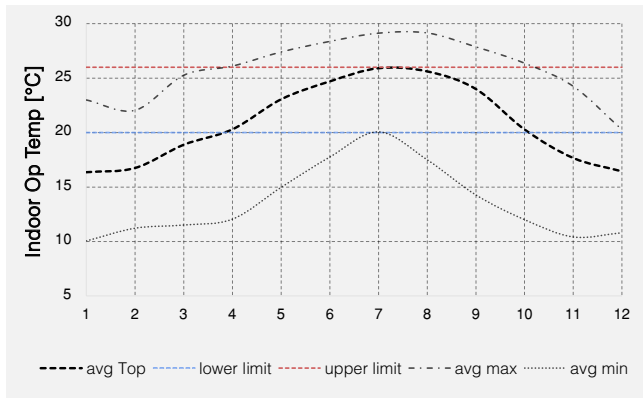


Figure b3.25
Average Op temperature and comfort range
- no solar radiation

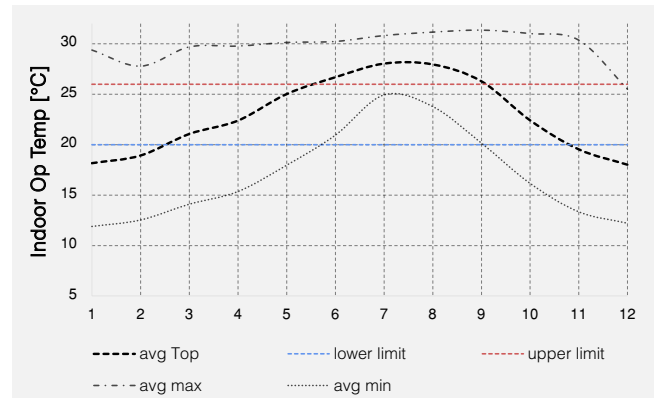


Figure b3.26
Average Op temperature and comfort range
- with solar radiation

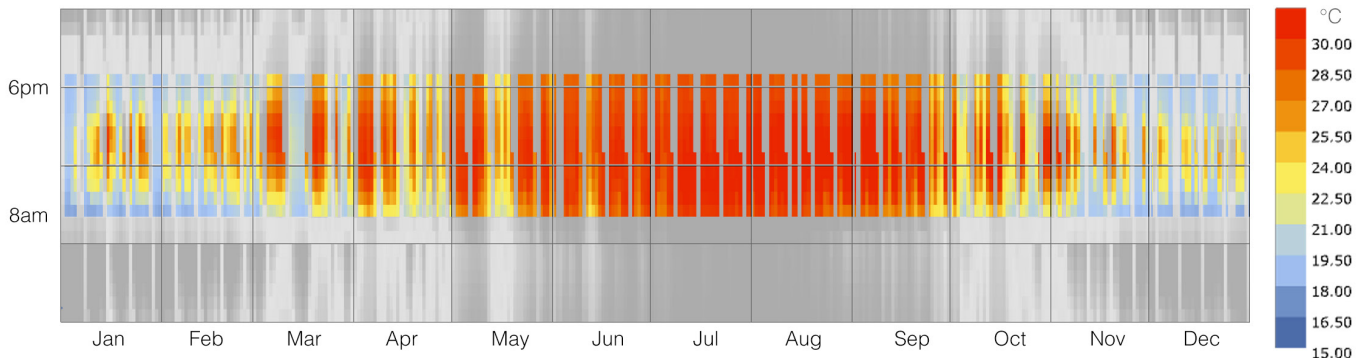


Figure b3.27 Indoor adjusted Operative Temperature - conditioned

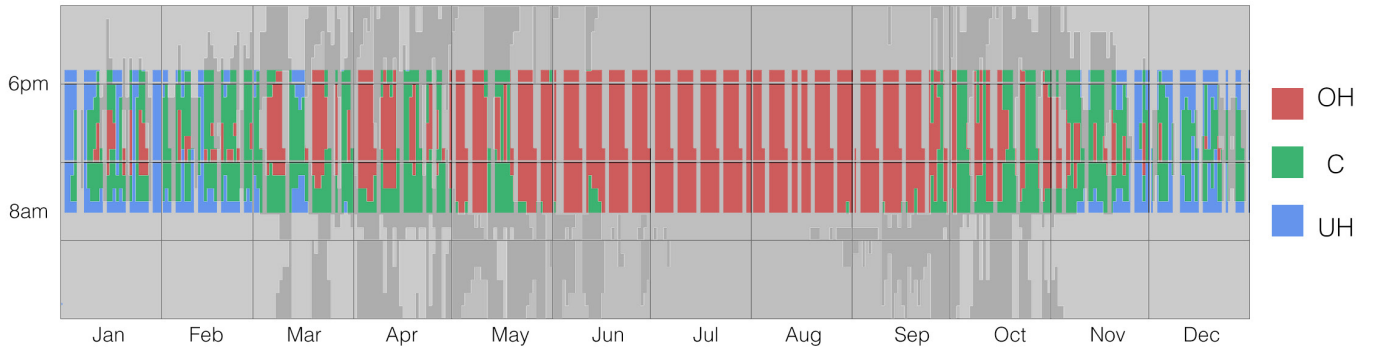
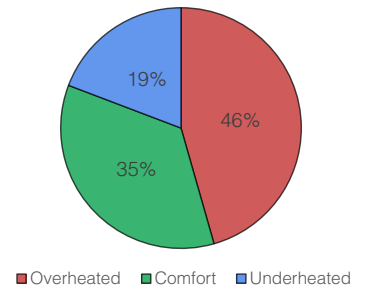


Figure b3.28 Mean Overheated, Comfort and Underheated annual plot ranges - conditioned



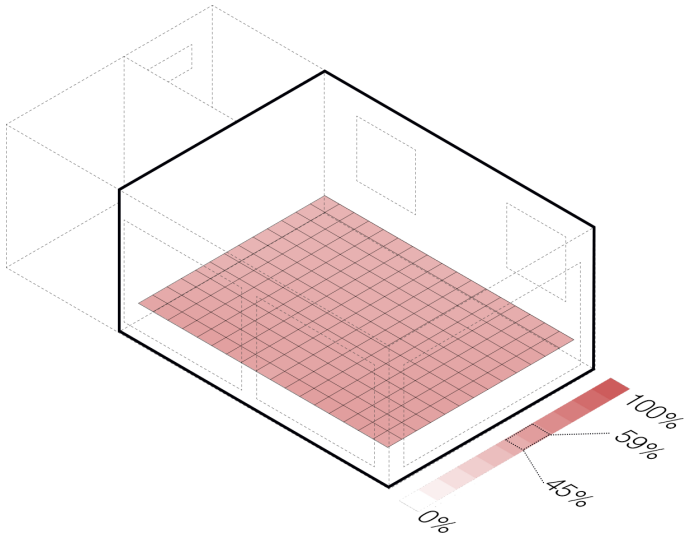


Figure b3.29 Over-heated map

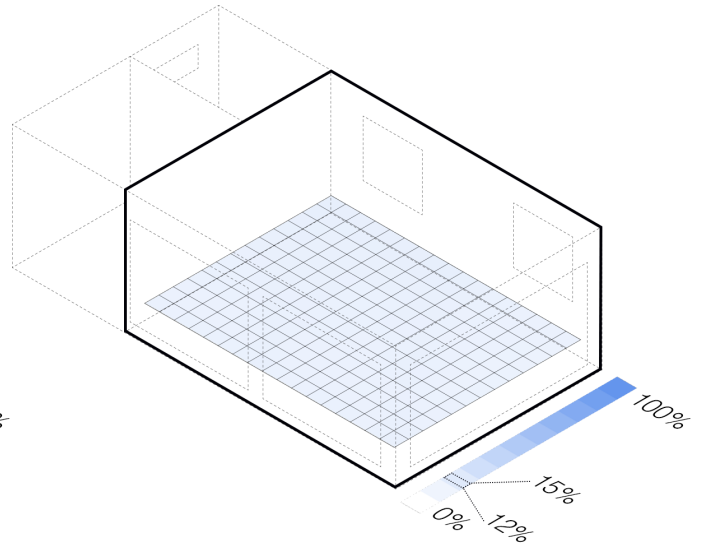


Figure b3.30 Under-heated map

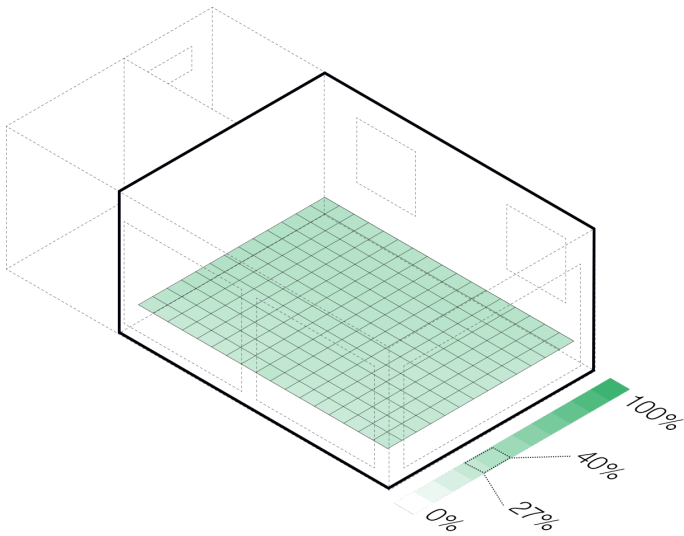


Figure b3.31 Thermal Comfort map

B4. CBDM & Daylight Analysis

Daylighting simulations produced results according to principal climate-based daylight modelling. As described in previous pages, these are Daylight Autonomy, Spatial Daylight Autonomy, Useful daylight Illuminance and Annual Solar Exposure.

Target illuminance set for Daylight Autonomy is 500 lx whereas UDI ranges are based on 100 lx as lower critical range (under-lit condition) and 3000 lx as upper critical range (over-lit condition).

In particular, high window surface in east and south façade produces high illuminance values, often critical. More than 50% of occupied time is in the over-lit range, especially area closer to south and east windows (see figure b4.5). High lx values and $UDI > 3000 \text{ lx} > 50\%$ of occupied time indicates high risk and potential for glare

conditions. This is stressed in figure b4.6 with ASE mapping zone area where at least 250 h of occupied time is beyond or equal to 1000 lx. As the reader can see, just 13 pts (6% total area), closer to north west area, satisfy this condition. In particular, map shows, through gradient colouring, the degree of numbers of hours when exceeding condition (more than 250 hrs) occurs.

Acceptable condition of Spatial Daylight Autonomy is considered as 50% of occupied time where target illuminance of 300 lx is reached. Figure b4.2 shows also preferable condition according to which 75% of occupancy shall be considered. Both conditions are fully satisfied.

Daylight autonomy indicates that all space receives high degree of natural lighting. This is confirmed by verification of Spatial Daylight overtaking both threshold of 50 and 75% of space.

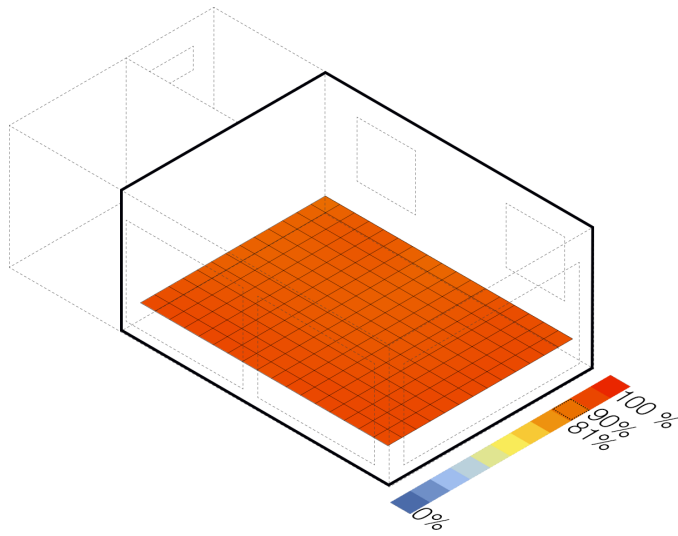


Figure b4.1 Daylight Autonomy

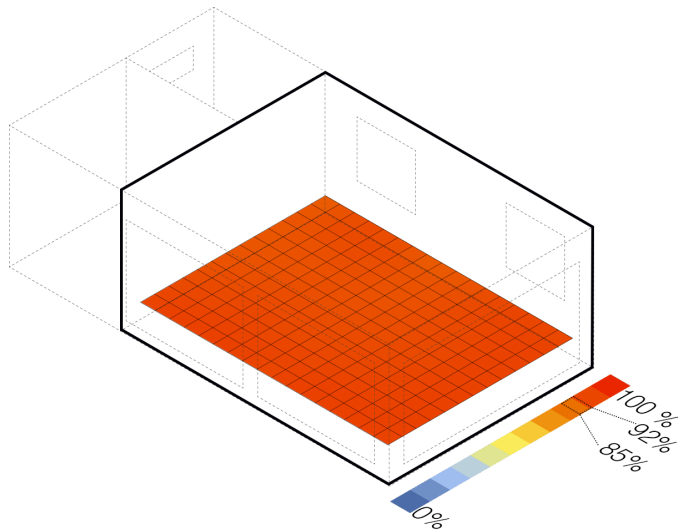
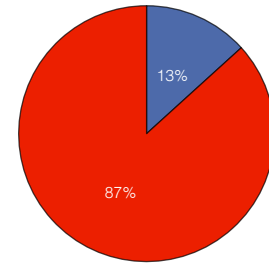
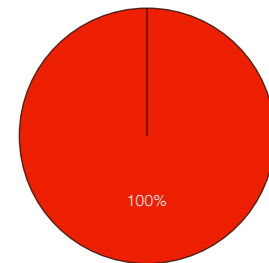


Figure b4.2 Spatial Daylight Autonomy



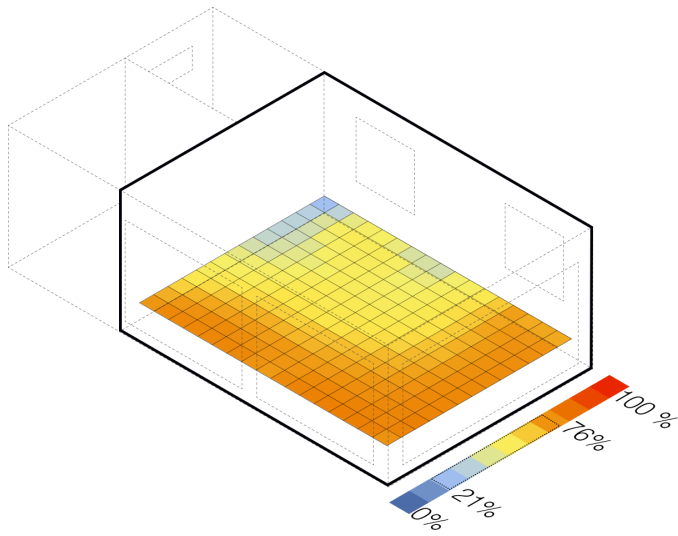


Figure b4.3 UDI > 3000 lx

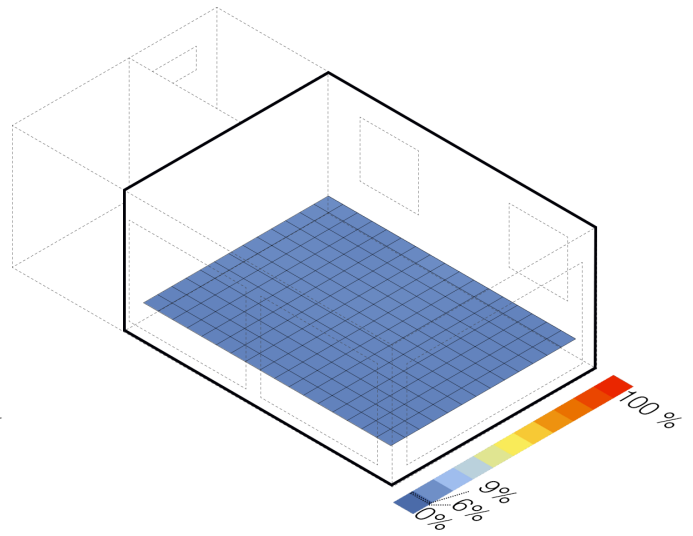


Figure b4.4 UDI < 100 lx

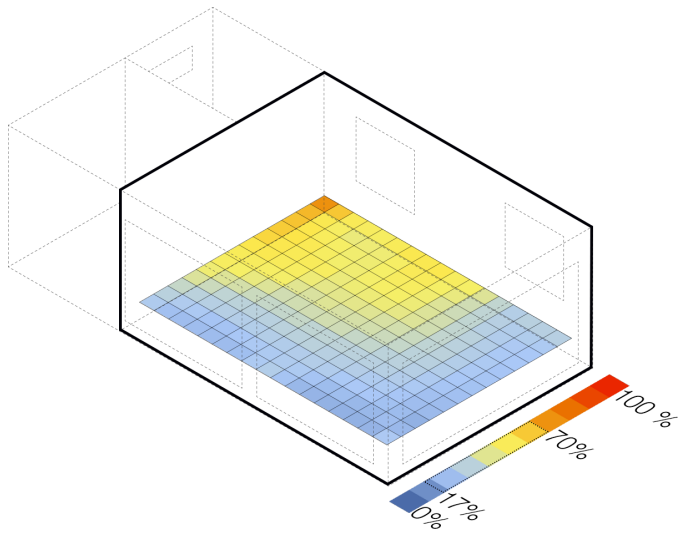


Figure b4.5 UDI, achieved

On the contrary, UDI_{achieved} is not verified.

Ranges in-between 100 and 3000 lx varies from 17 to 70%. Half of space is in the blue area, which means that for more than half the occupied time, points are outside this range (under-lit or over-lit)

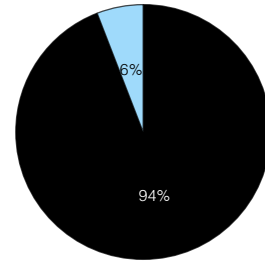
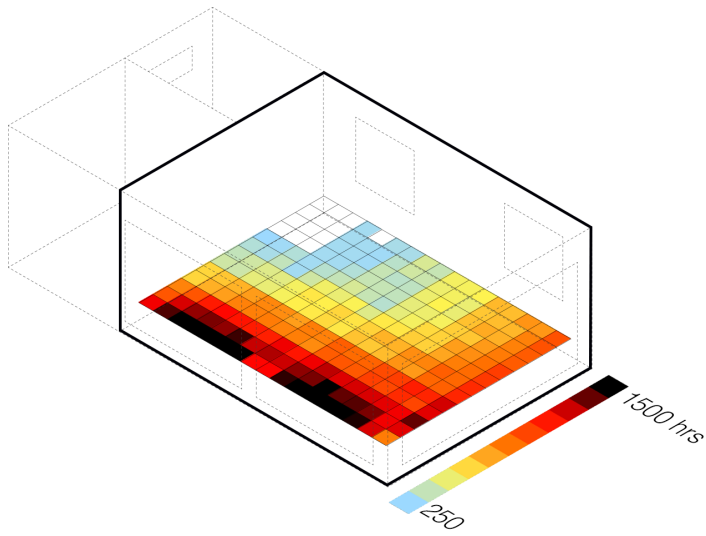


Figure b4.6 ASE_{250*1000}

ASE is not verified as well, with 94% of space receiving more than 1000 lx. As we can see, the more we get closer to south and east facade, the higher the number of hours exceeding the acceptable value.

B5. Ev + glare

Following images show mappings of vertical illuminances values scaled from 2500 lx to 5000 lx, both in east and south orientation, from 8 am to 16 pm. These specific range has been chosen in line with simplified DGPs methodology and thresholds (see pag. 33).

The reader can observe worse condition in winter where “black area” is bigger and maximum threshold in scale is reached. This happens in a shorter degree of time range (10am to 12pm). In summer, on the contrary, with values still being high, illuminances distribute in a larger time span, for the sun rises before and sets later.

This section offers a study of glare conditions. This is done both with produced HDR images, through Image Based Analysis, and annual Glare simulations. In particular, to calculate glare

occurrence for every point in space, repeating annual simulation for 221 times would be undoubtedly time consuming. For this reason, a simplified method is used.

This vertical illuminance values are used to define annual glare simulation for 4 specific points, two south oriented (54 and 58) and two east oriented (32 and 71), 1,5 and 3 m distant from windows respectively (see figure a.22 page 59). Moreover, spatial glare maps according to 0,4 dgp exceeding values are shown.

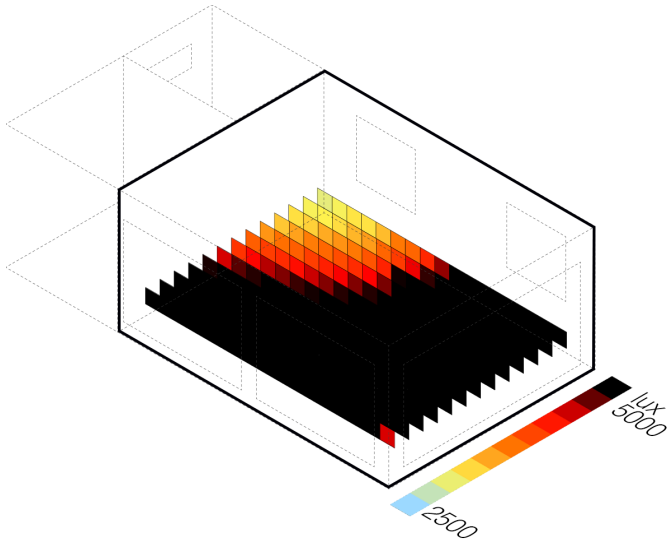


Figure b5.1 8 am

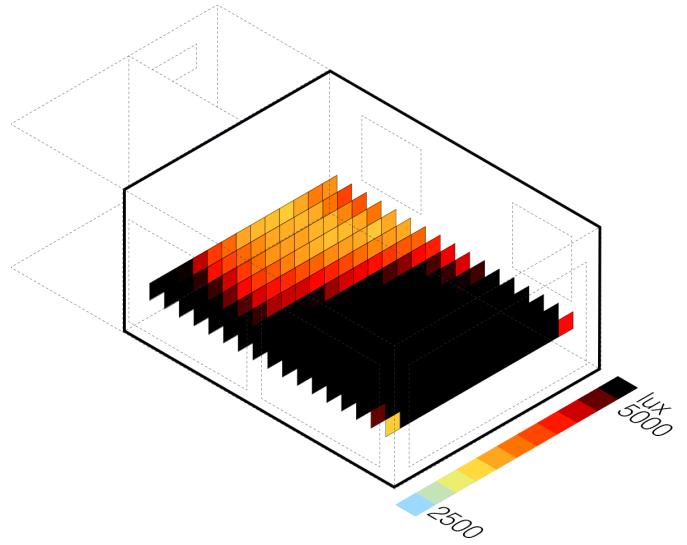


Figure b5.2 8 am

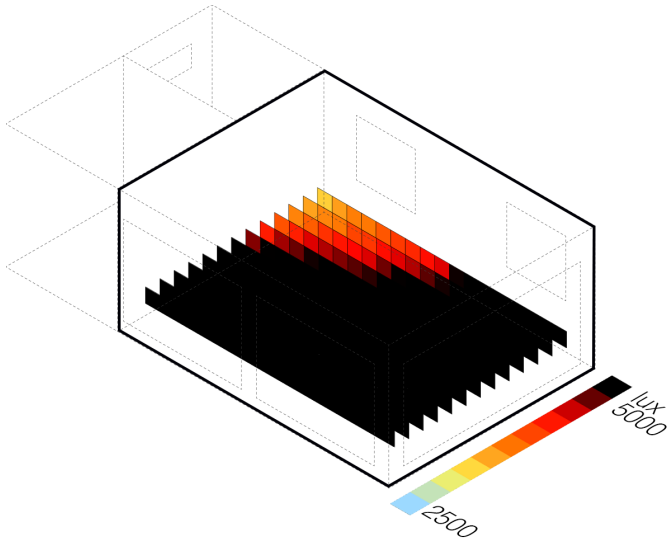


Figure b5.3 10 pm

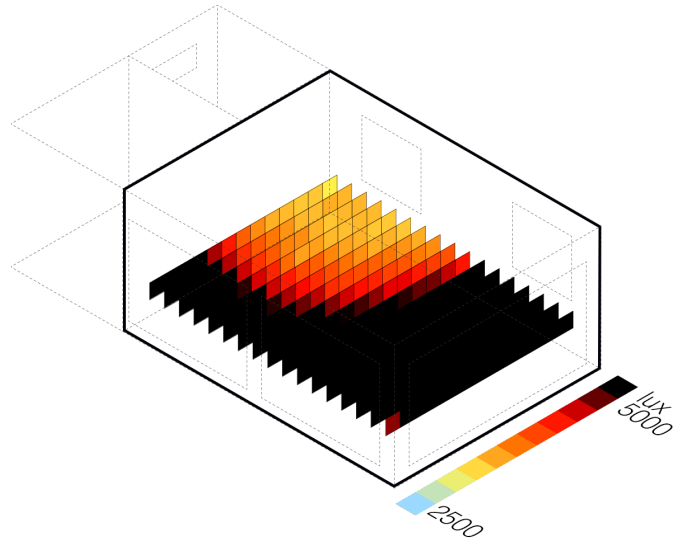


Figure b5.4 10 pm

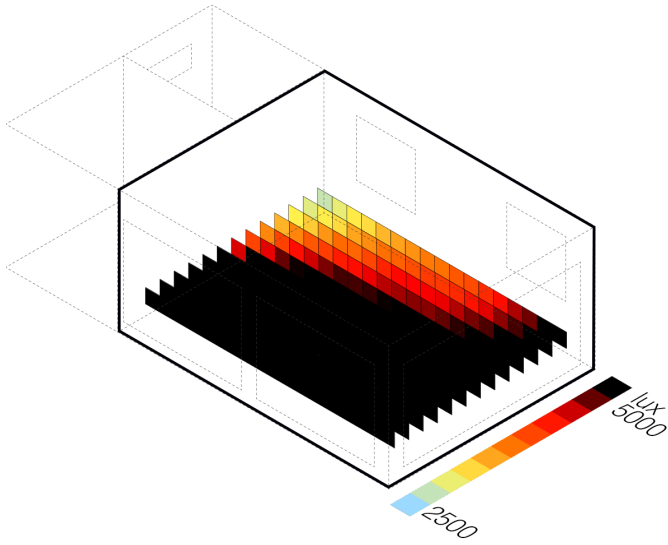


Figure b5.6 12pm

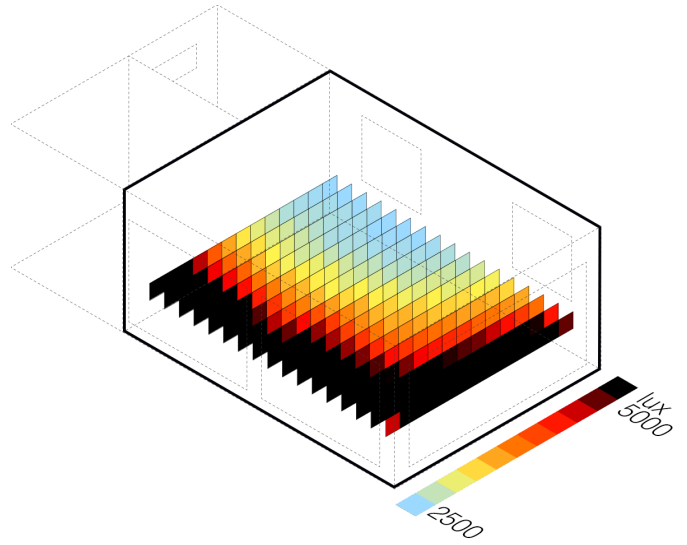


Figure b5.7 12pm

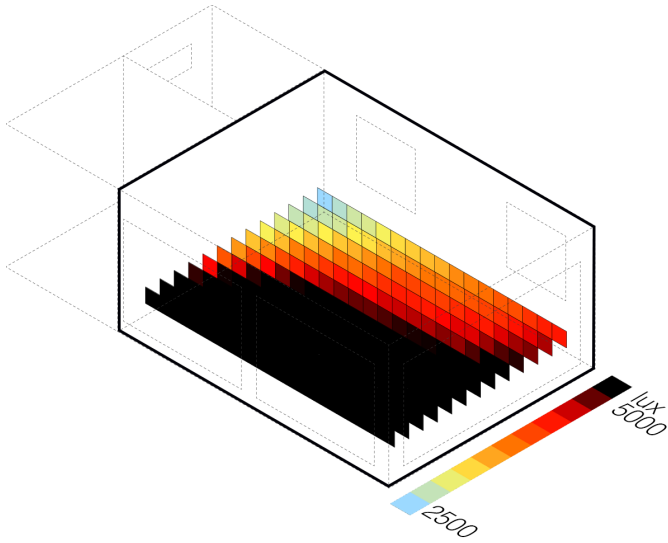


Figure b5.8 14 pm

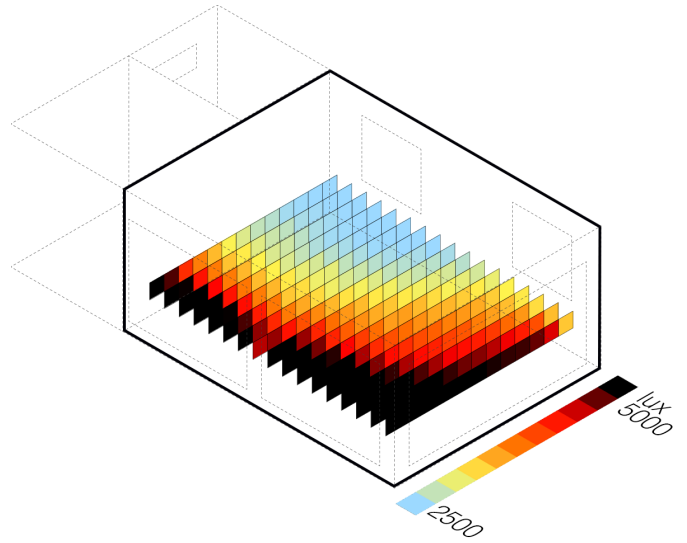


Figure b5.9 14 pm

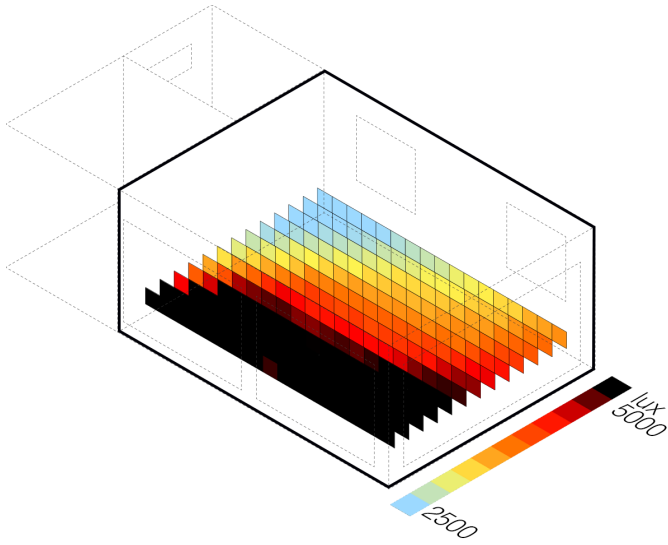


Figure b5.10 16pm

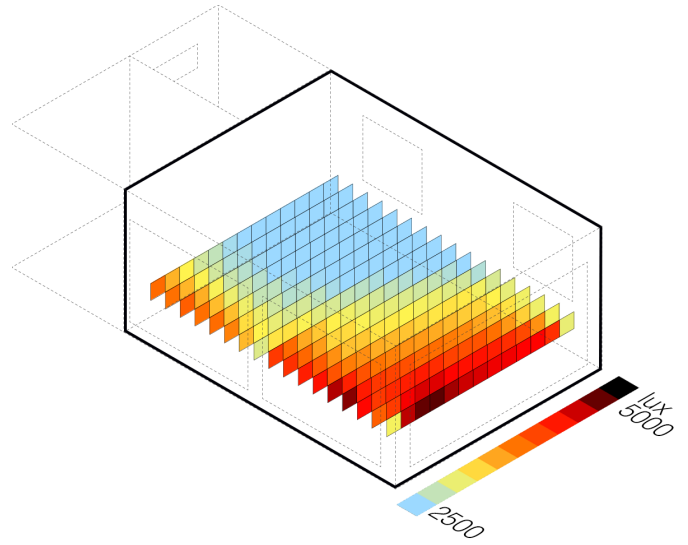


Figure b5.11 16pm

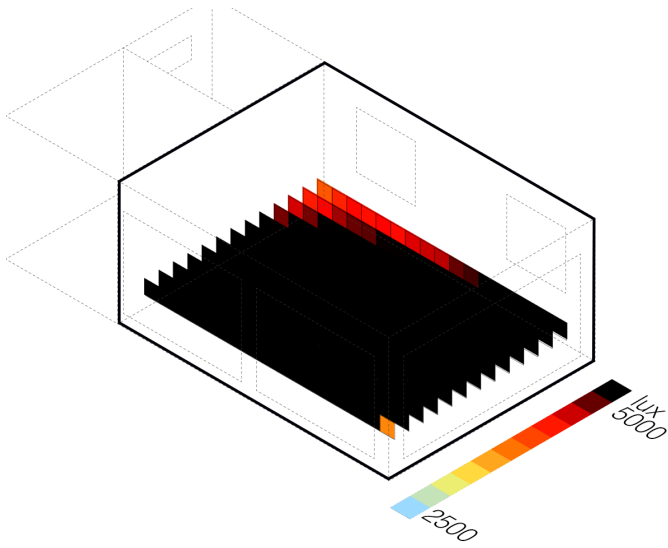


Figure b5.12 8am

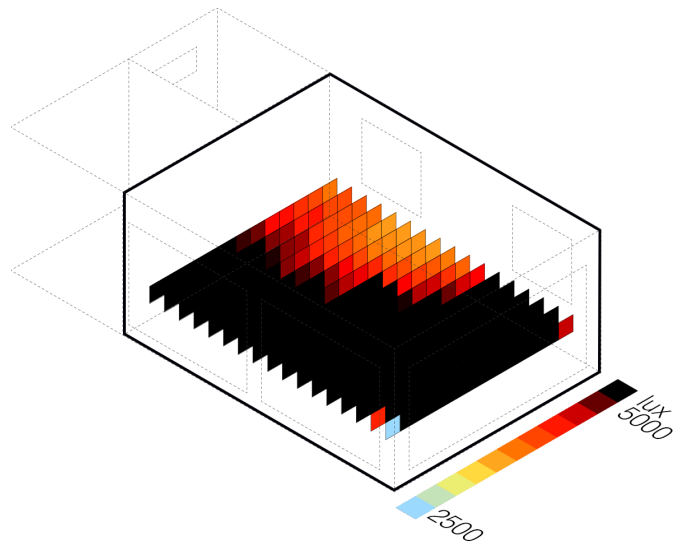


Figure b5.13 8am

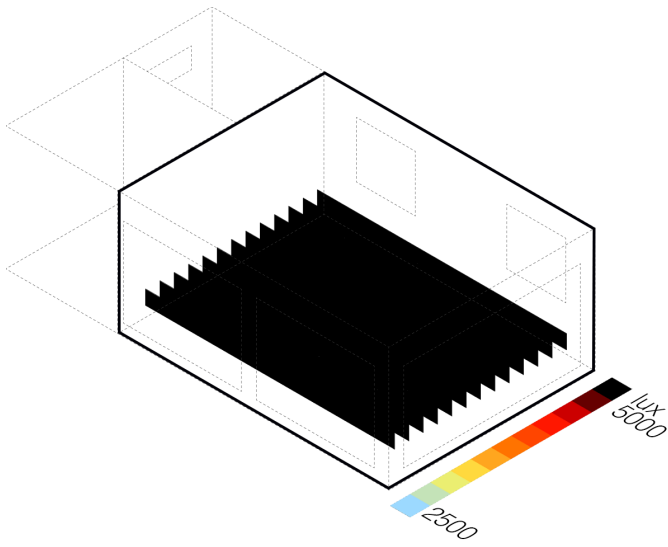


Figure b5.14 10 am

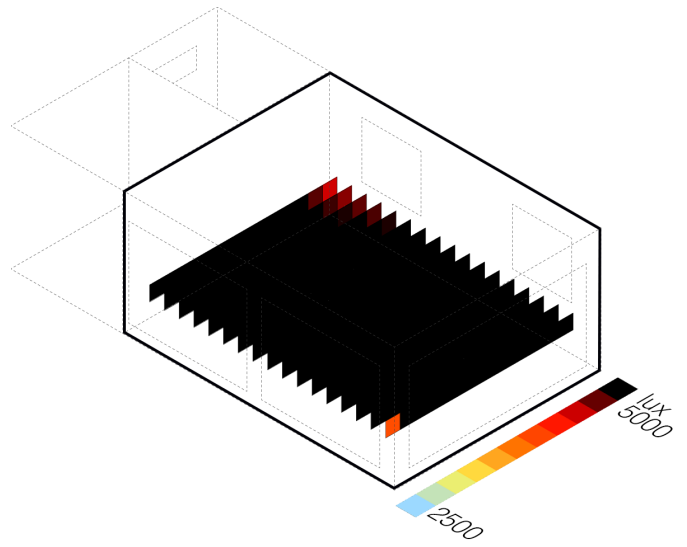


Figure b5.15 10 am

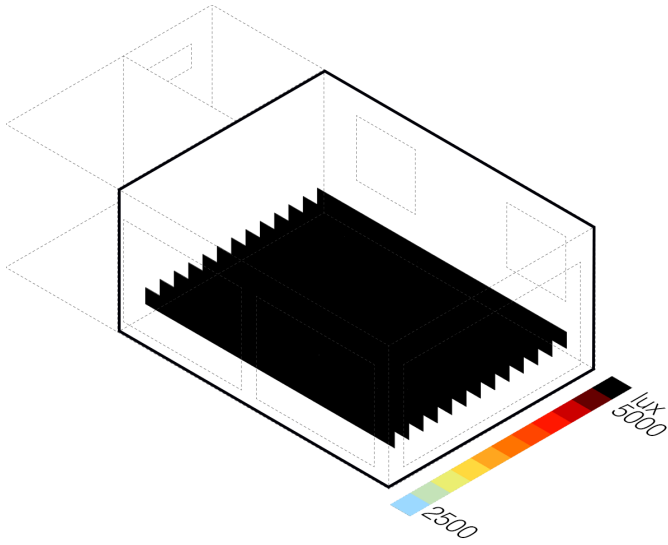


Figure b5.16 12 pm

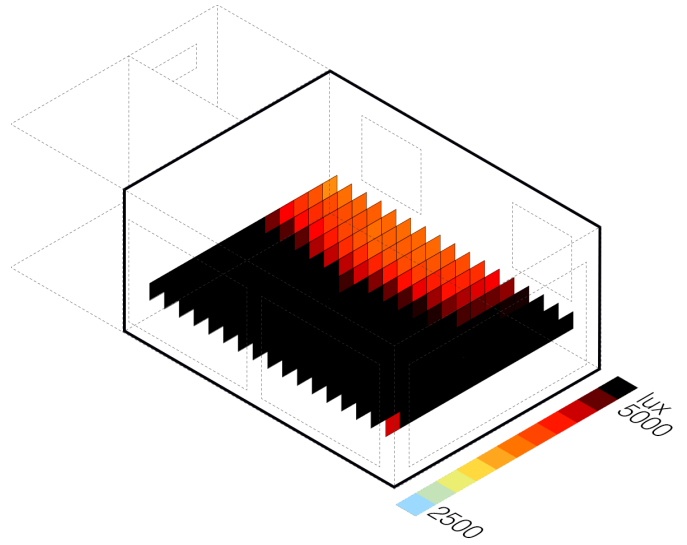


Figure b5.17 12pm

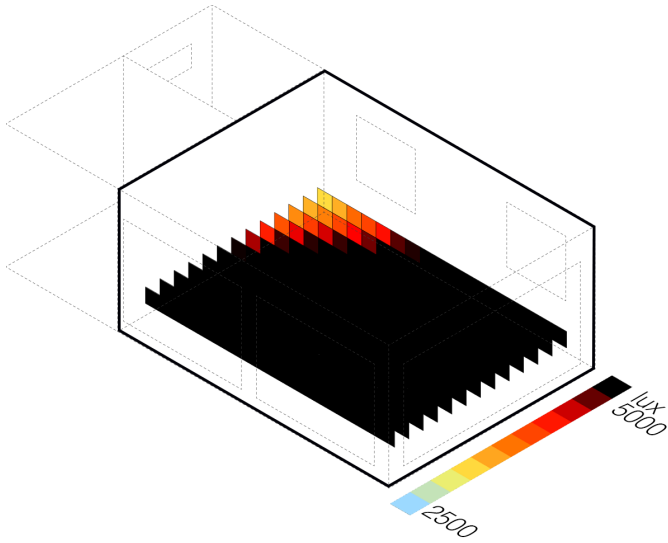


Figure b5.18 14pm

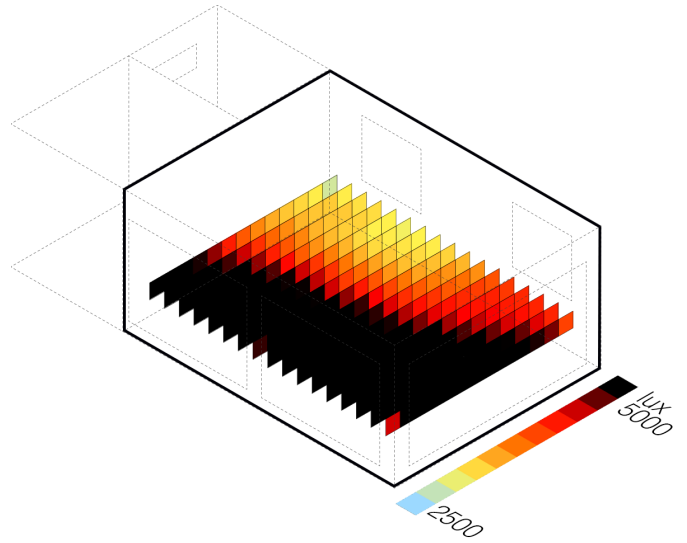


Figure b5.19 14pm

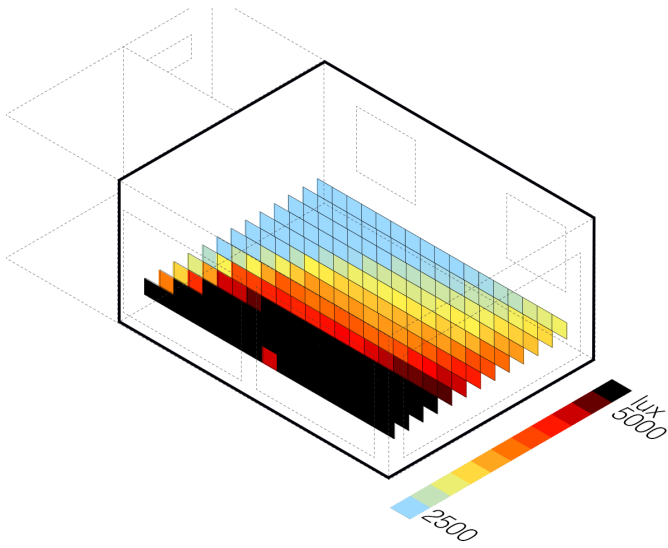


Figure b5.20 16pm

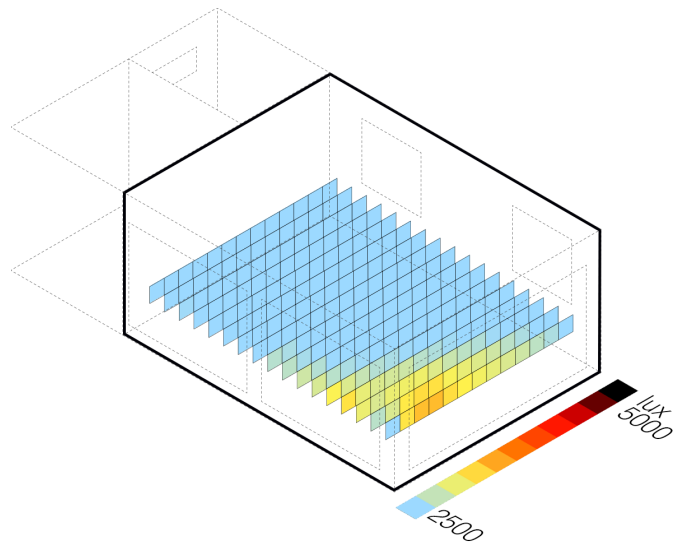


Figure b5.21 16pm

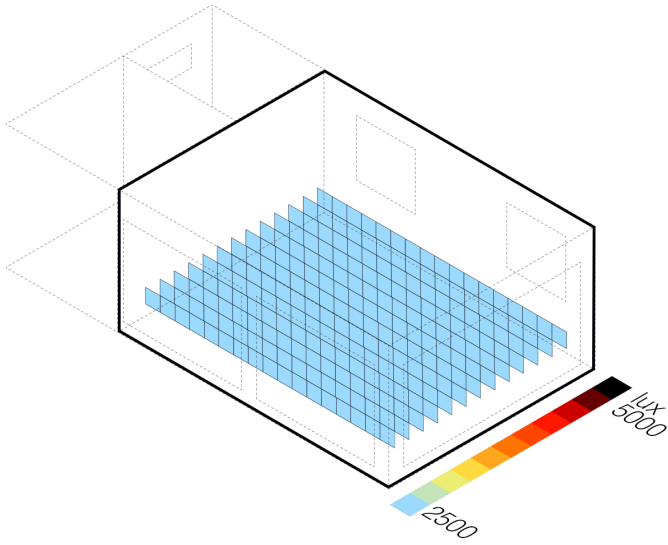


Figure b5.22 8 am

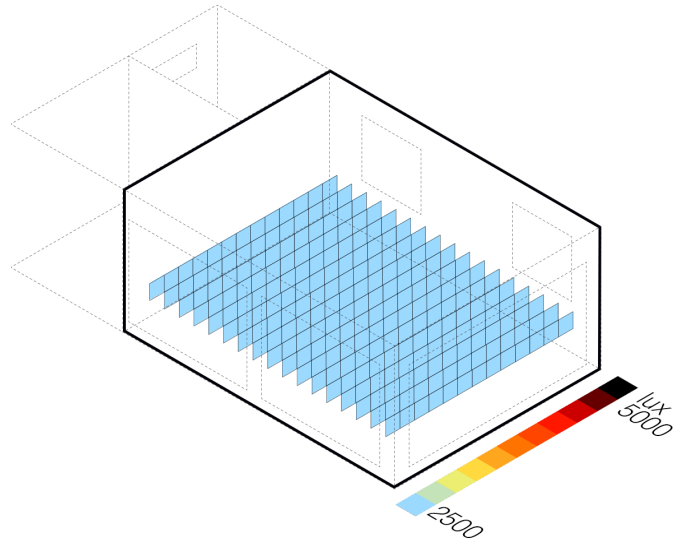


Figure b5.23 8 am

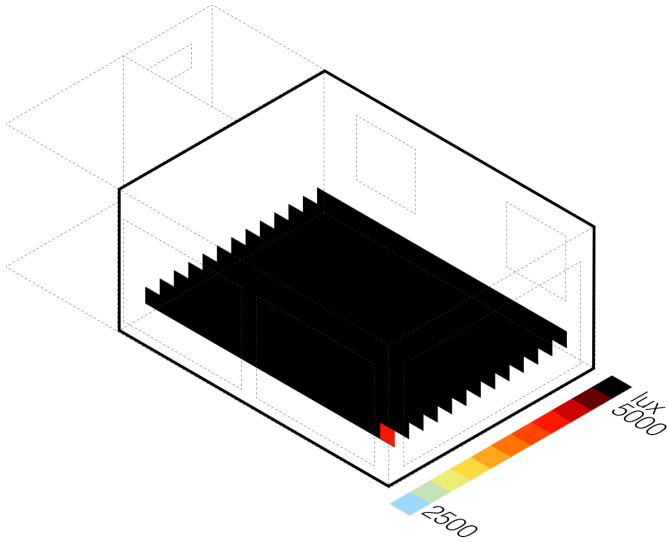


Figure b5.24 10 pm

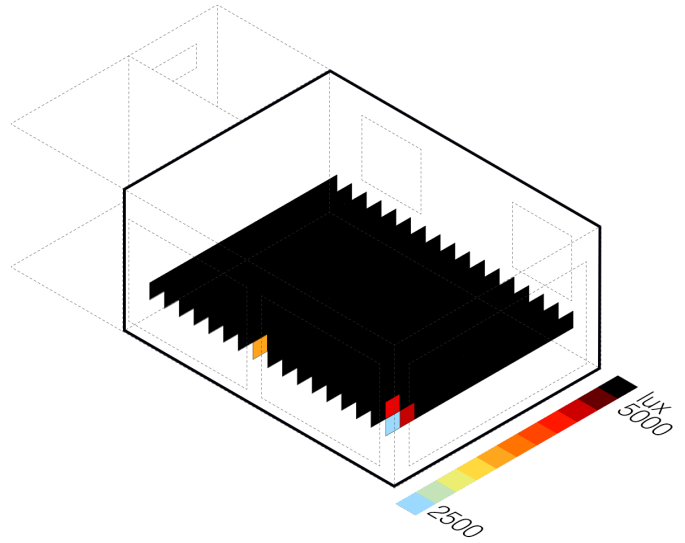


Figure b5.25 10 pm

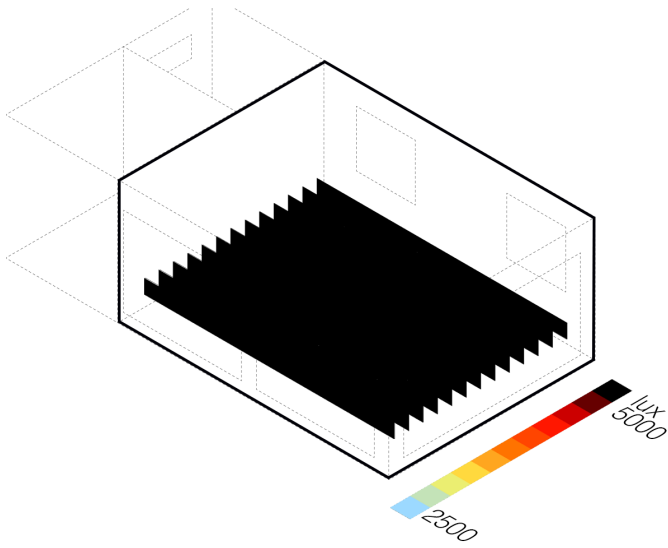


Figure b5.26 12pm

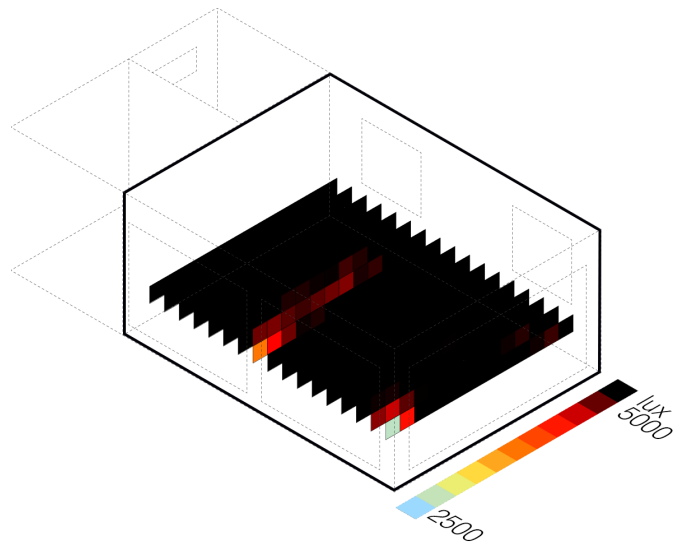


Figure b5.27 12pm

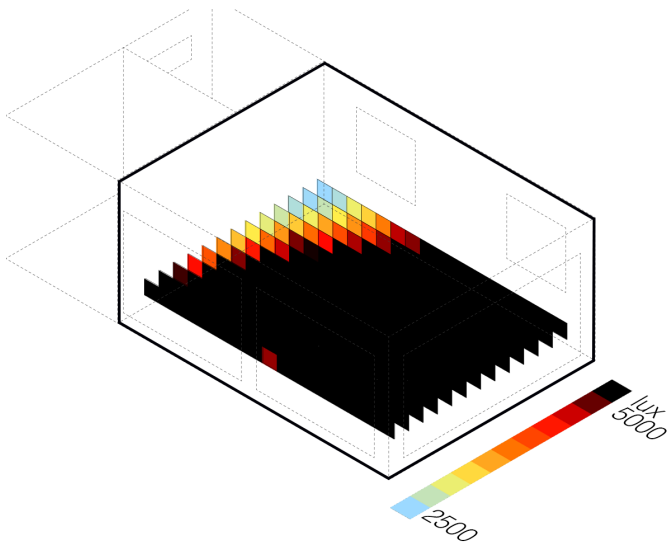


Figure b5.28 14 pm

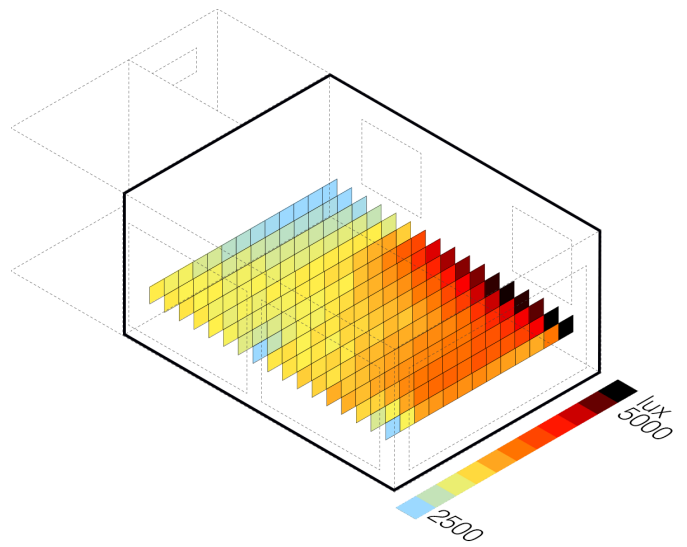


Figure b5.29 14 pm

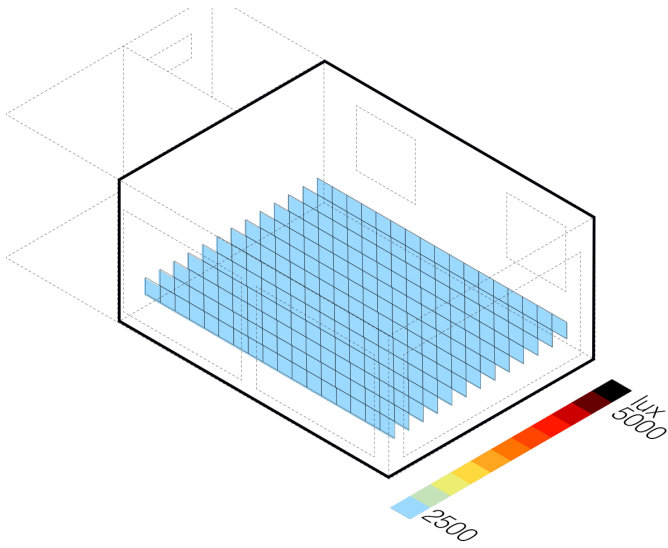


Figure b5.30 16 pm

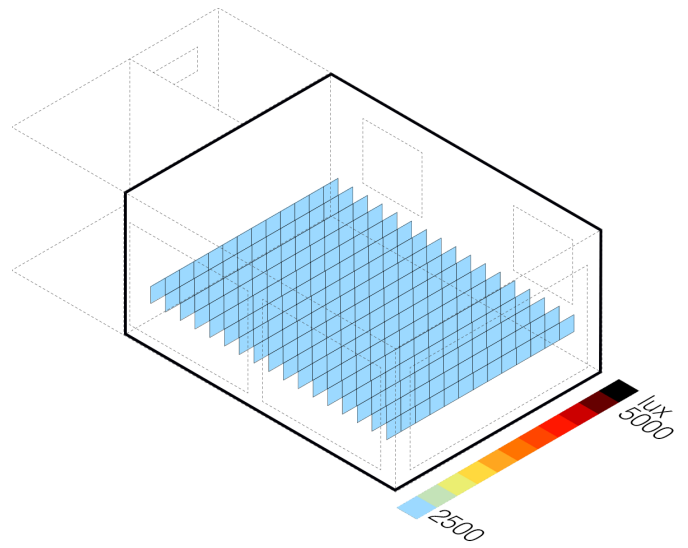


Figure b5.31 16 pm

south - Annual glare simulations

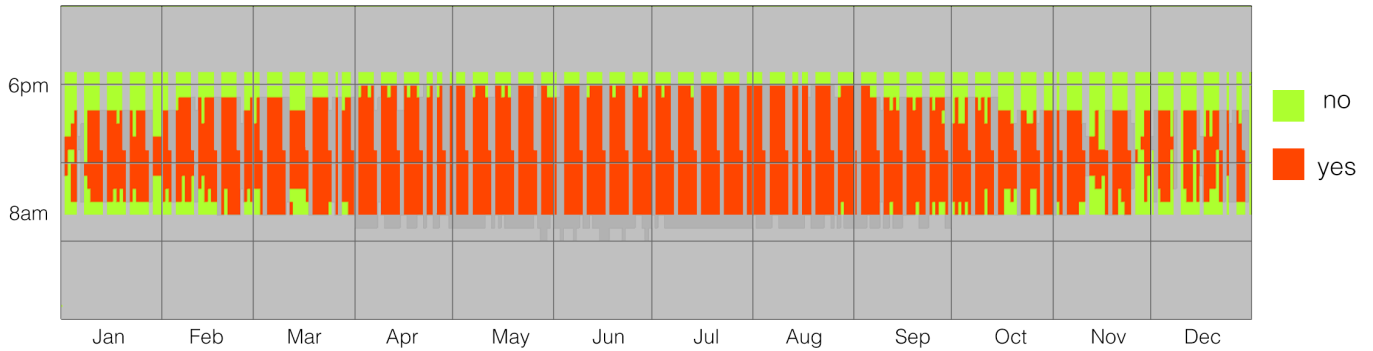


Figure b5.32 point 54 annual glare simulation (see figure a.22 pag 59)

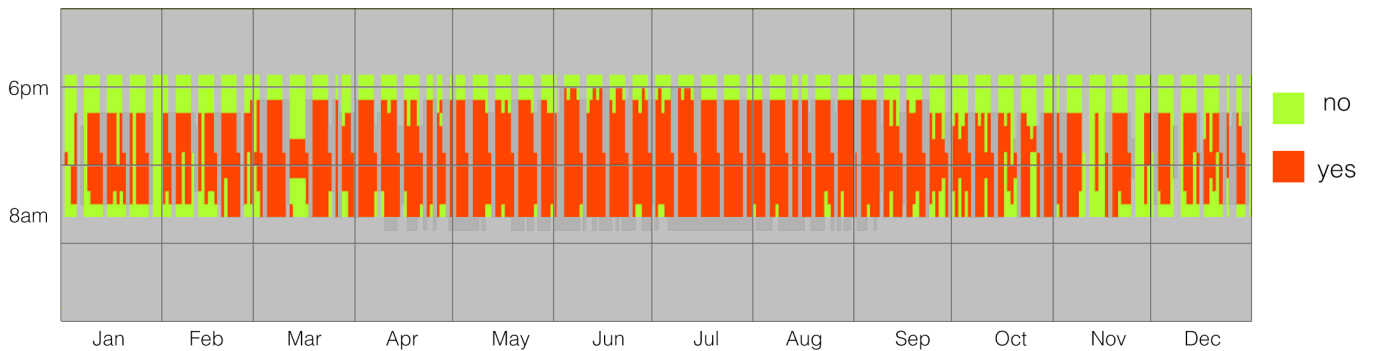


Figure b5.33 point 58 annual glare simulation (see figure a.22 pag 59)

South Oriented points display glare condition most of the time of the year, during full occupancy (from 8am to 6pm).

south - spatial glare maps

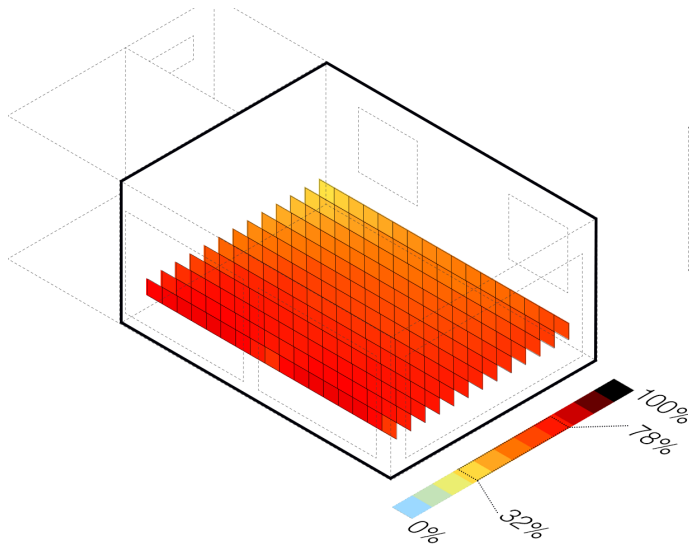


Figure b5.34 South glare map

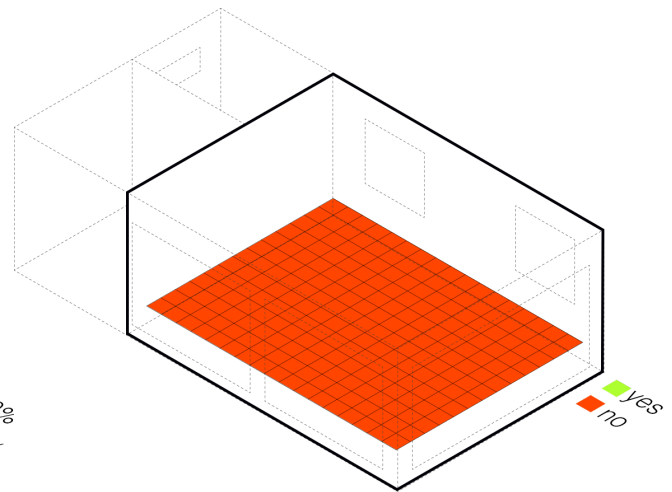


Figure b5.35 South glare map - verified/not verified condition

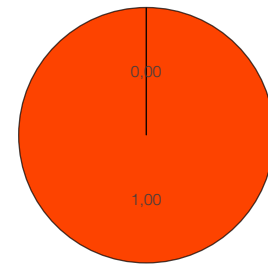


Figure b5.34 show % of time when dgp occurs in relation to south oriented Ev results. Up to 78% of time is in glare condition, which is about 2362 hours. None of the points is under or equal to a maximum of 150 hours of glare

east - Annual glare simulations



Figure b5.36 Point 32 annual glare simulation (see figure a.22 pag 59)

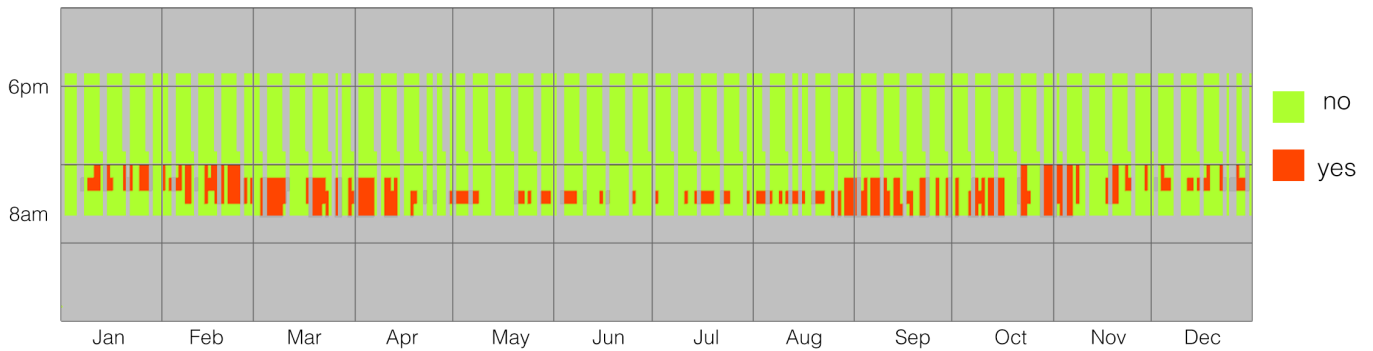


Figure b5.37 Point 71 annual glare simulation (see figure a.22 pag 59)

East Oriented points display glare condition just in morning time till 12pm

east - spatial glare maps

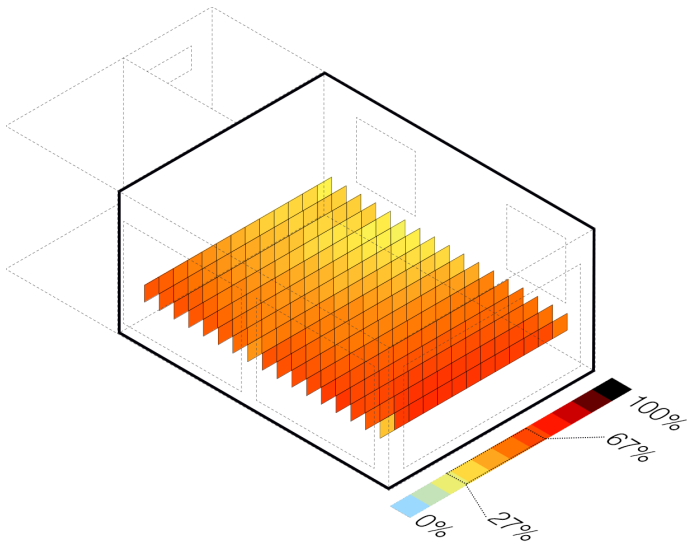


Figure b5.38 East glare map

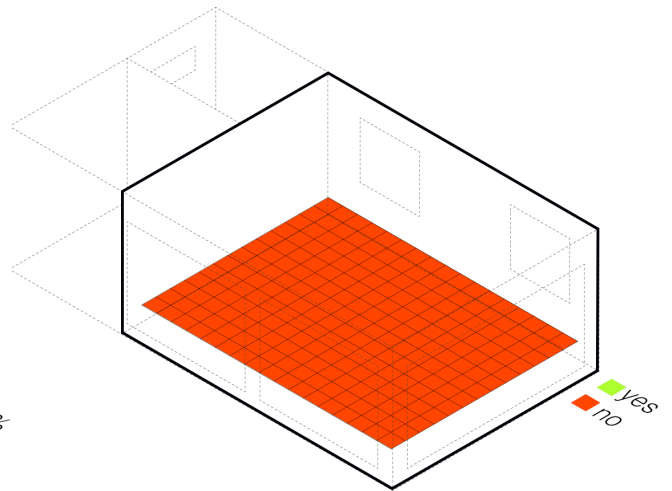
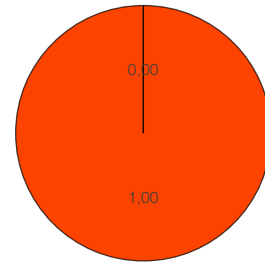


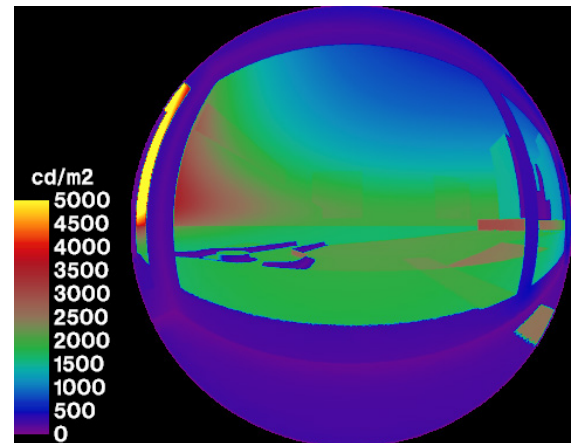
Figure b5.39 East glare map - verified/not verified condition



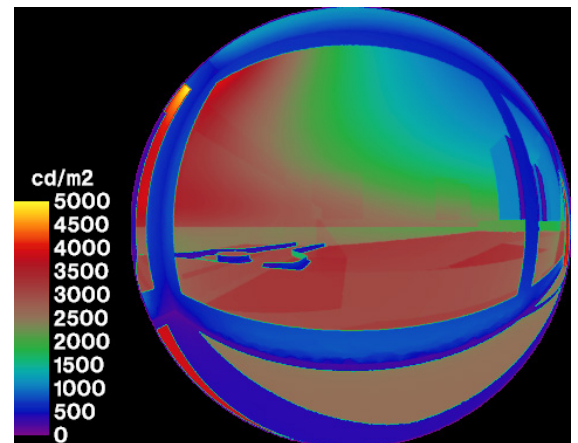
Following Images based on Evalglare analysis show, from 8am to 4pm, worse values in mid-day summer and winter hours (10-14pm), with winter having higher critical values.

East view presents disturbing to intolerable glare conditions in the hour range between 10 am and 12 pm.

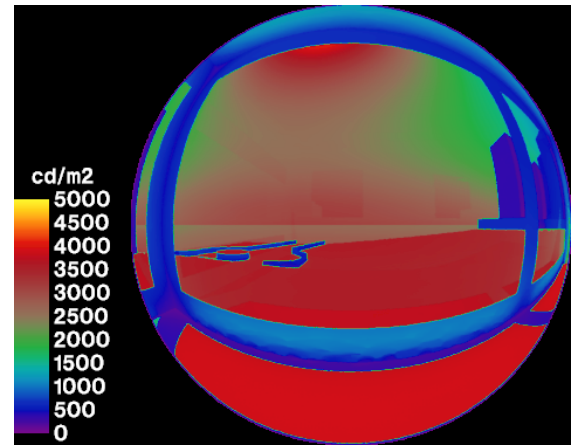
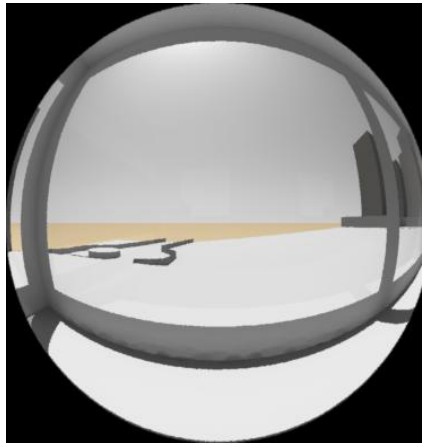
8 am
DGP = 36%



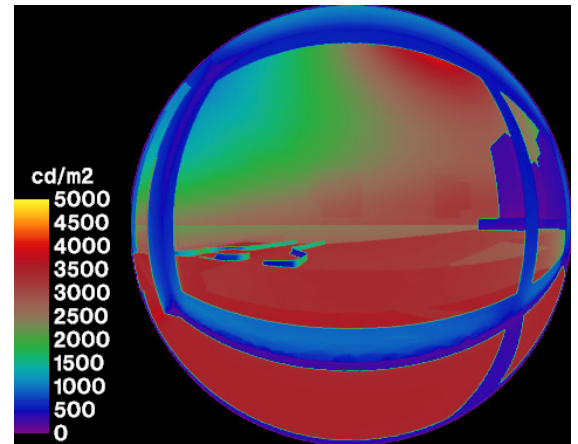
10 am
DGP = 50%



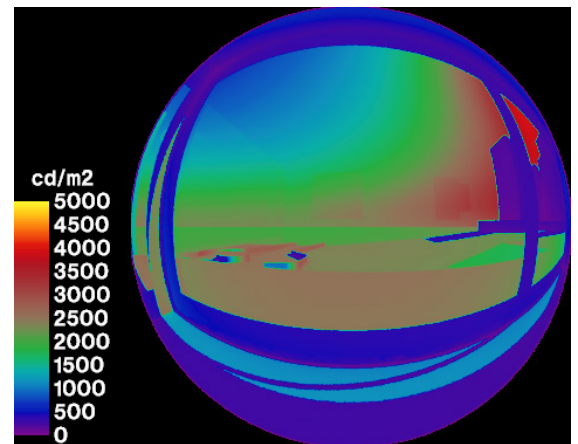
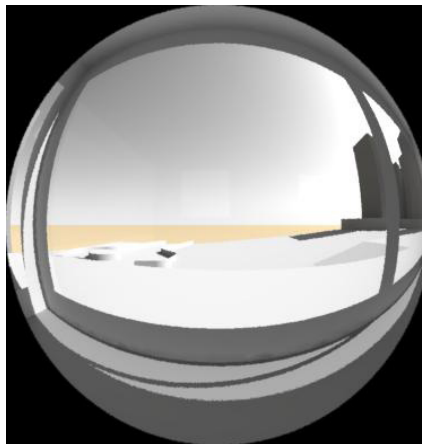
12 μm
DGP = 59%



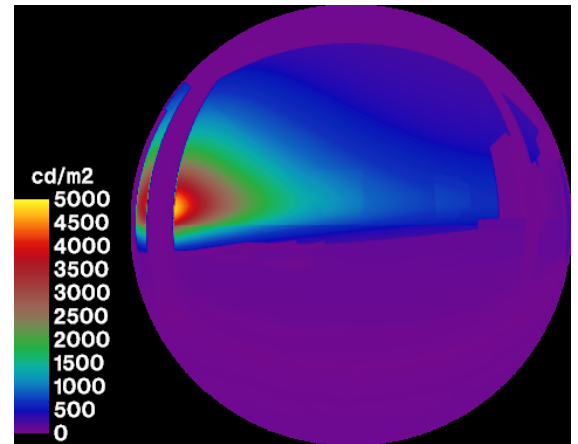
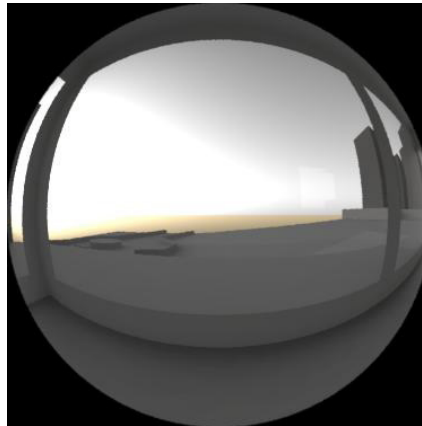
2 μm
DGP = 55%



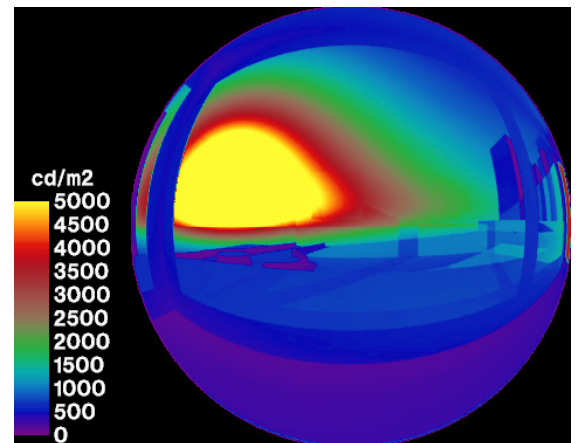
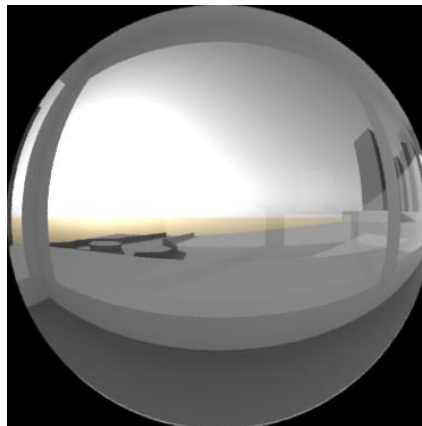
4 μm
DGP = 40%



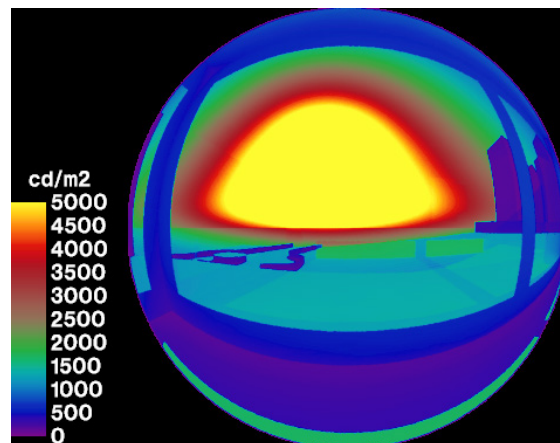
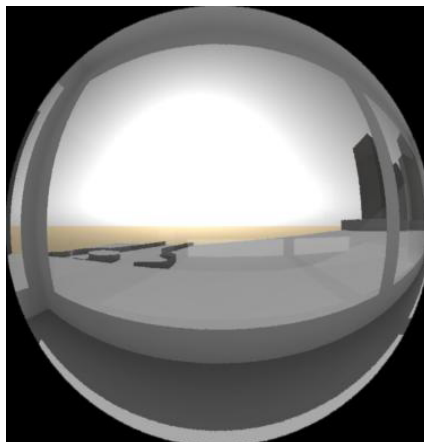
8 am
DGP = 24%



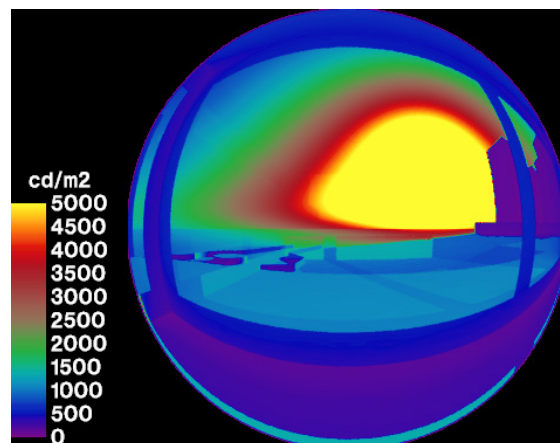
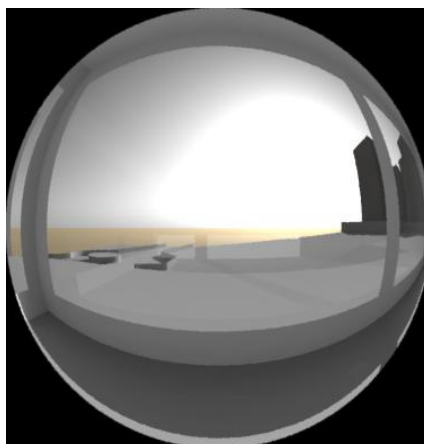
10 am
DGP = 100%



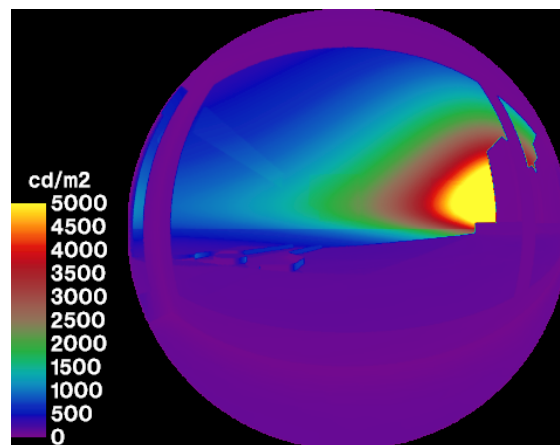
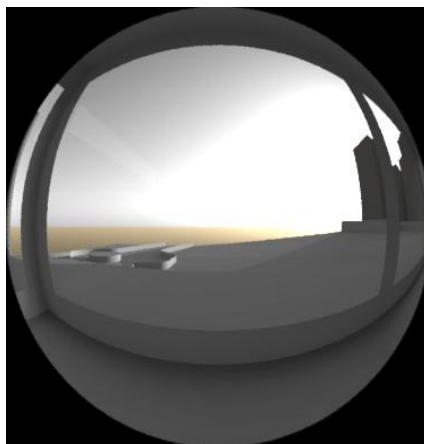
12 pm
DGP = 100%



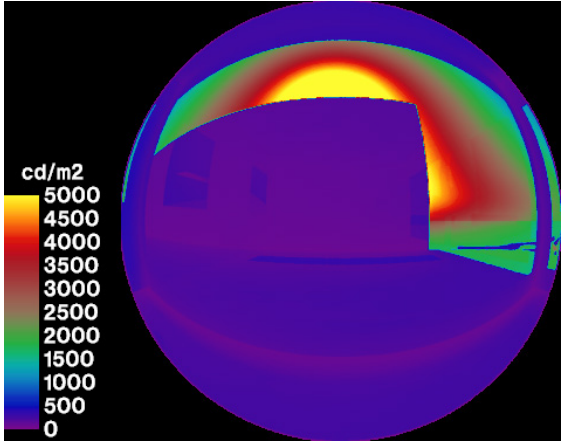
2 pm
DGP = 100%



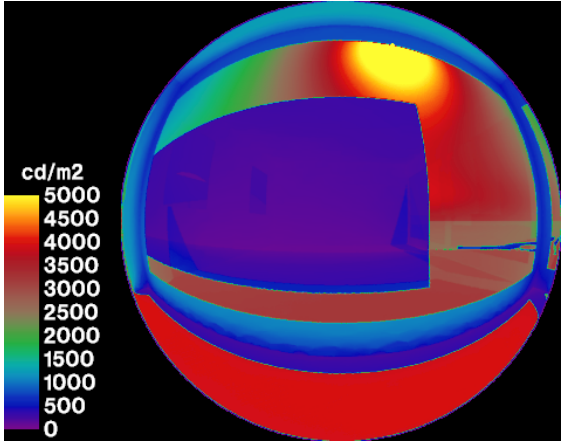
4 pm
DGP = 29%



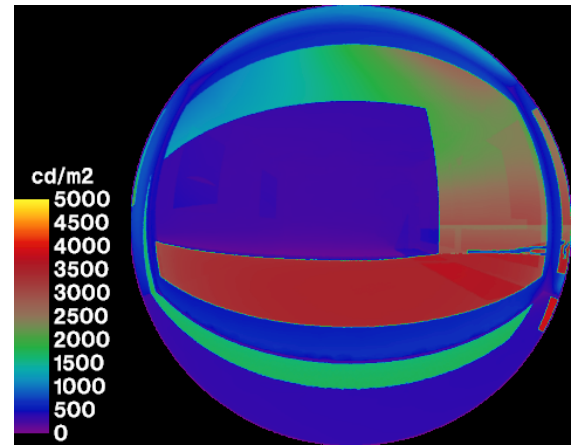
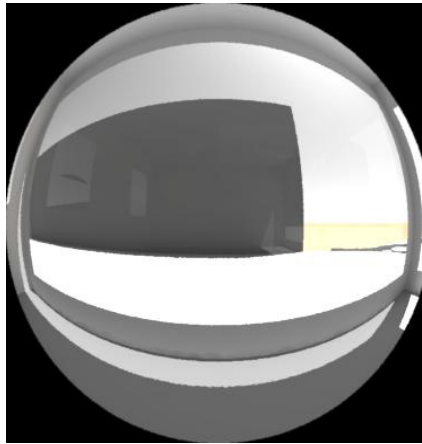
8 am
DGP = 31.4%



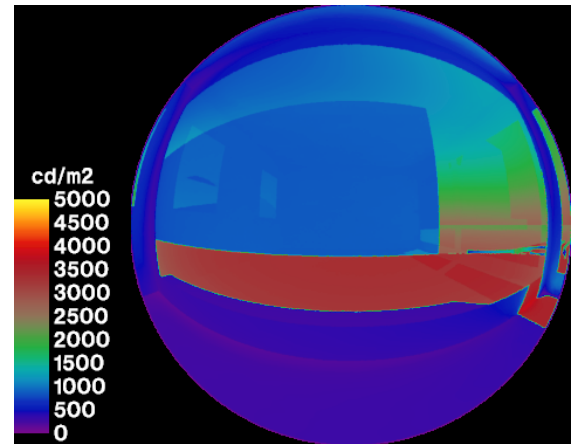
10 am
DGP = 100%



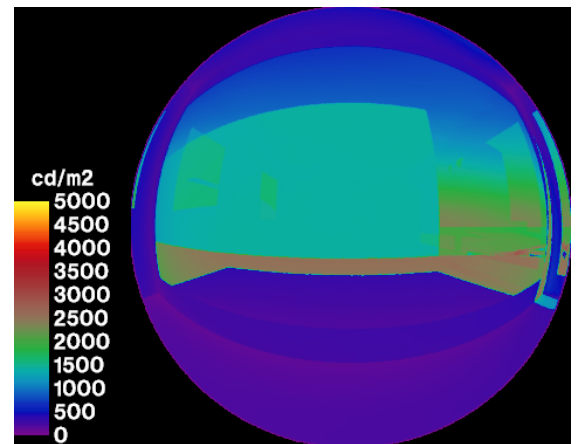
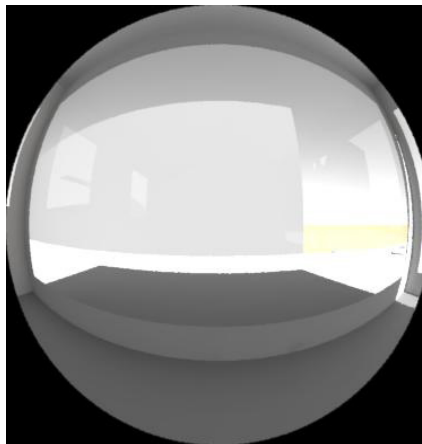
12 pm
DGP = 39%



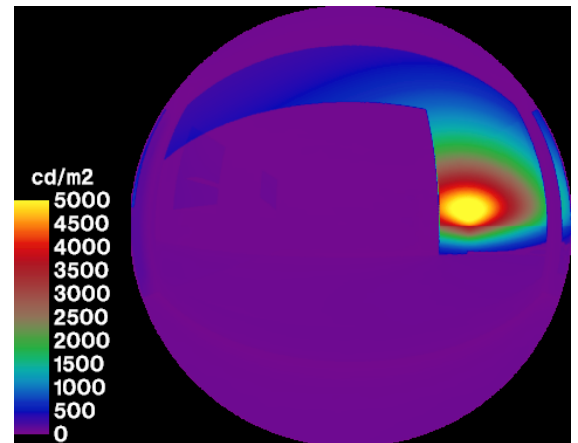
2 pm
DGP = 36%



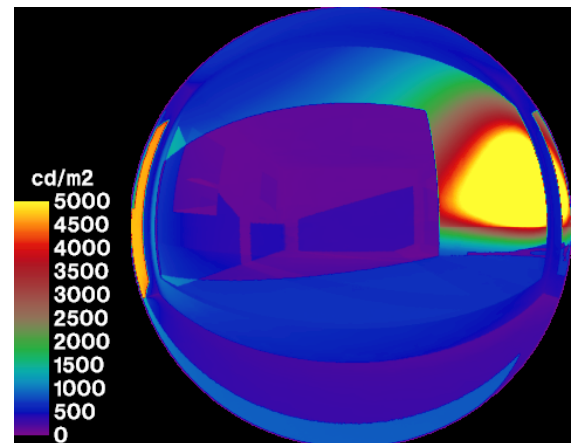
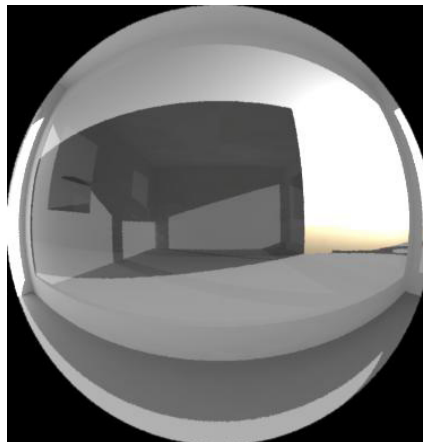
4 pm
DGP = 32%



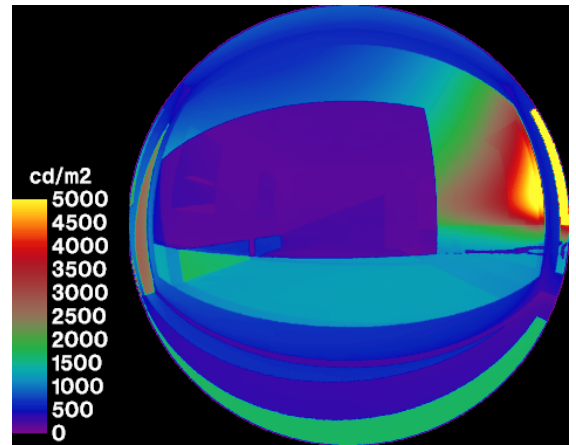
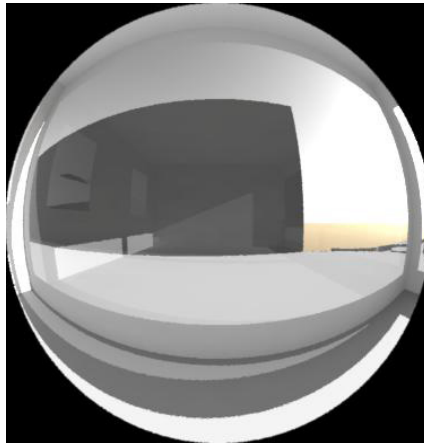
8 am
DGP = 24%



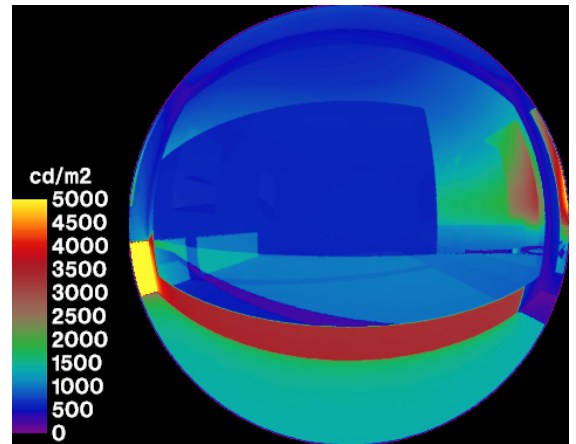
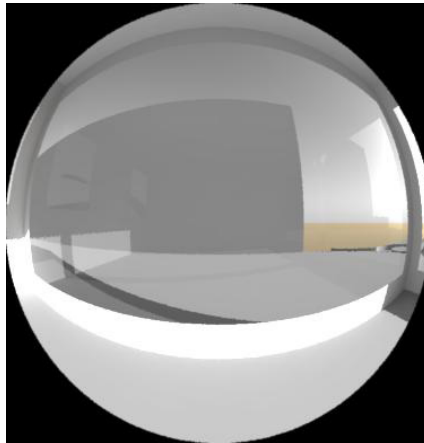
10 am
DGP = 100%



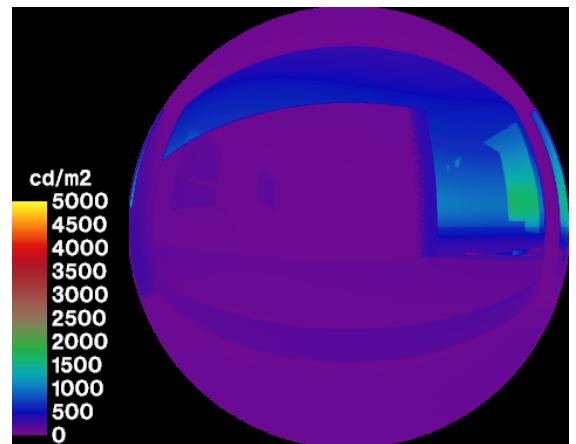
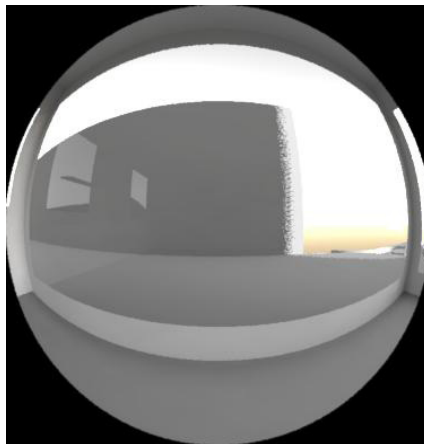
12 μm
DGP = 73%



2 μm
DGP = 37%



4 μm
DGP = 20%



B7. Thermal + visual comfort

This section aims at comparing both thermal and visual comfort analysis.

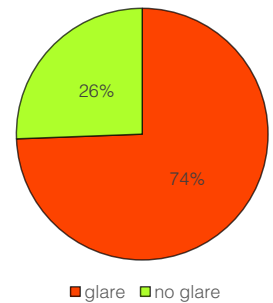
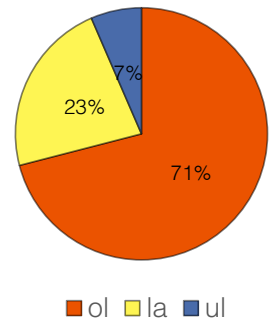
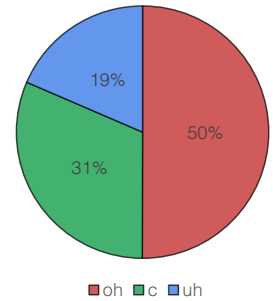
In particular, based on results from simulation “b” and application of PMV comfort model, Over-heated, Comfort and Under-heated Range will be related to Over-lit, Luminous Autonomy and Under-lit ranges for chosen point in space (e.g. point 54)

Moreover, Glare analysis results from previous section, obtained with simplified method, will also be considered in an “overall” comfort evaluation among these parameters, thus having a comparison between 7 variables. First, thermal and visual variables will be represented separately. Secondly, an attempt to put them together will be presented.

We have defined Thermal Ranges in previous pages. Luminous Autonomy can be defined as

the percentage of occupied time when a specific target condition is satisfied on a point (area). This is very similar to Daylight Autonomy. In this case, similarly to Won Hee Koa et Al. [19], Luminous Autonomy will be computed according to the definition of $UDI < 100$, $100 < UDI < 3000$ and $UDI > 3000$, corresponding to under-lit, luminous autonomy and over-lit range. Thus, the percentage of time during which a point is in between 100 and 3000 lx is considered autonomous.

Again, for glare thresholds, each time a point overtakes 0.4 dgp %, is considered as “not comfortable”.



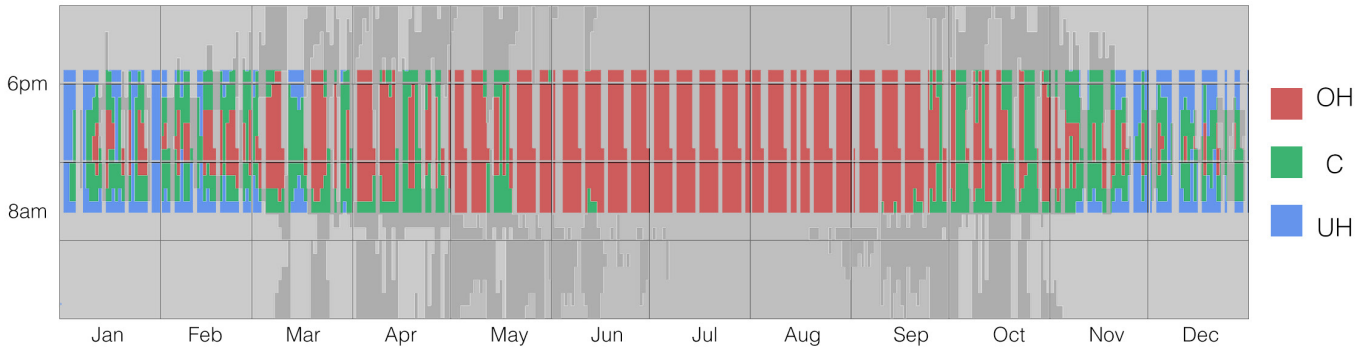


Figure b7.1 Overheated (OH), Comfort (C) , Underheated (UH) hours

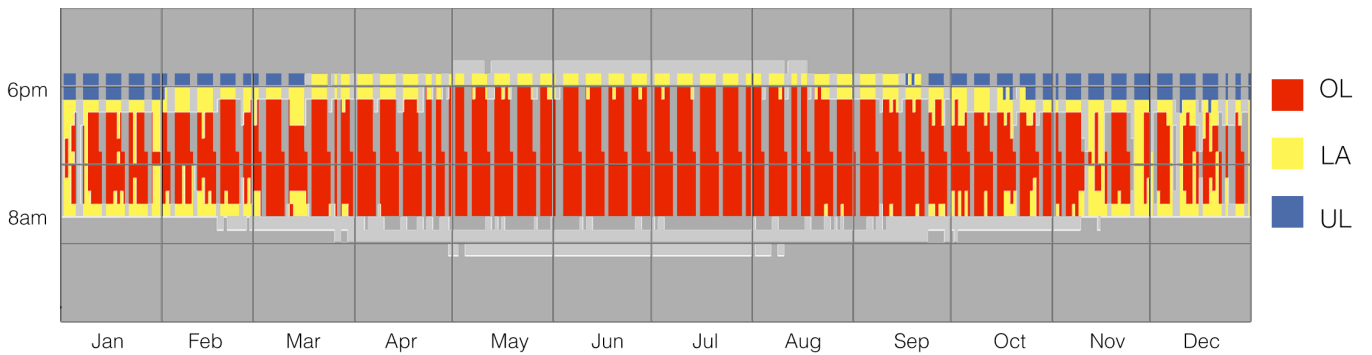


Figure b7.2 Overlit (OL), Luminous Autonomy (LA), Underlit (UL) hours

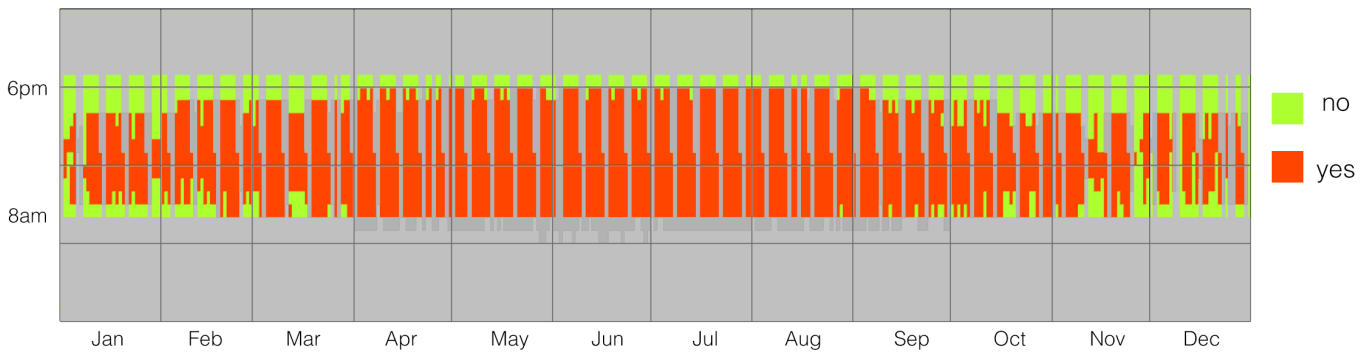


Figure b7.3 Yes/No glare - 0.4 dgp threshold

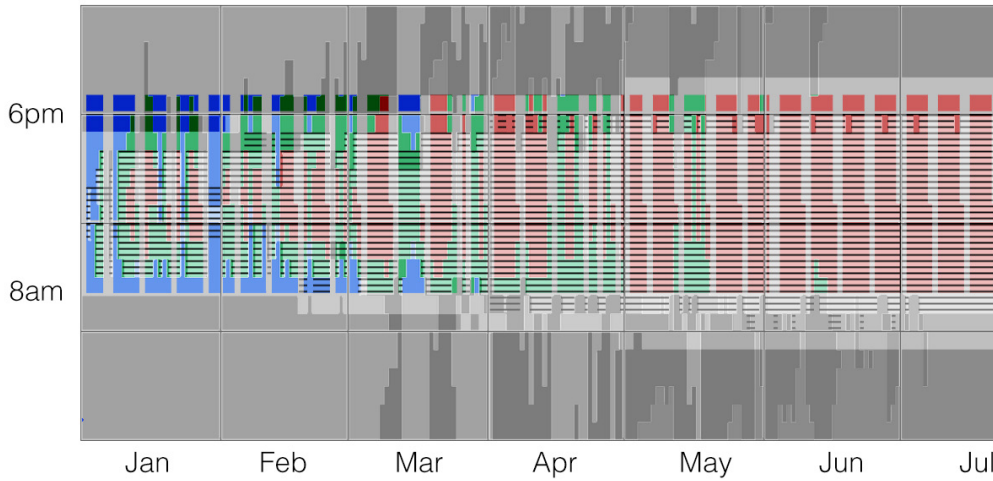
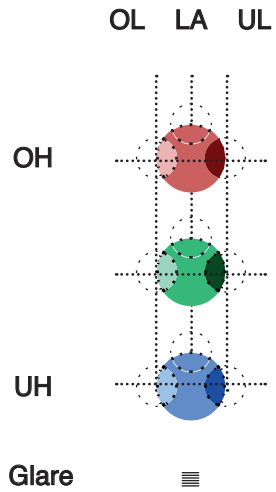
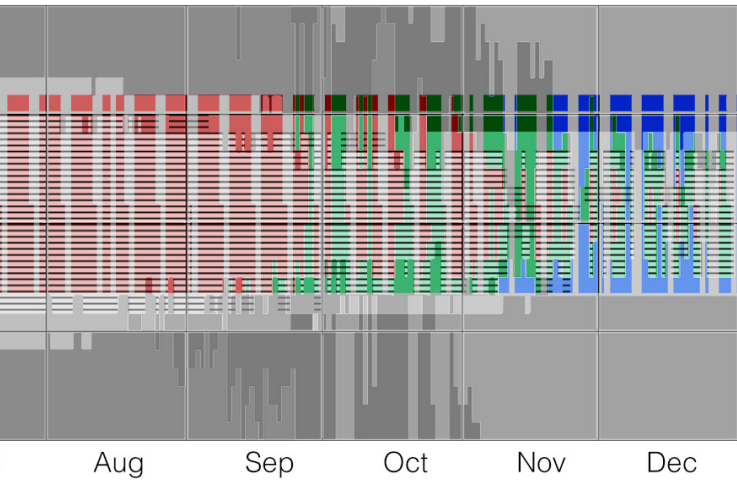
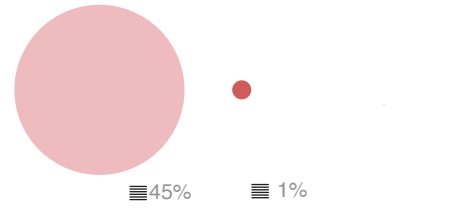


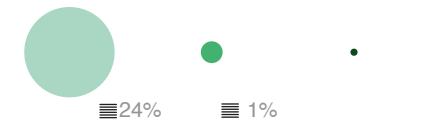
Figure b7.4 Thermal + Visual Comfort evaluation. Point 54



45% 5% 0%



24% 6% 2%



2% 12% 4%



Findings & comments p1

Without considering solar radiation falling on occupants, Adaptive Model simulation results show almost the same degree of thermal comfort reached in simulations with HVAC system on. Simulation b1 indicates 31% of thermal autonomy, 55% of under-heating and 14% of overheating occurring in July and August, whereas simulation b2 reveals a comfort zone range of 32%, a slightly higher amount of overheating (21%), in comparison to under-heated hours (47%). Yet, with HVAC system, there is a good degree of ventilation autonomy, which suggests lower concentration of CO₂. Moreover, when HVAC is on, there is a better control on humidity range as well, stabilizing it in the acceptable range of 30 – 50/60 % (compare figure b1.4 and b2.2).

Annual Radiation Analysis and SolarCal model application highlight considerable ARD (annual radiation discomfort) values. In particular, as it is visible in figures b3.17, more than half of test points receive ARD for more than 50% of Occupied time. Major-than-4° DeltaMRT is many times occurring. This is reflected on thermal simulations (both Adaptive and PMV), based on adjusted Top,

**up to
1787 hrs
overheated**

showing overheated % area ranging from 45 to 59%, corresponding to 1787 hours (see figures b3.28-b3.29).

Similar trend is found in Daylight analysis, where, whether Spatial daylight Autonomy and

very low under-lit area depicts high quantity of natural light during the year, overlighting and glare occurs. This is stressed in “ASE” evaluation and “UDI more-than range”. Exceeding ASE is measured for 94% of space, while UDI>3000 exceeds with an average of 59% of time. Vertical illuminances show most critical values on September 21st, reaching and going beyond 5000 lx, but glare conditions seem to

**up to
2362 hrs
glare**

occur frequently during the year, due to high and wide critically oriented glass surfaces. Image b5.34 shows south glare ranges from 32% to 78% of occupied time, which is up to 2362 hrs when glare occurs. Interestingly, point 54 simplified glare

0%

Thermal comfort %

evaluation depicts a very similar annual plots to UDI over-lit % of time (images b7.2-3).

for increasing thermal and visual discomfort.

This can be done at least by:

To sum up, as it is visible from Figure b7.4 (see pag.116-117), baseline simulation results highlights high degree of

a. improving window properties and adopting more solar-control glass

a)Over-heating, in particular:

b. designing shading to block undesired direct sun exposure and solar gains

From Jan to Febr, Oct to first half of Nov:

- 11am to 16pm

March to April:

- 9am to 17pm

May to Sept:

- 8am to 5/6pm

45% of total over-heating time is over-lit, which suggests a clear intervention in window design envelope.

b)high degree of Over-lit time, up to 71% of time.

0%

UDI achieved %

According to BPS performance parameters explained on page 38, none of these is verified.

Test laboratory needs design solutions to decrease excessive solar radiation, main responsible

0%

glare protection %

C - new glass specs

C1. Thermal Comfort Analysis



Figure c1.1 Concept scheme of solar energy through glazing

When solar radiation hits a glazing, there are three main components involved:

a. E_{DT} which is direct transmitted radiation

	baseline			new glass		
	s windows	n windows	e window	s windows	n windows	e window
g val	0,37	0,37	0,35	0,17	0,4	0,26
vt	0,7	0,7	0,7	0,2	0,6	0,35
U val	1,4	1,4	1	1,1	1,1	1,2

Figure c1.3 Window specs in comparison with previous scenario

b. E_R which is reflected radiation
 c. E_A which is absorbed radiation

Moreover, as we can see from figure c1.1, there are two more sub-elements involved, coming from the energy absorbed by the glazing. In particular, one is re-emitted inside and a part of it is re-emitted outside.

As we can see from figure c1.2, solar spectrum is characterized by 5% ultraviolet (UV), 43% visible light (VL) and around 52% near-infrared (NIR). UV and VL covers shorter wavelengths, hence carrying higher amount of energy, while infrared region covers larger quantity of solar spectrum.

Common strategies to reduce solar gains is to adopt solar control glazing with reflective coatings (low-e glass), which are characterized by a lower “g-value”. “g value” or “SHGC” (solar heat gain coefficient) is the fraction of incident solar radiation transmitted through the glazing, usually in the range 0,2-0,7.

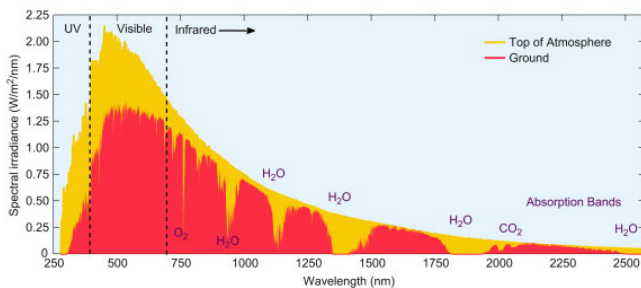


Figure c1.2 Solar Spectrum according to Wavelength

Lower the value the lower the solar gain. Note that, by manipulating this coefficient, there is influence on such parameters as “visible transmittance”. Hence, very low g values usually indicates lower visible transmittance of light through glazing. Whether this could mean reducing overheating, it could worsen daylight conditions in the ambient.

In this chapter, different glass properties are applied to previous baseline scenario. In particular, 3 main parameters are considered:

- a. g value
- b. Visible transmittance “ τ_v ”
- c. thermal transmittance “U”

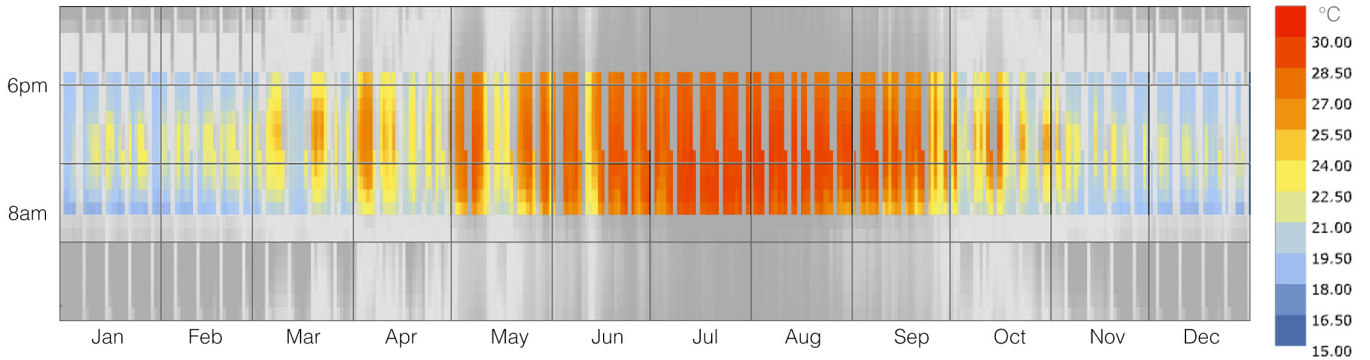


Figure c1.4 Adjusted Operative Temperature - new glass scenario

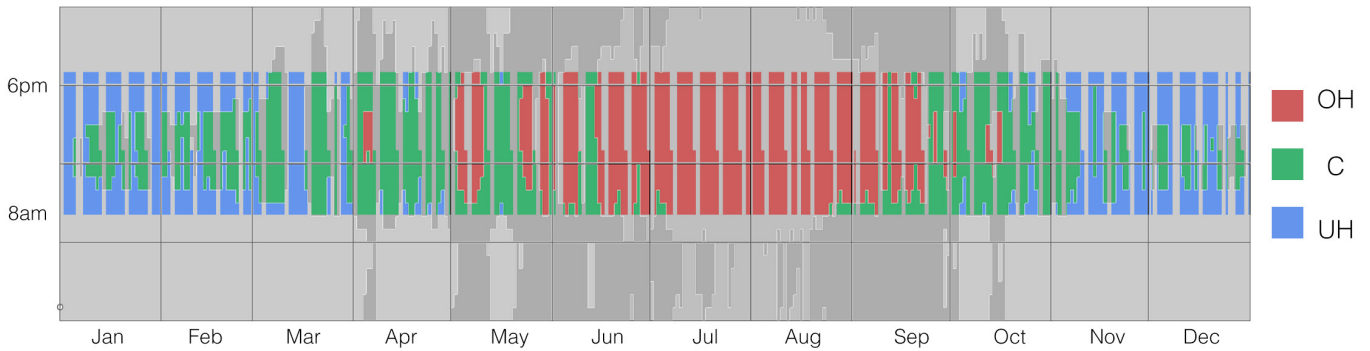
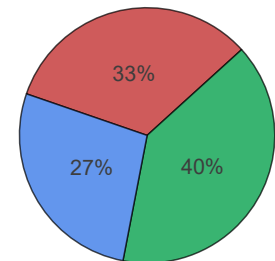


Figure c1.5 Over-heated, Comfort and Under-heated ranges - new glass scenario

Figure c1.5 and c1.6 shows that, even if applying strict glass properties to both south and east windows (glazing in baseline scenario is already low-e), 33% of over-heating still remains, mainly from June to September. A little increase in both Comfort % and Under-heated % is found.



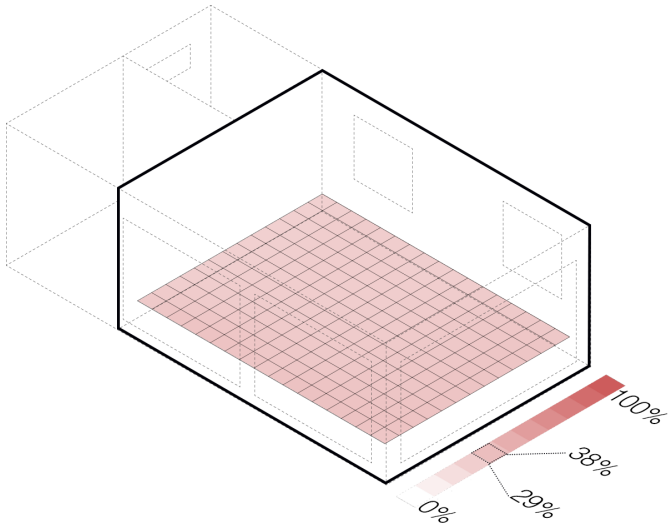


Figure c1.6 Over-heated map

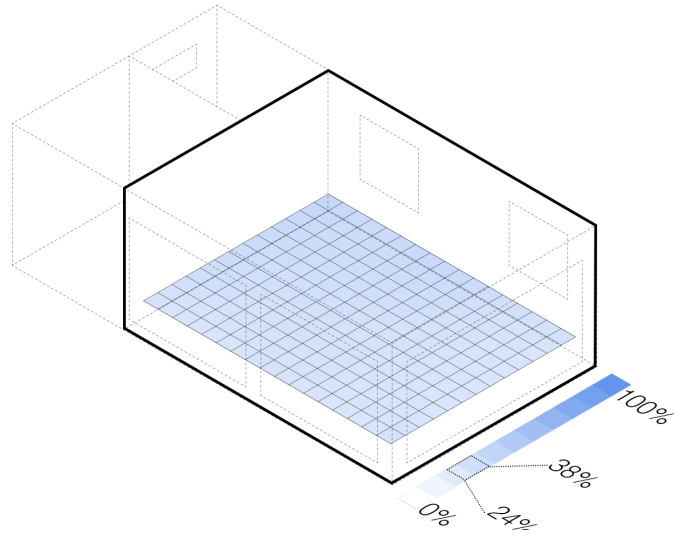


Figure c1.7 Under-heated map

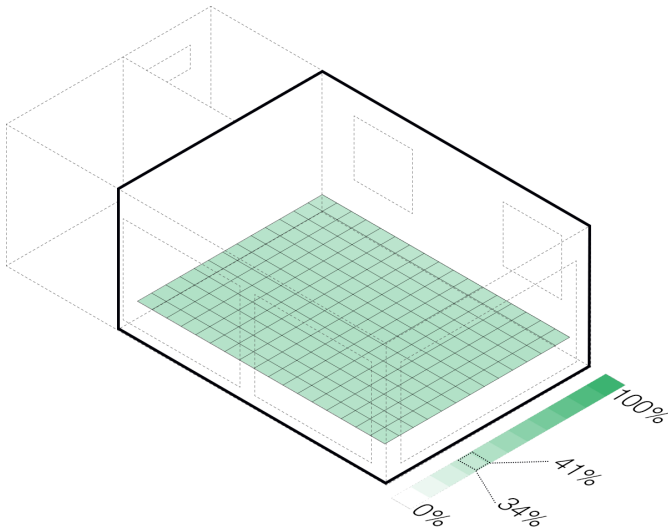


Figure c1.8 Comfort map

C2. CBDM & Daylight Analysis

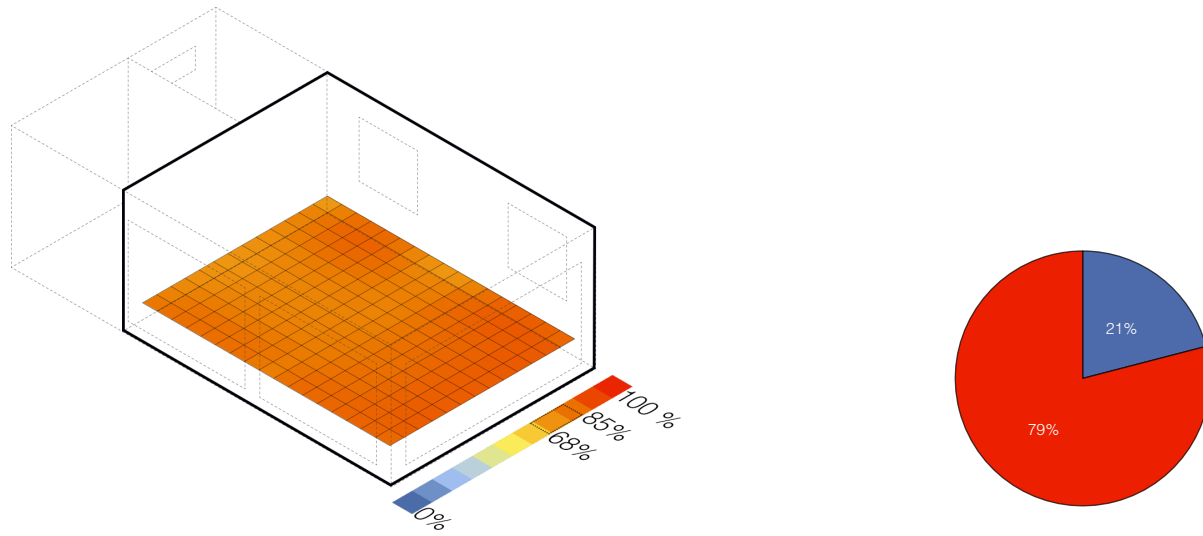


Figure c2.1 Daylight Autonomy

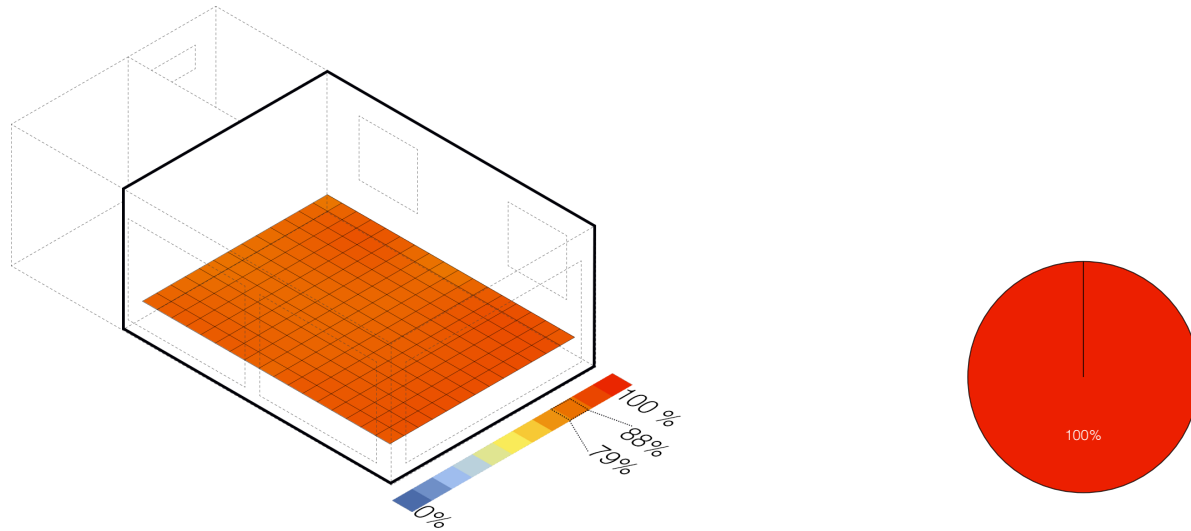


Figure c2.2 Spatial Daylight Autonomy

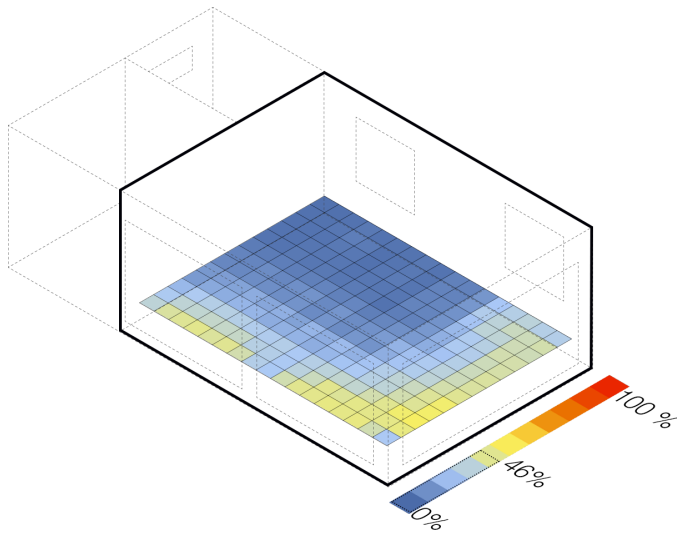


Figure c2.3 UDI>3000 lx

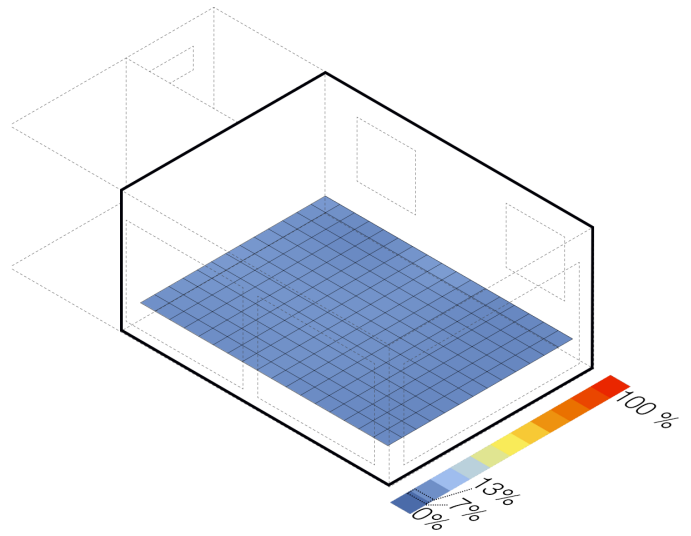


Figure c2.4 UDI<100 lx

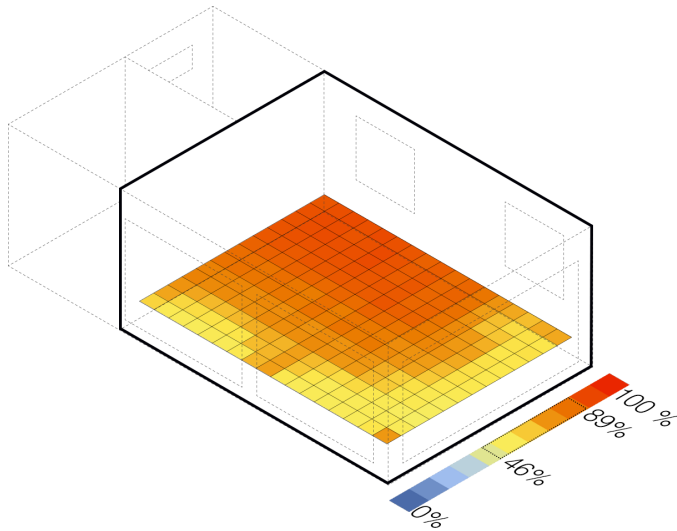


Figure c2.5 UDI,achieved

Figure c2.5 shows UDI in-between 100 and 3000 lx. Area closer to east and south windows reaches lower % values up to 46%, indicating less than half of occupied time outside the luminous autonomy range. In other words, there is still too much asymmetry in the illuminance distribution across the space.

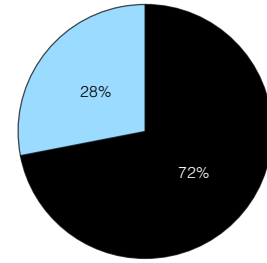
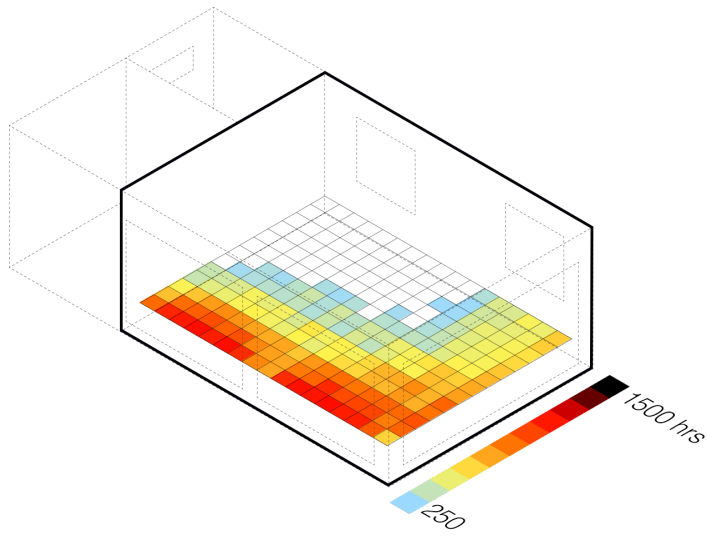


Figure c2.6 ASE

In Figure c2.6 Annual solar Exposure is not verified for 72% of space. Some points still overtake acceptable value up to 4-5 times (see red area).

Luminous Autonomy - 3 points

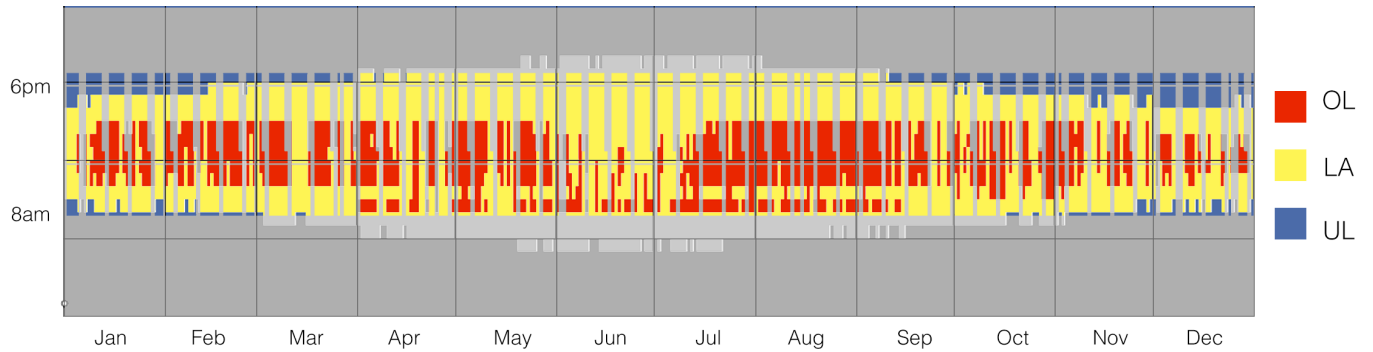


Figure c2.7 Over-lit (OL), Luminous autonomy (LA) and Under-lit (UL) range - point 54

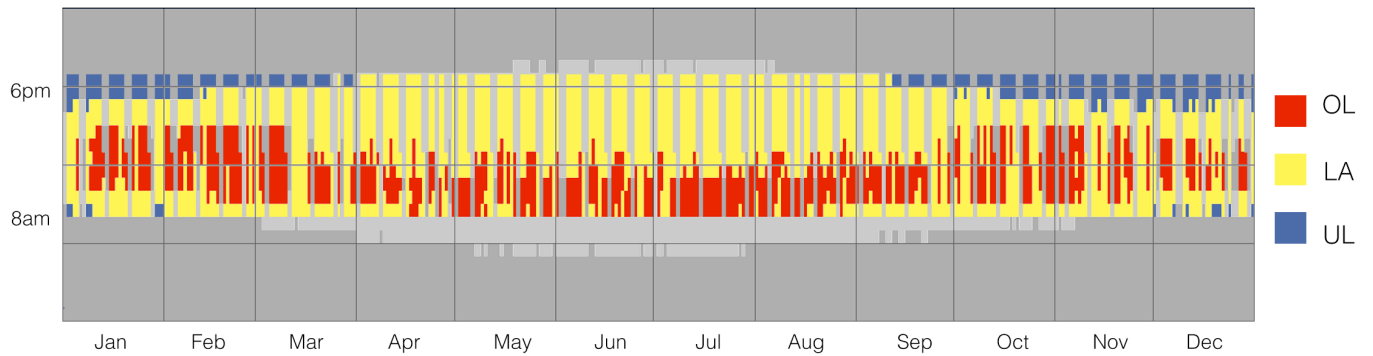


Figure c2.8 Over-lit (OL), Luminous autonomy (LA) and Under-lit (UL) range - point 32

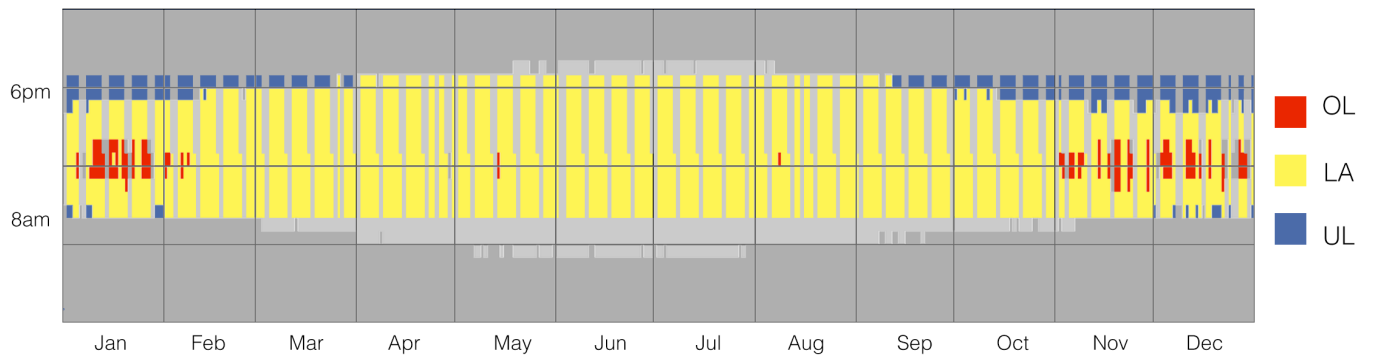


Figure c2.9 Over-lit (OL), Luminous autonomy (LA) and Under-lit (UL) range - point 179

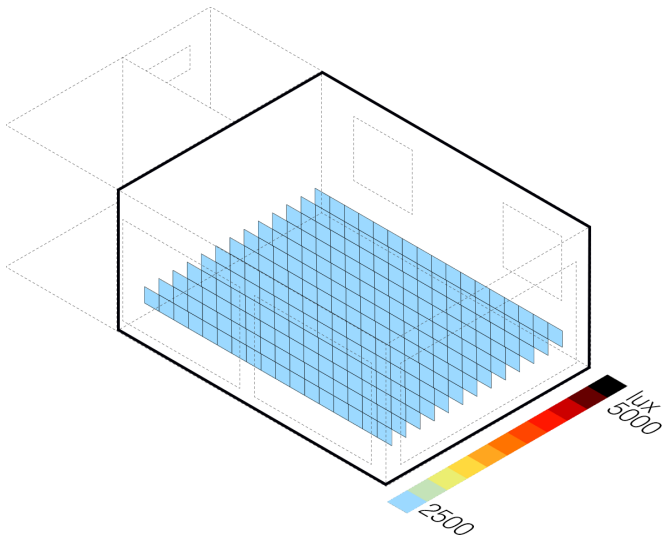


Figure c3.1 8 am

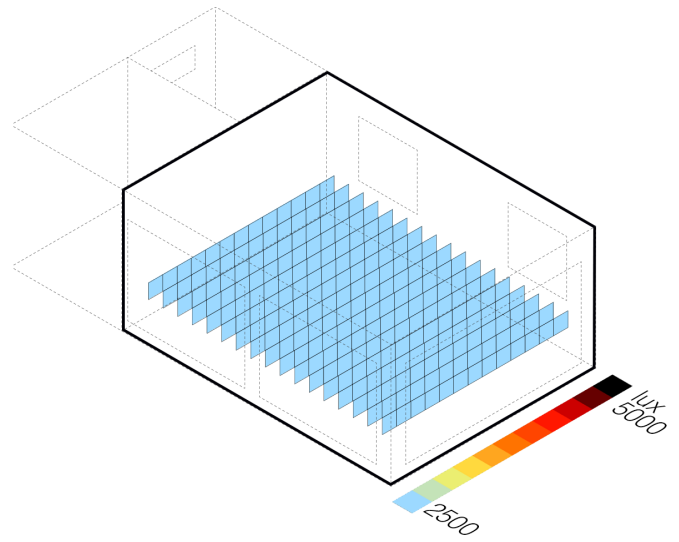


Figure c3.2 8 am

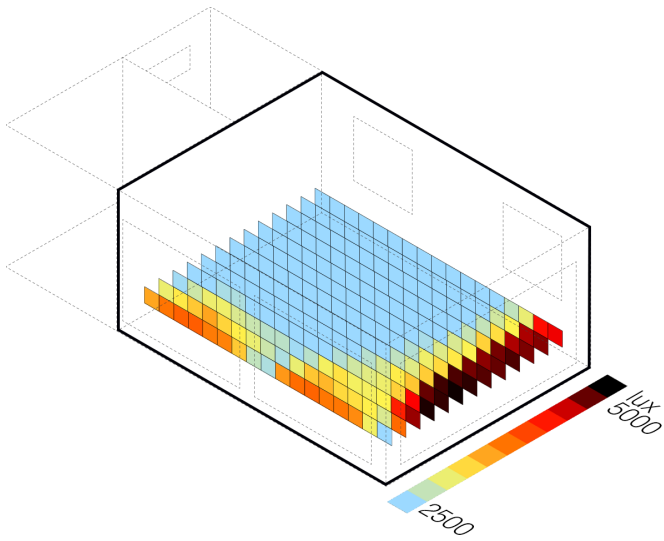


Figure c3.3 10 am

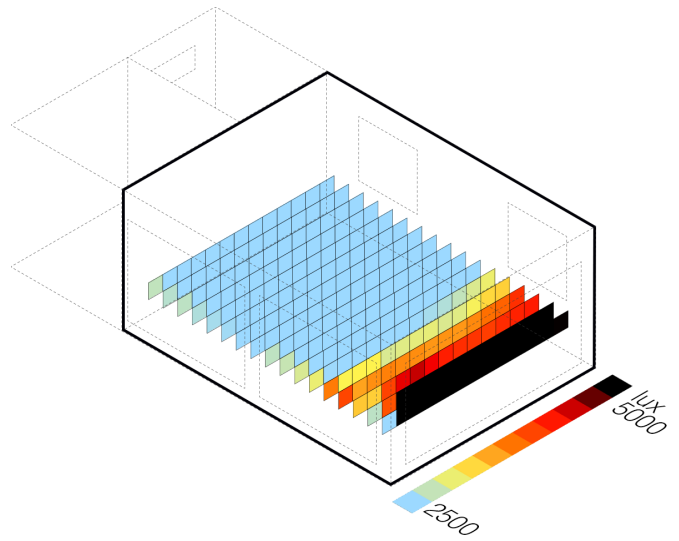


Figure c3.4 10 am

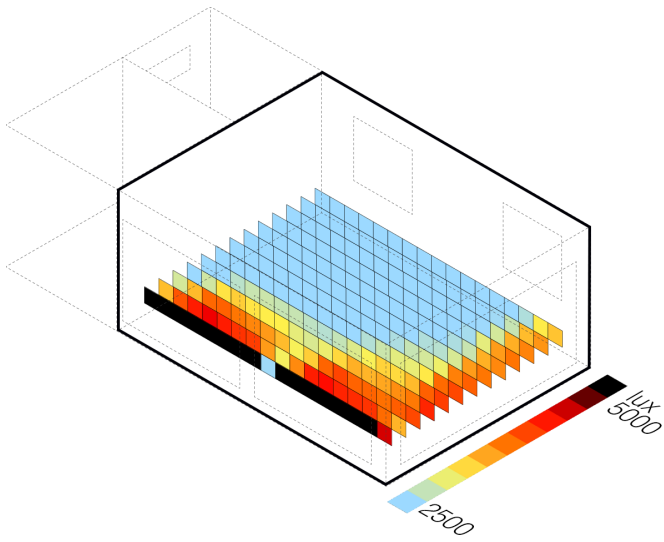


Figure c3.5 12 pm

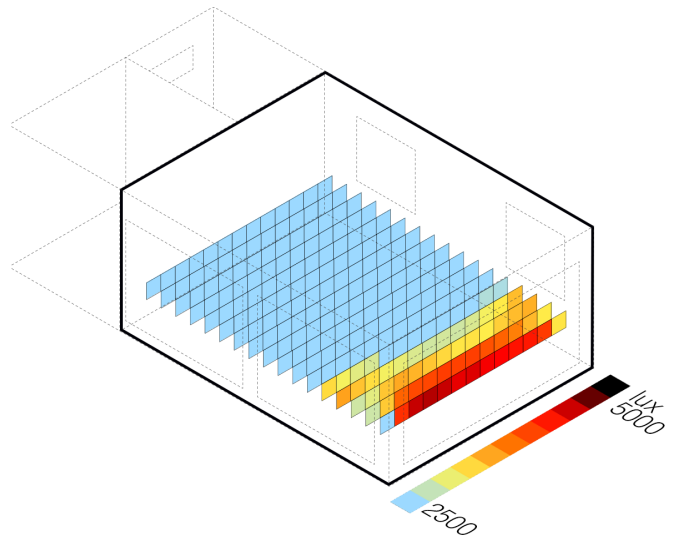


Figure c3.6 12pm

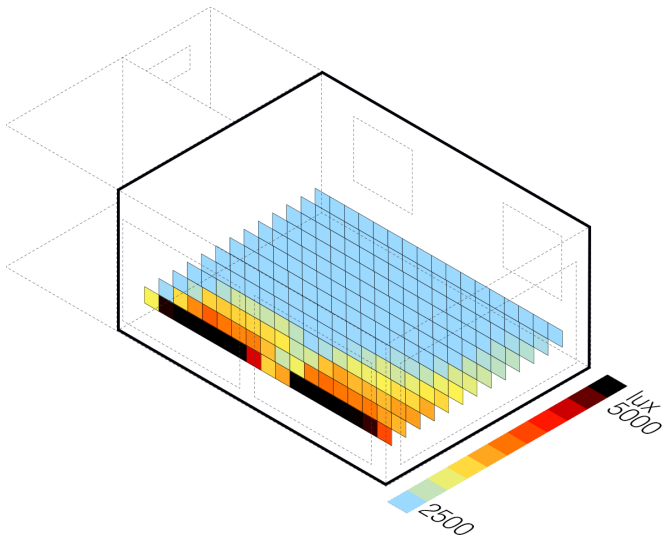


Figure c3.7 14 pm

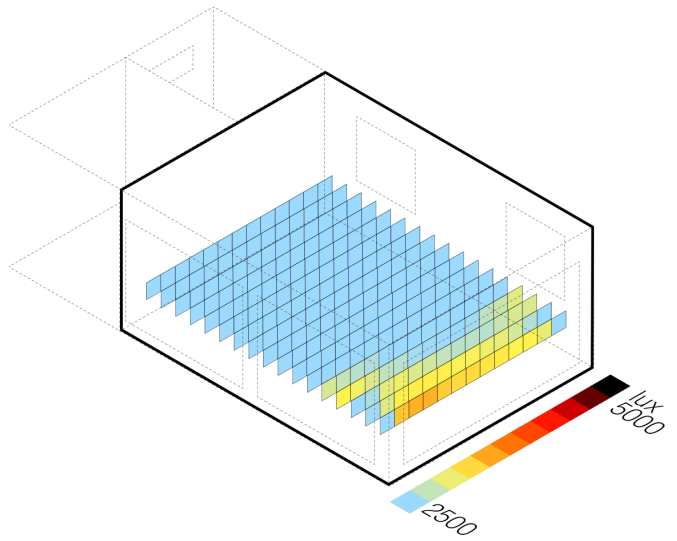


Figure c3.8 14 pm

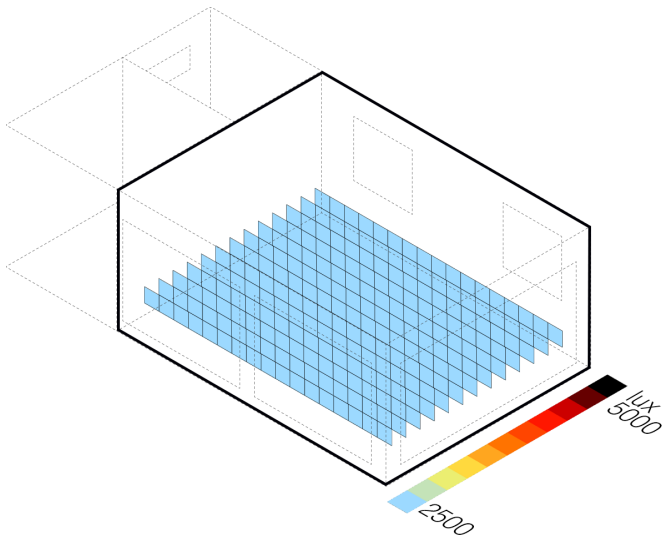


Figure c3.9 16 pm

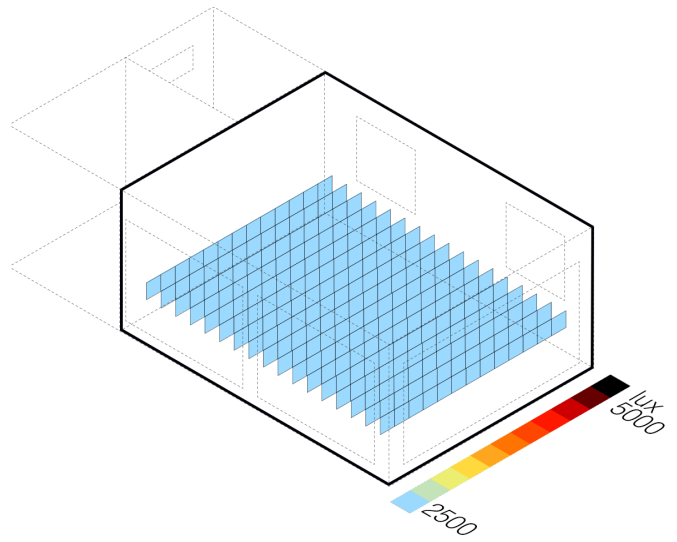


Figure c3.10 16pm

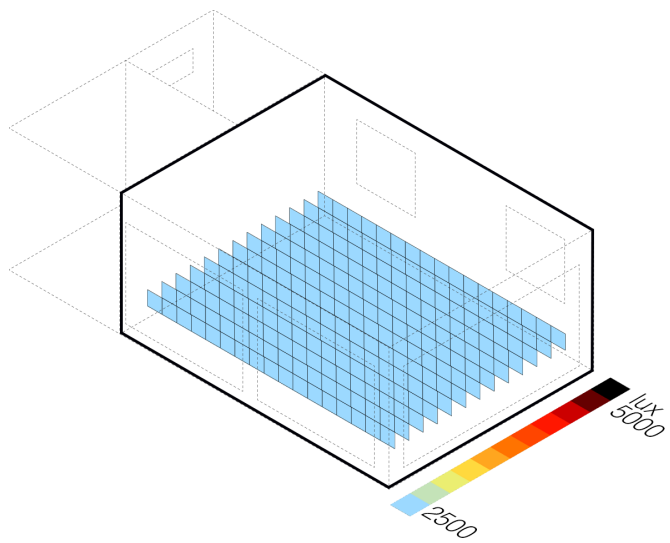


Figure c3.11 8 am

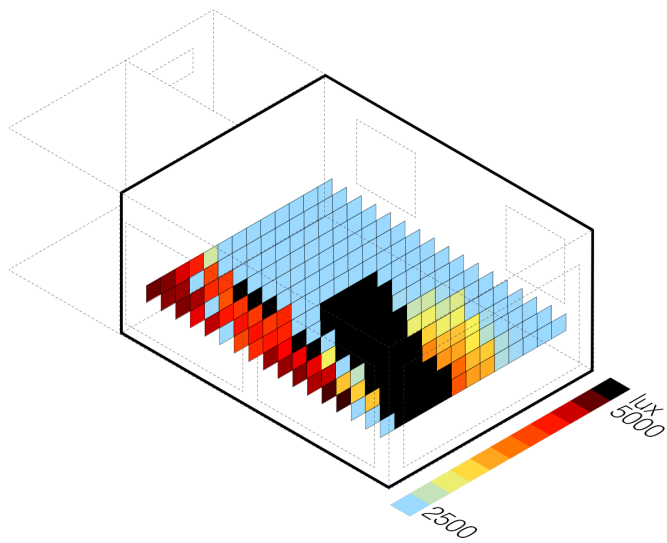


Figure c3.12 8 am

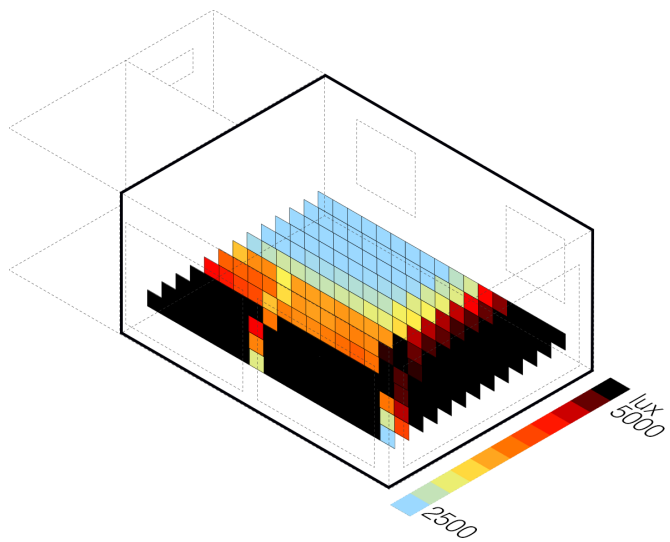


Figure c3.13 10 am

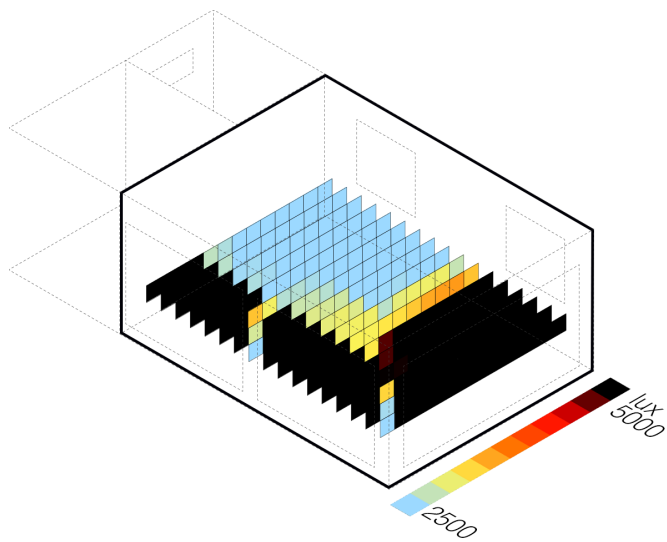


Figure c3.14 10 am

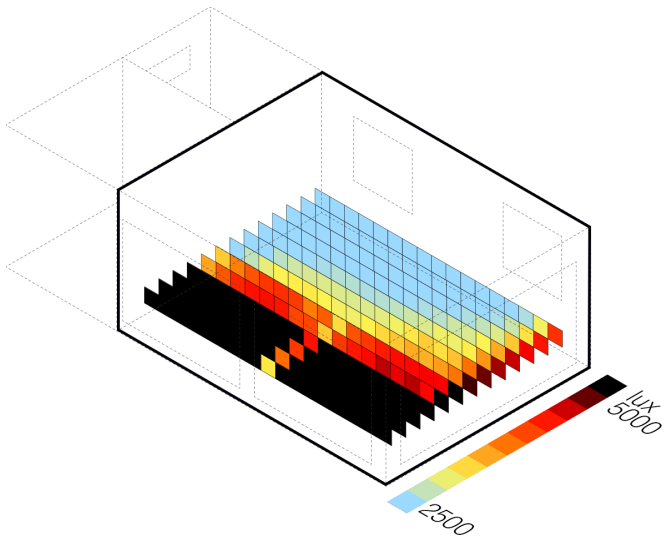


Figure c3.15 12 pm

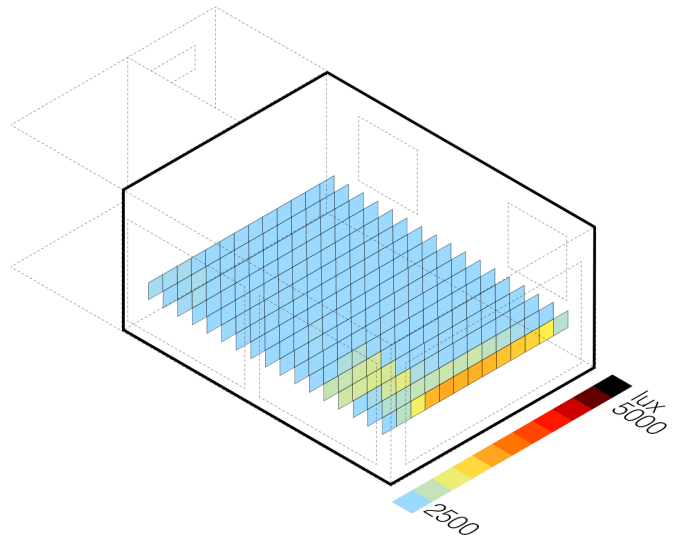


Figure c3.16 12pm

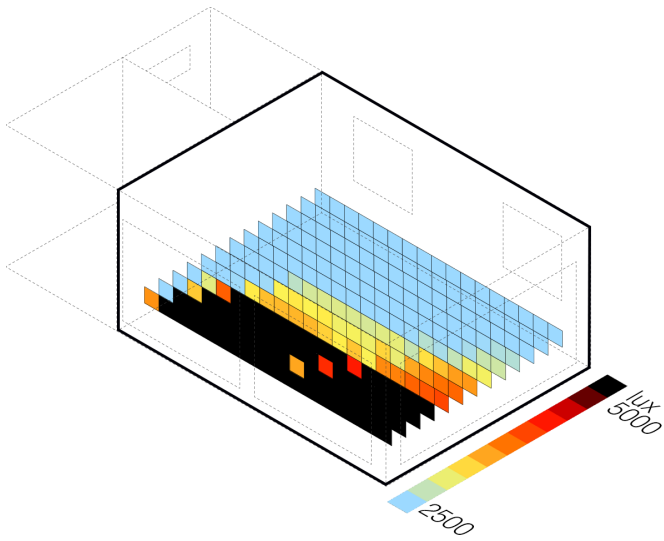


Figure c3.17 14 pm

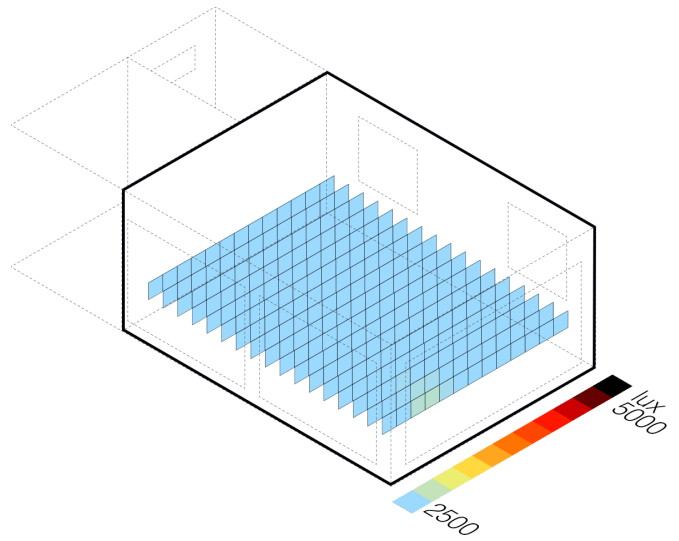


Figure c3.18 14 pm

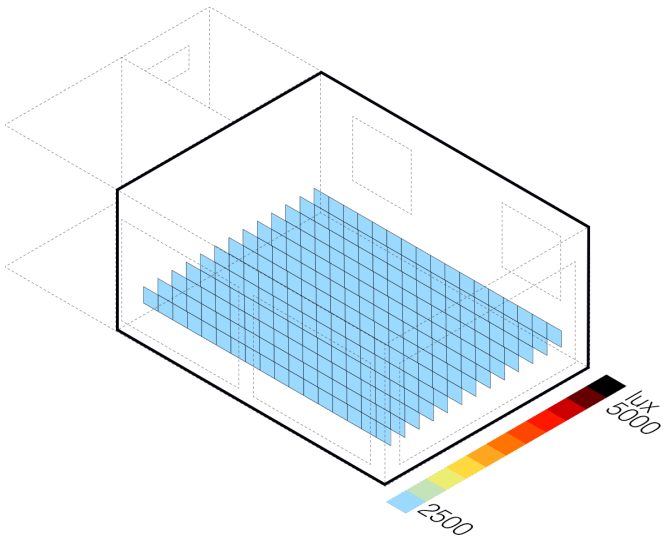


Figure c3.19 16 pm

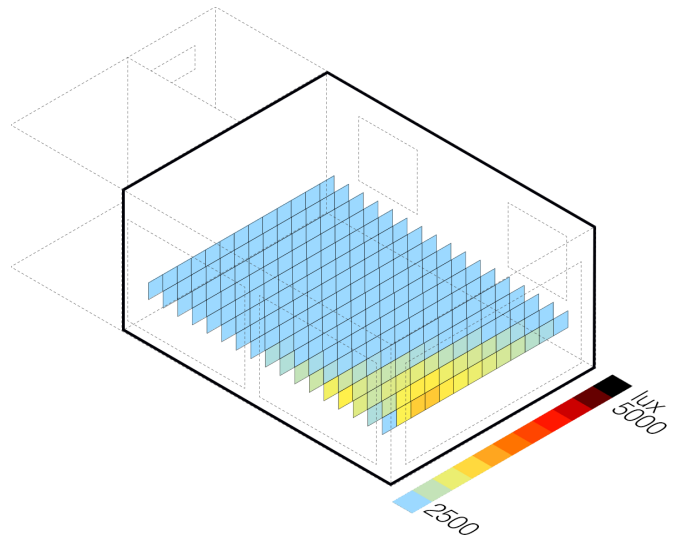


Figure c3.20 16pm

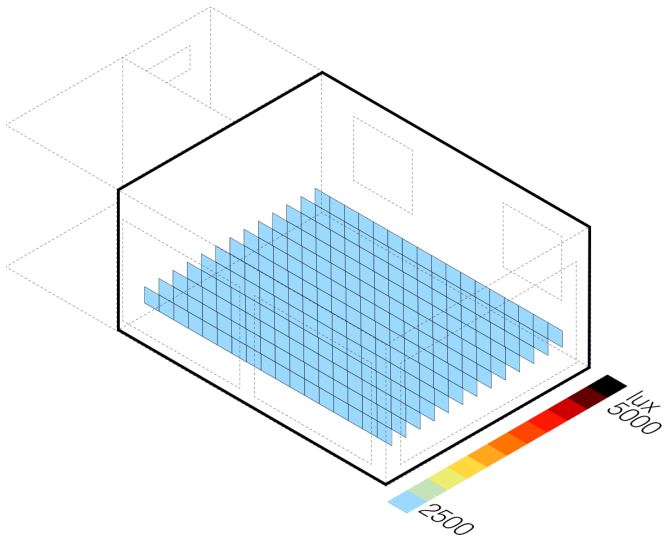


Figure c3.21 8 am

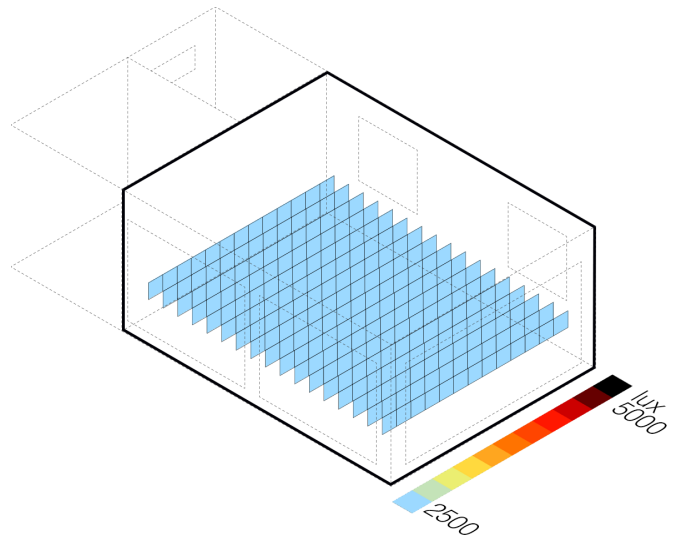


Figure c3.22 8am

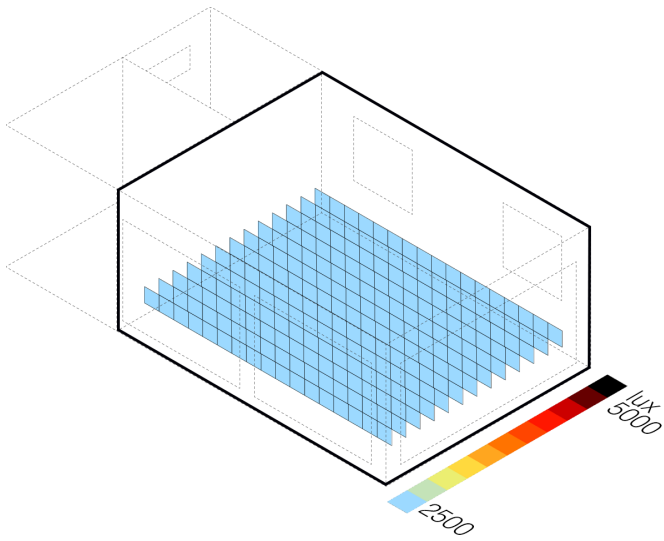


Figure c3.23 10 am

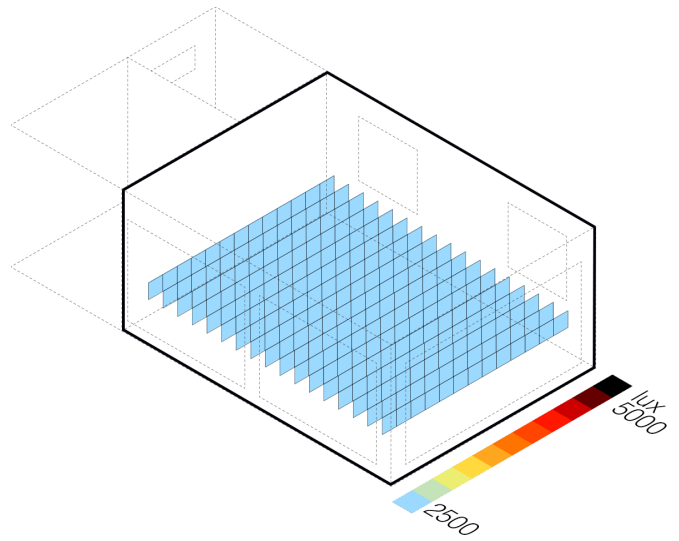


Figure c3.24 10 am

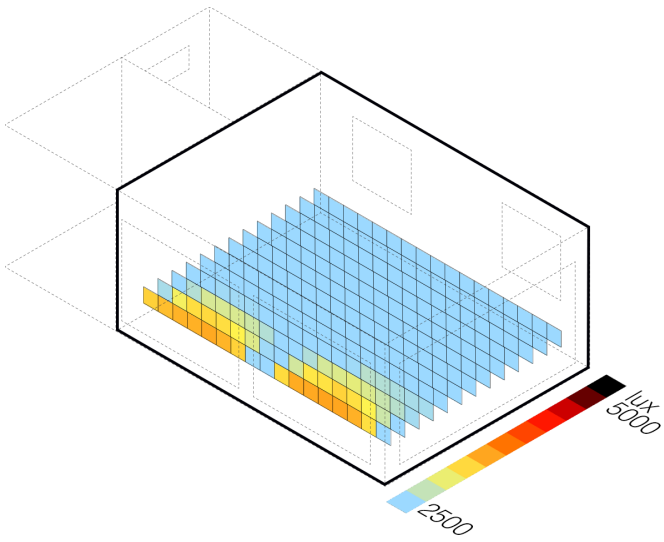


Figure c3.25 12 pm

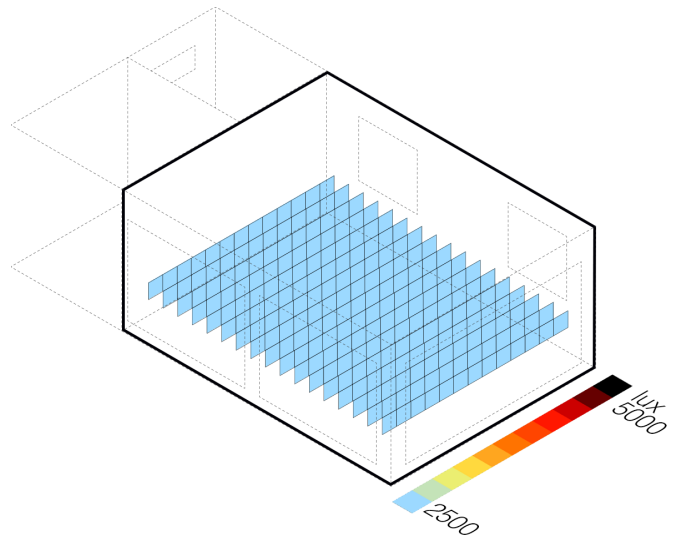


Figure c3.26 12pm

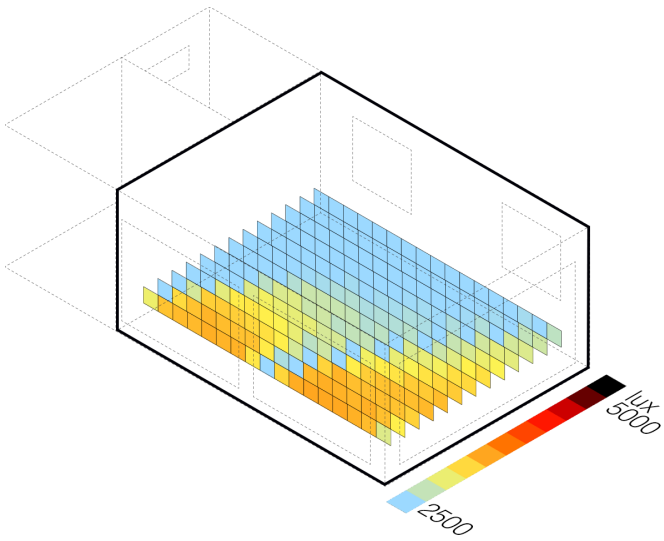


Figure c3.27 14 pm

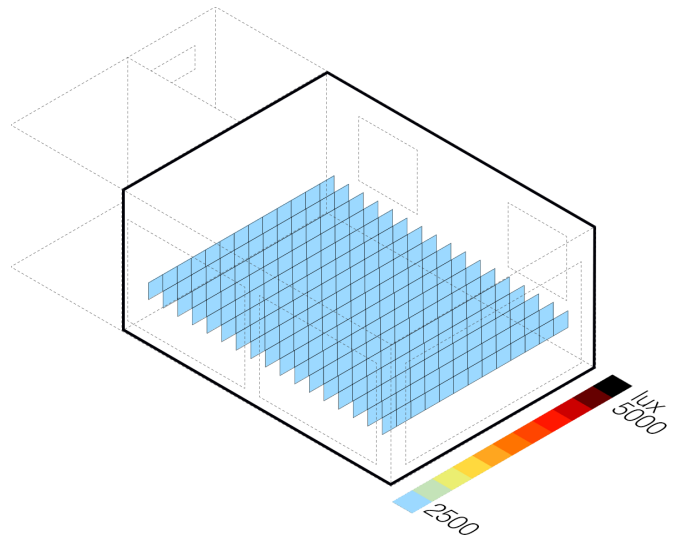


Figure c3.28 14 pm

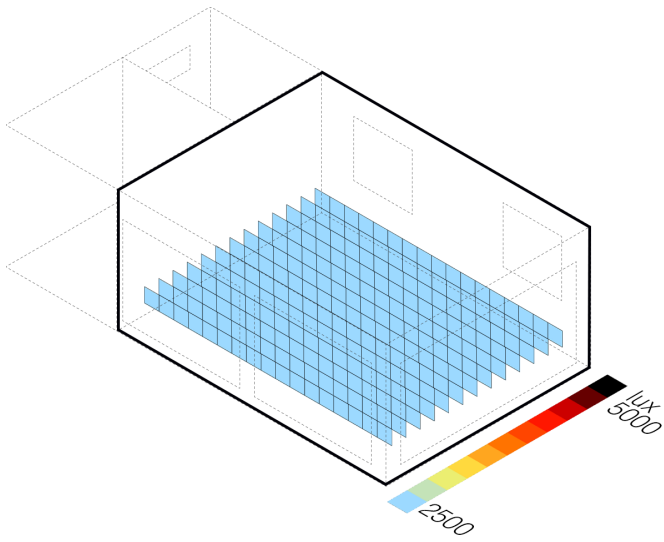


Figure c3.29 16 pm

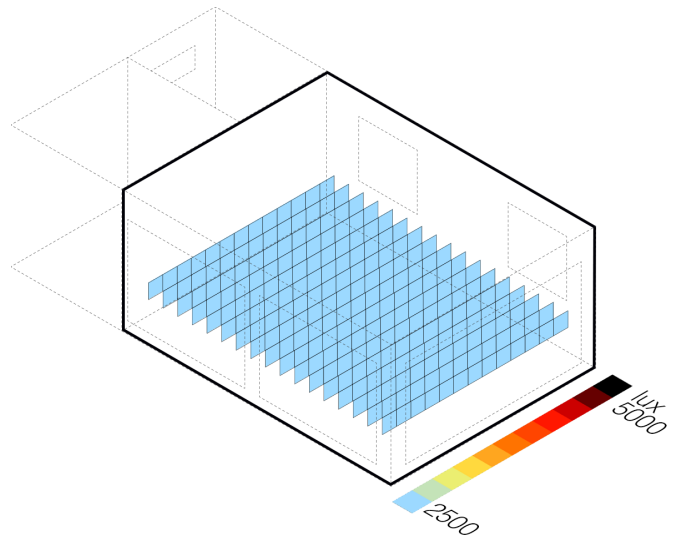


Figure c3.30 16pm

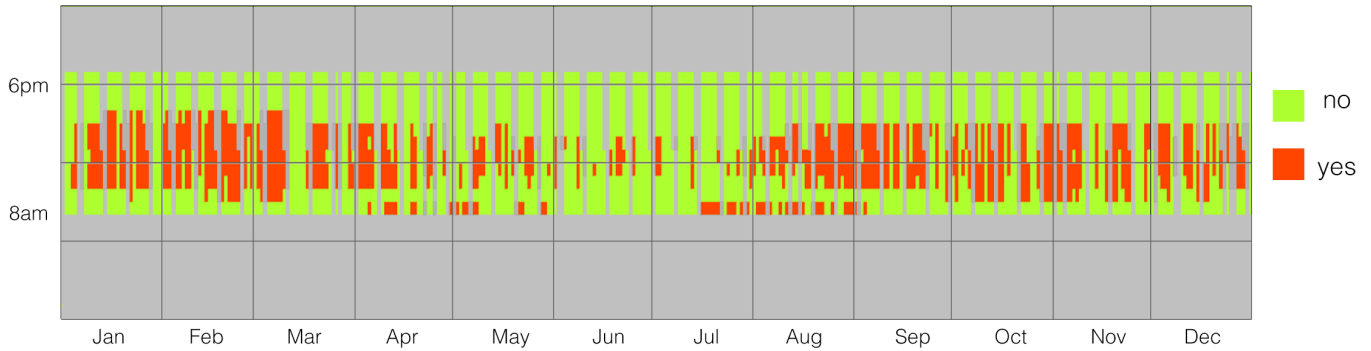


Figure c3.31 Annual glare simulation - point 54 (see figure a.22 pag 59)



Figure c3.32 Annual glare simulation - point 58 (see figure a.22 pag 59)

Figure c3.31 and c3.32 shows annual glare simulation according to simplified method. $D_{gp} \geq 0,4$, which is here related to vertical illuminance values over 3473 lx, show glare occurring from January to April and from August to December.

Point 58, 3m distant from south window, does not present glare conditions in the summer season at all.

south - spatial glare maps

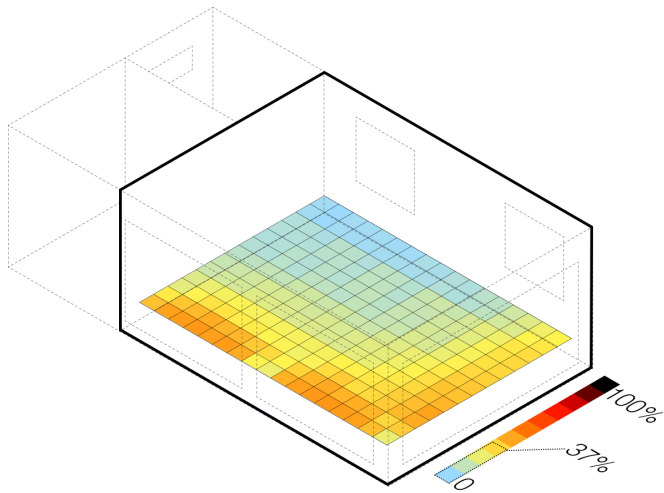


Figure c3.33 Glare Map

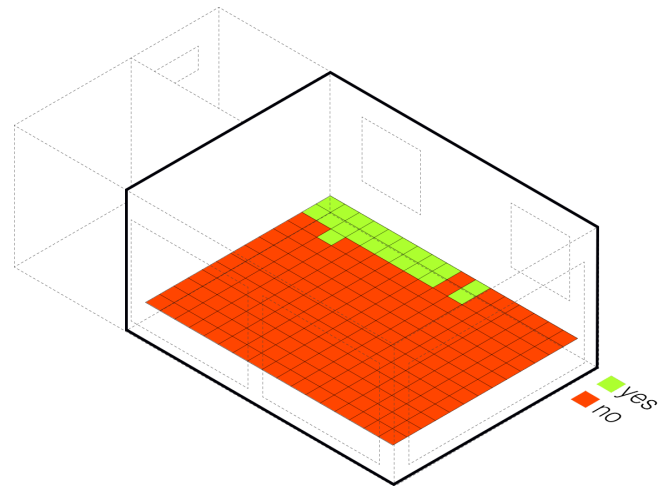


Figure c3.34 Glare Map - verified/ not verified

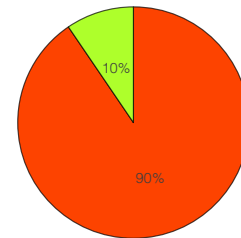


Figure c.33 reveals some of points in space where $dgp \geq 0,4$ occurs up to 37% of occupied time, which is about 1120 hours.

east - Annual glare simulations

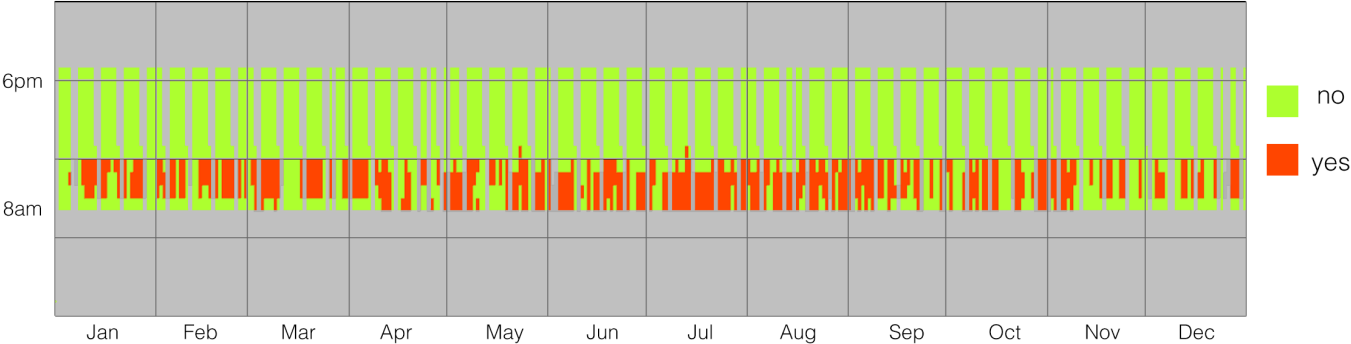


Figure c3.35 Annual glare simulation - point 32 (see figure a.22 pag 59)

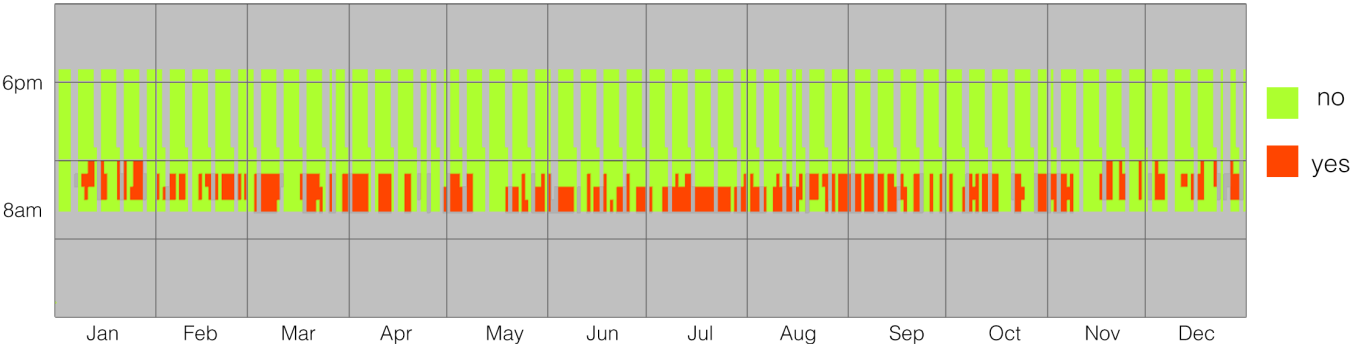


Figure c3.36 Annual glare simulation - point 71 (see figure a.22 pag 59)

East points present glare conditions all over the year, yet in a shorter period of time, from 8am to 11-12pm in the morning.

east - spatial glare maps

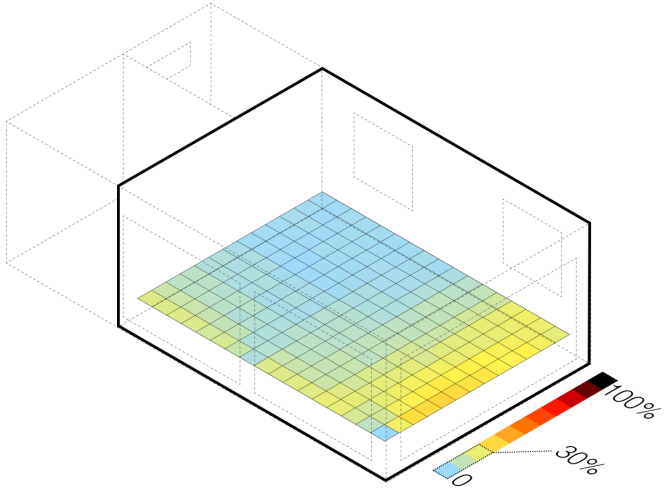


Figure c3.37 Glare map

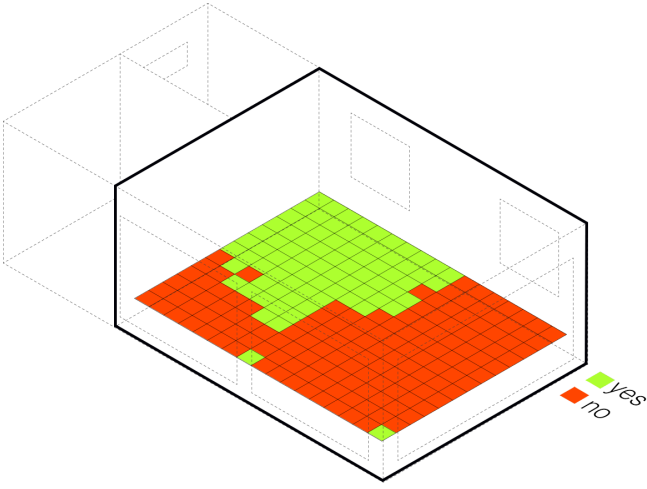
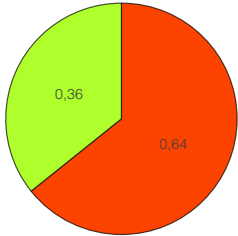


Figure c3.38 Glare Map - verified/not verified



As visible in figure c3.38 and Pie chart on the right, 36% of area exposed to east does not present glare condition.

C4. Thermal + visual comfort

Following image c4.1 (see below) represents combination of thermal ranges (over-heated, comfort and under-heated) with luminous ranges (over-lit, luminous autonomy and

under-lit). Colored circles on the right indicate percentages relative to each of the nine configurations. In particular, Over-heated and Over-lit time of the year covers 17% of occupied

time, typically from 11am to 3pm in winter and spring season and also from 8am to 9am in summer season. In June there is no over-lighting. There is an increase in under-lit area up to

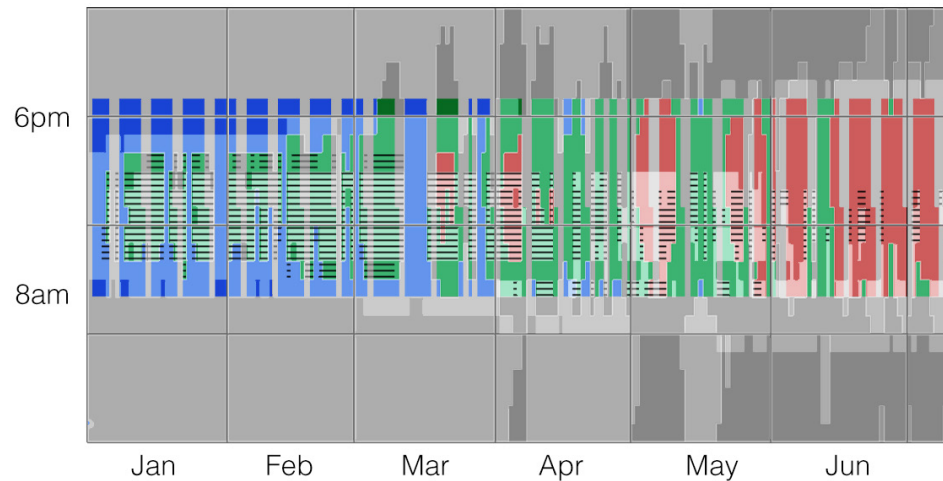
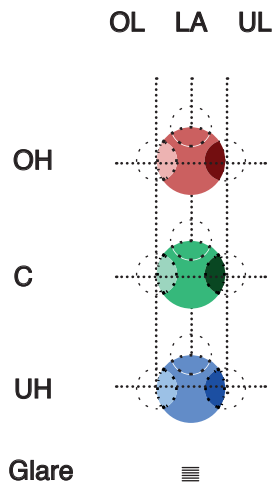
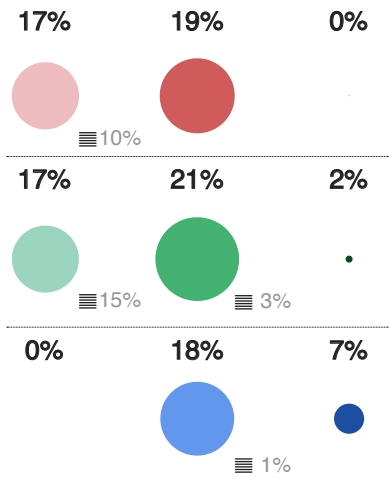
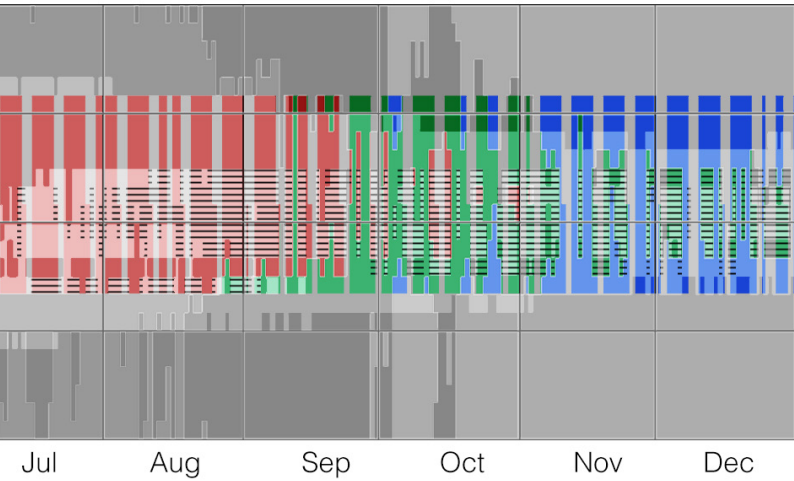


Figure c4.1 Thermal + Visual Comfort evaluation. Point 54

7% of time, typically in the winter season afternoons from 4pm to 6pm.



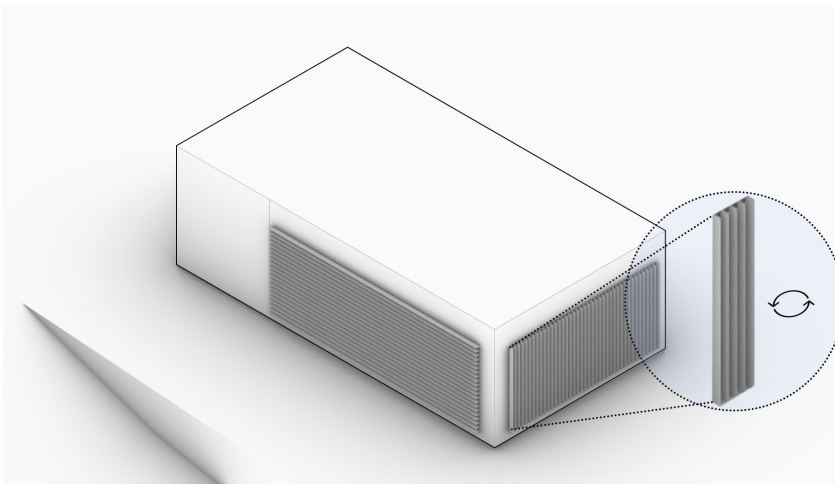
D - dynamic shading

D1. Thermal Comfort Analysis

This chapter focuses on results deriving from simulation with daysim conceptual dynamic shading.

In order to proceed with simulation, it was necessary to manually modify the “.idf” file through EnergyPlus before. The .idf file is the file generated by EnergyPlus, where all types of input data can be managed for specific simulation purposes. Indeed, it was necessary to ideally model horizontal and vertical blinds, both with a 0,5 reflectivity and assign them an operating schedule, so that, whenever a normal radiation of $50\text{W}/\text{m}^2$ was found on the facade, these would be activated and shield solar beams through a cut-off angle (total shielding).

This is done to observe how the Lab respond in case a dynamic shading is applied (tough threshold of $50\text{W}/\text{m}^2$ may result



Model of Exterior Venetian blinds implemented in EnergyPlus file
Each blind is 0,15 m wide and 0,1 m distant from glass surface

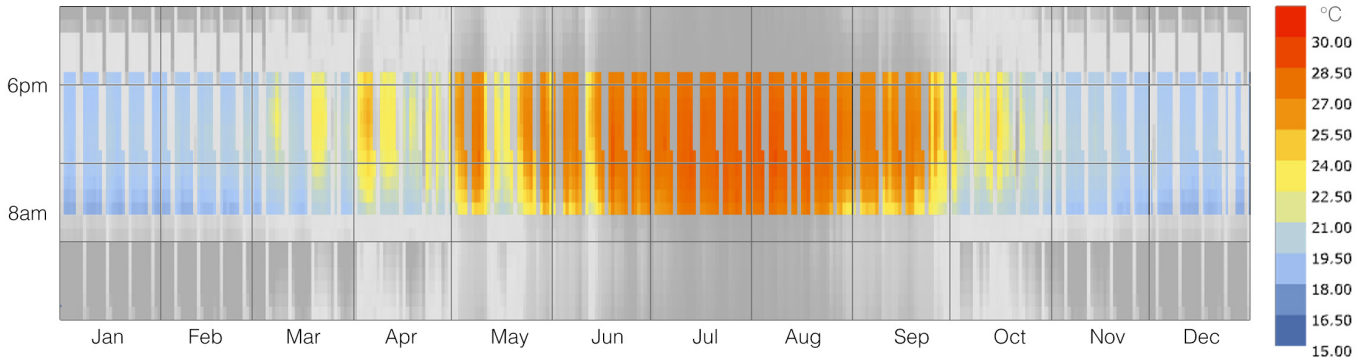


Figure d1.1 Adjusted Operative Temperature - dynamic shading scenario

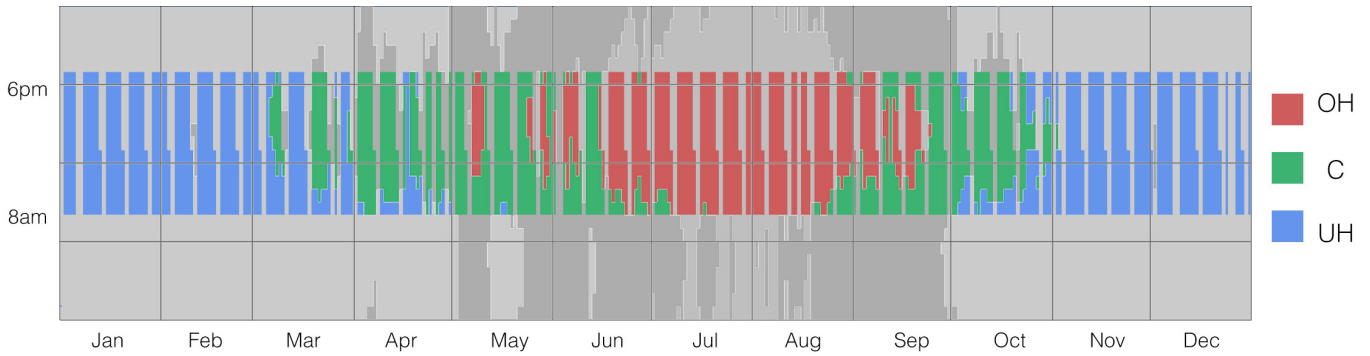


Figure d1.2 Over-heated, Comfort and Under-heated range - dynamic shading scenario

too severe).

Simulation results hint at reduction in Over-heating and Comfort % hours with an increase in Under-heating with a mean value of 42%.

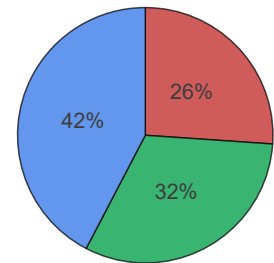


Figure b3.

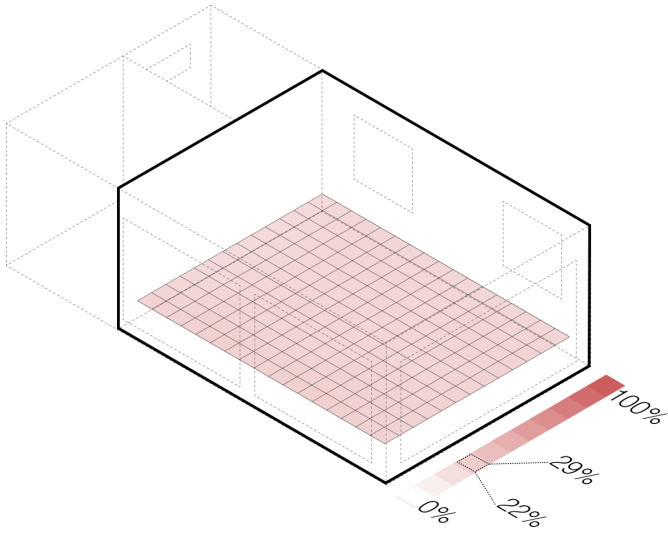


Figure d1.3 Over-heated Map

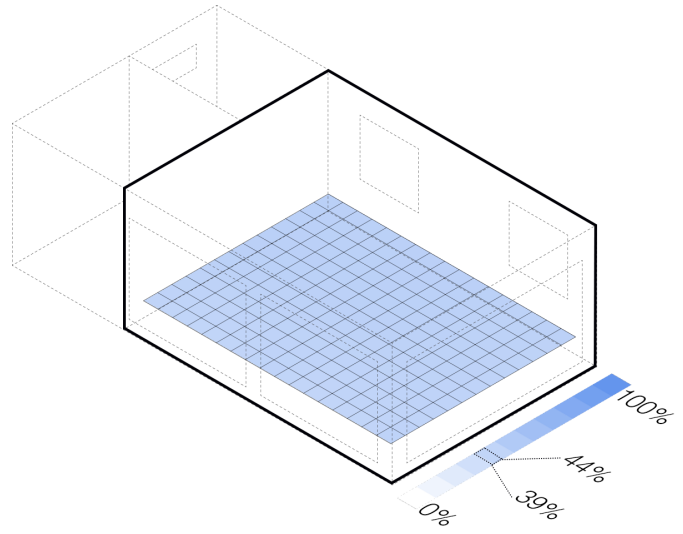


Figure d1.4 Under-heated Map

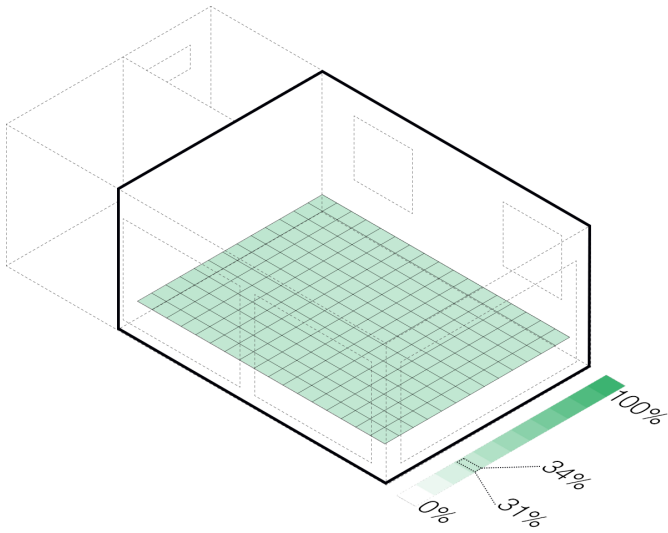


Figure d1.5 Comfort Map

D2. CBDM & Daylight Analysis

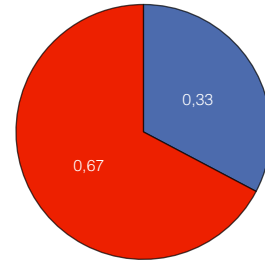
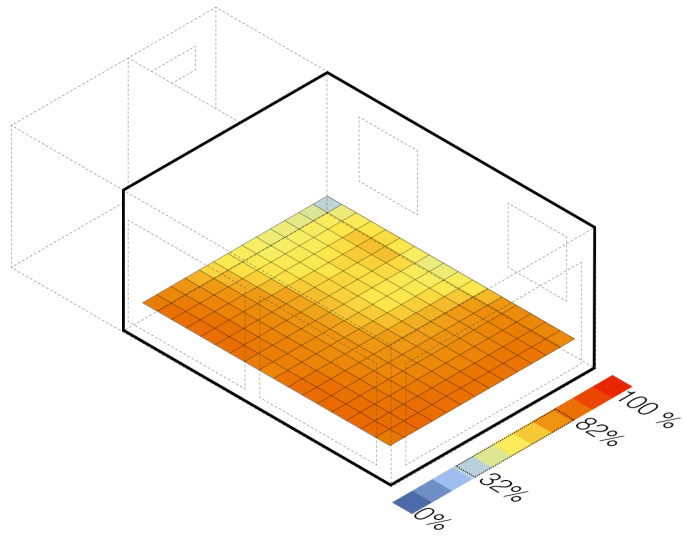


Figure d2.1 Daylight Autonomy

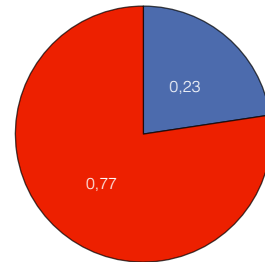
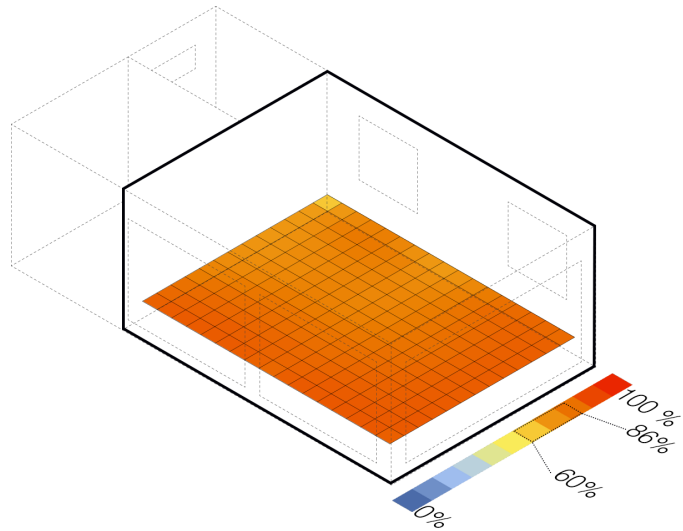


Figure d2.2 Spatial Daylight Autonomy

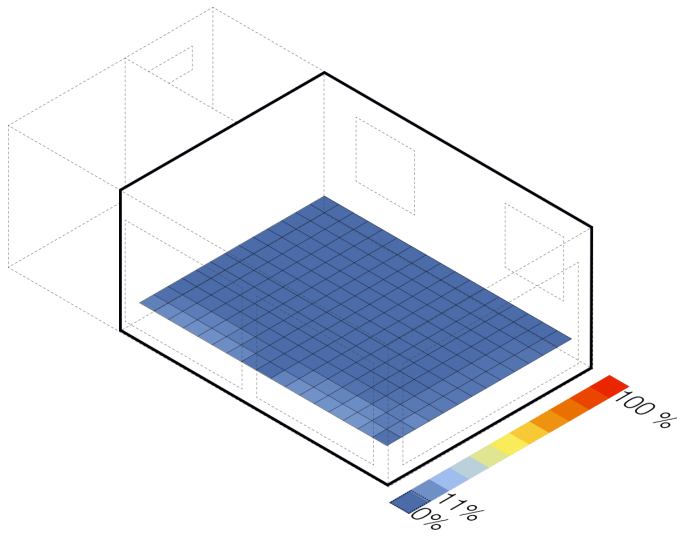


Figure d2.3 UDI > 3000 lx

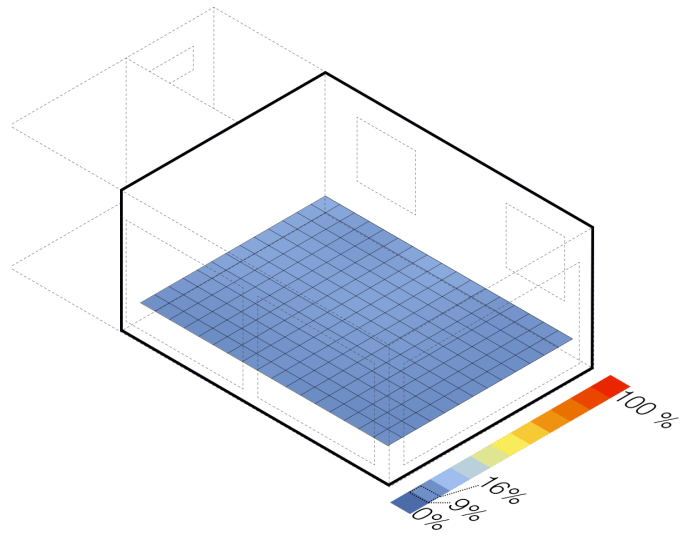


Figure d2.4 UDI < 100 lx

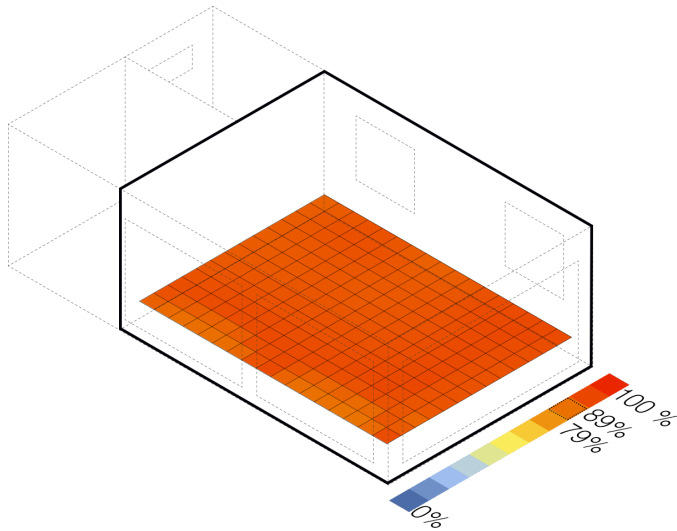


Figure d2.5 UDI,achieved

Whether UDI,achieved is quite constant according to spatial configuration in figure d2.5, Daylight Autonomy in figure d2.1 (see previous page) presents nearly half of LAB area with values lower than 50% of occupied time. Yet Spatial Daylight Autonomy is still verified with both acceptable and preferable values (50% and 75% of space).

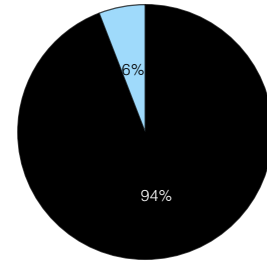
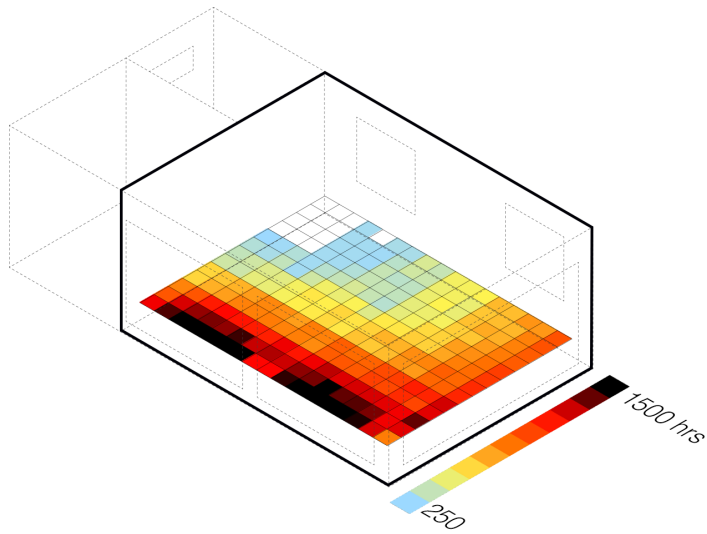


Figure d2.6 ASE

ASE in figure d2.6 has to be considered the same for the case when no dynamic blinds are on (baseline scenario). Yet, when blinds are fully on, Solar radiation is highly shielded and ASE drops to 0%, meaning that under no circumstances over the year is space equal to or over 1000 lx for at least 250 hours of occupied time.

Luminous Autonomy - 3 points

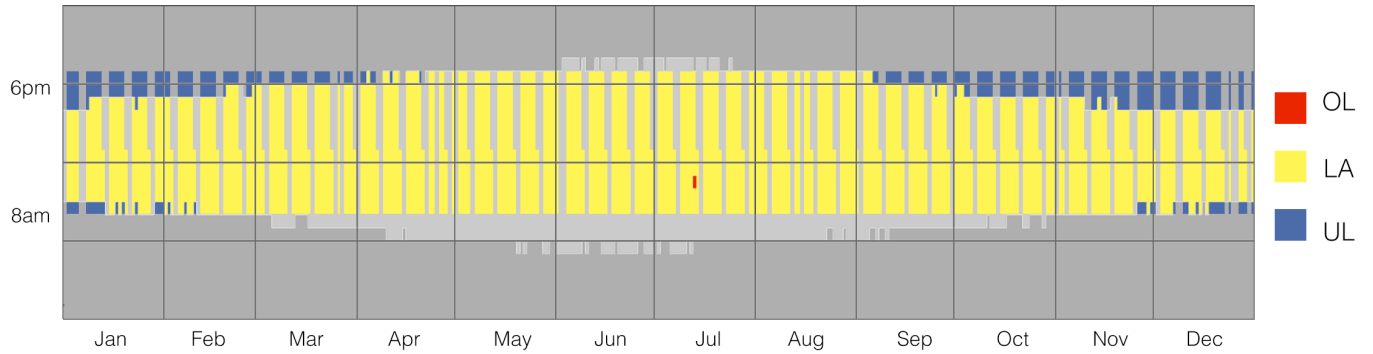


Figure d2.7 Over-lit (OL), Luminous autonomy (LA) and Under-lit (UL) range - point 54

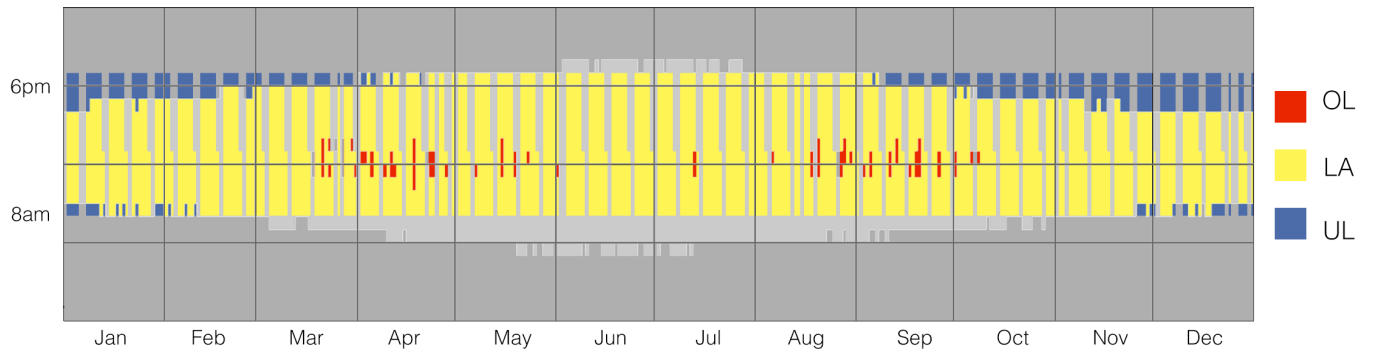


Figure d2.8 Over-lit (OL), Luminous autonomy (LA) and Under-lit (UL) range - point 32

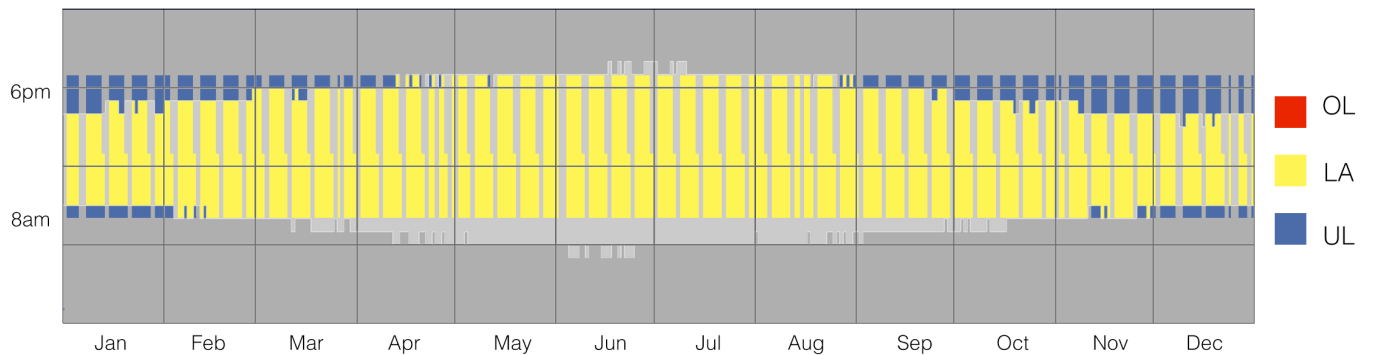


Figure d2.9 Over-lit (OL), Luminous autonomy (LA) and Under-lit (UL) range - point 179

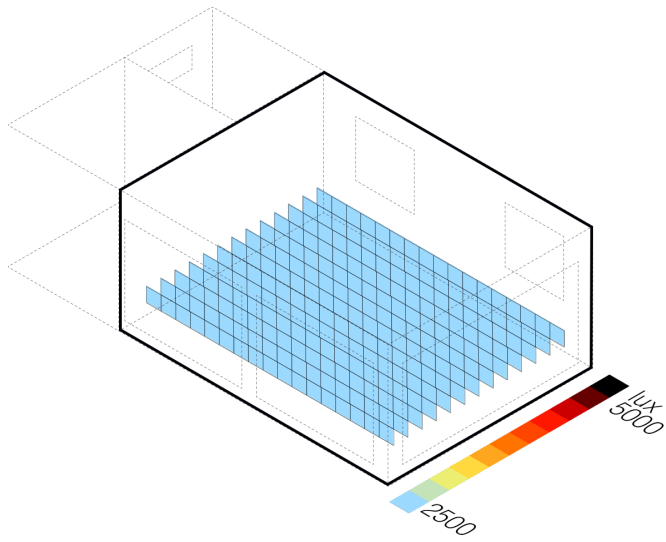


Figure d3.1 8 am

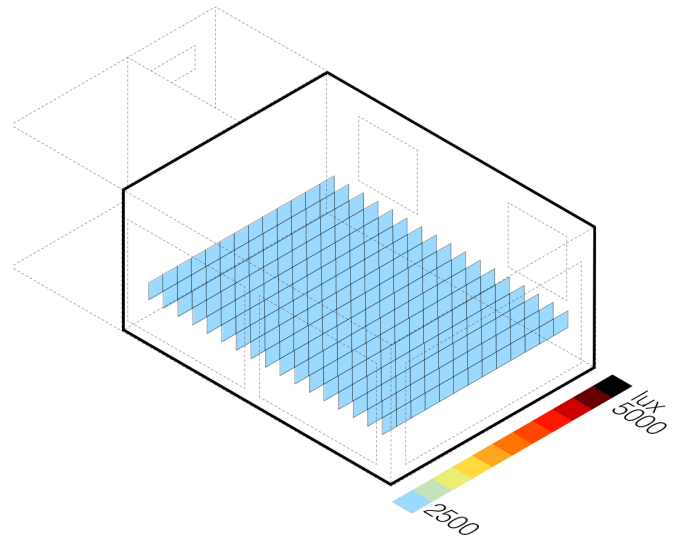


Figure d3.2 8 am

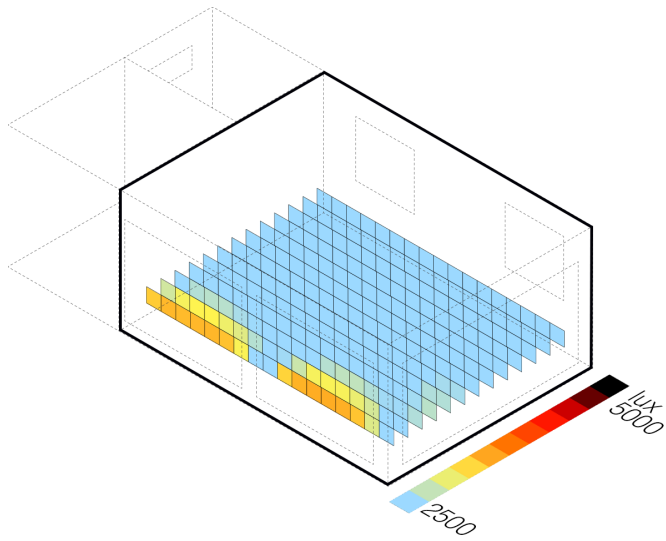


Figure d3.3 10 am

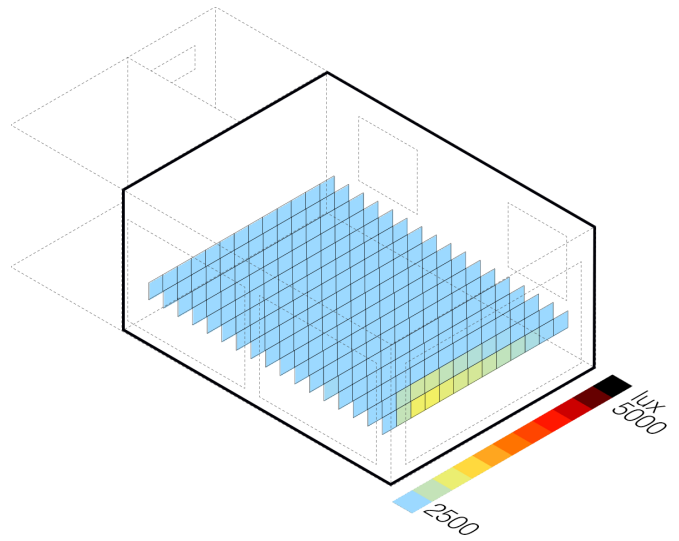


Figure d3.4 10 am

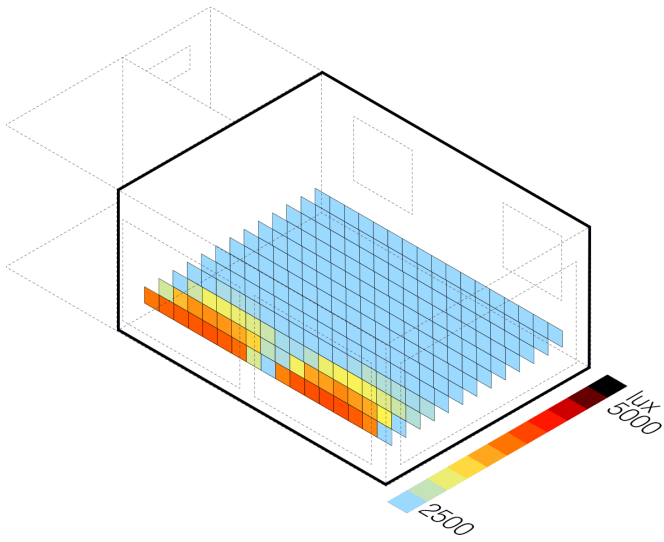


Figure d3.5 12 pm

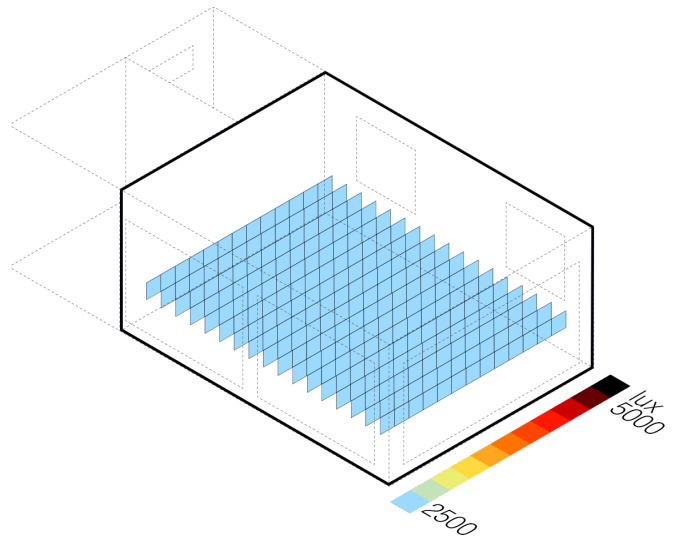


Figure d3.6 12pm

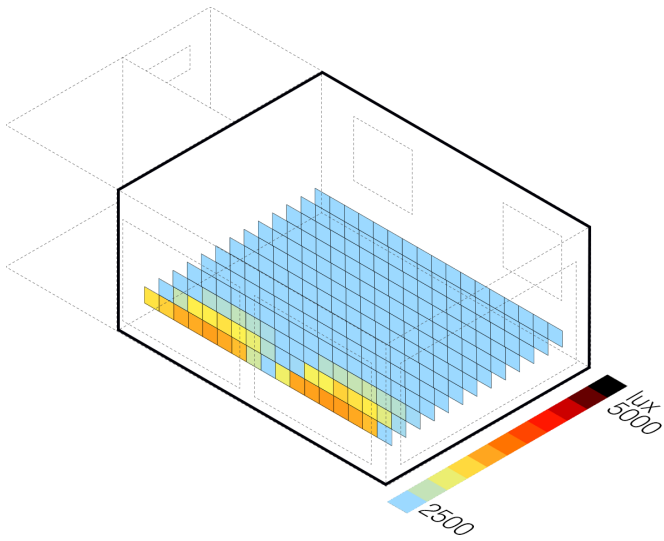


Figure d3.7 14 pm

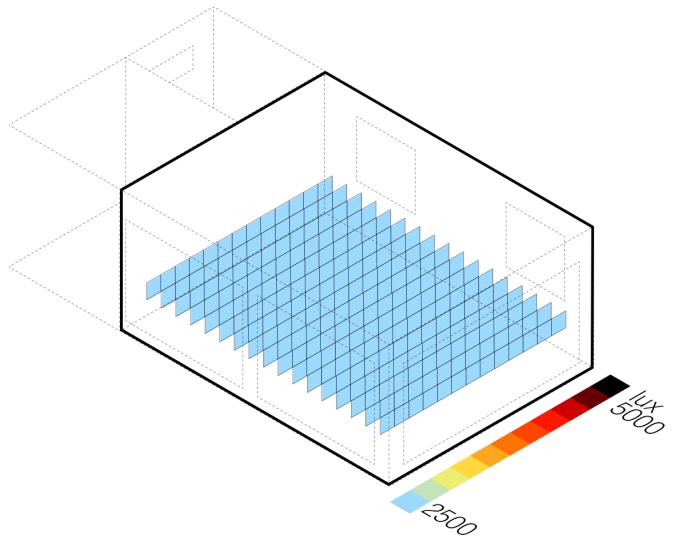


Figure d3.8 14 pm

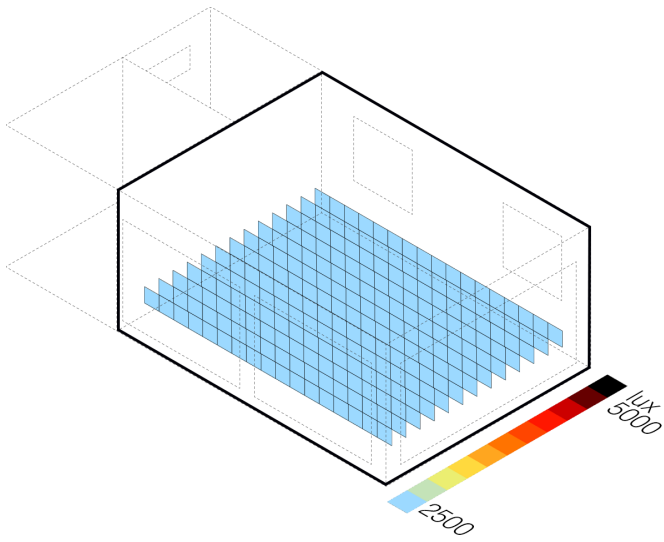


Figure d3.9 16 pm

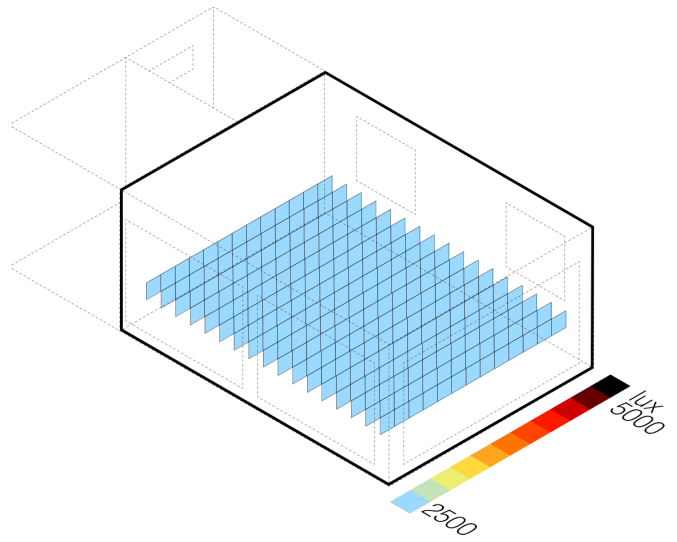


Figure d3.10 16pm

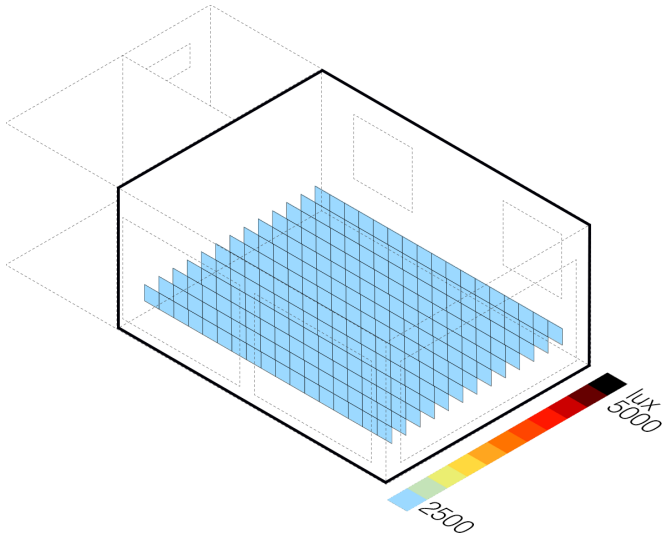


Figure d3.11 8 am

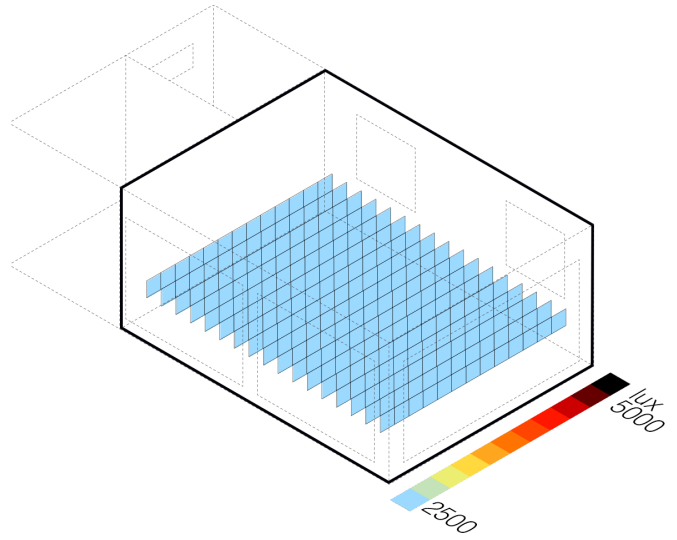


Figure d3.12 8 am

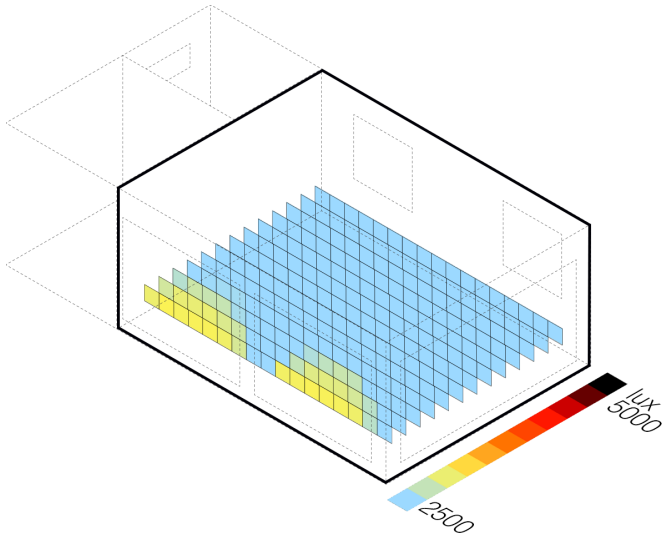


Figure d3.13 10 am

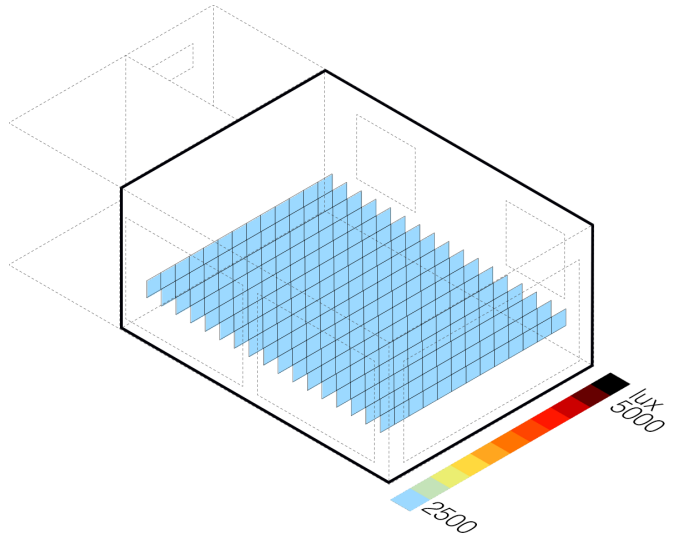


Figure d3.14 10 am

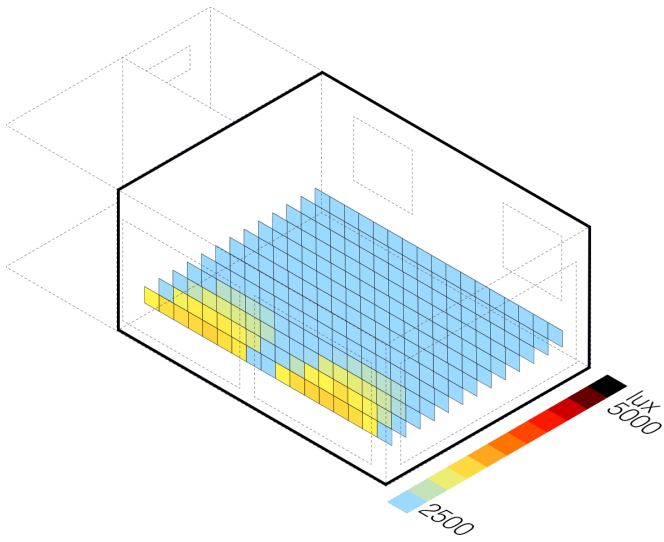


Figure d3.15 12 pm

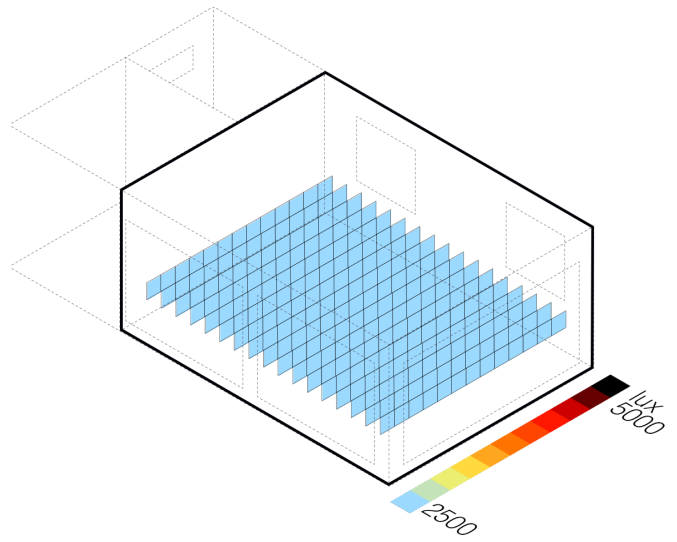


Figure d3.16 12pm

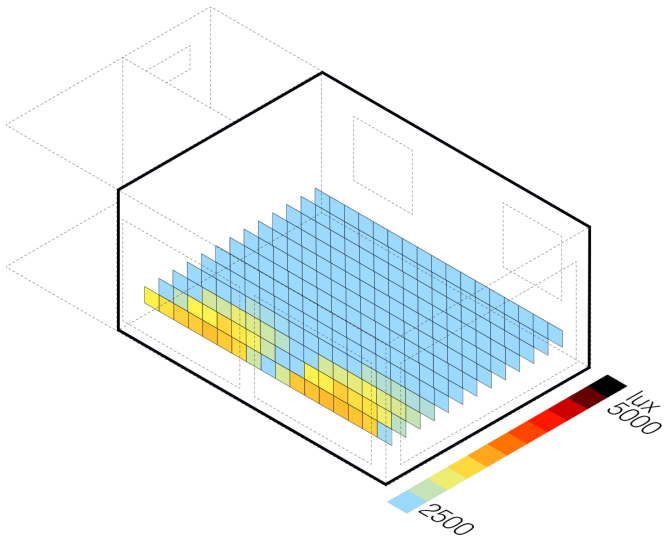


Figure d3.17 14 pm

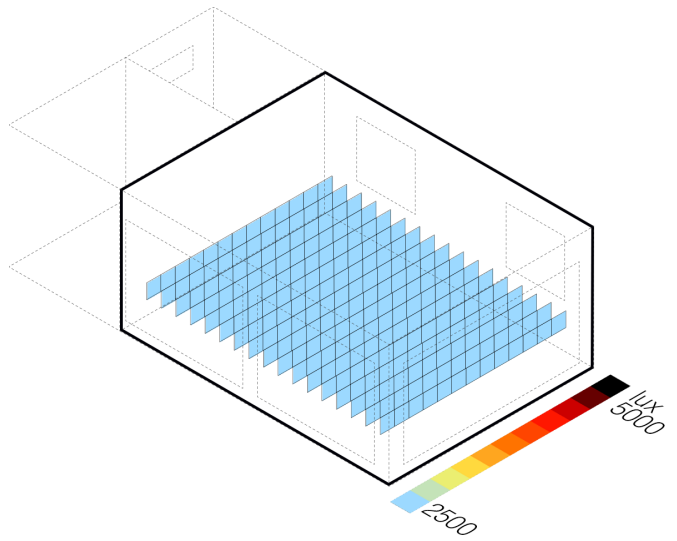


Figure d3.18 14 pm

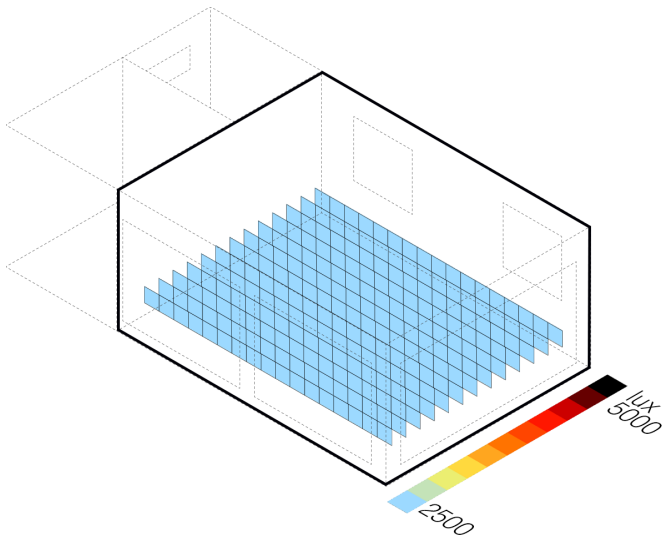


Figure d3.19 16 pm

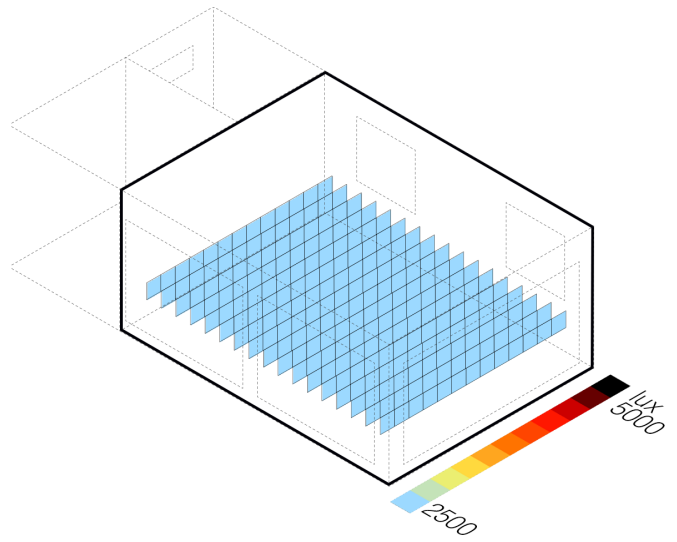


Figure d3.20 16pm

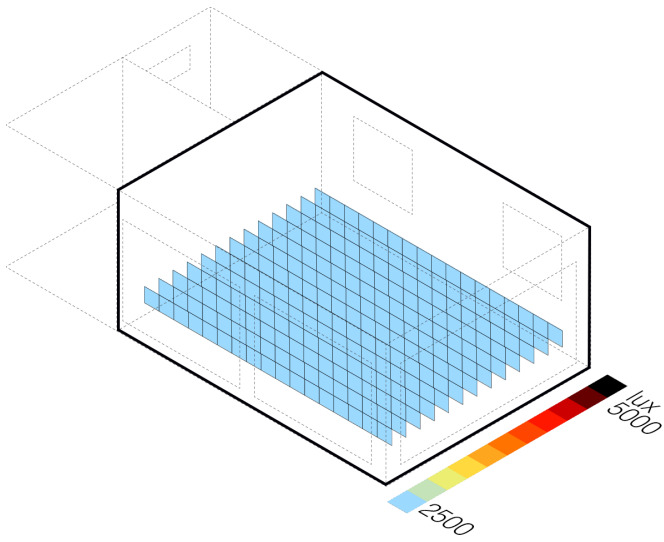


Figure d3.21 8 am

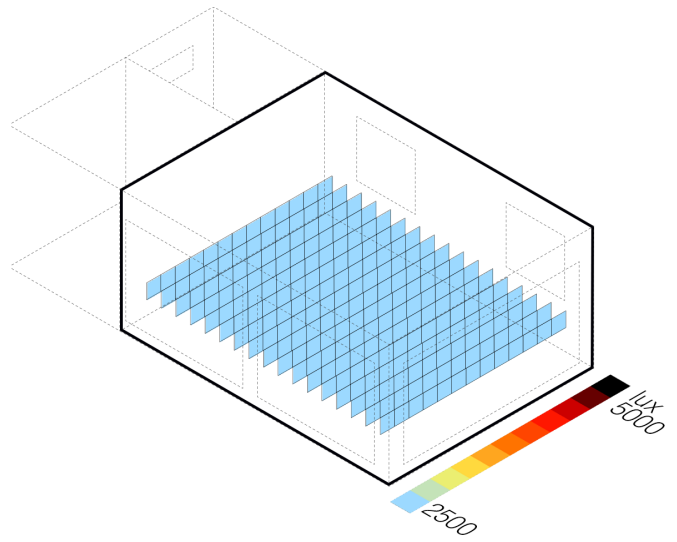


Figure d3.22 8 am

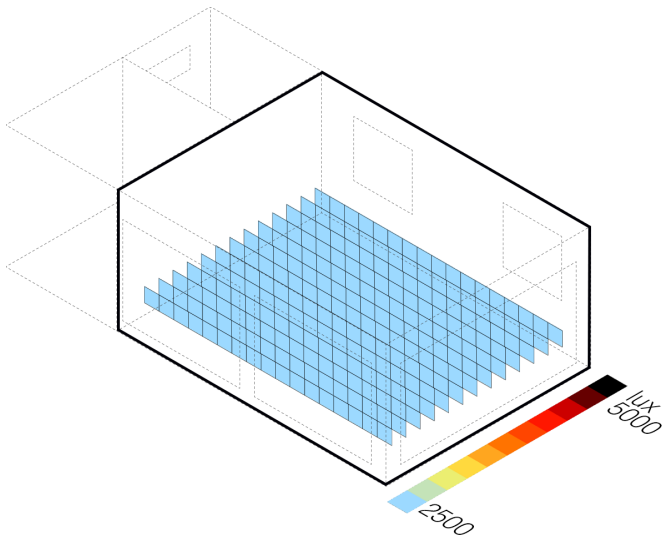


Figure d3.23 10 am

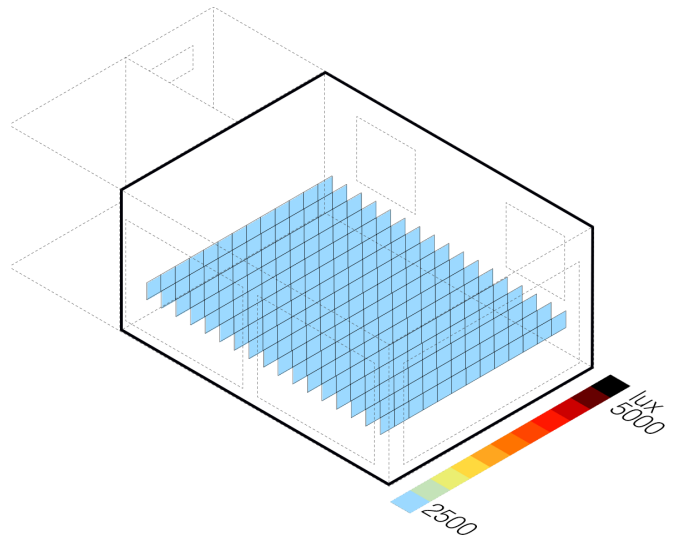


Figure d3.24 10 am

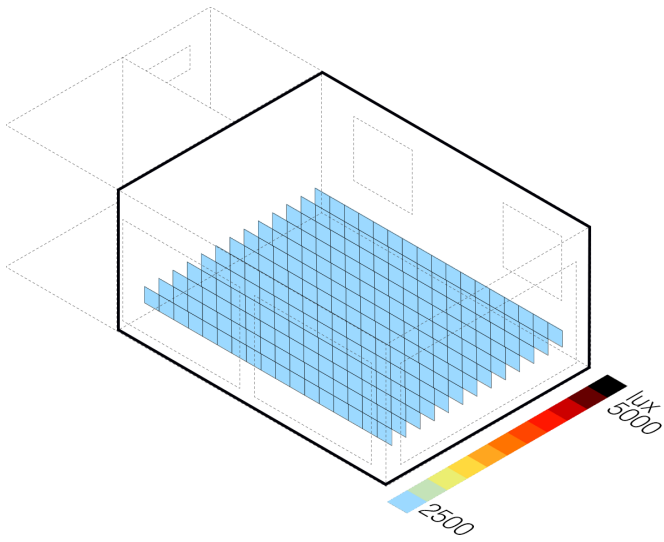


Figure d3.25 12 pm

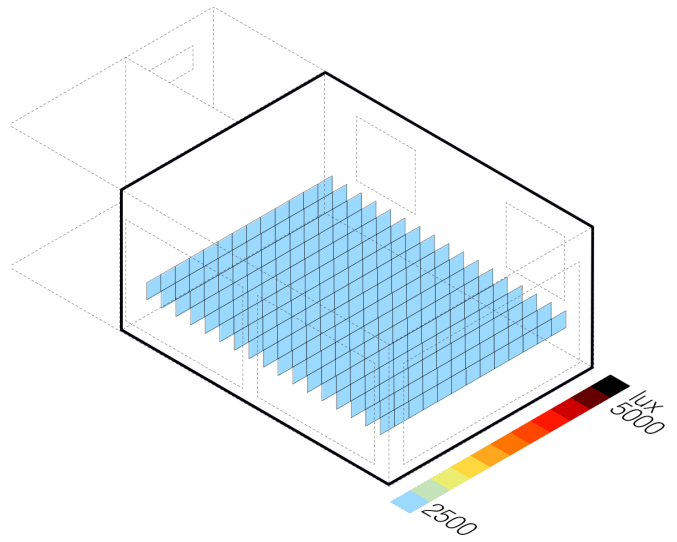


Figure d3.26 12pm

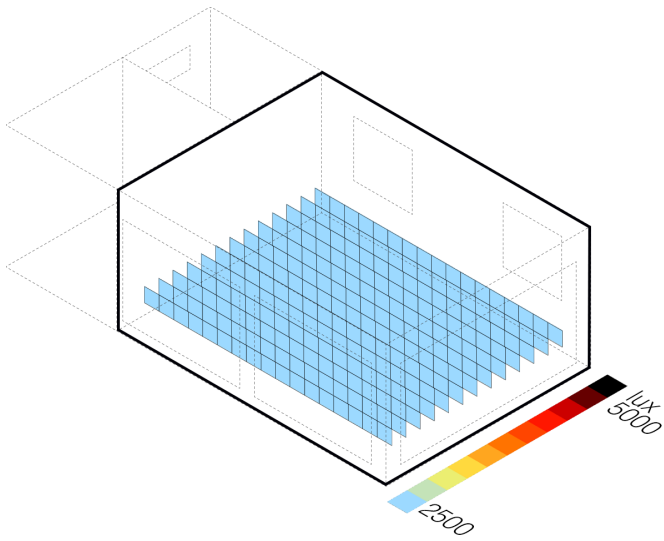


Figure d3.27 14 pm

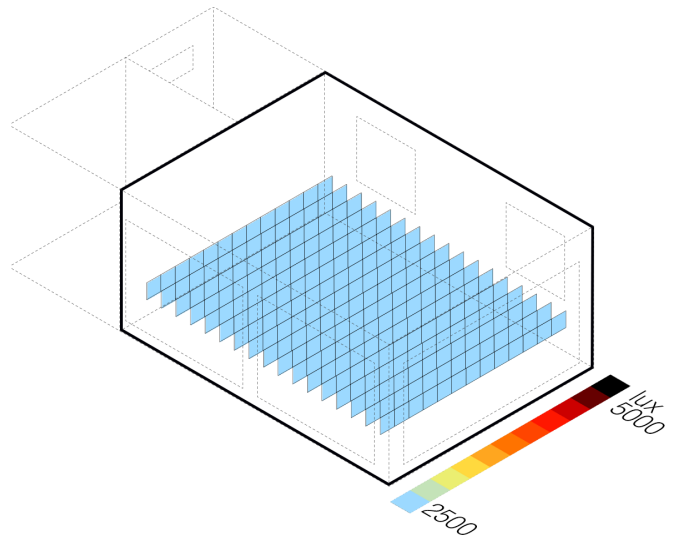


Figure d3.28 14 pm

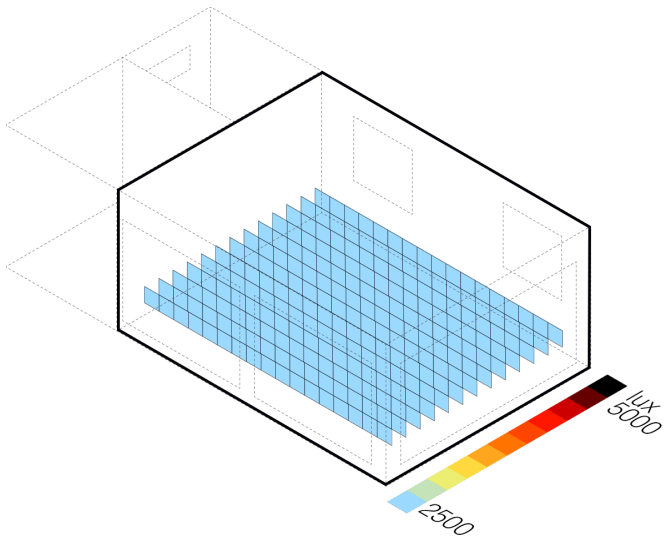


Figure d3.29 16 pm

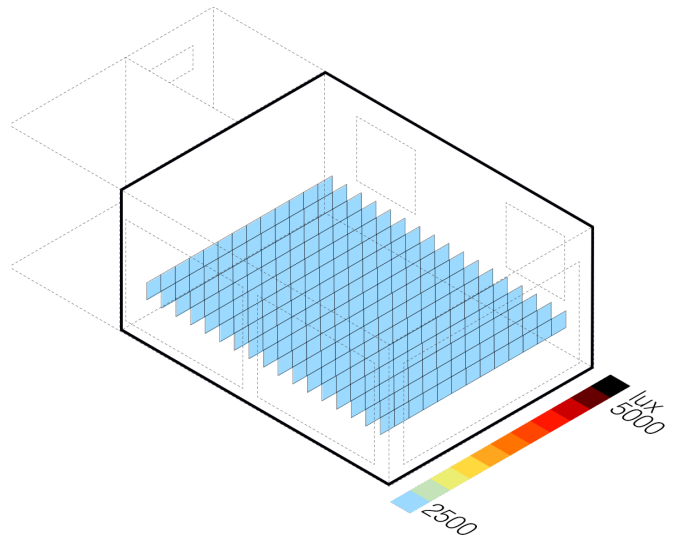


Figure d3.30 16pm

south - Annual glare simulations

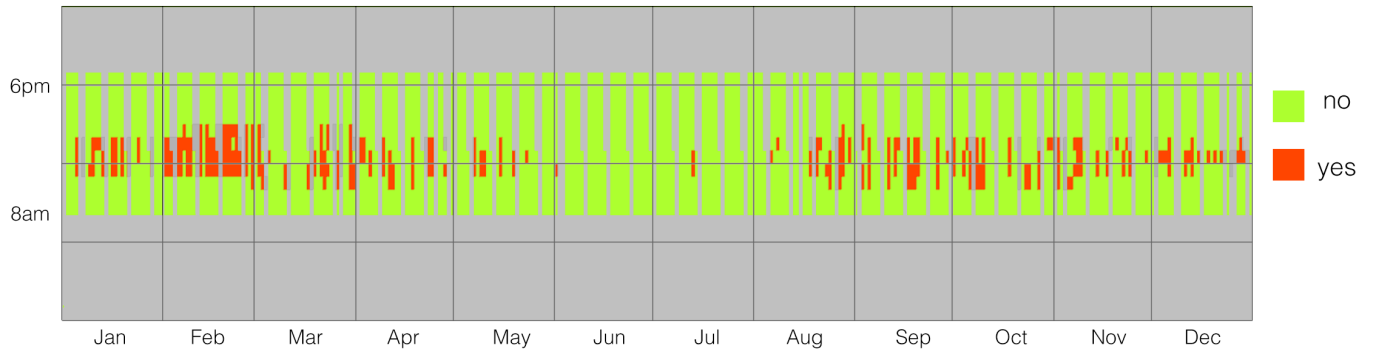


Figure d3.31 Annual glare simulation - point 54 (see figure a.22 pag 59)

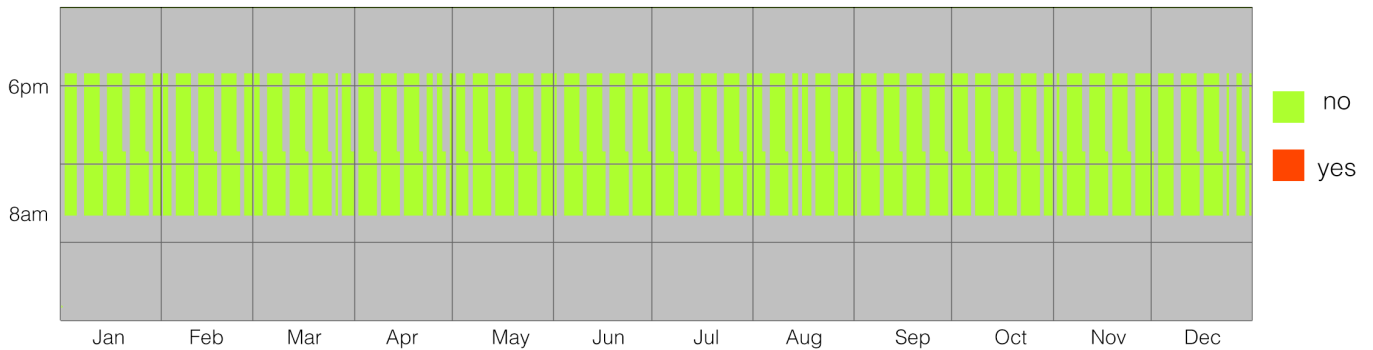


Figure d3.32 Annual glare simulation - point 58 (see figure a.22 pag 59)

Figure d3.31 shows glare condition still occurring from 11am to 15pm, especially during February.

South oriented point 58 is not exposed to glare all over the year.

south - spatial glare maps

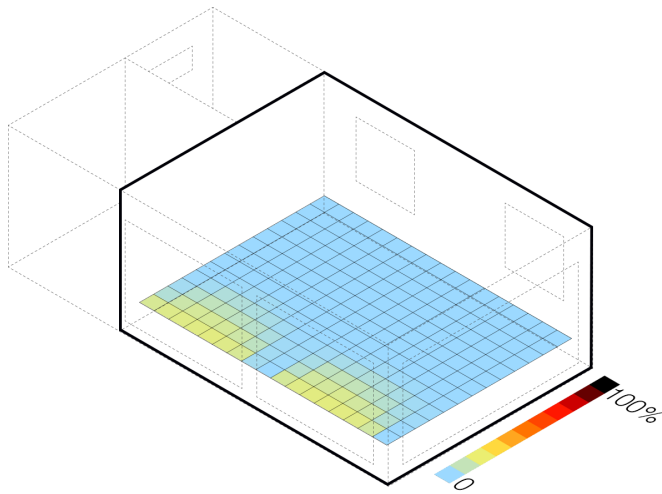


Figure d3.33 Glare Map

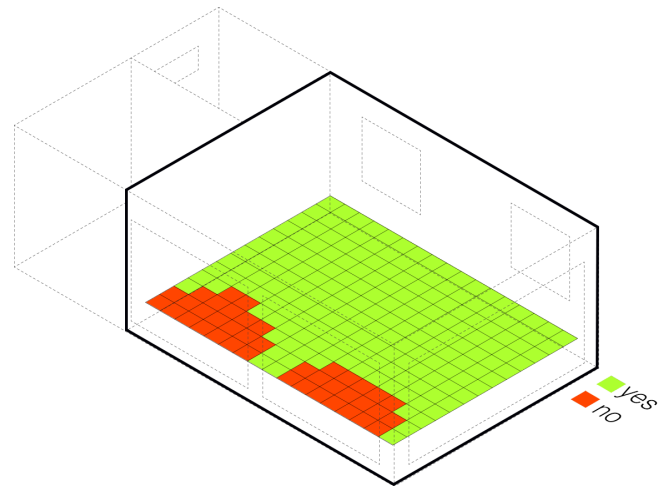
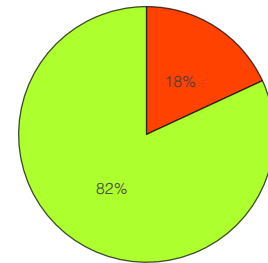


Figure d3.34 Glare Map - verified/ not verified



South oriented points still presents glare conditions happening within 2m from facade. On the contrary, east side is fully verified.

east - Annual glare simulations

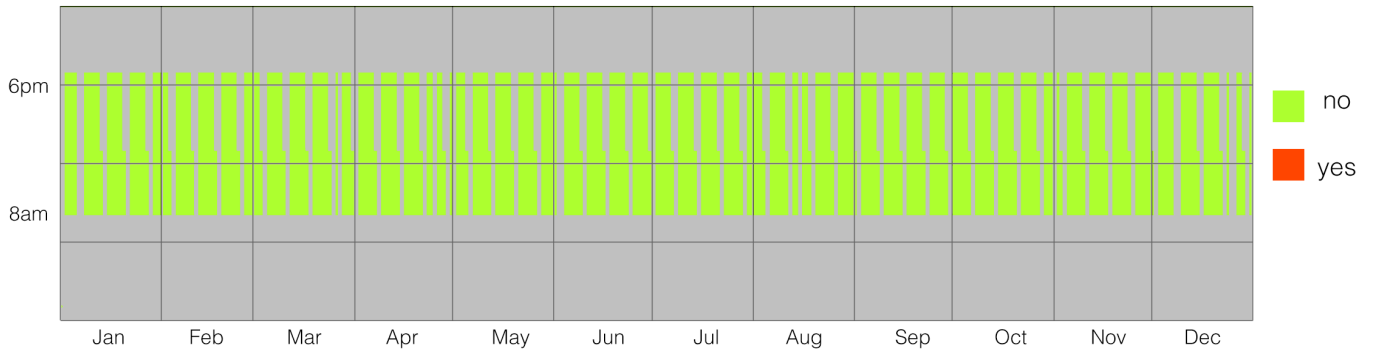


Figure d3.35 Annual glare simulation - point 32 (see figure a.22 pag 59)

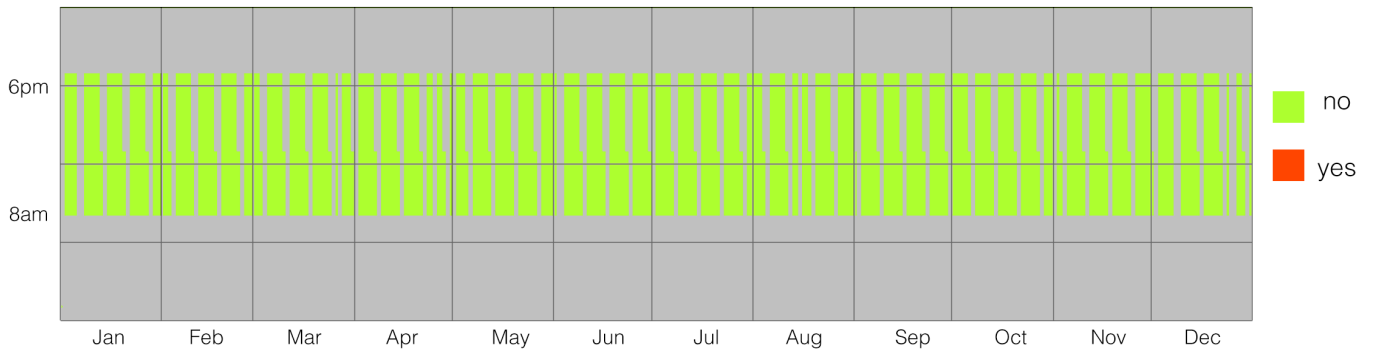


Figure d3.36 Annual glare simulation - point 71 (see figure a.22 pag 59)

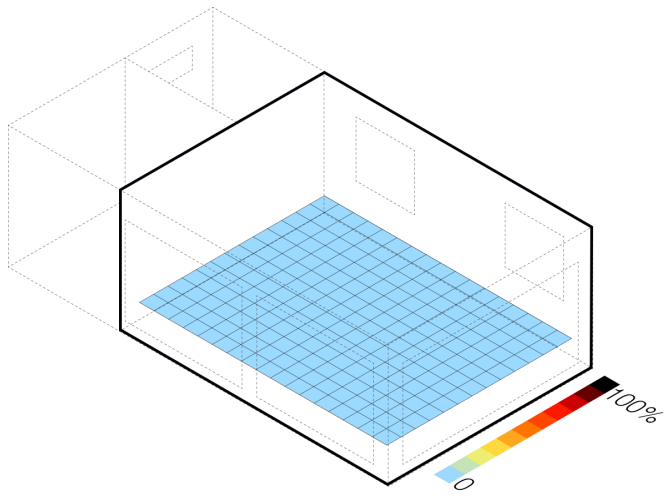


Figure d3.37 Glare Map

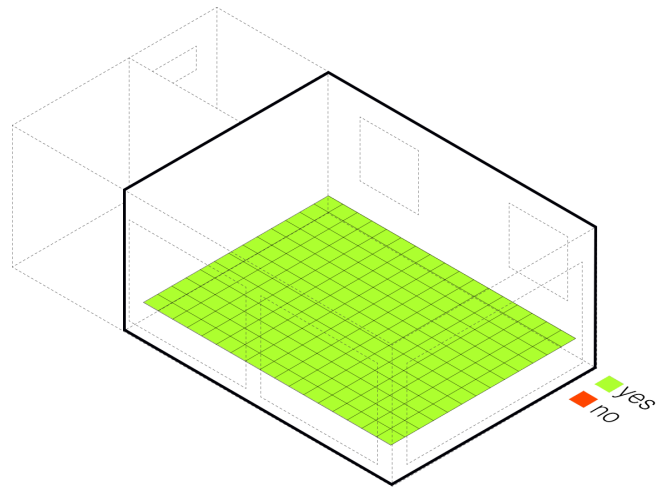
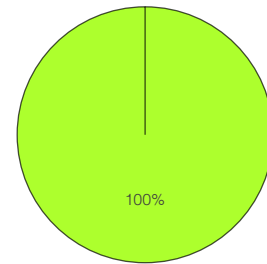


Figure d3.38 Glare Map - verified/ not verified



D4. Thermal + visual comfort

Combined results show reduction in upper and lower ranges (under-lit and over-lit) for over-heating and comfort zone. Increase in under-heated and under-lit hours up to 9% of

occupied time is observed, equal to about 266 hours.

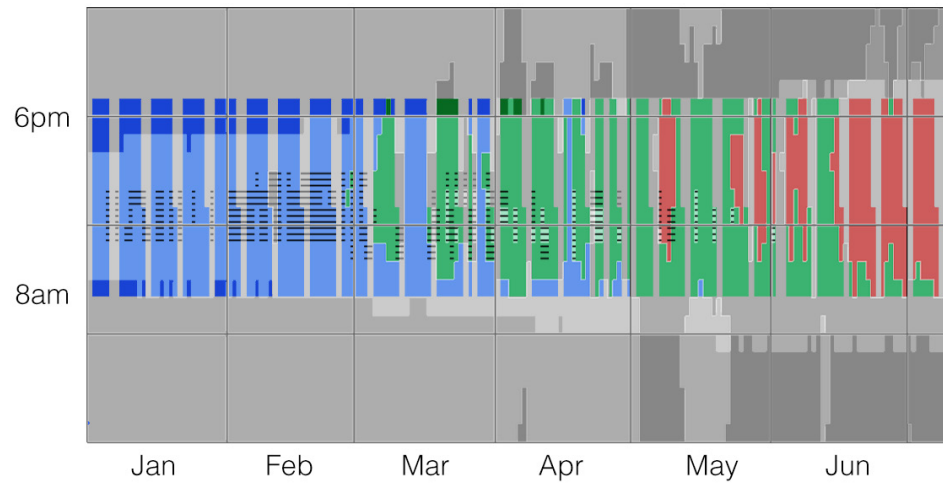
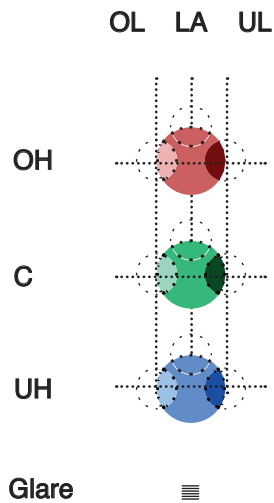
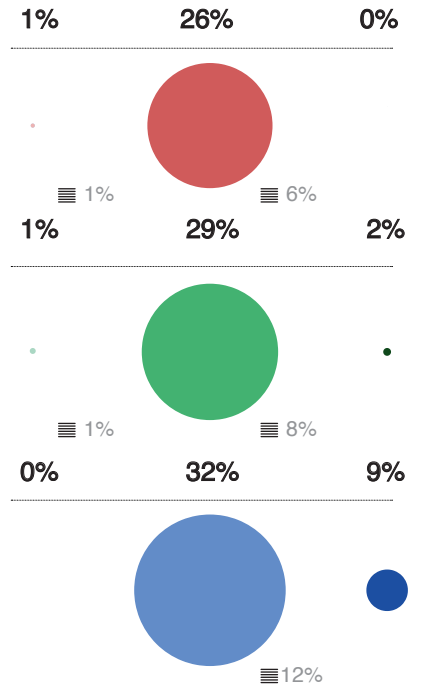
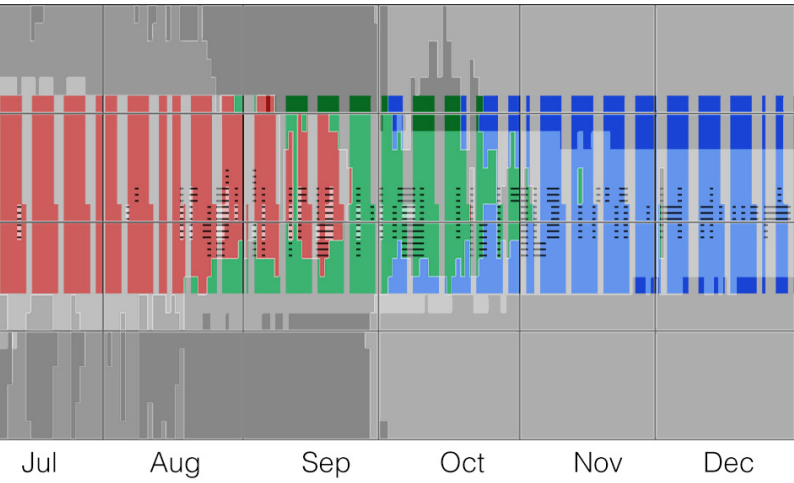


Figure d4.1 Thermal + Visual Comfort evaluation. Point 54



E - fixed shading

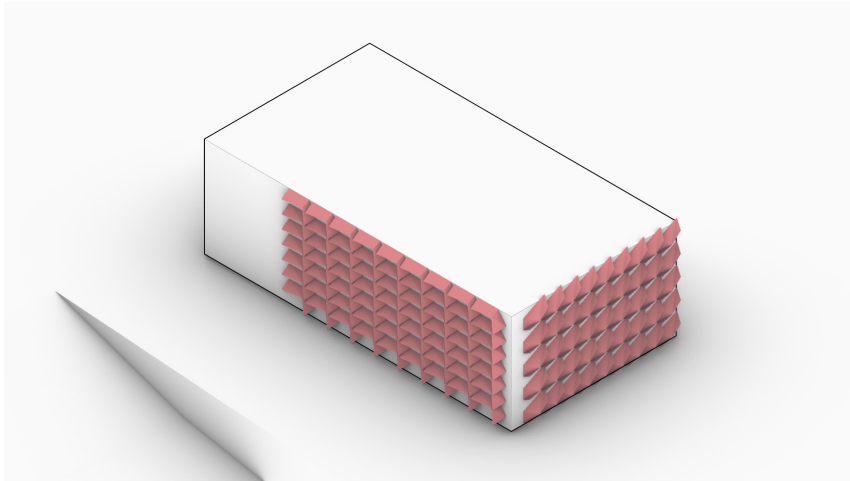


Figure e1.1 Designed Shading system (colored in red)

E1. Solar Study & Shading Masks

This section provides a final simulation with application of a fixed shading system (see figure on previous page). The latter is designed according to basic solar study, HSA and VSA (solar altitudes and amplitudes respectively) [20].

Moreover, a ladybug tool is used to draw shading masks and compute shading deriving from both building obstructions and designed system.

According to previous results and a large span of Over-heating mainly occurring from March to September, shading masks are drawn in order to cover sun-path relative to critical months (see images on next pages).

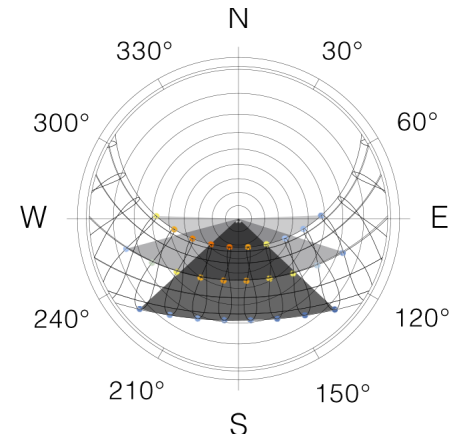


Figure e1.2 Summer, Winter and Equinox position of the sun in Turin

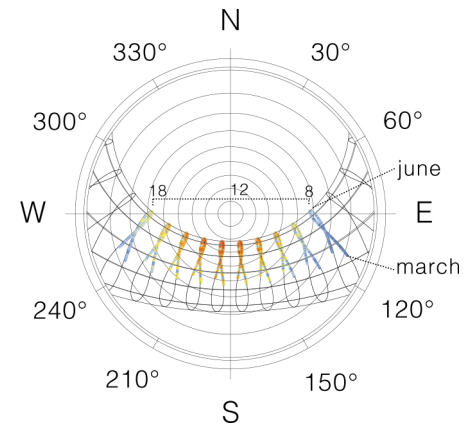


Figure e1.3 Sun path from March to September

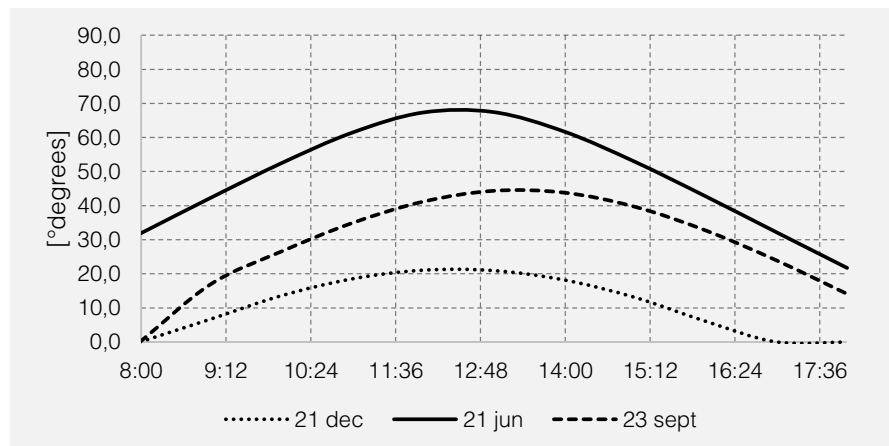


Figure e1.4 Different Sun altitudes in Turin

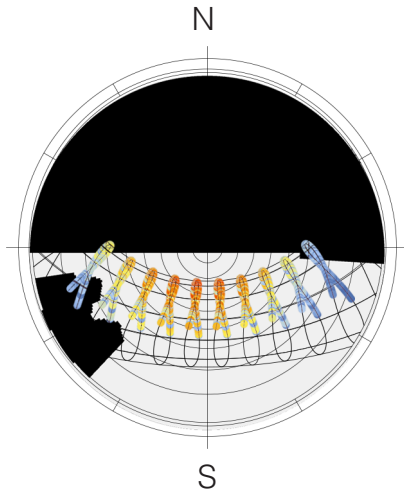


Figure e1.4 Shading Mask with obstructions alone - south

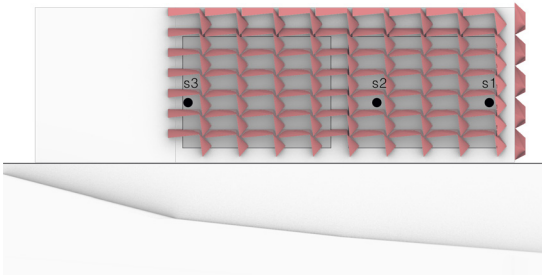
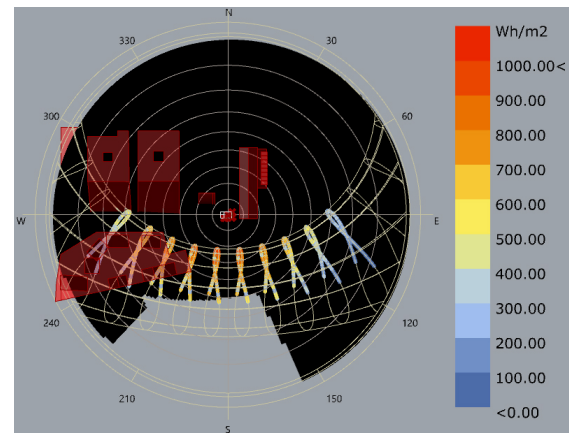
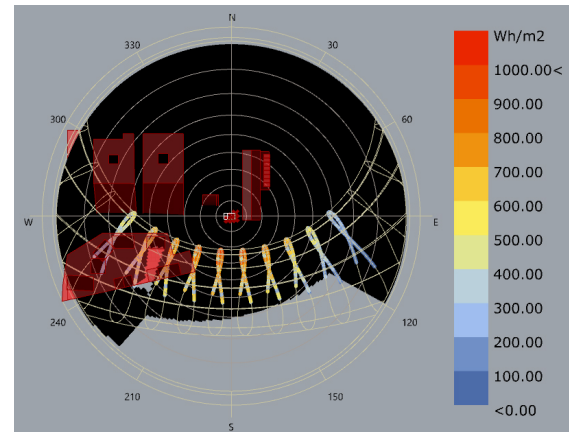
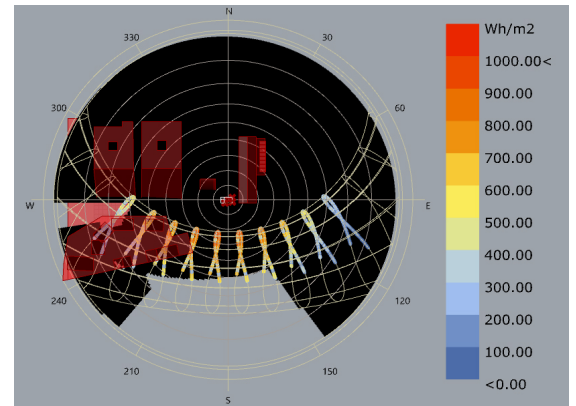


Figure e1.5 Front view - shading mask points

On the right, in order of appearance:
 shading mask for point s1
 shading mask for point s2
 shading mask for point s3



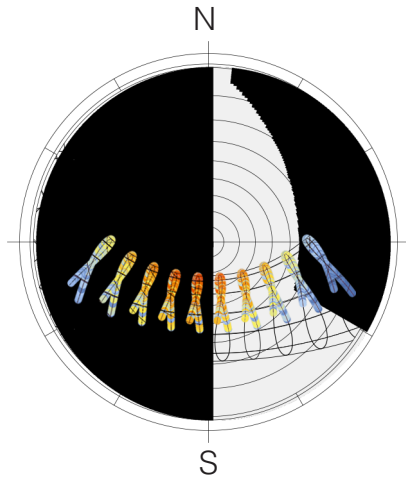


Figure e1.4 Shading Mask with obstructions alone - east

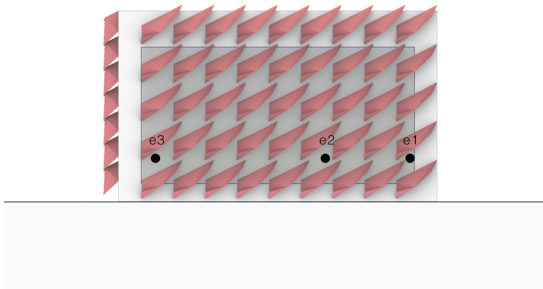
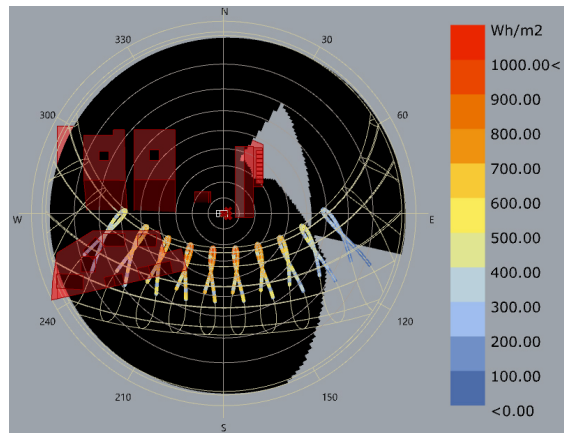
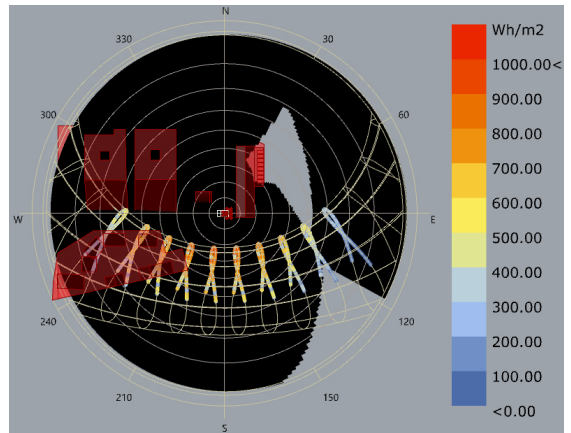
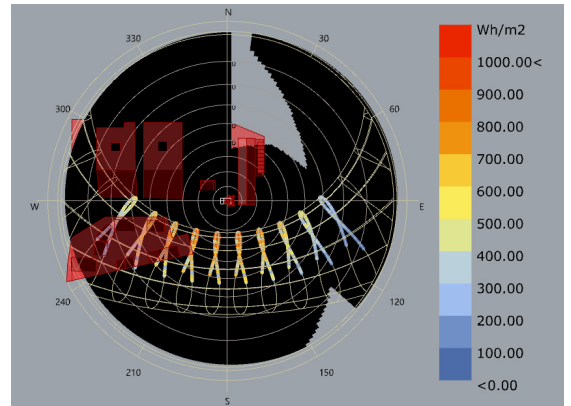


Figure e1.5 East view - shading mask points

On the right, in order of appearance:
 shading mask for point e1
 shading mask for point e2
 shading mask for point e3



E2.Thermal Comfort Analysis

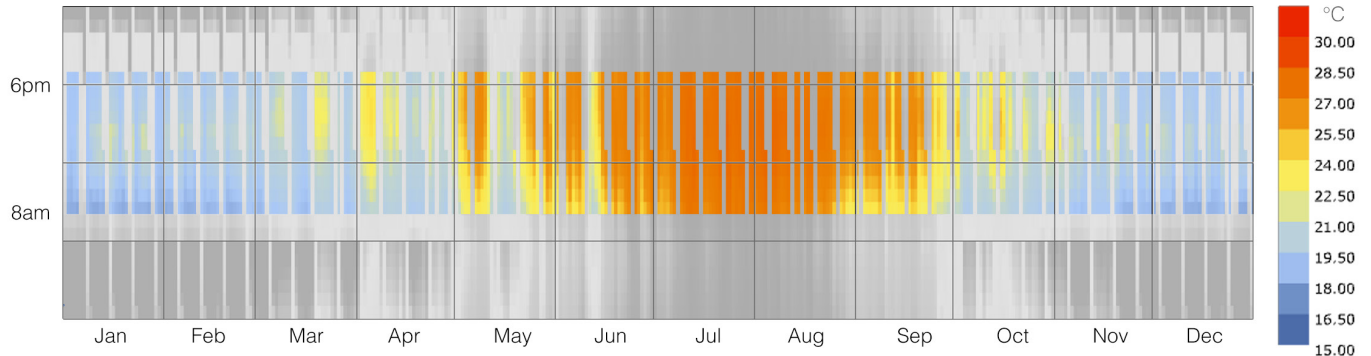


Figure e2.1 Adjusted Operative Temperature - fixed shading scenario

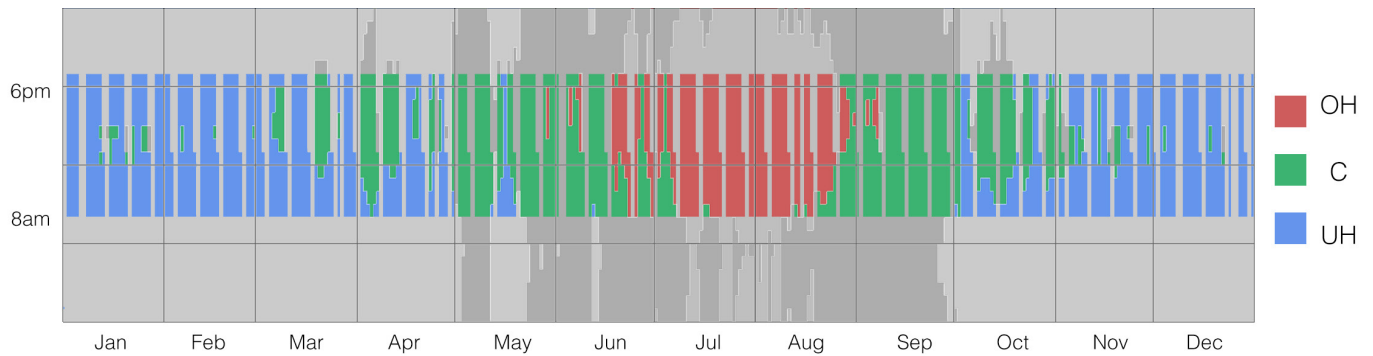


Figure e2.2 Over-heated, Comfort and Under-heated range - fixed shading scenario

Figure e2.2 shows a considerable reduction in Over-heating, now dropped to an average of 18%. Also, Comfort % sees a small increase, parallel to a consistent increase in the number of

under-heated hours (46%).

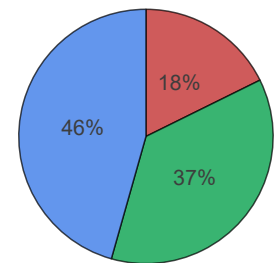


Figure b3.

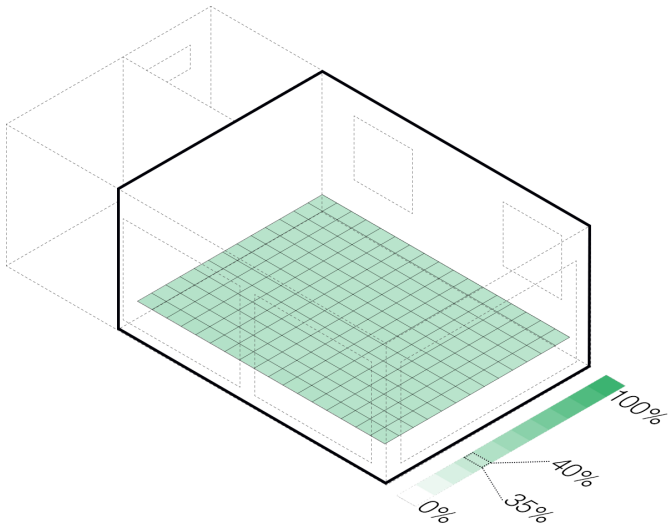
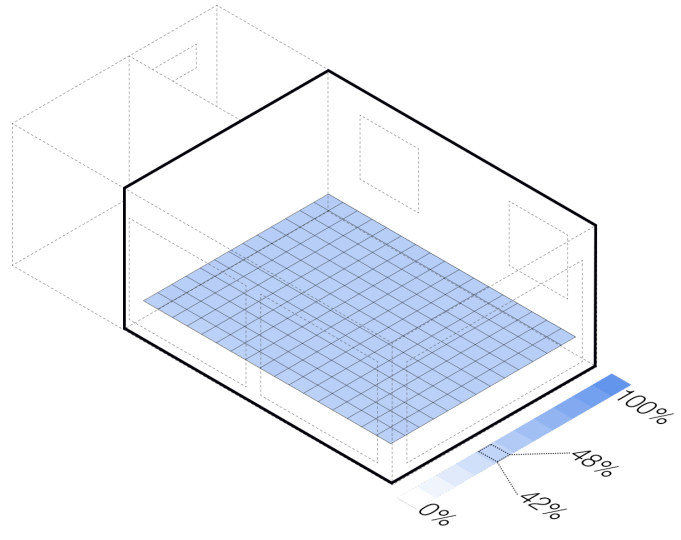
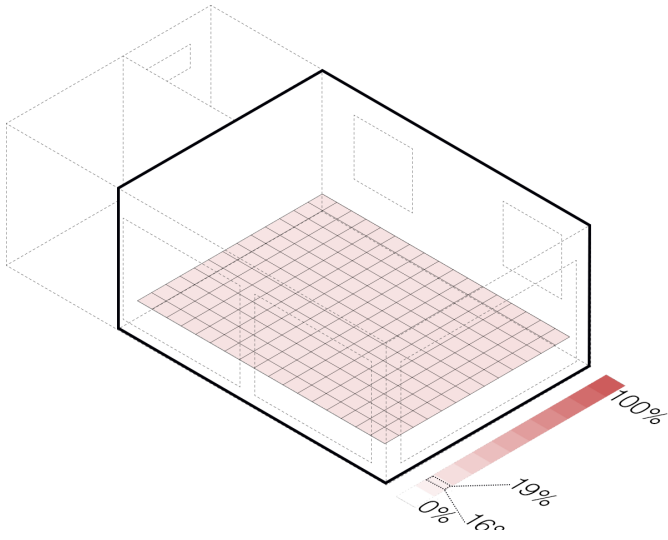


Figure e2.5 Comfort Map

E3. CBDM & Daylight Analysis

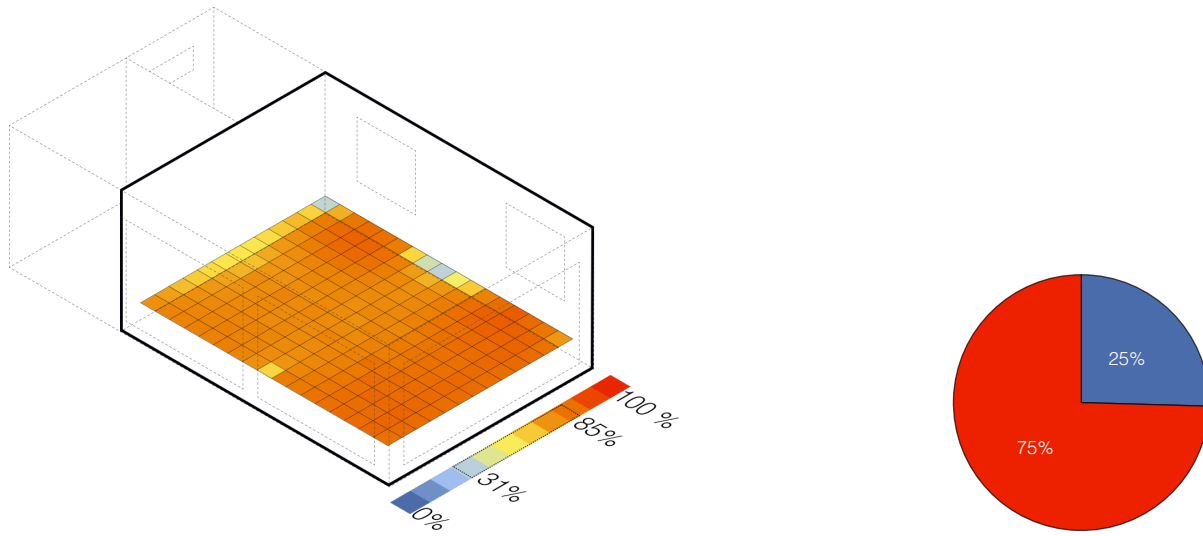


Figure e3.1 Daylight Autonomy

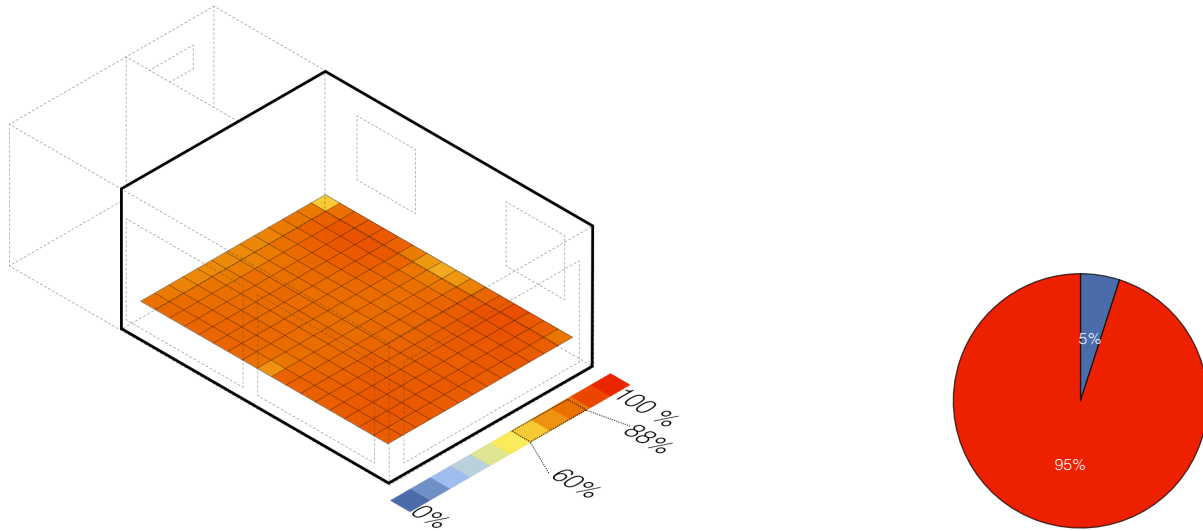


Figure e3.2 Spatial Daylight Autonomy

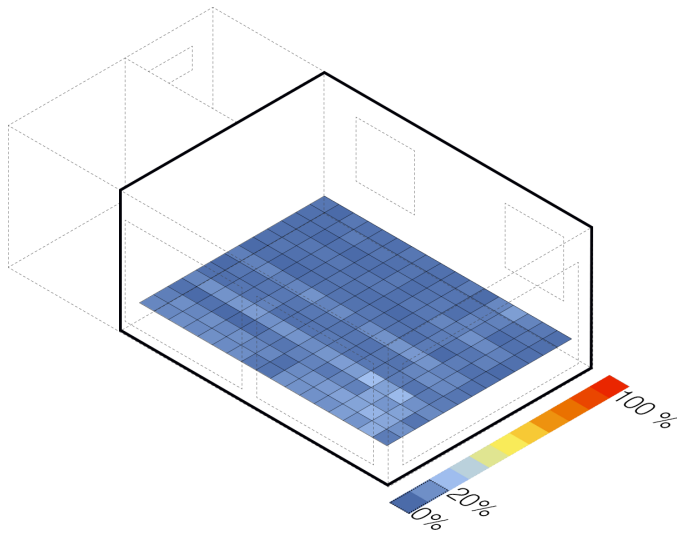


Figure e3.3 UDI>3000 lx

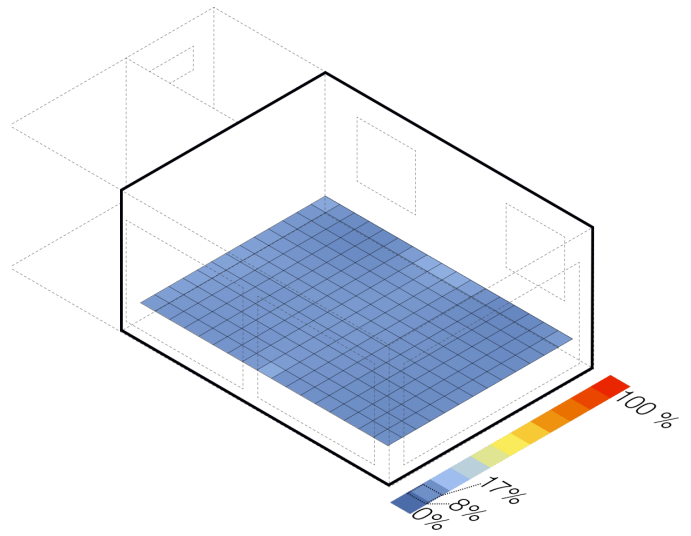


Figure e3.4 UDI<100 lx

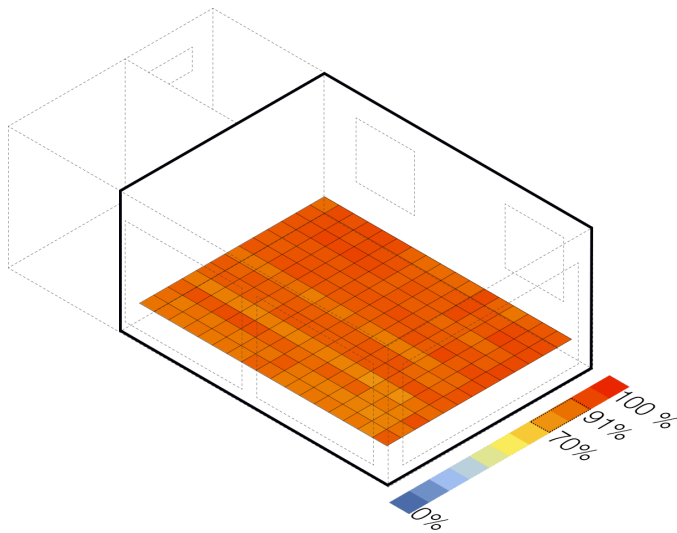


Figure e3.5 UDI,achieved

All this figures show constant distribution of daylight levels across the space. Daylight Autonomy range varies from 31 to 85%, yet the area with lower values is limited to few points along the perimeter of the zone (in particular west side). UDI,achieved range varies from 70 to 91%

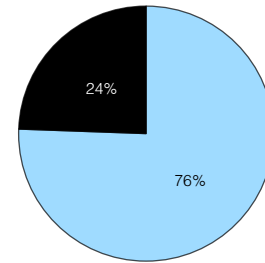
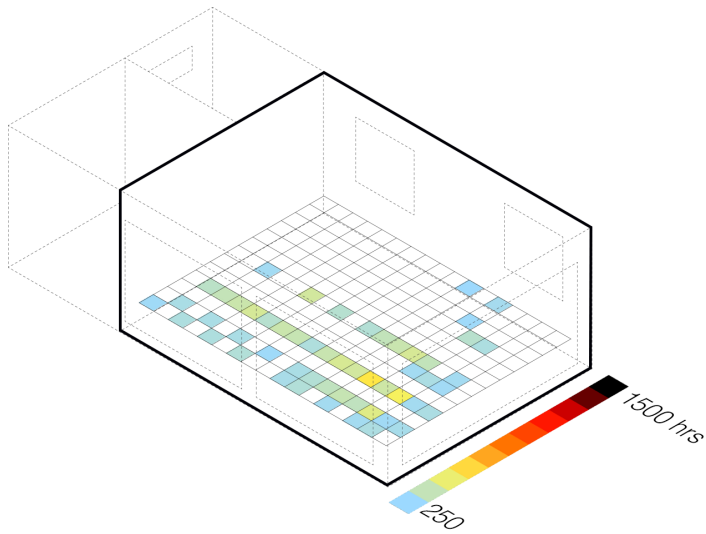


Figure e3.6 ASE

ASE shows a big reduction in exceeding values. Despite not being verified yet, those points that are beyond acceptable value of 250 hours per year, display a great reduction in exceeding hours in respect of this specific value, thus being really close to it.

Luminous Autonomy - 3 points

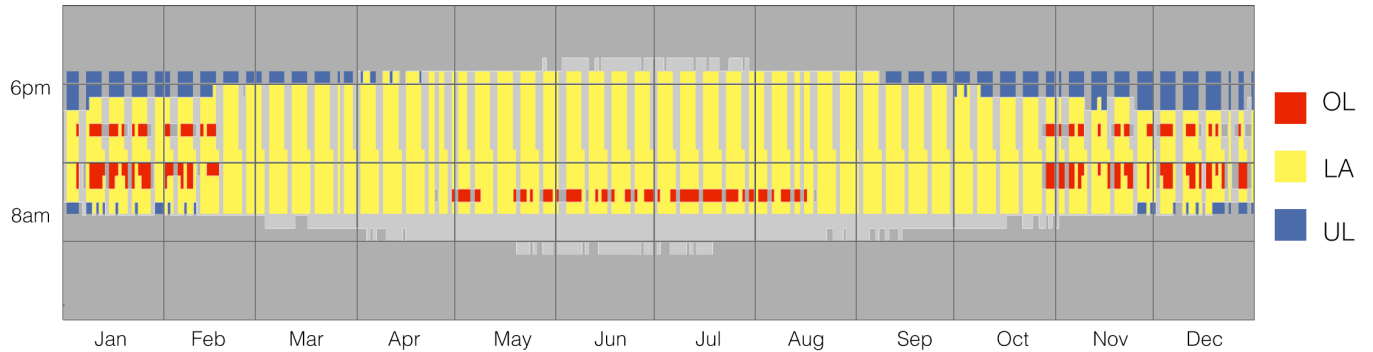


Figure e3.7 Over-lit (OL), Luminous autonomy (LA) and Under-lit (UL) range - point 54

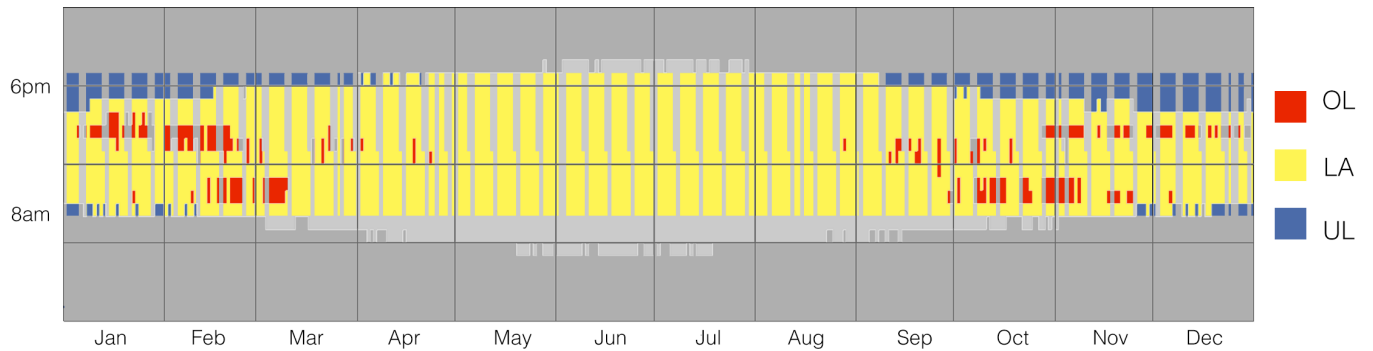


Figure e3.8 Over-lit (OL), Luminous autonomy (LA) and Under-lit (UL) range - point 32

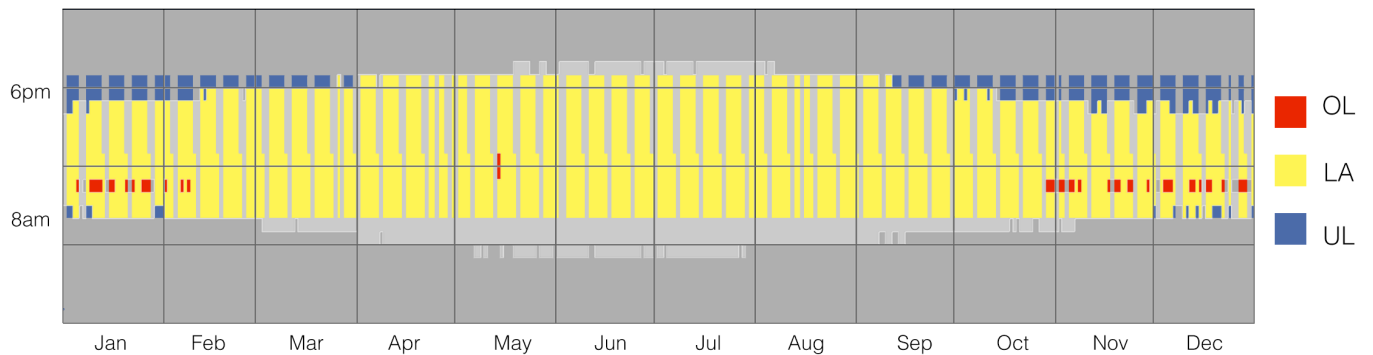


Figure e3.9 Over-lit (OL), Luminous autonomy (LA) and Under-lit (UL) range - point 179

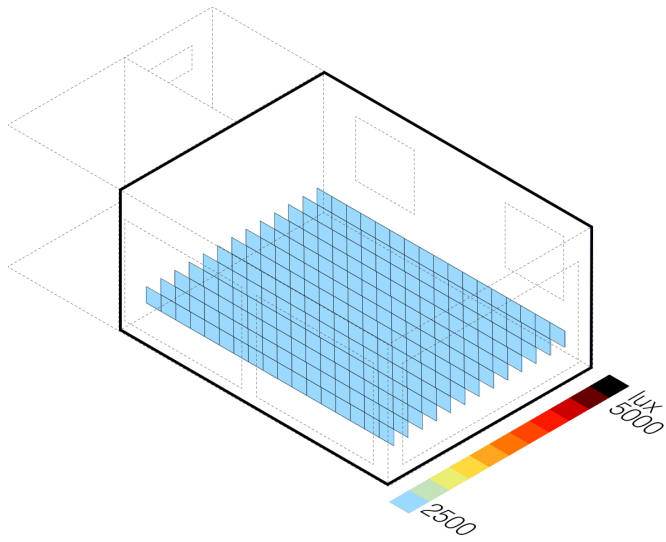


Figure e4.1 8 am

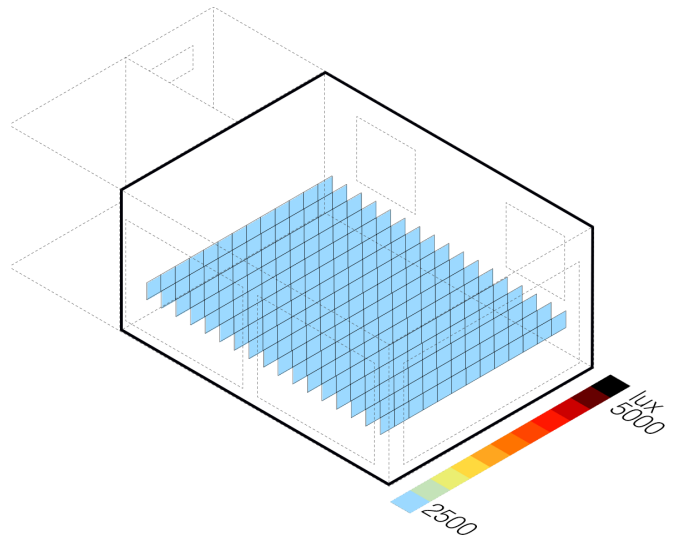


Figure e4.2 8 am

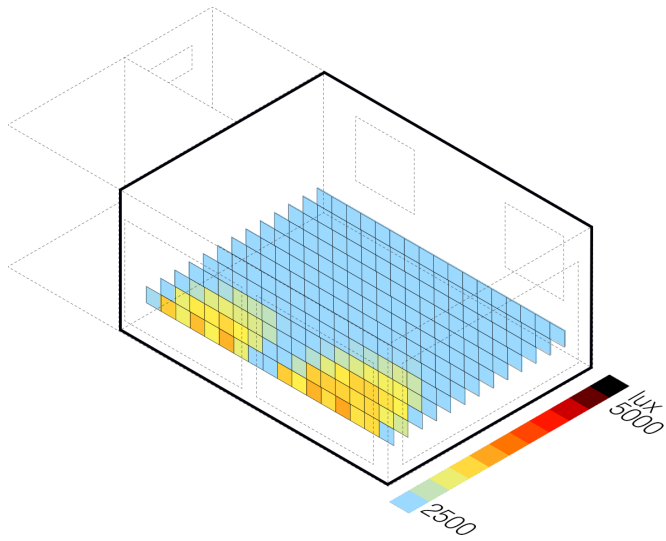


Figure e4.3 10 am

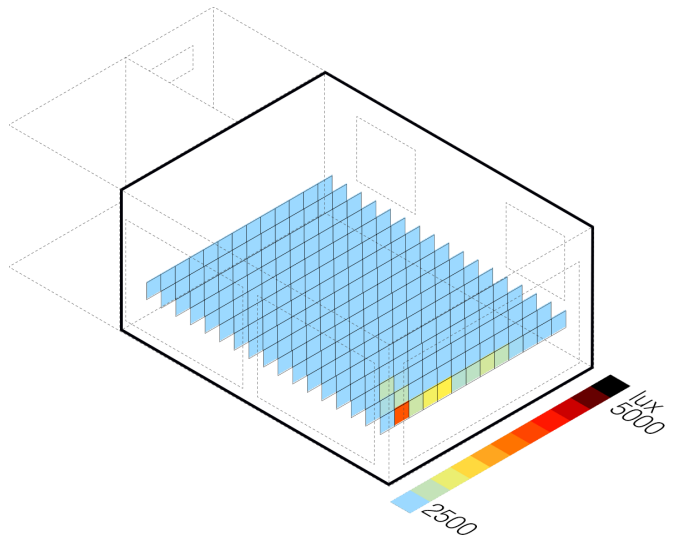


Figure e4.4 10 am

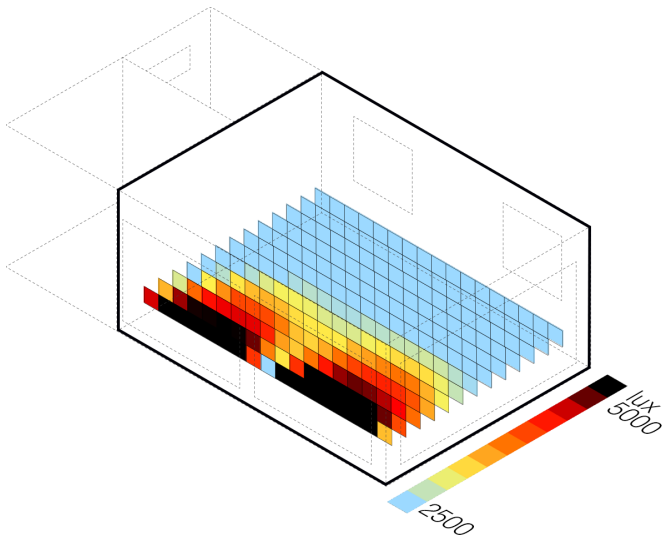


Figure e4.5 12 pm

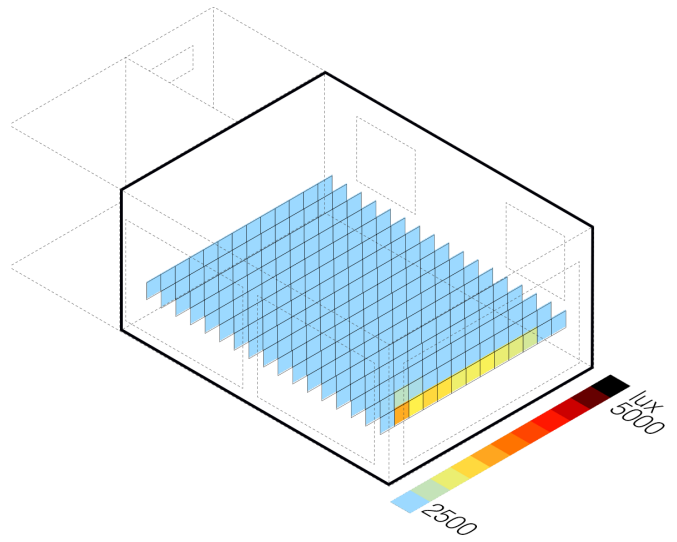


Figure e4.6 12pm

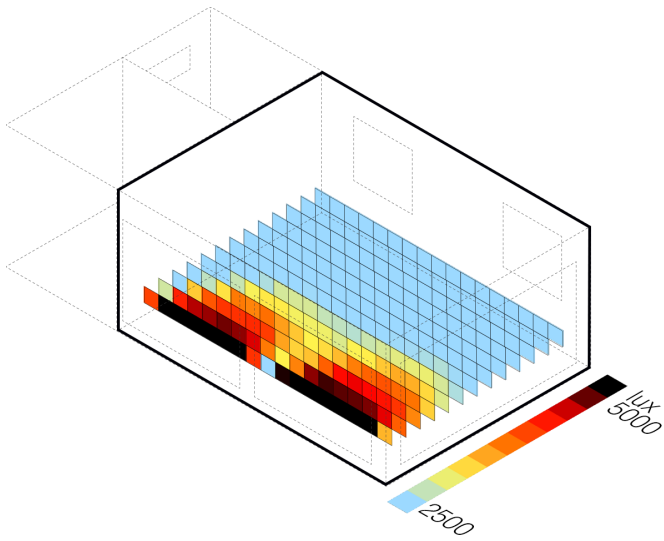


Figure e4.7 14 pm

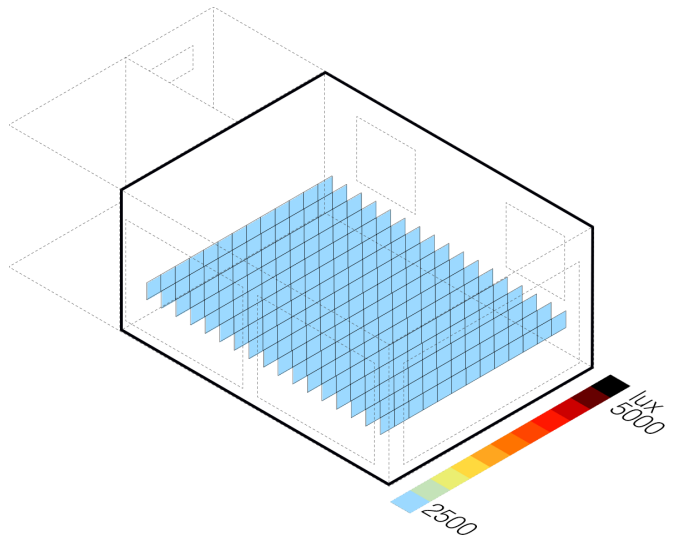


Figure e4.8 14 pm

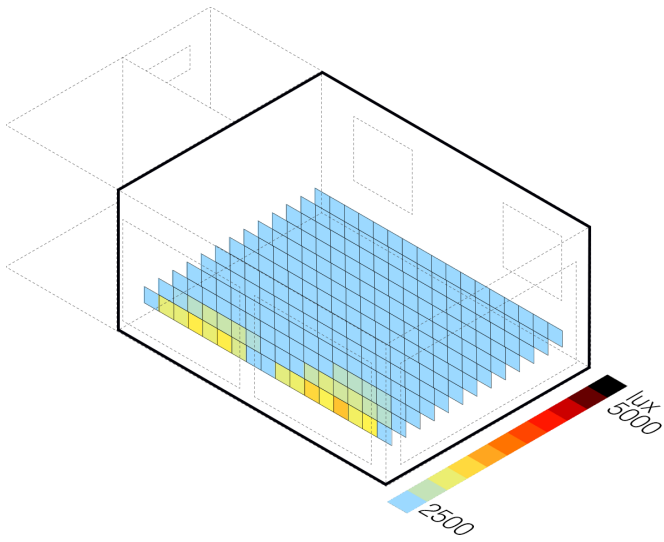


Figure e4.9 16 pm

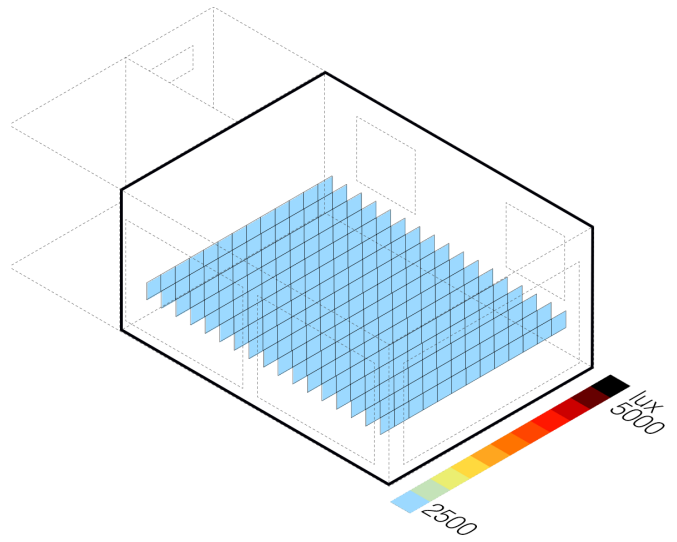


Figure e4.10 16pm

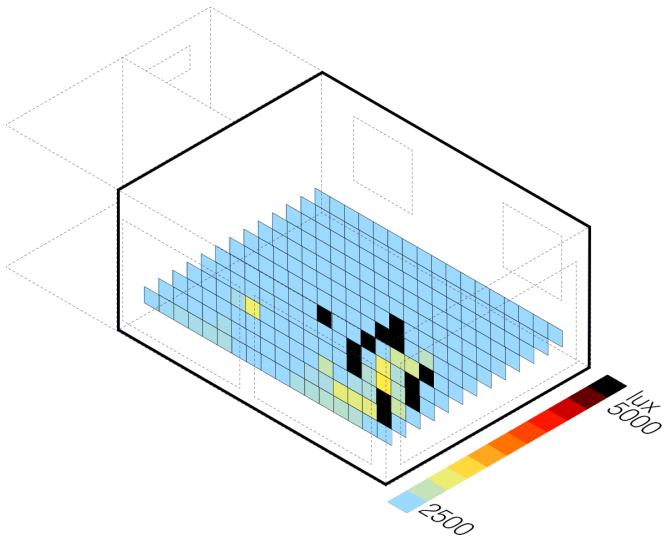


Figure e4.11 8 am

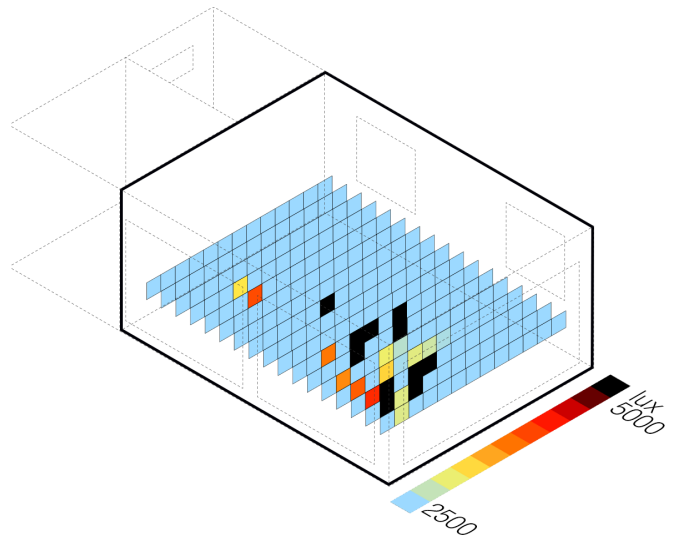


Figure e4.12 8am

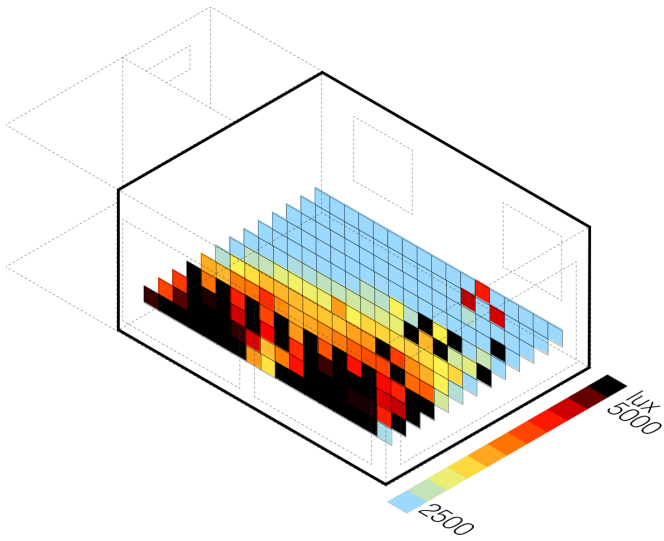


Figure e4.13 10 am

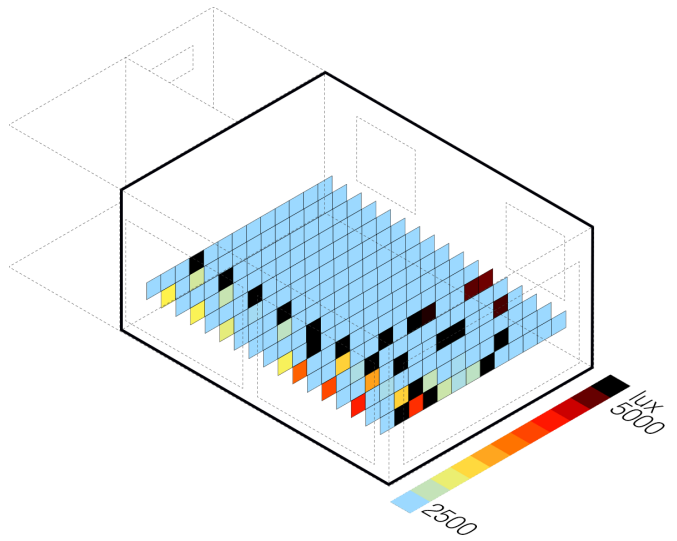


Figure e4.14 10 am

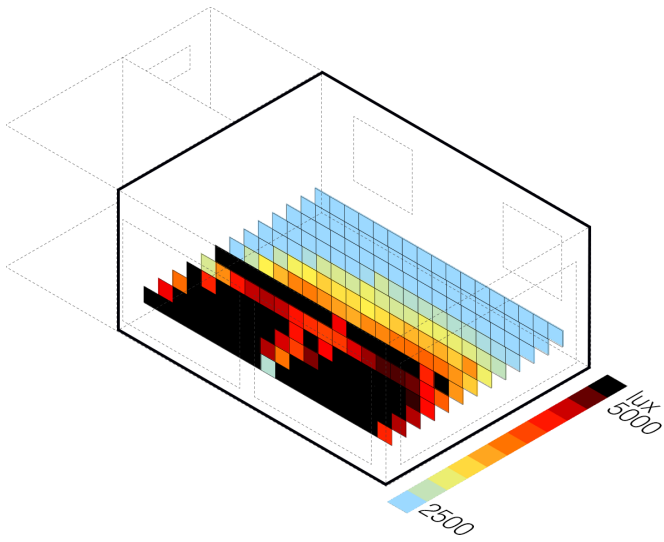


Figure e4.15 12 pm

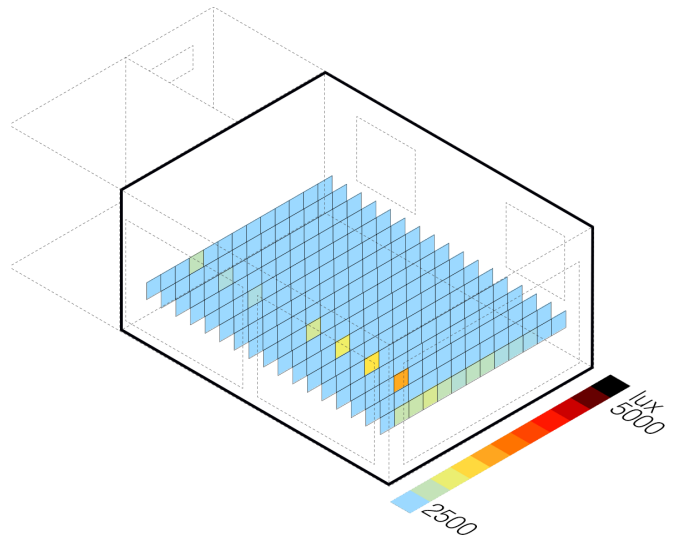


Figure e4.16 12pm

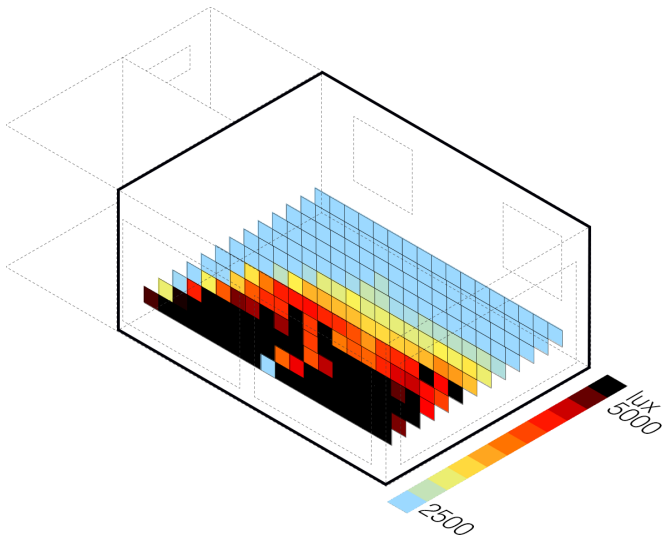


Figure e4.17 14 pm

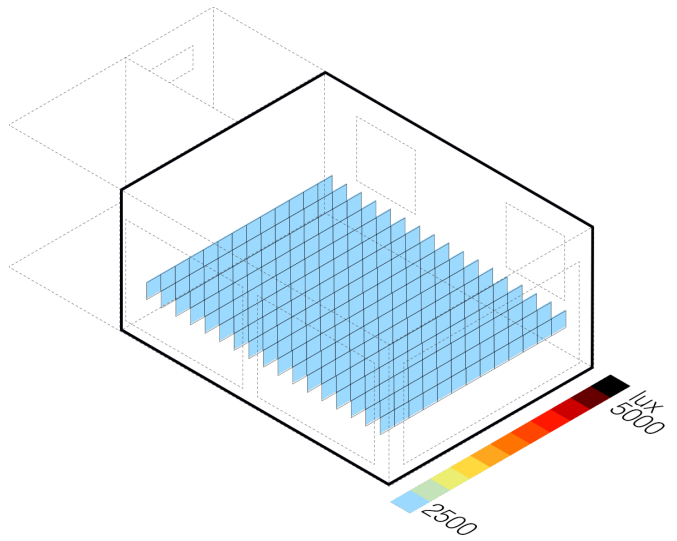


Figure e4.18 14 pm

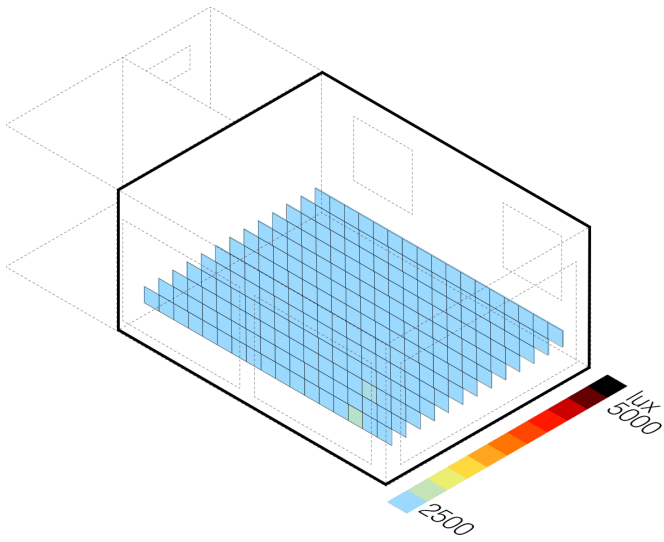


Figure e4.19 16 pm

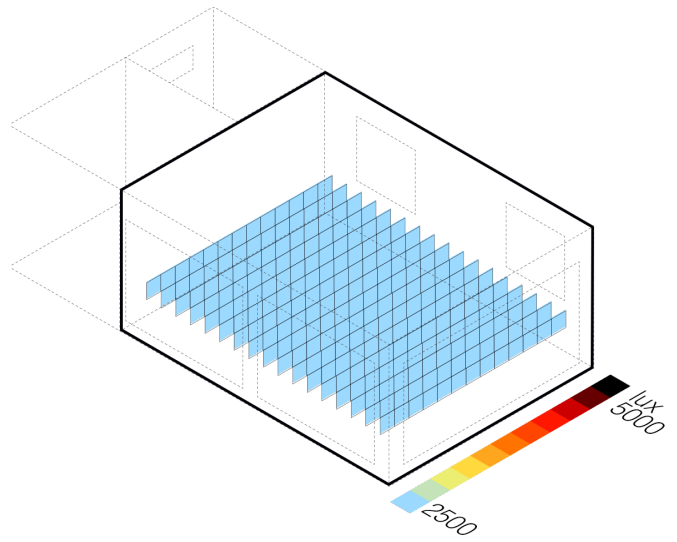


Figure e4.20 16pm

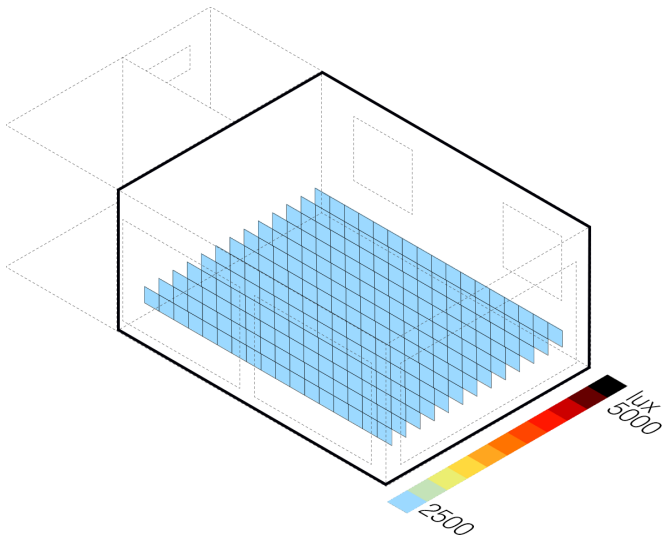


Figure e4.21 8 am

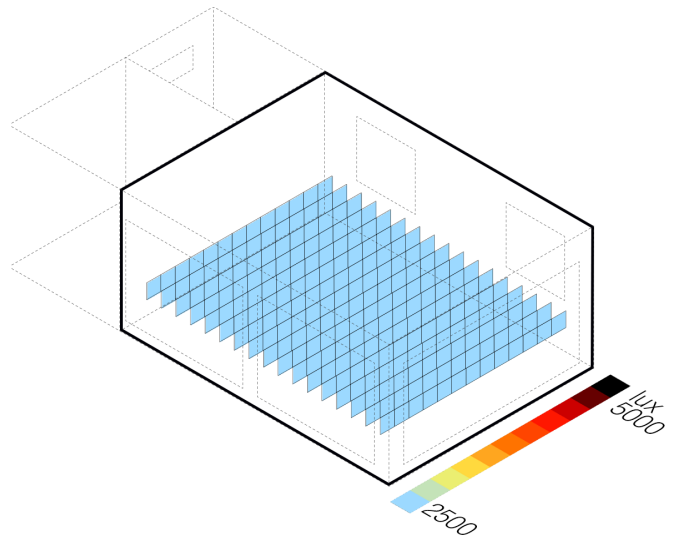


Figure e4.22 8am

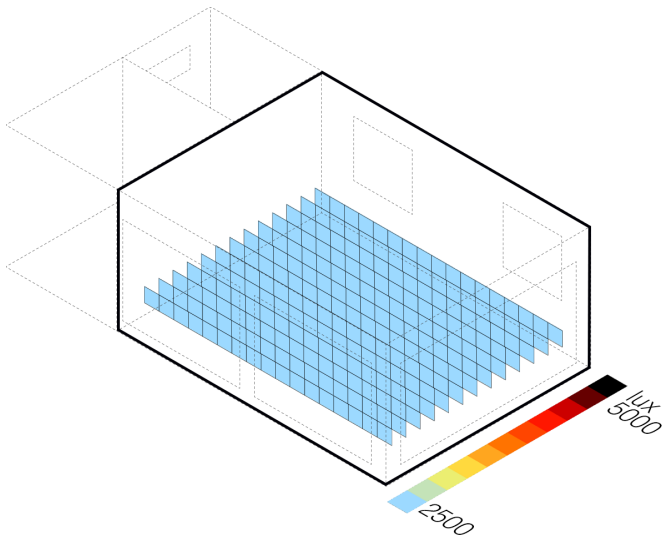


Figure e4.23 10 am

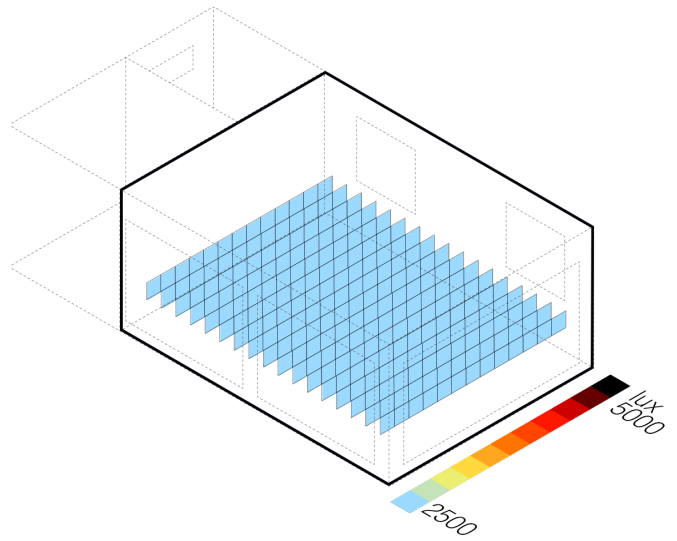


Figure e4.24 10 am

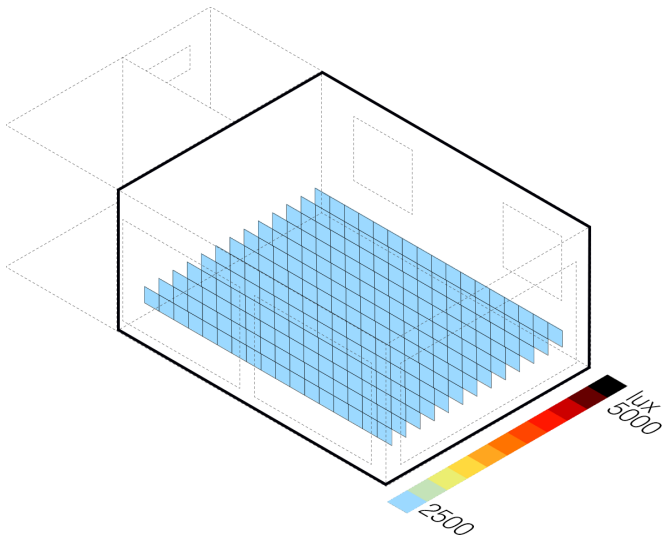


Figure e4.25 12 pm

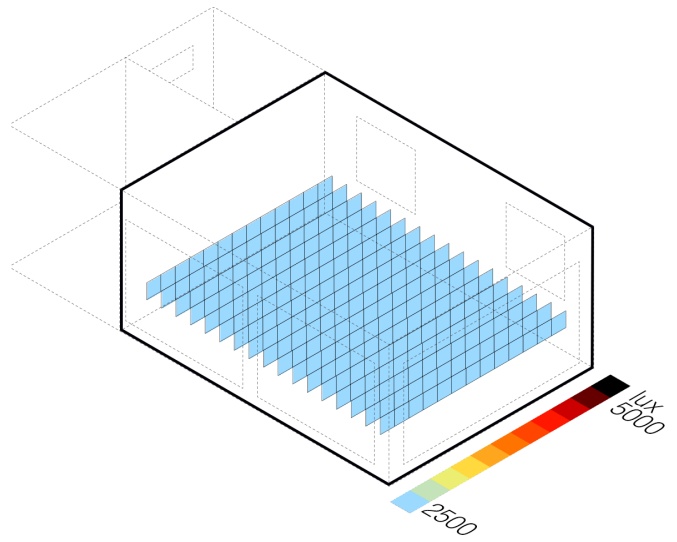


Figure e4.26 12pm

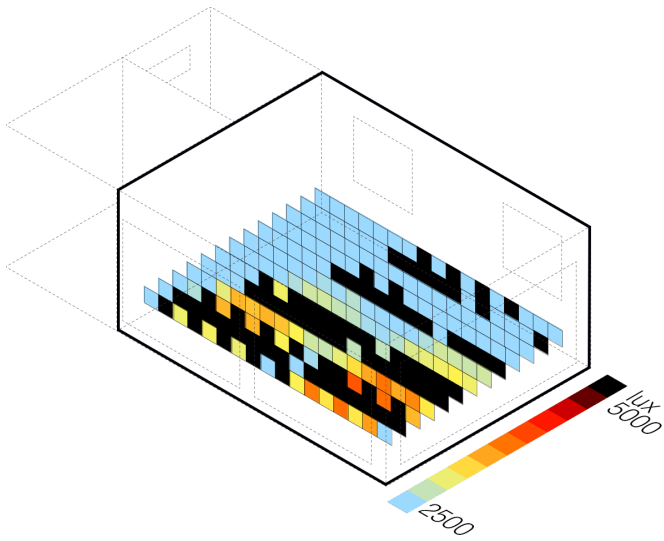


Figure e4.27 14 pm

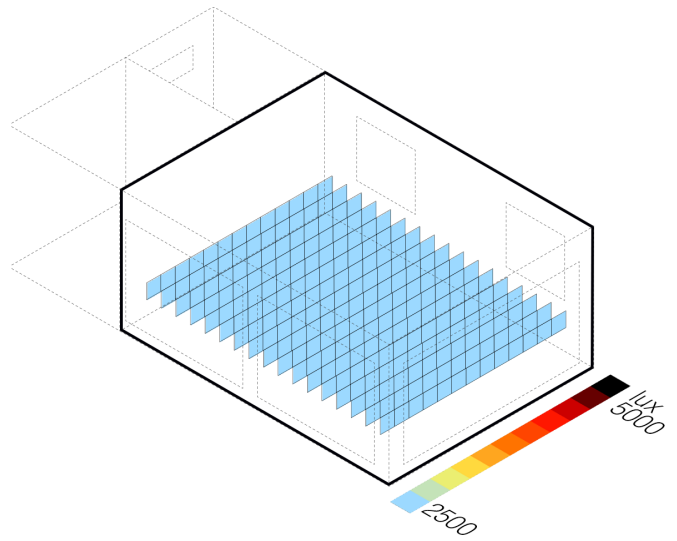


Figure e4.28 14 pm

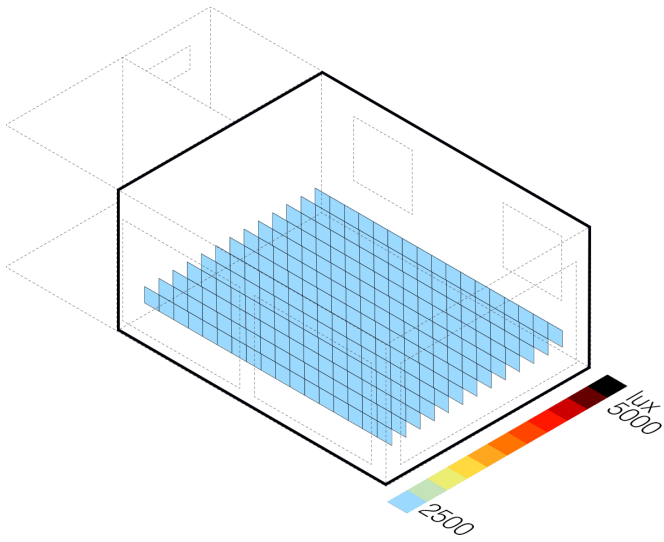


Figure e4.29 16 pm

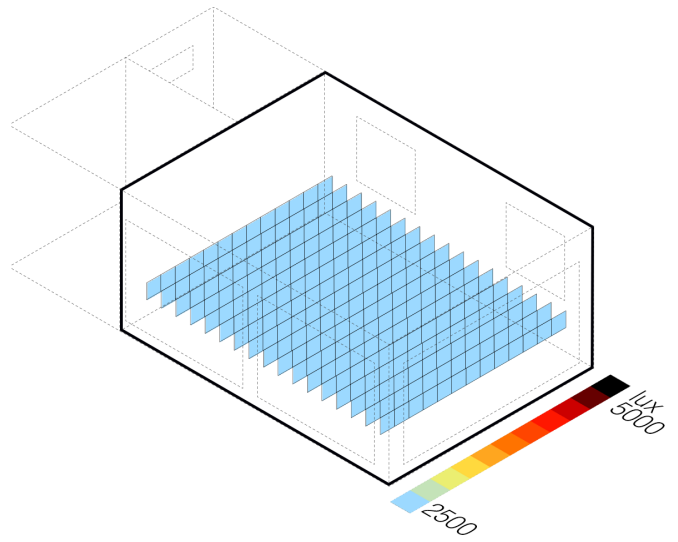


Figure e4.30 16pm

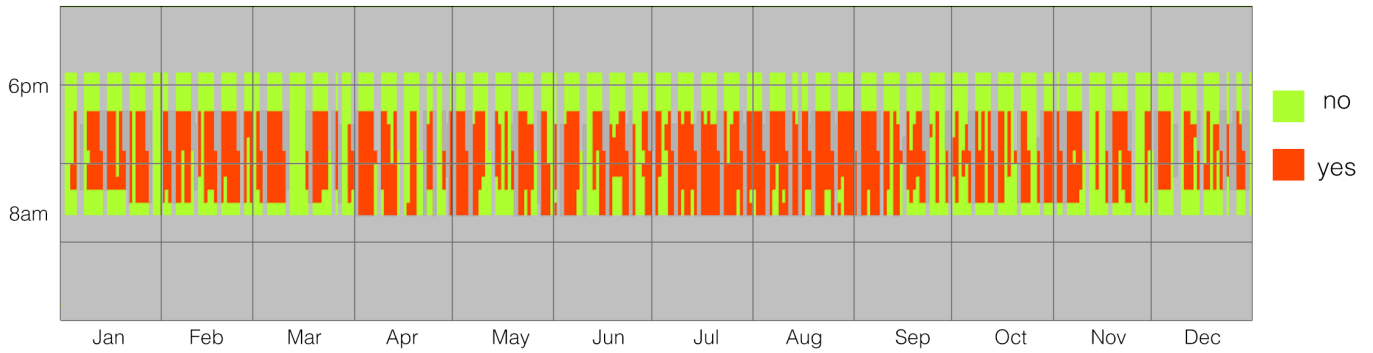


Figure e4.31 Annual glare simulation - point 54 (see figure a.22 pag 59)

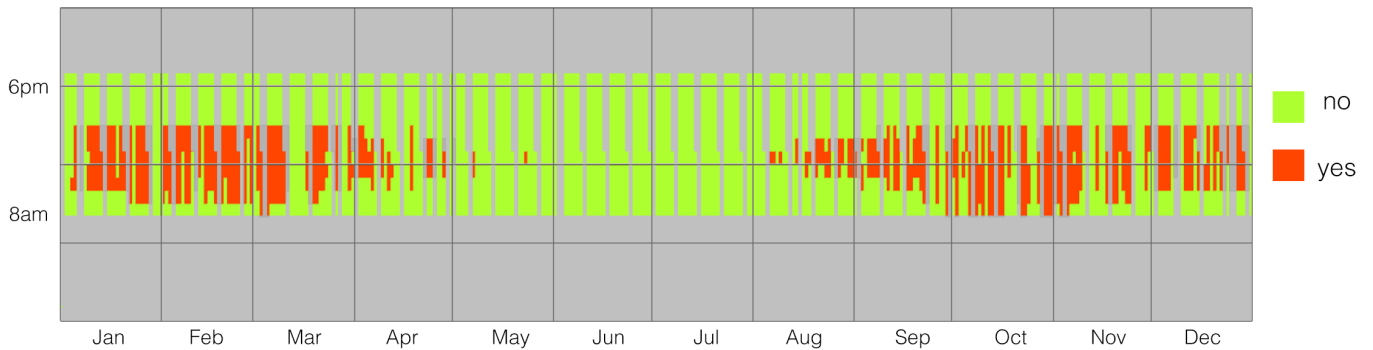


Figure e4.32 Annual glare simulation - point 58 (see figure a.22 pag 59)

By looking at south orientation, both vertical illuminances (figures e4.5, e4.7, e4.15, e4.17) and annual glare plots (figures above) show critical results. Point 58 reveals glare condition from January to April and from August to December.

south - spatial glare maps

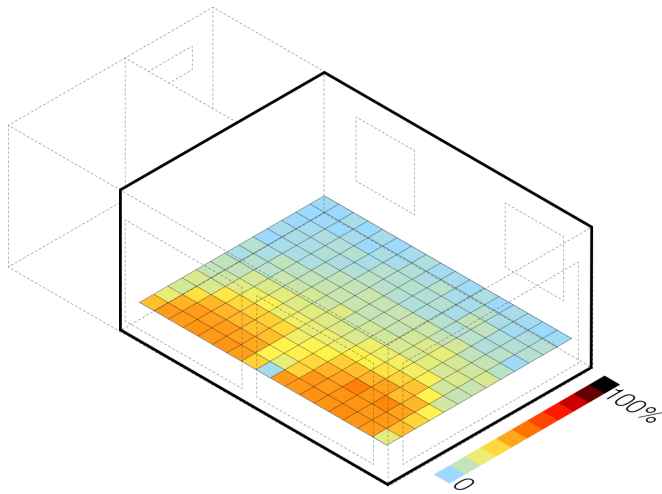


Figure e4.33 Glare Map

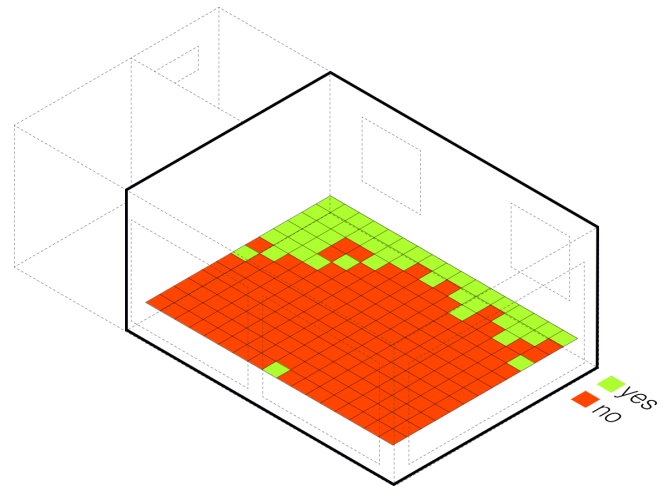
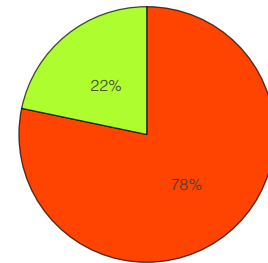


Figure e4.34 Glare Map - verified/ not verified



As already discussed, south orientation is still critical. First 3m presents points with occurring glare around 40-50% of occupied time

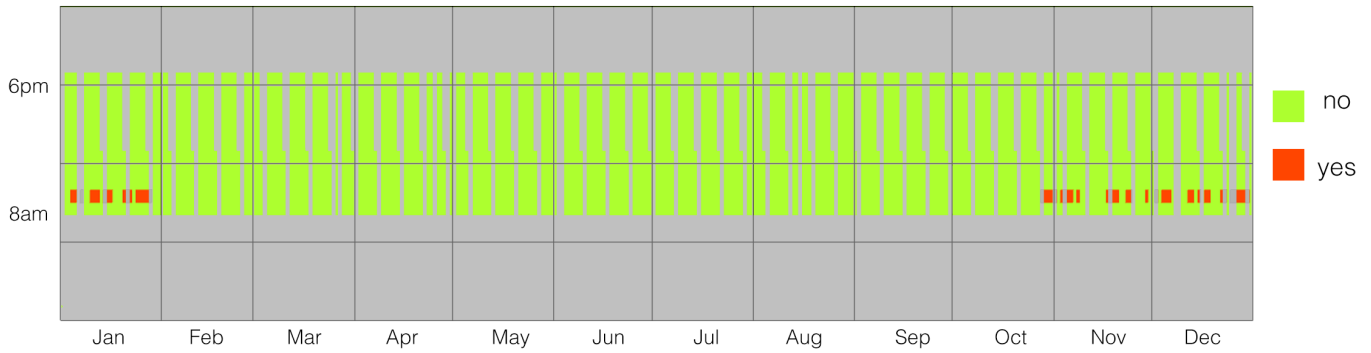


Figure e4.35 Annual glare simulation - point 32 (see figure a.22 pag 59)



Figure e4.36 Annual glare simulation - point 71 (see figure a.22 pag 59)

Shading system better works for east orientation. Point 32 has glare from 9am to 10am in January, November and December. Point 71, which is 3 m from east facade, presents more glare occurring from late February to beginning of April

and from end of August to beginning of November, from 8am to 10am.

east - spatial glare maps

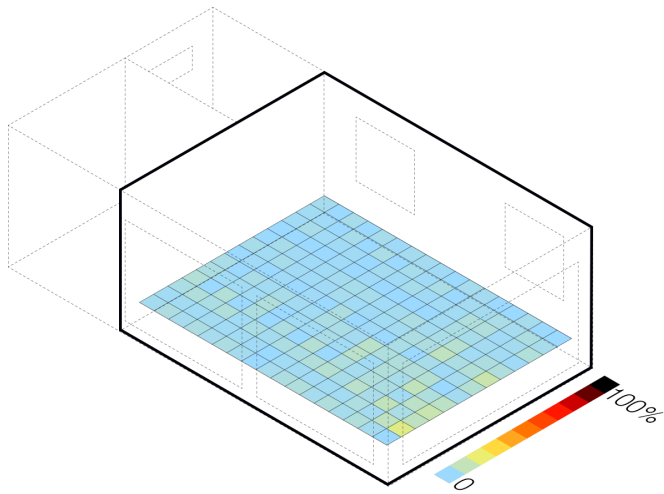


Figure e4.37 Glare Map

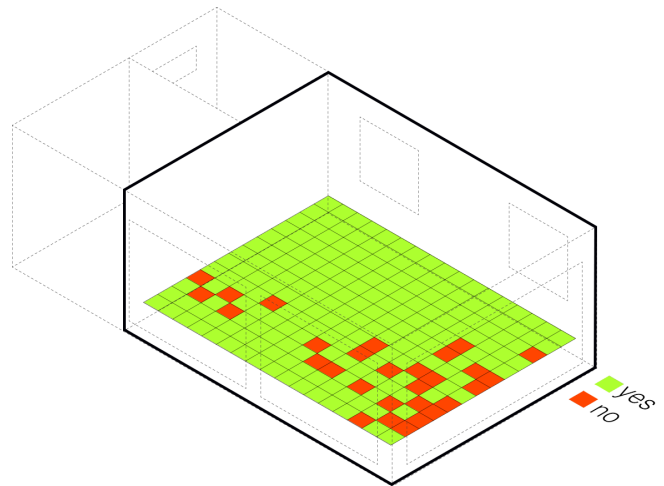
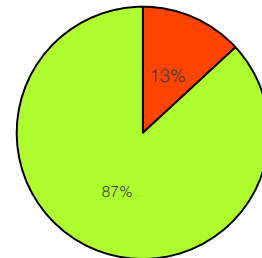


Figure e4.38 Glare Map - verified/ not verified



East orientation has 87% of points not having glare condition for more than 5% of occupied time.

E5. Thermal + visual comfort

18% Over-heated range, which correspond to 545 occupied hours, does not present over-lit or under-lit cases. Comfort range is associated to highest amount of glare hours (18%, same hours of

over-heating). Under-heated and Under-lit hours covers 8% of occupied time.

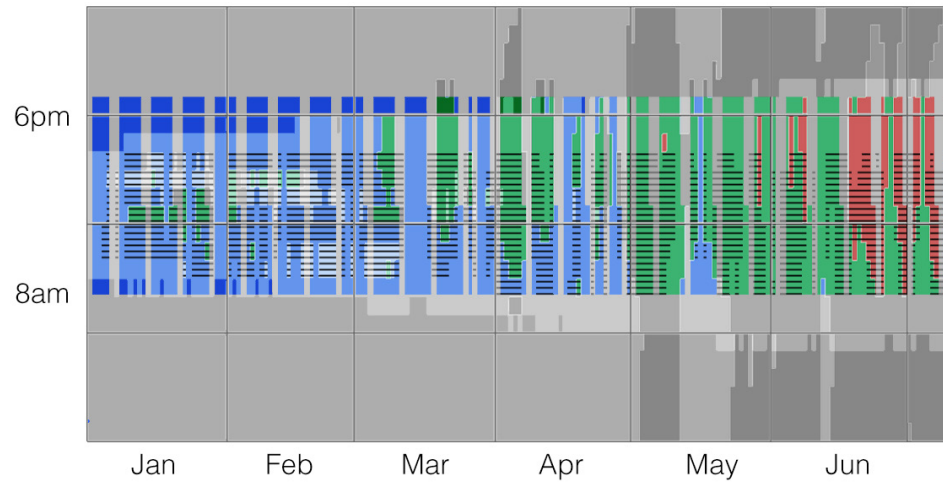
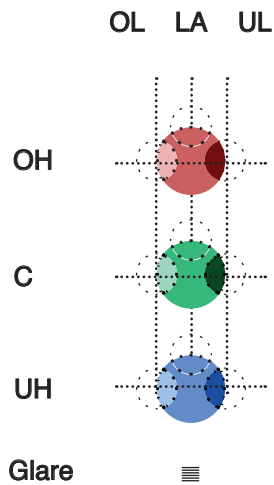
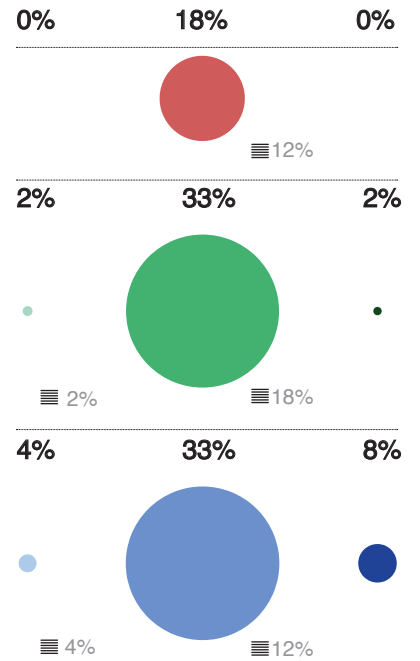
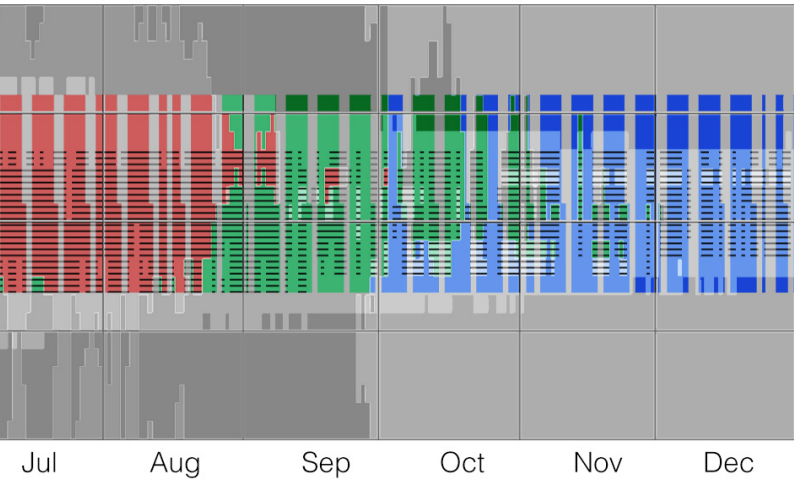


Figure e5.1 Thermal + Visual Comfort evaluation. Point 54



F - findings & comments

F. Findings & Comments

Baseline scenario results showed a high degree of over-heating and insufficient daylight values according to UDI, achieved ranges and in terms of luminous autonomy.

Figure f.1 shows total solar gains relative to baseline scenario, according to its default window properties.

For this reason, an attempt to mitigate or even reduce discomfort was proposed through three methodologies:

- a. application of new window properties
- b. use of dynamic shading
- c. use of fixed shading

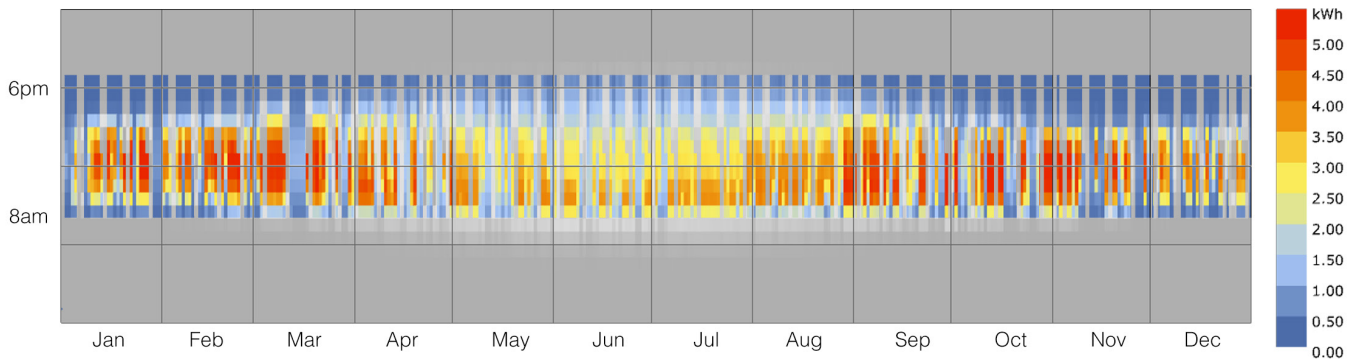


Figure f.1 Annual Plot of Total Solar Gains - baseline scenario

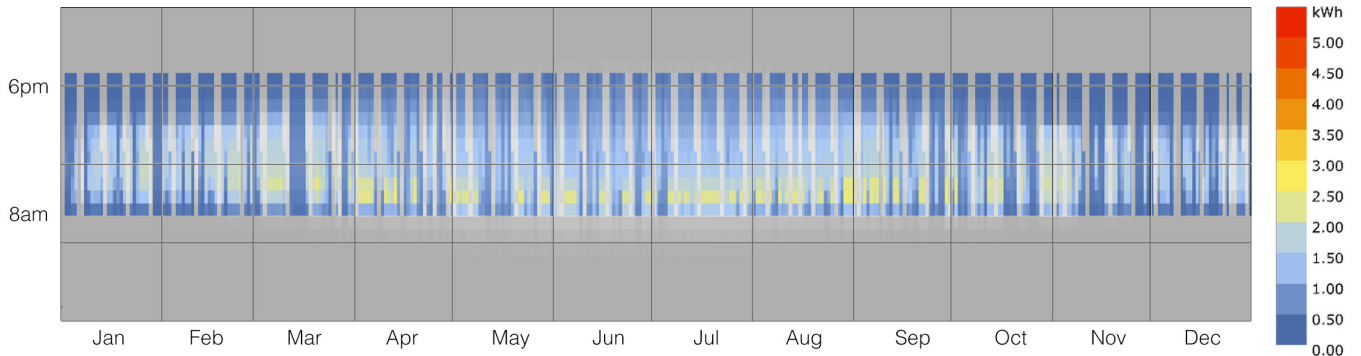


Figure f.2 Annual Plot of Total Solar Gains - new glass properties

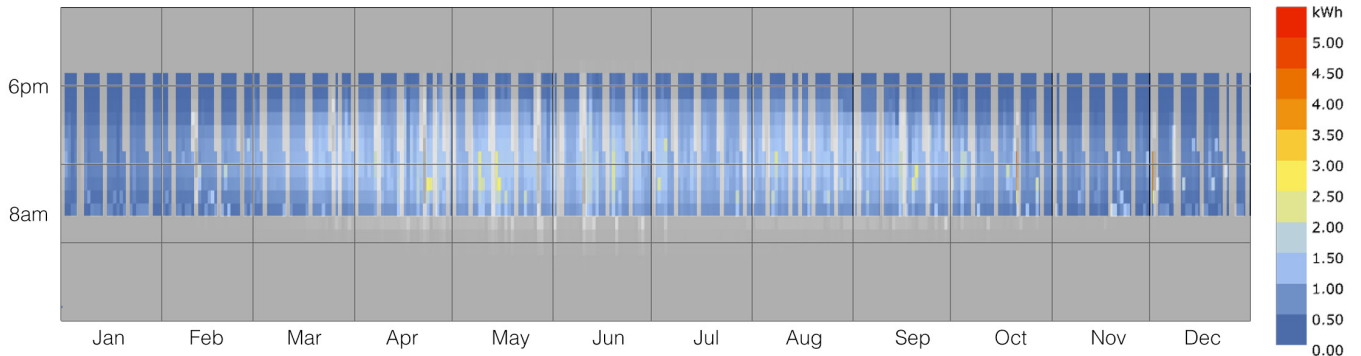


Figure f.3 Annual Plot of Total Solar Gains - dynamic shading

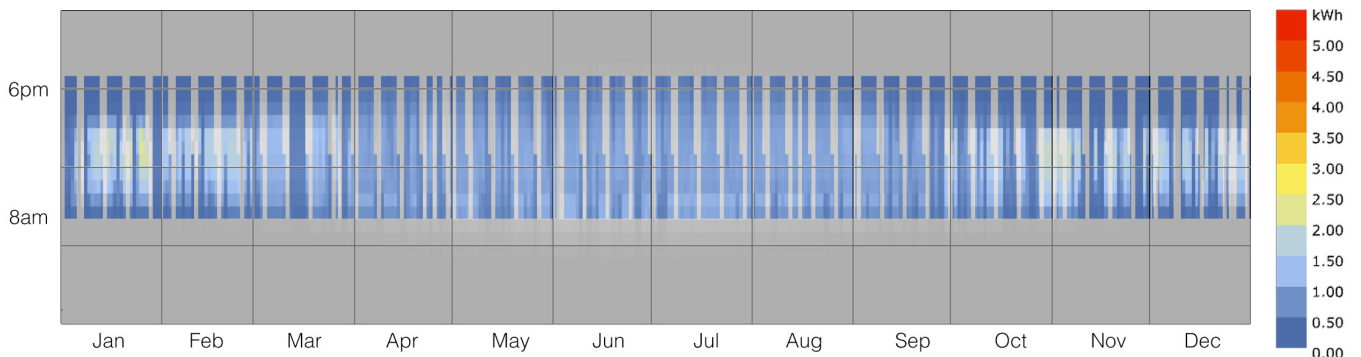


Figure f.4 Annual Plot of Total Solar Gains - fixed shading

Figures f.2-3-4 show reduction in Solar gains according to the followed strategy.

In particular, fixed shading leads to the highest reduction during spring and summer time while keeping some in winter time. This happens because the shading was designed according to sun path from April to September.

Case with different window properties results more efficient in limiting solar gains during winter time than summer. This could be unwanted for passive strategies implications which could be helpful for a climate similar to that of Turin. Similarly, daysim shading seems to be limiting winter gains more than summer ones, with these being a little higher compared to the case in which fixed shading is present.

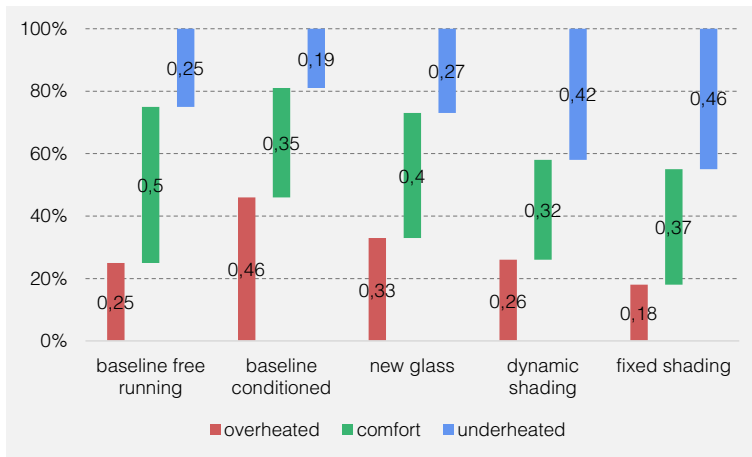


Figure f.5 Thermal ranges of 5 simulations scenario in comparison

Figure f5 compares all five simulation scenarios according to Thermal analysis results.

None of these cases reach sufficient or acceptable comfort.

What is visible is a bigger shift in over-heating (18% to 46%) and under-heating (19% to 46%) ranges in spite of comfort, which seems to be more stagnant (37% to 50%, see figure f.5).

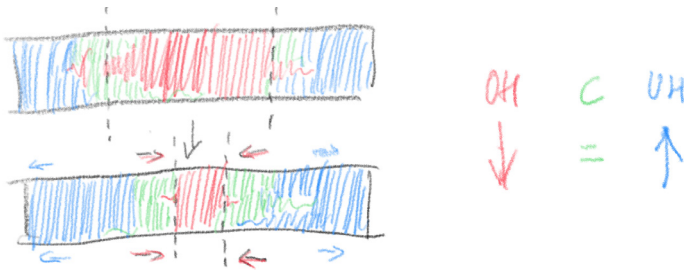


Figure f.7 Concept of Comfort range being more stagnant in comparison to over-heating and under-heating

Figure f.8 shows variations of thermal and daylight ranges according to four main different case scenarios. This kind of visualization sums up both a qualitative and quantitative shift of these ranges. Indeed, from baseline to fourth scenario with fixed shading, not only is over-heated reduced, but also the range of over-lit hours. Thus, the resulting 18% of fourth simulation is not associated to a daylight discomfort anymore (over-lit or under-lit). We have seen that

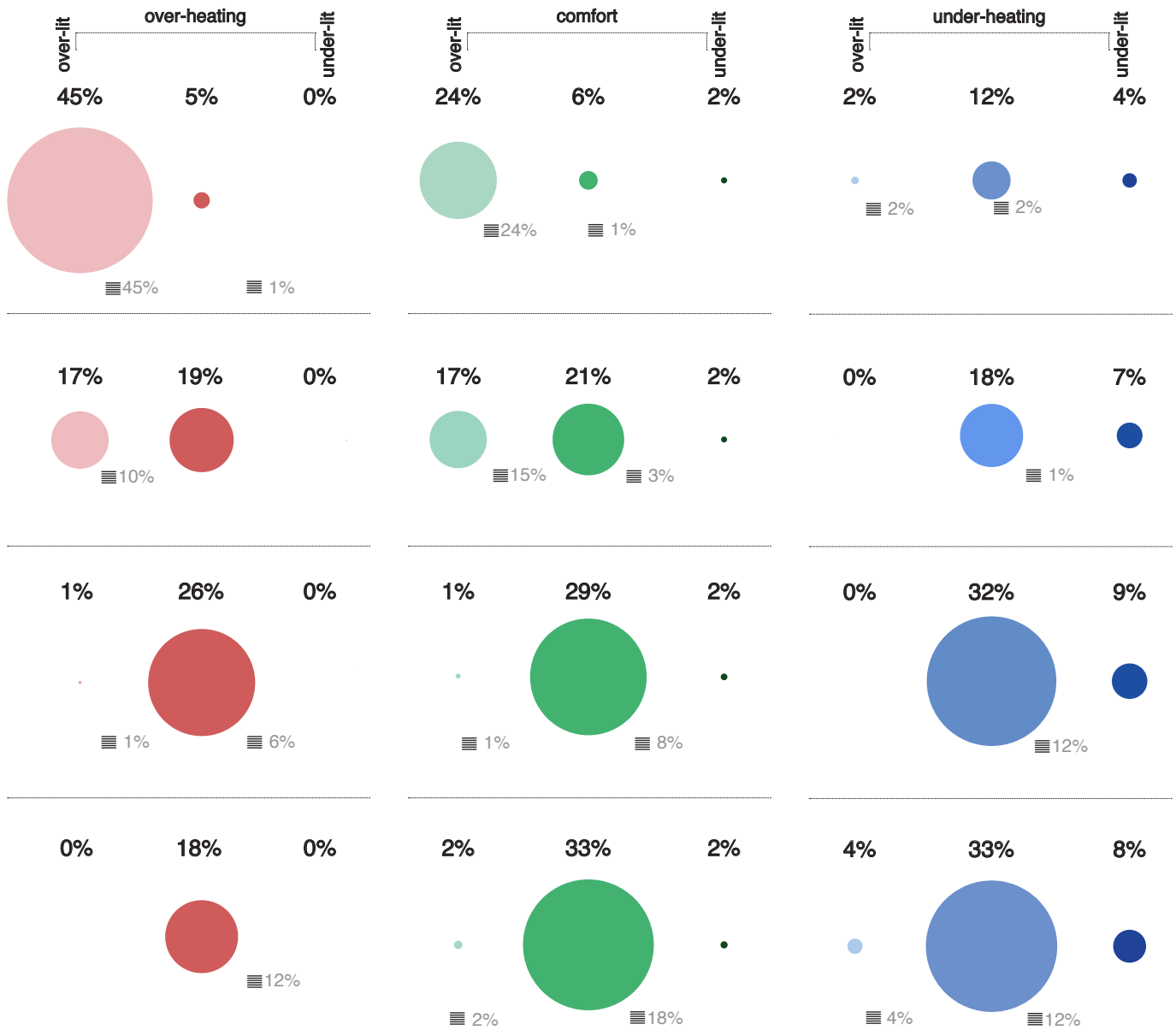


Figure f.8 Variation of thermal and daylight ranges according to different case scenarios

major comfort is reached in “new glass” simulation, but 17% of this range is associated to over-light-

ing. Fixed shading scenario on the contrary, achieves major comfort (33%) if we exclude ex-

ceeding daylight ranges. As for under-heated % of time, we can observe a worst picture, with an

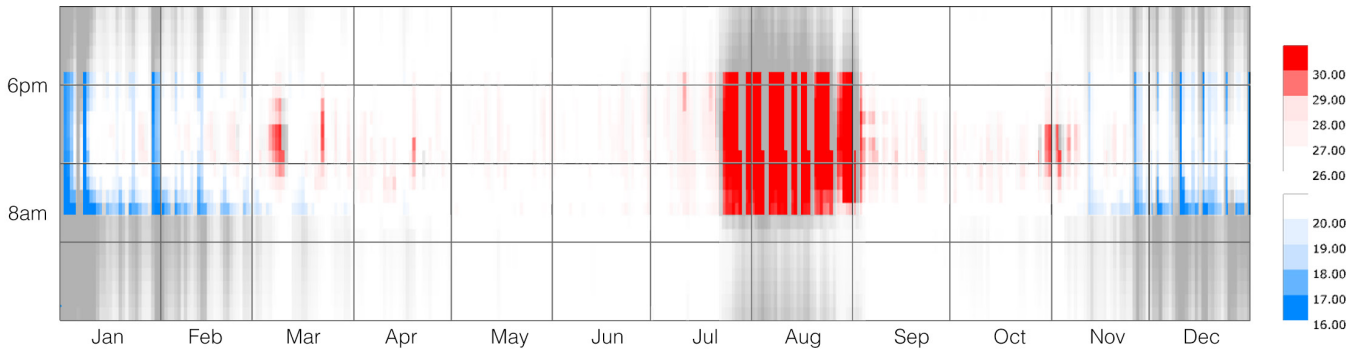


Figure f.9 Annual Plot of temperature delta - baseline free running scenario

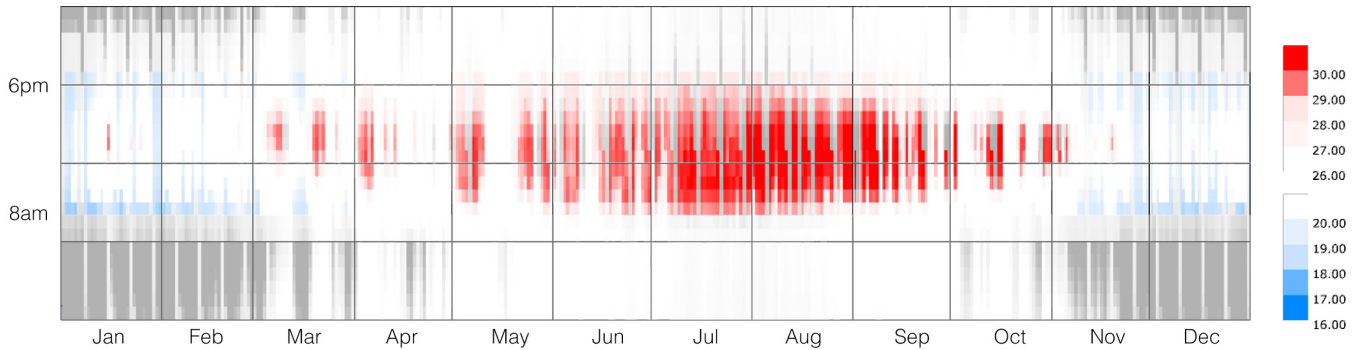


Figure f.10 Annual Plot of temperature delta - baseline conditioned scenario

increase in occupied hours below thermal comfort threshold, also with a small increase in daylight discomfort ranges (up to 4% and 8%).

Yet, by comparing annual plots of Operative Temperature and deltas from Comfort Zone, a

consistent change can be seen. Indeed, from different glass application to installation of fixed shading, deltas keep reducing and getting closer to the comfort zone thresholds (see images f.9-f.10-f.11-f.12-f.13).

Figure f.6 refers to simulation results in free running mode. Thermal Autonomy is achieved most in this case. Yet, as the image points out, early morning in winter time is characterized by very low temperatures (lower than 15°C), whereas late July and August, 205

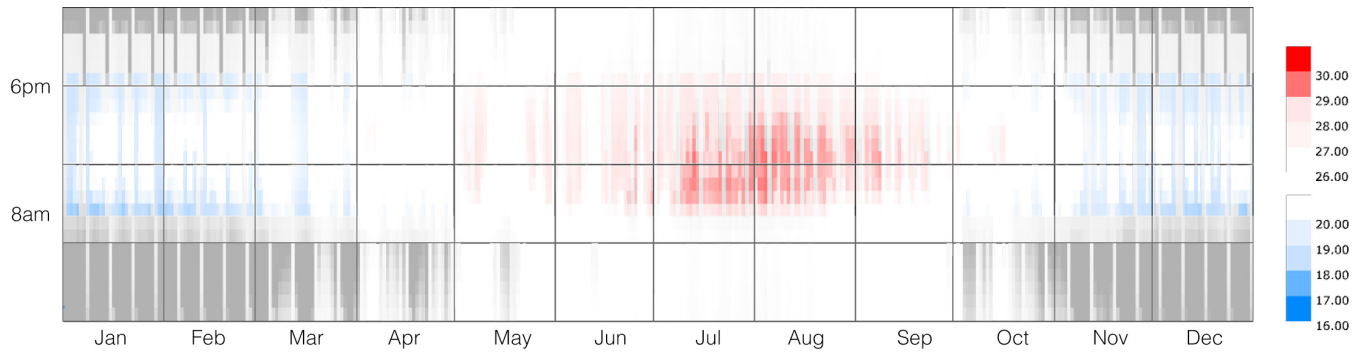


Figure f.11 Annual Plot of temperature delta - new glass scenario

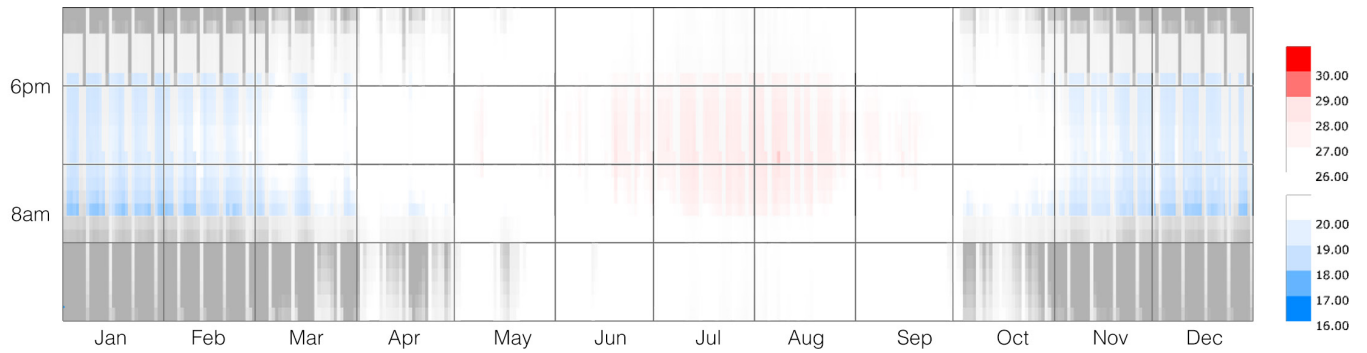


Figure f.12 Annual Plot of temperature delta - dynamic shading scenario

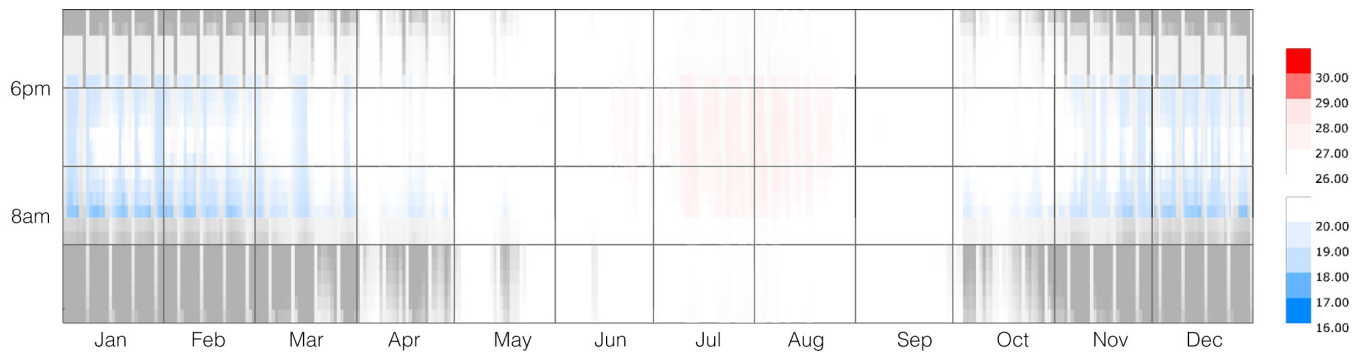


Figure f.13 Annual Plot of temperature delta - fixed shading scenario

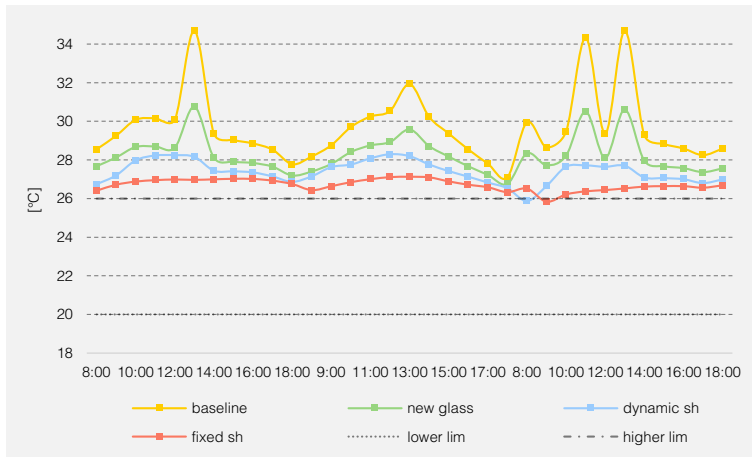


Figure f.14 Temperature variations in three consecutive days based on a typical summer week

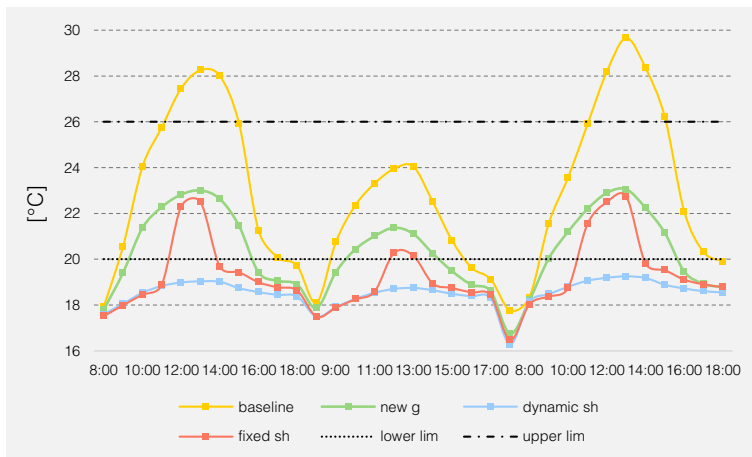


Figure f.15 Temperature variations in three consecutive days based on a typical inter week

which presents over-heating, have extreme high temperatures, even over 40°C.

Conditioned building shows a wider range of overheating, with temperature not as extreme as in previous case, but around 30°C and more

To better visualize temperature differences according to different scenarios, two charts were drawn, based on three consecutive days of a typical summer and winter day.

Figure f.14 shows a typical summer day, with reference to comfort range (20-26°C). In all scenarios over-heating is reached. Nonetheless, over-heating in baseline scenario (yellow line) reaches 35°C, almost 10° more than fixed shade scenario, where temperature exceeds comfort threshold by 1°C at most.

Similarly, winter typical day shows even some over-heating

happening in baseline scenario, with temperature reaching almost 30°C during midday. Exceeding temperatures and deriving thermal discomfort aspects during the heating season can be found in the article of Kalmar et Al. [21].

Under-heating, which is more common in the remaining three scenarios, occurs with deltas around 1-2 degrees from comfort range. On one day, there is a drop to 16°C, with the highest delta from range of 4°C.

Application of fixed shading, which shows smallest deltas and closer values to comfort range, almost solves issue of over-heating in summer.

Under-heating seems still a bit excessive, especially for dynamic shading scenario, which, as seen in previous pages, is responsible of limiting higher quantity of solar gains during winter time.

Whether Thermal Comfort % is not satisfied (though a sensible

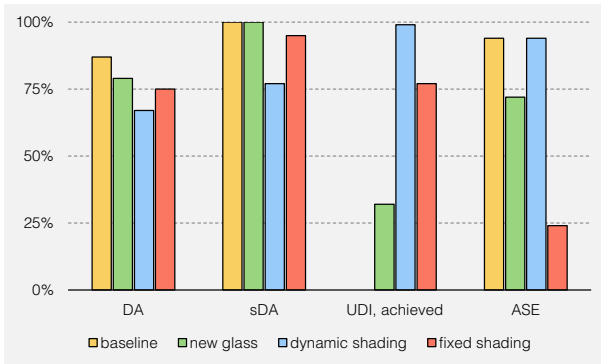


Figure f.16 DA, sDA, UDIach. and ASE according to different simulations

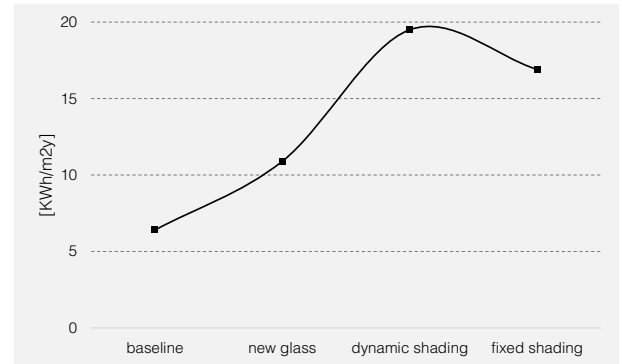


Figure f.19 Variations of lighting consume according to four simulations

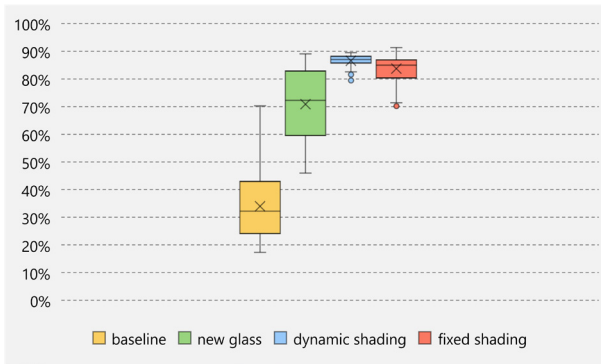


Figure f.17 Variations of UDIach. among the four simulations

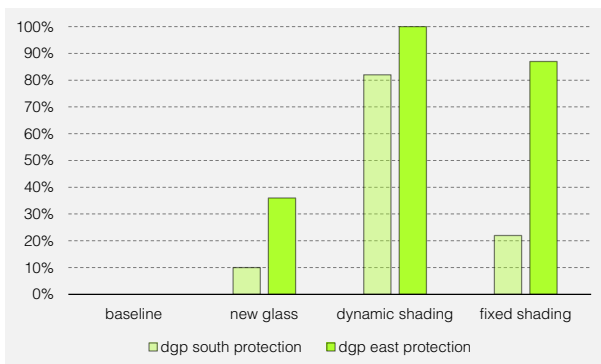


Figure f.18 Variations of Glare protection among the four simulations

difference in temperature delta is found), Visual comfort Parameters such as $UDI_{achieved}$ show better results.

Figure f.16 shows variations of daylight autonomy, spatial daylight autonomy, UDIachieved and ASE, according to four different scenarios. In particular, baseline case presents insufficient values of UDI in-between 100-3000 lx. This is better visible in figure f.17, where Dynamic shading and fixed shading simulations show better results, for they not only verify (or almost) performance parameter of luminous autonomy, but also

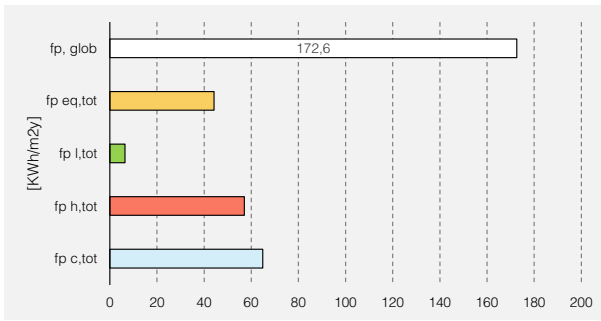


figure f.20 baseline

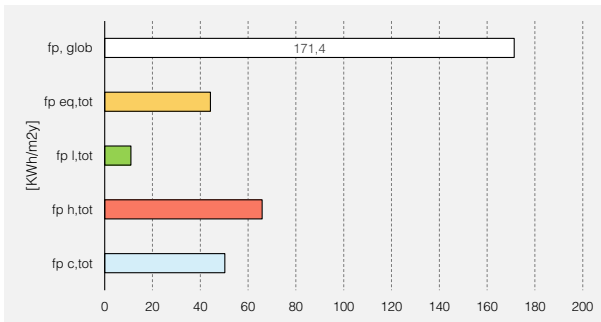


figure f.21 new glass

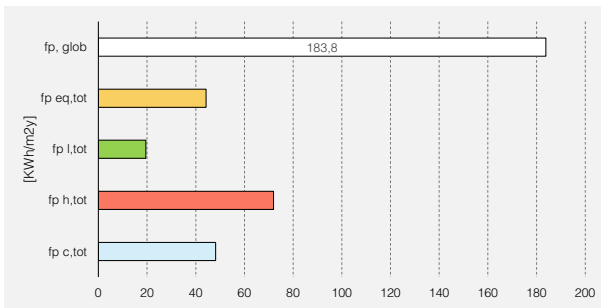


figure f.22 dynamic shading

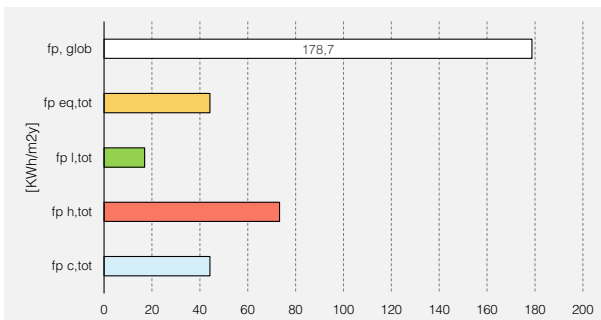


figure f.23 fixed shading

represent less space asymmetry (box plot is narrower).

In these two cases there is also more glare protection (with verified values occurring in east orientation according to the case with dynamic shading).

Whether shading solves some issues related to daylight and glare, more electrical consumptions are registered, as we can read from figure f.19.

Images on the left show Energy Results converted in Primary Energy according to different energy vectors [22]. In particular, according to following legend:

- equipment
- lighting
- heating
- cooling

Baseline scenario presents higher consumes in cooling vs. heating. This trend inverts with next three strategies (new glass, dynamic shading and fixed shading) as we can see from figures f.21, f.22 and f.23. Also, Lighting varies according to the simulation. Dynamic

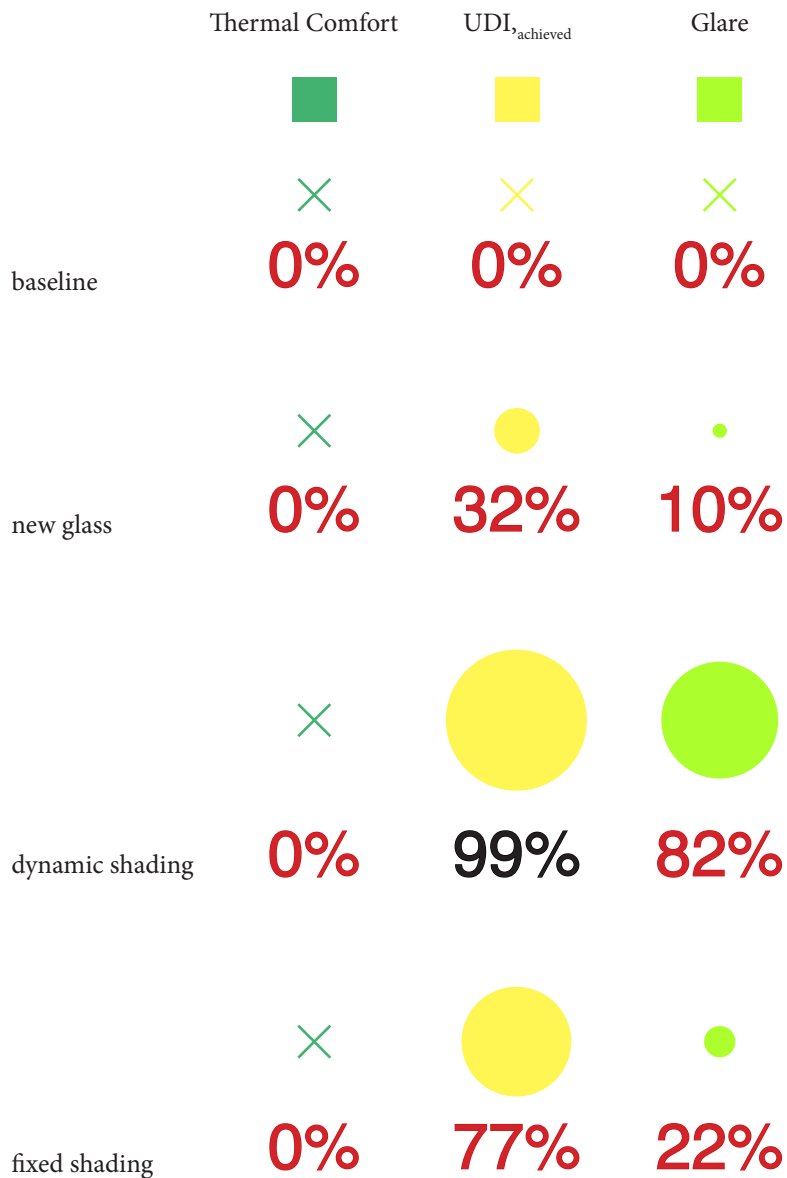


figure f.24 Synthesis of Performance Parameters according to Thermal Comfort, UDI_{achieved} and Glare

shading is the one where lighting consumption is the highest among the three applied strategies.

Overall, baseline new glass simulation reveals lowest global energy value.

Figure f.24 sums up results according to three performance parameters based on % of space. Though a better qualitative inside has already been reported, these numbers show that Thermal comfort and glare is not achieved in none of the four cases. Only dynamic shading scenario succeeds in UDI_{achieved} (though fixed shading misses just 3% of space).

Future Work

One of the principal properties of H-IEQ Lab is its flexibility. Different Windows can be installed as well as different shading systems of various dimensions.

Three exposure, south, east and

north even amplifies the range of possible experimentations.

Great part of future work can focus on comparison between software thermal and visual results with real life tests, once the laboratory will be fully built and ready-to-use. Besides, simulations with different window-to-wall ratios, “g values” and more performative “U values” may lead to interesting outputs and findings.

In conclusion, though with significant improvements (see figure f.25), thermal comfort and glare (considering south as the most critical orientation) parameters are not achieved in none of the four cases.

As for thermal comfort, this dissertation simply displays application of Thermal Comfort Models such as Adaptive and PMV. Next work could focus more on ventilation strategies and scheduling in thermostat

combining a mixed-mode simulation with periods of conditioning and natural ventilation, which would also lead to noticeable increase in comfort hours. Moreover, as it happens in the summer season for fixed shading scenario, small deltas from comfort temperature could be easily turned into comfortable by slightly adjusting clothing levels and focusing more on the adaptive behaviour of occupants.

As for daylight and glare, not only can iterative shading design with implementation of interior blinds drastically reduce glare risk to a minimum (nowadays most buildings combine use of exterior shading and interior blinds), but also reduce those exceeding over-lit hours (3% in case of fixed shading) and lead to verification of daylight parameters.

Finally, interesting outputs and

studies can be fulfilled with CFD or “Computational Fluid Dynamics”, which could be essential in a better understanding of indoor climate.

“- 848”
overheated
hrs

“+77%”
UDI achieved
area

“- 70%”
sun exposed
area

figure f.25 Principal “fixed shading”
scenario results in comparison to baseline
case

References

- [1] IPCC, 2014: Climate Change 2014: Synthesis Report. Contribution of Working Groups I, II and III to the Fifth Assessment Report of the Intergovernmental Panel on Climate Change [Core Writing Team, R.K. Pachauri and L.A. Meyer (eds.)]. IPCC, Geneva, Switzerland, 151 pp.
- [2] UN Environment and International Energy Agency (2017): Towards a zero-emission, efficient, and resilient buildings and construction sector, Global Status Report 2017, p. 14
- [3] Worldwatch Institute, Renner M. (2016, May 10). State of the world: Can a City be Sustainable. Washington D.C., US: Island Press
- [4] S. G. Hodder, K. Parsons, The effects of solar radiation on thermal comfort, Int J Biometereol, 2007, 51, pp. 233-250
- [5] E. Arens, T. Hoyt, X. Zhou, L. Huang, H. Zhang, S. Schiavon, Modeling the comfort effects of short wave solar radiation, Indoor Environmental Quality, “2015, V.88, pp. 3-9: retrieved on <http://escolarship.org//uc/item/89m1h2dg>
- [6] ANSI/ASHRAE 55 -2017, Thermal Environmental Conditions of Human Occupancy, 2017
- [7] CEN FINAL DRAFT prEN 15251, Indoor environmental input parameters for design and assessment of energy performance of buildings addressing indoor air quality, thermal environment, lighting and acoustics, (2006)
- [8] CEN /TC 169/WG 11, Daylight in buildings, (2017), p. 23
- [9] The Well Building Standard v1 with May 2016 addenda.
- [10] Chris Mackey, Pan Climatic Humans, Shaping Thermal Habits in an unconditioned Society, B.A. Ar-

chitectural Design, Yale University, 2010, p.24.

[11] A. O'Donnel, M. Stefanowicz, Refined distribution of frit: Method and design tool for improved thermal comfort in glazed spaces, Lund University, p.10

[12] L. Giovannini, Design and operation of transparent adaptive facades from a visual comfort and energy use perspective, (2019), p3

[13] Jan Wienold, Dynamic Simulations of blind control strategies for Visual Comfort and energy balance analysis, Proceedings: Building Simulations, 2007, pp. 1198-1204.

[14] R. Bacetti, Progettazione di una facility sperimentale per la valutazione della qualità ambientale interna in ambienti ad uso ufficio, (2019), p. 36

[15] S. Haddad, P. Osmond, S. King, Relationship between children's comfort temperature and outdoor climate: some methodological issues, Proceedings of 9th Windsor Conference: Making Comfort Relevant, 2016, p. 1273

[16] A. Zani, H. D. Richardson, A. Tono, S. Schiavon, E. Arens, A simulation-based design analysis for the assessment of indoor comfort under the effect of solar radiation, SimAUD 2019 April 07-09 Atlanta, Georgia, 2019

[17] A. Zani, A. G. Mainini, J. Cadena et al., A new modeling approach for the assessment of the effect of solar radiation on indoor thermal comfort, Building Performance Analysis Conference and SimBuild co-organized by ASHRAE and IBPSA-USA, Chicago, IL, 2018, retrieved from: <https://escholarship.org/uc/item/2jx680d7>

[18] A. Zani, H. D. Richardson, S. Schiavon, E. Arens, Annual Radiation Discomfort: A new climate-based framework for modeling short-wave solar radiation in indoor spaces, Center of the Built Environment, University of California, Berkeley, Ca, USA

- [19] Won Hee Koa, Stefano Schiavon, Gail Brager, Brendon Levitt, Ventilation, thermal and luminous autonomy metrics for an integrated design process, *Building and Environment*, 145 (2018), pp 153-165
- [20] L. E. Lopez Ponce de Leon, Shading design workflow for architectural designers, TU Delft
- [21] Ferenc Kalmar, Tunde Kalmar, Thermal Comfort Aspects of Solar Gains during the Heating Season, *Energies*, 13 (2020), pp. 1-15
- [22] Federico Arieti, Progettare edifici a energia zero: percorso metodologico, indicazioni applicative, dettagli costruttivi, *Progettare per costruire sostenibile*, 2017, pp. 297-300

